THE
PHYSICAL
SOCIETY

MEMOIRS

OF THE

COLLEGE OF SCIENCE

KYOTO IMPERIAL UNIVERSITY

SERIES A

VOL. XI, No. 5

SEPTEMBER 1928

KYOTO

Some Notes on Solar Research*

By

Issei Yamamoto

(Received June 20, 1928)

Abstracts

In 1923, when I was studying solar phenomena from the data observed at Mt. Wilson Observatory, I found a peculiar relation between the distance of the positive and negative magnetic poles and the maximum intensity of the magnetic field in the bipolar sun-spot. Generally the relation is linear, the field intensity increasing with the distance between the poles; but there is apparently a lower limit of the latter for a range of the former, so that the graphical form of the relation as a whole is more or less logarithmic.

On the other hand, I found a tendency for the distance between the magnetic poles to occur in a wider range if a spot is nearer the solar equator. The evidences are similar in both northern and southern hemispheres.

There is no logical connection between the above two phenomena. But, if we assume an hypothetical idea that the bipolarity of the sun-spot is a physical consequence of the velocity changes between the successive layers of the solar atmosphere, then the first phenomenon will suggest a discontinuity of the circulating velocity in a certain depth of the atmosphere, and the second phenomenon seems to indicate a gradual change of the relative depths and the radial distribution of the layer velocities according to heliographical latitudes. It seems to me that the depths of the atmosphere considered herewith are beyond the range of penetration with spectroscopic or other instrumental powers, so that the evidences above mentioned cannot be examined otherwise than by heliographic study.

1. *Introduction.* In 1923 I spent some months at the Mount Wilson Observatory, and carried out a research to examine a possible relation

---

* This paper was read at the 32nd Annual Meeting of the American Astronomical Society, held at Dartmouth College, Hannover, N. H., on August 5, 1924, and the Abstract was published in Publications of the Society, Vol. **5**, p. 196, or in Popular Astronomy, Vol. **32**, p. 627. (1924).

between the variable "solar constant" and some heliographic disturbances. The materials then used were, on the one hand, the most recent values of the solar constant observed under Dr. C. G. Abbot, and on the other hand, the spectroheliographic records as well as the heliomagnetic observations obtained by Mt. Wilson observers.*

The present notes are some of the casual results obtained during the above-mentioned examinations of the materials, and principally from the visual observations of the magnetic properties of sun-spots which had been carried out as routine work, since some years ago, at Mt. Wilson by Mr. F. Ellerman and others.

2. *Polar distances and the magnetic field intensity of bipolar sun-spots.* It is at present widely accepted, following Dr. G. E. Hale's brilliant researches, that a typical disturbance on the solar surface consists of a pair of sun-spots which form a group and are oppositely polarized in magnetism. The "following member" of the sun-spot group is usually not so stable as the "preceding" one in its heliographic configurations. But according to my observations, the distance between the two dominating centers of magnetic fields is fairly durable as well as the field intensity of the preceding spot. Consequently I took the heliographical distance of such bipolar spots as abscissae, and the magnetic field intensity of the "preceding" spot as ordinates in a diagram, just to see their mutual relation, if any, graphically. Fig. 1 gives the feature. In my examinations of the original observations I made no statistical treatment, but selected those data of the day on which the solar disturbance examined reached a good degree of development and also became convenient for my quantitative estimation by approaching as near as possible to the central meridian of the solar disc. Some, however, had to be examined when they were not near the meridian because of their short duration or other circumstances. Accordingly I assigned proper weights to the quantities here estimated. In Fig. 1, the circles represent those which were observed within 1 centimeter of the central meridian of the original 43-cm solar disc, the dots those which were between 1 to 10 centimeters from the meridian, and the crosses, those which were more than 10 centimeters distant from it. A possible relation is apparent, although it is not very clear

* The results of this research has been published fully in Memoirs of the College of Science, Kyoto Imperial University **11**, 233 (1928); and its somewhat abridged report was published in Monthly Notices, Royal Astronomical Society, Vol. LXXXV, No. 1, (November 1924), pp. 71-78.

and definite. As a whole a linear relation seems to hold. But, if we take the relative weights into account, a greater or less curvature of the mean curve of regression is probable, so that a formula:

$$H - H_0 = M.\log\ (\rho - \rho_0) \qquad (1)$$

is suggested, where, H, the magnetic field intensity, ρ, the distance between the two spots, and H_0, ρ_0, and M are constants.

Fig. 1 was obtained by using the materials from the original observations of sun-spot magnetism made in the course of two and a half years, January 1921—September 1923, which should be considered to include the time when the solar activity is "minimum." Next, I treated similarly the original observations from another period of one year, July 1917—July 1918, which is representative of the "maximum" activity of the solar surface. The result is shown in Fig. 2. Here the circles denote those which were estimated within 1 cm. of the solar meridian, while the dots represent those which were between 1 and 5 cms. from the meridian. The tendency is generally the same as in Fig. 1. Moreover, the mean curve of both diagrams runs practically through the same points: in Fig. 2 the broken line B represents the mean curve of points in the same diagram, and the line A denotes the points on which the mean curve of the quantities of Fig. 1 runs.

It is true that these "mean curves" should not be too strictly considered in the physical sense; they are no more than a mathematical conventionalisation of the phenomenal appearance. There are wide deviations of individual points from these curves as seen in the two diagrams, and also a physical interpretation of the general character of these curves should be made sooner or later.

Nevertheless, it is too remarkable to be neglected in this connection that there is practically a lower limit in the mutual distance between the two spots in a bipolar sun-spot group, as is seen in the two diagrams: in both cases 0.5 cm. is the least distance ever observed, and yet this is clearly not due to observational difficulties, for the said limit is well within the possibility of visual examination.

In Fig. 3 I tried to plot the quantities of Fig. 1, retaining the same values for the abscissae, but taking for the ordinates the largest values of the magnetic field intensities ever observed in each sun-spot group, although these largest possible values were not always observed simultaneously with the corresponding interpolar distances. In its general features Fig. 3 is not very remarkably different from the other two, except that there is every possible augumentation of the ordinates. But a

close examination of the diagram shows, especially in the most weighted quantities, the curvature of the mean curve more clearly, and at the same time it reveals a slightly wider range, in ordinate, of occurrence of the lowest values of the polar distances.

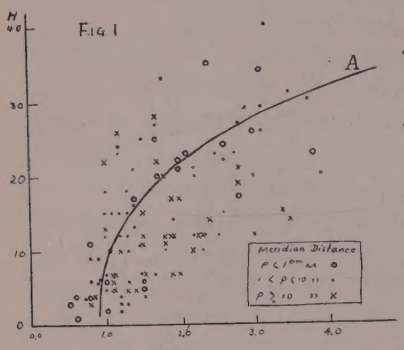

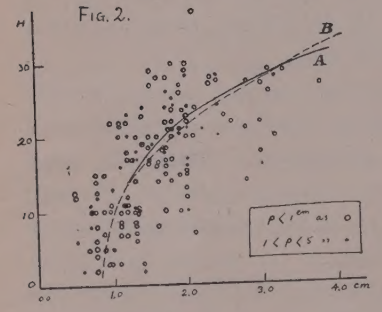

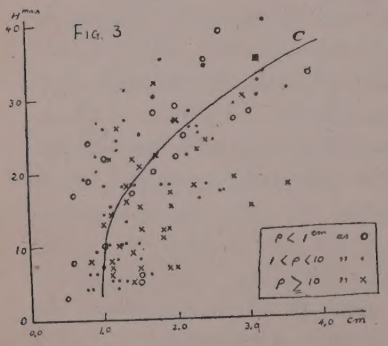

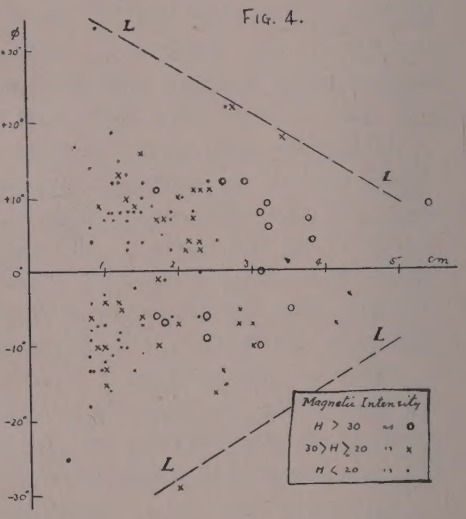

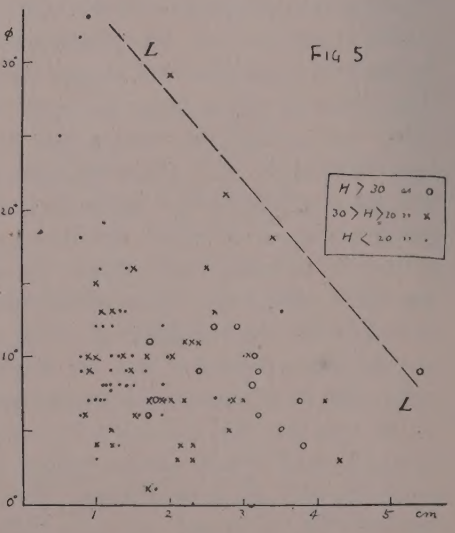

3. *Polar distances and the Heliographic latitudes of bipolar sun-spots.* Next, I took the heliographic latitudes of the sun-spot group as ordinates, while the abscissae denoting the interpolar distances remained the same as in Fig. 1. The new diagram thus obtained is shown in Fig. 4. In this case, the circles represent those whose magnetic field intensities are larger than 30 in Mr. Ellerman's scale, (in Mr. Ellerman's scale of the magnetic intensity unity is about 100 gausses,) the crosses, those between 20 and 30, and the dots, those which are less than 20 units. In Fig. 4 we see that the whole diagram is symmetrical about the solar equator, and also there is clearly and decidedly a wider range of interpolar distance occuring in lower heliographic latitudes than in higher latitudes. If we combine all the materials into a simpler diagram neglecting the distinction of north and south in the solar latitude, we get Fig. 5. The feature just mentioned is here more conspicuous, and the general tendency of a wider pair of sun-spots to occur in lower latitudes is so clear that a straight light line LL arbitrarily drawn upon the diagram appears a practical boundary of occurrence of the quantities.

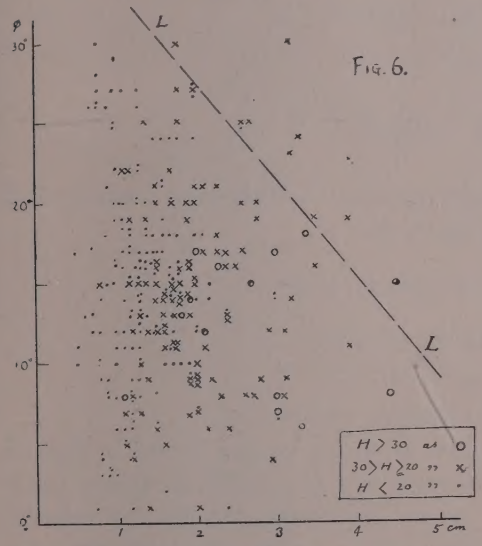

Fig. 6.

Fig. 6 is similar to Fig. 5, the material being however taken from ths years 1917–1918. Owing to the difference in the periods of solar activity, the distribution of the frequency of sun-spots in various latitudes differs in Figs. 5 and 6, which are widely recognized nowadays. Still the boundary line, which has been suggested in Fig. 5 to include all points between itself and the coordinate axes, appears to hold true just the same when it is *reproduced* in its exact position, as is shown in Fig. 6, limiting practically all points.

4. *Some physical suggestions from the above results.* There is apparently no logical connection between the two kinds of phenomena above mentioned. Now, if we assume an idea following Dr. G. E.

Hale that the bipolarity of sun-spot groups is caused by velocity-differences of successive layers of the solar atmosphere, then :

$$\frac{dv}{dr}\, dr = K.\ d\rho \qquad (2)$$

where v means current velocity of a solar atmospheric layer whose distance from the sun's center is r, and K a constant, while ρ means the distance between the two components of the bipolar group as previously mentioned. But, from (1)

$$d\rho = N.\ E^H.\ dH,$$

where $$N = \frac{1}{M} \cdot \frac{1}{E^{H0}},$$

and $$E = e^{1/M}.$$

Hence, $$\int \frac{dv}{dr}.\ dr = N \int E^H . dH.$$

If we assume that the correlation between the inter-polar distance and the magnetic-field intensity is linear, then

$$\frac{dv}{dr} = \text{constant, P say,}$$

and consequently the polar distance becomes

$$P(r - r_0) = N.E^H = N.e^{H/M}$$

or $$H = \text{constant. } \log(r - r_0).$$

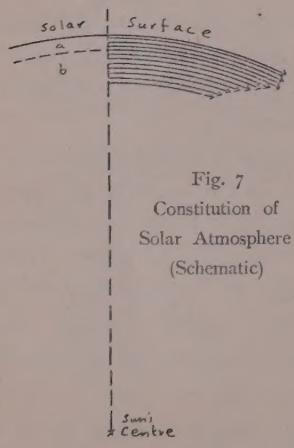

Fig. 7
Constitution of Solar Atmosphere (Schematic)

a=Layers of Constant Velocity
b= " " Varying "

But, as shown in Figs. 1 and 2, there is a lower limit of ρ, which is approximately 0.5 cm. in our scale, and this fact suggests that within a certain depth of the solar atmosphere from the uppermost surface we should have

$$\frac{dv}{dr} = 0.$$

The accompanying Fig. 7 shows the schematic view of a vertical section of the atmospheric currents of the sun. I cannot say how deep is the layer of discontinuity of the velocity, except a rough estimation of the order of

$$\frac{0.5}{43.0} = \frac{1}{90}$$

of the solar diameter.

Another fact revealed in Figs. 5 and 6 is that there a continuous variation of distribution of the atmospheric velocities according to heliographical latitudes, although the depth of the constant velocity in the uppermost part of the atmosphere is sensibly constant.

It seems to me that these considerations will be important in the theoretical treatment of the constitution of the solar atmosphere.

Harvard College Observatory,

July 3rd., 1924.

On some Functions defined by certain Infinite Products.

By

Yoshikatsu Watanabe.

(Received Jan. 23, 1928)

Introduction

Recently Mr. Mittag-Leffler[1] and Mr. K. Grandjot[2] presented some integral transcendental functions which tend to zero along any straight line or algebraical curve going to ∞. Is it impossible to construct a power series with a finite radius of convergence, which tends to zero by any radial approaching to the boundary?

This would not contradict the fact that the maximum modulus of a power series increases with the modulus of the variable z; for the maximum way defined by Mr. T. Matsumoto[3], may in this case touch the boundary, and along it the maximum modulus of the function may increase in any way while it tends to become zero by a radial approaching to the boundary.

Messrs. F. and M. Riesz[4], however, proved the impossibility, except in the case of a constant, of such a phenomenon for those power series which were considered by Mr. P. Fatou, *i. e.* on the condition that $\Sigma|\text{coefficient}|^2=\text{convergent}$; for this sort of power series, the aggregate of vanishing points on the circle of convergence should be only of zero-measure.

One example may be suggested by the well known non-continuable

1. Acta Mathematica, **42** (1920), p. 290.
2. Math. Annalen, **91** (1924), S. 316.
3. These Memoirs **1**, (1915), p. 163.
4. G. Szegö, Math. Ann., **84**, S. 233.

series $f(z)=\Sigma z^{2^n}$. At the points $z=1, \pm 1, \ldots\ldots \exp\left(2p\pi i\right)^{\frac{1}{2q}}, \ldots\ldots$, $f(z)$ becomes $+\infty$, so $F(z)=e^{-f(z)}$ vanishes at these points on the circle of convergence; but when e. g. $z=e^{\frac{\pi}{3}i}$, $e^{\frac{2}{3}\pi i}, \ldots\ldots$, $f(z)=-\infty$, and so $F(z)=+\infty$. When the argument of z be incommensurable to π, e. g. $1, 2, \ldots\ldots$radians, the imaginary part presents itself, and though $f(z)=\infty$ in Riemann's sense, as a matter of fact, $e^{-f(z)}$ or $e^{-[f(z)]^2}$ cannot be ascertained to vanish. Also if $F(z)=\frac{1}{f(z)}$ or $\frac{g(z)}{f(z)}$, and $f(z)$ becomes ∞, $F(z)$ vanishes, but inside the circle, possibly $f(z)=0$, an infinite number of times up to the circumference; hence $F(z)$ cannot be expressed by a single power series whose radius of convergence $=1$.

I endeavour in this note to seek a power series or function which tends to vanish at the prescribed enumerably infinite number of points on the circle of convergence; particularly the case where the aggregate of these points becomes dense. For this purpose, Mittag-Leffler's generalized factor-theorem cannot be applied since the given points must be isolated in his case[1]. Also the original Weirstrass's factor-theorem is not very convenient for the proof of convergency on the boundary, as M. É. Borel remarks[2]; the main difficulty lies in the fact that, the vanishing factor being removed, the remaining product does not show evident convergence.

I present a function defined by some new infinite product, which does not vanish inside the circle of convergence, but does or tends to vanish at the previously given points on the circle. When the aggregate of these points is dense, wholly or partly on the circumference, it cannot be continued analytically across the arc, because if it be continuable over it, the continued element must vanish an infinite number of times in the inside of its own convergence-circle; consequently it should be equal to 0, which, except in the trivial case, is impossible. I have also discussed the behaviour of the function at the derived point, which does not belong to the given aggregate, and find two types: one still becomes zero, while the other becomes some finite value not zero.

As analytical application, besides the determination of a power series which is analytically singular at the prescribed points or on the arcs of the circle of convergence, I try to construct, by the aid of our function, a function which tends to given values l_n at given points $a_n (n=1, 2, \ldots\ldots)$ on the circle, though the result is not yet satisfactory.

1. Osgood, Functionentheorie, Bd. I, S. 548.
2. Function entière, p. 14.

I. Existence-theorem.

1. Definition. We mean by $Z^u=(Re^{i\Theta})^u$, $\exp u(\log R+i\Theta)$ where $R>0$ and $-\pi<\Theta\leqq\pi$[1], so Z^u is a holomorphic function of z in some domain, if u and Z be so. Let $a_1, a_2, \ldots\ldots(\mathfrak{A})$ be an aggregate of given enumerably infinite points, all lying on the unite circle; *i. e.* $a_n=e^{i\alpha_n}$, α_n being any angle not necessarily restricted in magnitude, but it can and should be reduced to the interval $(-\pi^{\ast\ast}, \pi)$ or $(0, 2\pi^{\ast\ast})$, if necessary.

Let $u_1, u_2, \ldots\ldots$be an infinite series of constant or variable terms (index-series). Form the product

$$F(z)=\prod_{n=1}^{\infty}\left(1-\frac{z}{a_n}\right)^{u_n}$$

$$=\exp\sum_{n=1}^{\infty}u_n\log\left(1-\frac{z}{a_n}\right)$$

$$=\exp f(z, u).$$

To make our proposal somewhat clearer, let us conceive possible forms of u_n:

If u_n be the n-th term of a power series

$$\phi(x)=c_1x+c_2x^2+\ldots\ldots\ldots+c_nx^n+\ldots\ldots\ldots$$

of a real (or complex) variable with real (or complex) coefficients,

$$f(z, x)=\sum_{n=1}^{\infty}c_nx^n\log\left(1-\frac{z}{a_n}\right);$$

and particularly

$$f(z, 1)=\sum_{n=1}^{\infty}c_n\log\left(1-\frac{z}{a_n}\right),$$

which is mainly discussed in this paper, and sometimes simply denoted by $f(z)$. Also

$$f(z, z)=\sum_{n=1}^{\infty}c_nz^n\log\left(1-\frac{z}{a_n}\right),$$

which suggests a more general form

1. Sometimes we make it $0\leqq\Theta<2\pi$; but then it will be explicity noticed.

$$f(z, u) = \sum_{n=1}^{\infty} u_n(z) \log\left(1 - \frac{z}{a_n}\right).$$

But, in this paper, none of these except $f(z, 1)$ is so much treated.

2. Defining domain. We notice first of all that $\log\left(1-\frac{z}{a_n}\right)$ is holomorphic and even bounded in a certain domain S_n. S_n will be obtained from the Gauss plane by cutting away a sort of fundamental loop: Describe a circle about $a_n = e^{i\alpha_n}$ with radius ϵ and a circle about 0, $|z| = R$. Make a cross cutting line $\theta = \alpha_n$ from $a_n(1+\epsilon)$ towards ∞ up to Ra_n. Draw a parallel cut starting from $a_n(1+\epsilon e^{i\delta})$ and ending also on the circle $|z|=R$. The remaining domain, the boundary inclusive, will give S_n. For, let $z = re^{i\theta}$, $1 - \frac{z}{a_n} = 1 + re^{i(\pi+\theta-\alpha_n)} = \zeta_n = \xi_n + \eta_n i = \rho_n e^{i\varphi_n}$. Taking the ζ-plane's origin at $z=-1$, and the ξ-axis coincident with the x-axis of the z-plane, it is easily seen geometrically (Fig. 1) that, for all z in the domain, the corresponding ζ_n falls in $|z| \leqq R$, the portion obtained by revolving the portion cut away before, about $z=0$ by angle $\pi - \alpha_n$ being excluded.

Fig. 1.

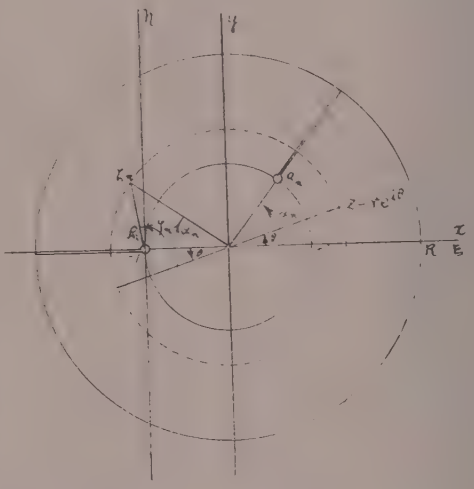

In whatever way z may wander in the domain, ζ cannot make a complete revolution around the point $\zeta = 0$, and $-\pi < \varphi_n \leqq \pi$, $0 < \epsilon \leqq \rho_n \leqq R+1$. Thus $\log\left(1 - \frac{z}{a_n}\right) = \log \rho_n + i\varphi_n$ is one valued and even bounded. Let the greater of $1 + \sqrt{(\log \epsilon)^2 + \pi^2}$ and $1 + \sqrt{(\log 2R)^2 + \pi^2}$ be M; then

$$\left|\log\left(1 - \frac{z}{a_n}\right)\right| < M.$$

It is to be noted that M is independent of a_n. Hence if we cut out from $z \leqq R$ similar loops made for all $a_1, a_2, \ldots\ldots$, *all* $\log\left(1 - \frac{z}{a_n}\right)$ *are bounded uniformly for all* z *and for all* n, *in a star-figured domain* S *above obtained.*

When the aggregate $\mathfrak{A}$ is dense, the small circles with radii ϵ, having centers at a_{n_1}, a_{n_2},....., whose derived points form an arc C, give somewhat like an envelope which is some arc of $|z|=1-\epsilon$, parallel to C, so to speak. If C becomes the whole unit circle, the evelope becomes the whole circle $|z|=1-\epsilon$, and S should be only the domain $|z|\leqq 1-\epsilon$. If, on the other hand, there exists some finite arc $\mathfrak{C}$ which contains no a_n (we call such an arc *regular*), certainly S can be extended beyond a sub-arc of $\mathfrak{C}$, if we make e. g. $2\sin^{-1}\frac{\epsilon}{2} < \frac{1}{2}$ (*length of* $\mathfrak{C}$).

Our domain S is not necessarily simply connected, since $\epsilon \neq 0$. But it becomes so ultimately if we make $\epsilon \to 0$, $\delta \to 0$.

3. Existence of our functions. We are now in a position to prove the existence of our function defined in § 1.

Theorem 1 (general existence-theorem). *Let* $u_n(z)$ *be holomorphic in* z *and* $\sum_{n=1}^{\infty} u_n(z)$ *be uniformly and absolutely convergent in some domain* U; *then*

$$f(z, u) = \sum_{n=1}^{\infty} u_n(z)\log\left(1 - \frac{z}{a_n}\right)$$

is holomorphic in the common domain T *of* S *and* U.

For, every summand is holomorphic in T; also

$$\sum_{n=n_0}^{\infty} \left| u_n \log\left(1 - \frac{z}{a_n}\right)\right| < \sum_{n=n_0}^{\infty} |u_n|\, M.$$

But by hypothesis, for a prescribed small quantity $\sigma > 0$, we can find N such as

$$\sum_{n=n_0}^{\infty} |u_n| < \sigma \quad \text{for all } n_0 \geqq N \text{ and for all } z \text{ in } T.$$

Hence $$\sum_{n=n_0}^{\infty} u_n \log\left(1 - \frac{z}{a_n}\right)\Bigg| < M\sigma.$$

Thus $f(z, u)$ is also uniformly convergent in z in T, and therefore, by Weirstrass's series-theorem, it is holomorphic in T. Q. E. D.

Particularly if $\Sigma u_n(z)$ be an integral function, U becomes the whole Gauss plane and T coincides with S; the exterior radius R may be taken of any length however great.

More particularly if u_n be a constant term c_n (or $c_n x^n$, x being another independent variable), the simple hypothesis that Σu_n is absolutely convergent is enough, and the derived function is given by

$$f'(z)=\sum_{n=1}^{\infty}\frac{c_n}{z-a_n}$$

which is the logarithmic derivative of $F(z)$. For $f'(z)$ we do not need any cut at all.

It is well to remark that, when c_n is real, the real part of our function $\Re f(z)$, is a one-valued continuous function in the whole Gauss plane except $z=a_n$, and the straight cut may be given up entirely. On the other hand, for the imaginary part $\Im f(z)$, only the straight cut is needed, since $\Im f(z)$ is uniformly continuous in S ($\delta=0$, $\epsilon=0$).

The case where Σc_n is only conditionally convergent, will be treated by example later on (§ 16). But with this, or even when Σc_n is divergent, if there exist a convergent power series $\Sigma c_n x^n$, we have still a holomorphic function $f(z, x)$.

Among cases where u_n are really functions of z, it is interesting to consider the case $\Sigma u_n(z)=\Sigma c_n z^n=p(z)$, a power series of z. If $p(z)$ has a finite radius of convergence R_0, U beoomes $|z|\leqq R<R_0$. Hence if $R_0>1$, and there is some regular arc $\mathfrak{C}$, S may be extended over $\mathfrak{C}$, while if $R_0<1$, S becomes U.

$f(z)$ being thus defined, $F(z)=\exp f(z)$ is also holomorphic in T. If U contains the unit circle, T or S may be extended to contain almost all the inner points of the unit circle as nearly as we please. $F(z)$ being expressed by a power series, the power series thus obtained does not vanish inside the uinit circle.

4. Representation by a power series. For some special cases, we are able to show the above existence in another way, and at the same time, to represent it by a power series.

Theorem 2. *The function $f(z, z)$ is holomorphic inside the circle $|z|=r_0$, where r_0 is the smaller of R_0 (the radius of convergence of $p(z)=\Sigma c_n z^n$) and unity.*

$$\text{For}\quad f(z,z)=\sum_{n=1}^{\infty}c_n z^n\log\left(1-\frac{z}{a_n}\right)$$

$$=-\sum_{n=1}^{\infty}c_n z^n\left(\frac{z}{a_n}+\frac{1}{2}\left(\frac{z}{a_n}\right)^2+\dots\right),\qquad |z|<r_0\leqq 1;$$

hence the dominant function is less than $\sum_{n=1}^{\infty}\left|c_n z^n\right|\frac{|z|}{1-|z|}$.

But since $|z|<R_0$, $\sum_{n=1}^{\infty}c_n z^n$ is absolutely convergent; hence the expansion

in z of $f(z, x)$ is absolutely convergent. Thus it can be rearranged in powers of z:

$$f(z, x) = -\sum_{n=1}^{\infty} z^{n-1}\left(\frac{1}{n}\frac{c_1}{a_1^n} - \frac{1}{n-1}\frac{c_2}{a_2^{n-1}} + \cdots - \frac{c_n}{a_n}\right),$$

which defines a holomorphic function in z, $|z| < r$: $r = 1$ if $K \geqq 1$, and $r = K$ if $K < 1$.

Theorem 3. *If $p(x) = \Sigma c_n x^n$ has a radius of convergence $K > 0$, $f(z, x)$ is holomorphic in $|z| < 1$, $|x| < K$. Specially, if $K \geqq 1$, $f(z, 1)$ is* ***holomorphic in*** $|z| < 1$.

The proof is similar to the above. But to obtain a compact form, we have

$$f(z, x) = \sum_{n=1}^{\infty} c_n x^n \log\left(1 - \frac{z}{a_n}\right)$$

$$= -\sum_{n=1}^{\infty} c_n x^n \sum_{m=1}^{\infty} \frac{1}{m}\left(\frac{z}{a_n}\right)^m, \qquad \left|\frac{z}{a_n}\right| < 1$$

$$= -\sum_{n=1}^{\infty} \frac{z^n}{n} \sum_{m=1}^{\infty} \frac{c_m x^m}{a_m^n}, \qquad |x| < R_0.$$

Particularly if $p(x)$ is an integral transcendental function, $f(z, x)$ exists for all values of x when $|z| < 1$.

When $K > 1$, putting $x = 1$

$$f(z, 1) = -\sum_{n=1}^{\infty} c_n \log\left(1 - \frac{z}{a_n}\right) = -\sum_{n=1}^{\infty} \frac{z^n}{n} \sum_{m=1}^{\infty} \frac{c_m}{a_m^n}$$

$$= -\sum_{n=1}^{\infty} \frac{z^n}{n} \varphi(n).$$

We shall hereafter denote $f(z, 1)$ by $f(z)$ simply.

Now $$\frac{1}{n}\varphi(n) < \frac{1}{n}\sum_{n=1}^{\infty} |c_n| = \frac{C}{n},$$

where $C > 0$ and is finite, (except in the trivial case that all $c_n = 0$, in which case $F(z)$ reduces to unity).

Hence $$\lim_{n=\infty} \sqrt[n]{\frac{1}{n}\varphi(n)} \leqq 1.$$

Hence r_0, the radius of convergence of $f(z)$ is not less than 1.

When all c_n's are real and positive (or negative) throughout, we shall see that really $r_0=1$, since at the prescribed point a_n, $f(z)$ becomes infinity, as shown in the next section.

Further

$$\sum_{n=1}^{\infty}\left|\frac{1}{n}\varphi(n)\right|^2<\sum_{n=1}^{\infty}\frac{1}{n^2}\sum_{m=1}^{\infty}|c_m|^2=\frac{\pi^2}{6}\sum_{m=1}^{\infty}|c_m|^2;$$

but Σc_m being absolutely convergent, *a fortiori* $\Sigma |c_m|^2$ is convergent, and the above is convergent. Thus when $r_0=1$, our $f(z)$ reduces to one of Fatou's functions[1].

It is known that for such functions,

$$\lim_{r=1-0} f(re^{i\theta})=f(e^{i\theta})$$

exists everywhere on the circle of convergence, except possibly some points whose aggregate is only of zero-measure; and besides, $f(e^{i\theta})$ takes every complex value with a frequency of zero-measure. But our purpose being rather to determine whether a point given on the circle is one of the very exceptional points or not, we must discuss more in detail. Thus when $e^{i\theta}$ belongs to neither the given aggregate $\mathfrak{A}$ nor to its derived aggregate $\mathfrak{A}'$, we can find a finite arc $\mathfrak{C}$, which contains no a_n, and in the interior of which $e^{i\theta}$ lies. And we can construct a star-figured domain S (§ 2), in the interior of which $e^{i\theta}$ lies. Hence by our general existence theorem, whatever path of approach may be taken,

$$\lim_{z=e^{i\theta}} f(z)=f(e^{i\theta})$$

is finite and determinate.

This is not, I think, merely a direct consequence of Riesz's theorem.

Also Riesz's proposition apparently contains three things: the existense of $\lim_{r=1-0} f(re^{i\theta})$ and $f(e^{i\theta})$ and their equality. But in virtue of Abel's continuity theorem and Littlewood's converse theorem[2] for a power series whose coefficients are of the same order as $\frac{c}{n}$, where c is finite, we have only to assume the existence of either one.

But in our case it is somewhat difficult to consider the power series

$$-\sum_{n=1}^{\infty}\frac{z^n}{n}\sum_{m=1}^{\infty}\frac{c_m}{a_m^n}$$

1. G. Szegö, loc. cit. 4.
2. The converse of Abel's theorem on power series. Proc. Lond. Math. Soc. Ser. 2, Vol. 9, p. 434.

itself; and it is rather preferable to take for the given series

$$\sum_{n=1}^{\infty} c_n \log\left(1 - \frac{z}{a_n}\right).$$

Both are equal if $|z|<1$, or even on a finite arc of the unit circle, which does not contain any a_n as shown above. But since $\mathfrak{A}$ may be dense, we cannot assume their general equality on the boundary, and it is the latter that we have defined primarily. Hence we consider chiefly the latter expression, which seems to me to have nothing to do with the above two celebrated theorems. I therefore seek for a somewhat Abel-like theorem for our function. Thus the convergency of the former expression on the boundary is rather out of question, as we are concerned with the latter's continuity on the boundary. (When it is continuous the continuity of the former follows naturally.)

II. Behaviour on the boundary.

5. Some preliminary remarks. It is to be noticed that, since

$$f(z) = \sum_{n=1}^{\infty} u_n \log\left(1 - \frac{z}{a_n}\right)$$

is absolutely convergent in S, it is quite irrespective of the order of summation, by Weirstrass's theorem on double series. Thus

$$\sum_{n=1}^{\infty} = \Sigma' + \Sigma'' + \cdots\cdots,$$

where Σ', Σ'',.....denote sums of summands arbitrarily chosen from Σ, without either repeating or leaving any terms. This is really the cardinal point of the discussions in the following paragraphs. Also our prescribed points a_n's need not necessarily be all different. Let

$$a_{n_{1,0}} = a_{n_{1,1}} = a_{n_{1,2}} = \cdots\cdots,$$

$$a_{n_{2,0}} = a_{n_{2,1}} = \cdots\cdots,$$

$$\cdots\cdots,$$

where $n_{1,0} < n_{2,0} < \cdots\cdots < n_{p,0} < \cdots\cdots$, and for every p : $n_{p,0} < n_{p,1} < n_{p,2} \cdots\cdots$, the number of $n_{p,q}$ may be finite or infinite. By summing up in groups, we have in S

$$f(z) = \sum_{p} \sum_{q} u_{p,q} \log\left(1 - \frac{z}{a_{n_{p,q}}}\right)$$

$$= \sum_{p=1}^{\infty} v_p \log\left(1 - \frac{z}{a_{n_{p,0}}}\right)$$

where $v_p = \Sigma_{n_{p,q}}$: and in virtue of the absolute convergency of Σu_n, not only each v_p but also Σv_p is absolutely convergent. Hence in the following we may assume that all a_n are different. (In this respect our function is, though superficial, different from those infinite products of Weierstrass and Mittag-Leffler, since the number of repetitions of a_n is confined to be finite.)

It is not, however, in our power to arrange $\arg a_n = \alpha_n$ (reduced between $-\pi$, $+\pi$) or $-\pi^0$, π^0 in order of ascending magnitude in general. For, if $\mathfrak{A}$ be dense somewhere on the arc C, $\mathfrak{A}'$ has a closed interval C' in C whose end points do not belong to $\mathfrak{A}$, and in C', we can determine neither the maximum nor the minimum of α_n.

Nevertheless it must be noticed that $\mathfrak{A}$ can be divided into $\mathfrak{A}_1$, $\mathfrak{A}_2$,..... $\mathfrak{A}_m$,..... so that the arguments (reduced) of all the points of $\mathfrak{A}_m$ are greater than that (reduced) of any point of $\mathfrak{A}_{m-1}$. Thus we may divide the whole circumference into sub-arcs by taking points of division as, e. g.

$$0 \leqq \theta_1 < \theta_2 < \theta_3 < \ldots\ldots\ldots\ldots\ldots < 2\pi .$$

Making sub-summations, we have still in S

$$f(z) = \sum_{n=1}^{\infty} u_n \log\left(1 - \frac{z}{a_n}\right) = \Sigma_1 + \Sigma_2 + \ldots \ldots \Sigma_m + \ldots\ldots$$

where Σ_m means the summation of all the summands with those a_n's which lie on the arc $\theta\,(\theta_{m-1}, \theta_m^{\pm 0})$.

Now let us consider the behaviour of $f(z)$ when z becomes or tends to some point z_0 on the unit circle, assuming that all $u_n\,(=c_n)$ are real *positive* constants.

6. The value of $f(z)$.

1° When z belongs to neither $\mathfrak{A}$ nor $\mathfrak{A}'$, it has been seen that $f(z)$ is continuous at this point, and

$$f(z_0) = \lim_{z=z_0} f(z)$$

is finite and determinate.

2° When z_0 belongs to $\mathfrak{A}'$ but not to $\mathfrak{A}$, the real part $\Re f(z_0)$ becomes either $-\infty$ or finite and determinate. For, describing a circle C about z_0 with radius 1, consider

$$\sum_{n=1}^{\infty} c_n \log\left(1 - \frac{z_0}{a_n}\right) = \Sigma' + \Sigma''$$

(thought it might not be permissible at z_0 which is a point in the ultimate boundary of S), where Σ' concerns those a_n which fall in the circle C and Σ'' concerns all the remaining. All the summands of Σ' are negative, while those of Σ'' are positive. Σ'' must be finite and determinate by 1° and really $\geqq 0$, while Σ' becomes either finite and determinate or $-\infty$. If it is convergent and hence absolutely covergent, the above mode of summation is permissible by the well known theorem on the absolutely convergent series.

Hence we have

$$\Re f(z_0) = \Sigma' + \Sigma''$$

which is finite and determinate. On the other hand if Σ' becomes $-\infty$, $\Re f(z_0)$ or Σ becomes $-\infty$, because, it can be easily shown by means of the partial sums as usual, though this is not given explicitly in the form of a theorem. Thus $\Re f(z_0)$ becomes either finite and determinate or $-\infty$.

3° When z_0 is a point of $\mathfrak{A}$, a_p say, evidently $\Re f(z)$ becomes $-\infty$. For,

$$\Sigma = c_p \log\left|1 - \frac{z}{a_p}\right| + \Sigma'$$

and Σ' becomes $-\infty$ or finite and determinate by 2° or 1°; thus the real part should be $-\infty$. As to the imaginary part, thouge it is not defined in $z_0 = a_p$ at all, it is continuous up to z_0 in S (§ 2); and our main purpose being to seek the limiting value, we may define $\Im f(a_p)$ as $\lim_{z=a_p} \Im f(z)$ which is determinate in S.

7. Determination of the alternative. The alternative made about Σ in § 6, 2°, which is the same as that about Σ', depends partly upon the mode of condensation of a_n about z_0 and partly on the depression of the corresponding c_n. To determine it, we must know a_n's and c_n's in some more explicit forms and thus it is nessesary to proceed by examples. Here only some special categories will be treated: Let $z_0 = 1$. Otherwise, if $z_0 = e^{i\theta}$, it can be made so by a trivial transformation $z \,||\, ze^{-i\theta}$. Assume that $\mathfrak{A}$ (or its sub-aggregate which falls inside the circle C_0 about z_0 with a small radius ϵ) has only one regressive (or progressive) limiting point $z_0 = 1$, which is assumed not to belong to $\mathfrak{A}$. Let the arguments of the given points in C_0 be

$$(\epsilon >)\, a_1^{(0)} > a_2^{(0)} > \ldots\ldots\ldots (>0) \text{ with } \lim_{n=\infty} a_n^{(0)} = 0.$$

To decide the alternative we examine, first of all, whether

$$\lim_{n=\infty} c_n \log | a_n - 1 | = 0 \quad \text{or not};$$

(for the sake of brevity, (0) of $c_n^{(0)}$ and $a_n^{(0)}$ have been dropped). If this limit does not become zero, evidently the divergent case occurs. This condition may be put in other forms:

$$\lim_{n=\infty} | a_n - 1 |^{c_n} = 1, \quad \text{i. e. } \lim_{n=\infty} \left(2 \sin \frac{a_n}{2} \right)^{c_n} = 1.$$

Or more briefly $\lim_{n=\infty} a_n^{c_n} = 1$,

since $$\lim_{n=\infty} \left(\frac{\sin \frac{a_n}{2}}{\frac{a_n}{2}} \right)^{c_n} = 1$$

in virtue of $a_n \to 0$ and $c_n \to 0$.

But the above is only necessary for the convergency. Therefore it being satisfied, some further discussion is necessary as in the ordinary tests for the convergency of series.

Taking Cauchy's test, we know the convergency or divergency according as

$$\overline{\lim_{n=\infty}} \left| c_n \log 2 \sin \frac{a_n}{2} \right|^{\frac{1}{n}} \lesseqgtr 1.$$

But Σc_n being convergent, let

$$\overline{\lim_{n=\infty}} c_n^{\frac{1}{n}} = c = e^{-\lambda}, \qquad \text{where} \quad \lambda \geqq 0;$$

and since

$$\overline{\lim_{n=\infty}} \left| \log 2 \sin \frac{a_n}{2} \right|^{\frac{1}{n}} = \overline{\lim_{n=\infty}} \left| \log a_n \right|^{\frac{1}{n}},$$

we have the above alternative according as

$$\overline{\lim_{n=\infty}} \left| \log a_n \right|^{\frac{1}{n}} \lesseqgtr \frac{1}{c} = e^{\lambda};$$

i. e., assuming that $\lim c_n^{\frac{1}{n}}$, $\lim | \log a_n |^{\frac{1}{n}}$ are both determinate, we have

$$\left|\log a_n\right| \leqslant c_n^{-n}.$$

If they become equal, we must proceed further; e. g. using Cauchy's condesation-test[1]

$$\lim_{n=\infty} \frac{\log\left\{n \log n \log^2 n \ldots\ldots \log^{r-1} n \left| c_n \log 2 \sin \frac{a_n}{2} \right|\right\}}{\log^r n} \leqslant 0.$$

If we use the ratio-test, the convergency or divergency of Σ is determined according as

$$\lim_{n=\infty} \frac{c_n \log |a_n - 1|}{c_{n+1} \log |a_{n+1} - 1|} \gtrless 1,$$

which after reduction becomes

$$\lim_{n=\infty} \frac{a_n^{c_n}}{a_{n+1}^{c_{n+1}}} \leqslant 1;$$

i. e. ultimately $a_n^{c_n} \leqslant a_{n+1}^{c_{n+1}}$, and either one < 1 always.

Combining all these, we see that (i) if $a_n^{c_n}$ decreases, it can not reach 1 at all and, necessarily the divergent case occurs; (ii) even when it increases, if it does not go up to 1, it is still divergent; and (iii) when it increases up to 1 and further

$$\lim_{n=\infty} \frac{a_n^{c_n}}{a_{n+1}^{c_{n+1}}} = r_1 < 1, \text{ then the convergent case occurs;}$$

(iv) but if $r_1 = 1$, still the alternative remains undecided.

In the last case, the convergency or divergency is determined according as

$$\lim_{n=\infty} n \left[\frac{\log a_n^{c_n}}{\log a_{n+1}^{c_{n+1}}} - 1 \right] \gtrless 1,$$

or ultimately

$$n \log \left(\frac{a_n^{c_n}}{a_{n+1}^{c_{n+1}}} \right) \leqslant \log a_{n+1}^{c_{n+1}}$$

1. E. g. Crystal, Algebra, Part II (second edition), p. 126.

i. e. $$a_n^{nc_n} \leqq a_{n+1}^{(n+1)c_{n+1}}.$$

Turning to the comparison-test, e. g. taking Σn^{-s} as the series of comparison, we can determine the convergency or divergency according as ultimately

$$a_n^{c_n} e^{n^{-(1+\delta)}} \geqq 1 \quad \text{or} \quad a_n^{c_n} e^{n^{-1}} \leqq 1$$

where $\delta > 0$, however small, but necessarily finite; in case e. g. $\log a_n^{-c_n} = n^{-\left(1+\frac{1}{n}\right)}$, it becomes divergent.

We have assumed in the above that $\mathfrak{A}$ has only one regressive limiting point $z_0 = 1$, and no other in the vicinity of it. If the limiting point be $z_0 = e^{i\theta}$, we have only to replace a_n by $(a_n - \theta)$.

It is much more difficult in the case of non-isolated a_n's.

8. $\lim_{z=z_0} f(z)$. When $z_0 = e^{i\theta}$ is a regular point or an isolated prescribed point, it has been considered in § 6. Now let us examine the case where z_0 belongs to $\mathfrak{A}'$ but not to $\mathfrak{A}$. It may occur that $e^{i\theta}$ is an end point of $\mathfrak{A}'$. Otherwise, divide $\mathfrak{A}$ into two parts: one ($\mathfrak{A}_1$) lying on the arc $(\theta^{\ast}, \theta + \pi)$ and the other ($\mathfrak{A}_2$) on $(\theta + \pi^{\ast}, \theta + 2\pi^{\ast})$. Thus we may consider

$$f(z) = \Sigma = \Sigma' + \Sigma'',$$

where the summands of Σ' are those corresponding to $\mathfrak{A}_1$, while those of Σ'' correspond to $\mathfrak{A}_2$. Then $z_0 = e^{i\theta}$ becomes the end point of both $\mathfrak{A}_1'$, $\mathfrak{A}_2'$. Discussions of Σ' and Σ'' give that of Σ. Hence we assume the case where z_0 is an end point of $\mathfrak{A}'$. Also, for the sake of simplicity, we consider only the case $z_0 = 1$, since, by the transformation $z' = ze^{-i\theta}$, we have

$$\Sigma c_n \log\left(1 - \frac{z}{e^{i\alpha_n}}\right) = \Sigma c_n \log\left(1 - \frac{z'}{e^{i(\alpha-\theta)}_n}\right)$$

$$= \Sigma c_n \log\left(1 - \frac{z'}{a'_n}\right)$$

and the generality is by no means lost.

Let $a_1, a_2, \ldots\ldots$ be distributed only on the semi-circumference $\overset{\frown}{AB}$ $(0^{\ast}, \pi)$; the case $(0^{\ast}, -\pi)$ can be treated just similarly. Their arguments (reduced to $(0, \pi)$): $a_1, a_2, \ldots\ldots$ are not necessarily of descending magnitudes; but all a_n's lie between $(0^{\ast}, \pi)$ at any rate, with

$$\lim_{n=\infty} a_n = 0.$$

Divide the semi-circumference $\widehat{AB}$ into sub-arcs: $\widehat{BC^{\infty}}$, $\widehat{CC_1^{\infty}}$ $\widehat{C_1C_2^{\infty}}$,..... The argument of the first dividing point $C(=C_0)$ is $\frac{\pi}{3}$, and the subsequent dividing points are arbitrarily taken in order of descending arguments and indefinitely approach $A(\theta=o)$. Denote the summation of those

$$c_n \log\left(1-\frac{z}{a_n}\right),$$

of which a_n lies on the sub-arc $C_{s-1}C_s^{\infty}$ by Σ_s. In the inside of the unit circle, the order of summation being indifferent, we put

$$\Sigma = \Sigma_0 + \Sigma_1 + \Sigma_2 + \ldots\ldots + \Sigma_s + \ldots\ldots = \sum_B^A$$

Then, as has been seen in § 6, 2°,

$$\Re\left[\sum_B^A\right]_{z=1}$$

is either $-\infty$ or finite and determinate.

Fig. 2.

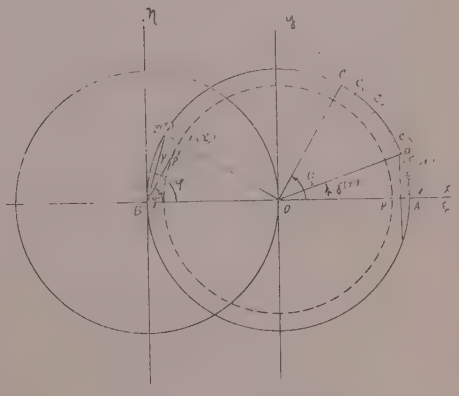

I say the same holds for its limiting value when $z\to 1$. This may be looked on as a corollary to Abel-Stolz's continuity-theorem[1]. But that theorem being only related to the case of power series, so far as I know we show now independently it is the case for our series.

Evidently Σ_0 being continuous at $z=1$ by theorem 1, we have only to consider

$$\Sigma_1 + \Sigma_2 + \ldots\ldots = \sum_C^A, \quad \text{(cf. Fig. 2).}$$

Let $$\zeta_n = 1 - \frac{1}{a_n} = 1 + e^{(\pi-\alpha_n)i} = \rho_n e^{i\varphi_n}$$

where $$\rho_n = 2\sin\frac{\alpha_n}{2}, \quad \varphi_n = \frac{\pi-\alpha_n}{2},$$ (α_n being reduced to the interval (o, π));

1. E.g. Nielsen, Functionentheorie, S. 287.

and $$\zeta'_n = 1 - \frac{\gamma}{a_n} = 1 + re^{(\pi-\alpha_n)i} = \rho'_n e^{i\varphi'_n}$$

where $$\rho_n = \sqrt{1-2r\cos a_n + r^2}, \quad \rho_n \cos\varphi'_n = 1 - r\cos a_n,$$
$$\rho_n \sin\varphi'_n = r\sin a_n.$$

Now $$\left(\frac{\rho'_n}{\rho_n}\right)^2 = \frac{(1-r)^2 + 4r\sin^2\frac{a_n}{2}}{4\sin^2\frac{a_n}{2}} \gtrless 1$$

according as $1 - r \gtrless 2\sin\frac{a_n}{2}$.

Let $\gamma(r) = 2\sin^{-1}\frac{1}{2}\sqrt{1-r}$; then for all $0 < a_n < \gamma(r)$, $1 > \rho'_n > \rho_n$; and for all $\gamma(r) < a_n < \frac{\pi}{3}$, $\rho'_n < \rho_n < 1$; when $a_n = \gamma(r)$ (if any), $\rho'_n = \rho_n = \sqrt{1-r}$. If the point $D\ (=e^{\tau i})$ lie on a sub-arc $\overset{\frown}{C_s C^{*}_{s+1}}$ we have for all a_n on $\overset{\frown}{CC^{*}_s}$ $\log\rho'_n < \log\rho_n < 0$, while $0 > \log\rho'_n > \log\rho_n$ for all a_n on $\overset{\frown}{C_{s+1}A^{*}}$. when $1-r$ converges to zero, $\gamma(r)$ tending to become null; thus if $P\,(z=r)$ approaches to $A\,(z=1)$, the sub-arc $\overset{\frown}{C_s C^{*}_{s+1}}$, together with the point of separation D, approaches to A.

Now consider the divergent case;

$$\sum_{C}^{A} c_n \log|a_n - 1| = -\infty.$$

Then we can find the dividing point C_s so that

$$\sum_{C}^{C_s} c_n \log|a_n - 1| < -\Omega$$

however great a positive number Ω may be. But if the point of separation $D(\equiv e^{\tau i})$ lies on $\overset{\frown}{C_s C^{*}_{s+1}}$

$$\sum_{C}^{A} c_n \log|a_n - r| < \sum_{C}^{C_s} c_n \log|a_n - r| < \sum_{C}^{C_s} c_n \log|a_n - 1| < -\Omega.$$

These inequalities hold for all $0 < 1 - r \leqq \delta$, since, when $r < r' < 1$, the corresponding D' lies nearer to A than D, and correspondingly $s' \geqq s$.

$$\therefore \quad \lim_{r=1-0} \sum_{C}^{A} c_n \log|a_n - r| = -\infty.$$

And Σ_0 being continuous at A, we have

$$\lim_{r=1-0} \Re\,(\Sigma_0 + \Sigma_1 + \ldots\ldots) = -\infty.$$

But inside the unit circle, however small $1-r=\delta$ may be, we have

$$\Re f(r) \equiv \sum_{n=1}^{\infty} c_n \log|a_n - r| = \Re(\Sigma_0 + \Sigma_1 + \Sigma_2 + \ldots\ldots)$$

Hence $\lim_{r=1-0} \Re f(r) = -\infty.$ Q. E. D.

9. Continued. Next we consider the convergent case. Let the point of separation D fall on $\overset{\frown}{C_s C_{s+1}^{\divideontimes}}$ as before. Now

$$\log\left|a_n - r\right| \lesseqgtr \log\left|a_n - 1\right|$$

according as the point a_n lies on the arc $\overset{\frown}{CD^{\divideontimes}}$ or $\overset{\frown}{DA^{\divideontimes}}$ or at D. Hence

$$0 > \sum_{D}^{A} c_n \log|a_n - r| > \sum_{D}^{A} c_n \log|a_n - 1|.^1$$

But $\sum_{C}^{A} c_n \log|a_n - 1|$ being convergent, $\sum_{C_s}^{A}$ and *a fortiori* $\sum_{D}^{A}$, can be made in absolute value as small as we please, by making C_s sufficiently near to A, i. e. by taking $1-r$ sufficiently small. In other words, if

$$\sum_{D}^{A} c_n \log|a_n - 1| = -\epsilon_1(r),$$

$\epsilon_1(r)$ represents a positive decreasing function with $\lim_{r=1-0} \epsilon_1(r) = 0$. Consequently

$$\epsilon_1(r) > \sum_{D}^{A} c_n \log|a_n - r| - \sum_{D}^{A} c_n \log|a_n - 1| > 0.$$

Also $$0 > \sum_{C}^{D} c_n \log\left|a_n - r\right| - \sum_{C}^{D} c_n \log\left|a_n - 1\right| = \sum_{C}^{D} c_n \log\left|\frac{a_n - r}{a_n - 1}\right|,$$

since the two series are absolutely convergent. Now if $|a_n - 1| = BZ$ and $|a_n - r| = BZ'$ (Fig. 2), we have

---

1. We have used the point of separation D for the sake of simplicity. To put it more exactly, making sub-summations as

$$\sum_{C_s}^{C_{s+1}^{\divideontimes}} = \sum_{C_s}^{D^{\divideontimes}} + \sum_{D}^{C_s^{\divideontimes}} = \Sigma' + \Sigma'',$$

we must write e. g. $\sum_{C_{s+1}}^{A} + \Sigma''$ instead of $\sum_{D}^{A}$.

$$1 > \frac{BZ'}{BZ} > \frac{BZ-ZZ'}{BZ} = 1 - \frac{ZZ'}{BZ} > 1 - \frac{1-r}{\sqrt{1-r}}$$
$$= 1 - \sqrt{1-r}.$$

Consequently $$0 > \sum_C^D c_n \log|a_n - r| - \sum_C^D c_n \log|a_n - 1| >$$
$$\sum_C^D c_n \log(1-\sqrt{1-r}) > \log(1-\sqrt{1-r}) \sum_{n=1}^{\infty} c_n = -\epsilon_2(\gamma),$$

where $\epsilon_2(r)$ is a positive decreasing function with $\lim_{r=1-0} \epsilon_2(r) = 0$.

Combining the two inequalities obtained above,

$$\epsilon_1(r) > \sum_C^A c_n \log|a_n - r| - \sum_C^A c_n \log|a_n - 1| > -\epsilon_2(r).$$

Hence $$\lim_{r=1-0} \sum_C^A c_n \log|a_n - r| = \sum_C^A c_n \log|a_n - 1|.$$

Thus

$$\lim_{r=1-0} \Re(\Sigma_0 + \Sigma_1 + \cdots\cdots) \text{ exists,}$$

and so $$\lim_{r=1-0} \Re f(r) \text{ exists.} \qquad \text{Q. E. D.}$$

Most probably all the above may be extended to the case of other modes of approaching as in Stolz's generalization of Abel's theorem. Further, in our case even the outward approaching may be considered. Here I will present one: Let $OQ = r' > 1$, and find the fourth harmonic point P of $A, Q, B,$:

$$\frac{AP}{AQ} = \frac{BP}{BQ} = \frac{1+r}{1+r'} = \lambda \text{ say,}$$

where $r = OP$. Then, for any point E on the unit circle, we have

$$PE : QE = \lambda \quad \text{and} \quad \log PE = \log QE + \log \lambda,$$

so that $$\Sigma c_n \log PE = \Sigma c_n \log QE + \Sigma c_n \log \lambda,$$

that is $$\Re f(r) = \Re f(r) + \log \lambda \, \Sigma c_n.$$

Let $r' \to 1$, then $r \to 1$, and $\lambda \to 1$.

Hence $$\lim_{r=1-0} \Re f(r) = \lim_{r=1+0} \Re f(r). \qquad \text{Q. E. D.}$$

We have investigated the case of $z \to 1$. In general, when $z \to e^{i\theta}$, as noted before, putting $\Sigma = \Sigma' + \Sigma''$, we have

$$\lim_{r=1} \Re \Sigma' = -\infty \text{ or finite determinate,}$$

and $\lim_{r=1} \Re \Sigma'' = -\infty$ or finite determinate.

Hence if one or both become $-\infty$,

$$\lim_{r=1} \Re \Sigma = -\infty ;$$

and if both be convergent, $\lim_{r=1} \Re \Sigma =$ finite determinate $= \Phi(\theta)$, say.

As to imaginary part of $f(z)$, we have

$$\lim_{r=1-0} \Im \sum_{n=1}^{\infty} c_n \log\left(1 - \frac{re^{i\theta}}{a_n}\right) = \text{finite determinate.}$$

For, when $\theta \neq \arg a_n$, every summand in the above is continuous in $r(0, 1)$ and

$$\left| \Im \sum_{n=n_0}^{\infty} c_n \log\left(1 - \frac{re^{i\theta}}{a_n}\right) \right| < \pi \sum_{n=n_0}^{\infty} c_n < \delta \quad \text{for all} \quad n_0 \geqq N.$$

Hence $\Im f(re^{i\theta})$ is uniformly continuous in $r(0, 1)$; and therefore we have

$$\lim_{r=1-0} \Im \sum_{n=1}^{\infty} c_n \log\left(1 - \frac{re^{i\theta}}{a_n}\right) = \Im \sum_{n=1}^{\infty} c_n \log\left(1 - \frac{e^{i\theta}}{a_n}\right)$$
$$= \Psi(\theta), \text{ say.}$$

Thus, in case of convergence, we have[1]

$$\lim_{r=1-0} f(re^{i\theta}) = \Phi(\theta) + i\Psi(\theta)$$

and $$\lim_{r=1-0} F(re^{i\theta}) = e^{\Phi(\theta)}(\cos \Psi(\theta) + i \sin \Psi(\theta)).$$

10. Main theorems. Summing up all the above we get

Theorem 4. *Given an enumerablly infinite number of points on the unit circle: $a_n = e^{i\alpha_n} (\mathfrak{A})$, taking an arbitrary positive convergent series Σc_n, we construct*

$$f(z) = \sum_{n=1}^{\infty} c_n \log\left(1 - \frac{z}{a_n}\right) = -\sum_{n=1}^{\infty} \frac{z^n}{n} \sum_{m=1}^{\infty} c_m a_m^{-n},$$

which is holomophic inside the unit circle. When z tends to a point z_0 on the unit circle radially, $f(z)$ tends to a determinate (finite or infinite) value. In detail:

i) *When z_0 belongs to $\mathfrak{A}$, $\Re f(z) = -\infty$;*

ii) *When z_0 does not belong to $\mathfrak{A}$ but belongs to $\mathfrak{A}'$, $\Re f(z)$ is $-\infty$ or finite and determinate;*

1. In this case $f(e^{i\theta})$ really exists by Littlewood's converse theorem, loc. cit. 8.

iii) *When z_0 belongs to neither $\mathfrak{A}$ nor $\mathfrak{A}'$, $f(z)=f(z_0)$, finite and determinate.*

Our choice of Σc_n being arbitrary (e. g. as $\Sigma \frac{1}{n^\sigma}$, σ any real number $>1+\delta$) there is a non-enumerably infinite number of the said functions. Moreover if $g(z)$ be any arbitrary power series whose radius of convergence >1, $\{f(z)+g(z)\}$ will have still the same character as $f(z)$.

Taking $F(z)=\exp f(z)$, it is still holomorphic inside the unit circle and can be represented by a power series of z. This power series tends to become zero when z tends to $a_n (n=1, 2, \ldots\ldots)$; so that the radius of convergence must be equal to 1. Thus we have

Theorem 5. *It is possible to construct power series which do not vanish inside the circle of convergence, but which tends to vanish at prescribed enumerably infinite points on the circle, and elsewhere on the circle, becomes still determinately zero or finite.*

There is a non-enumerably infinite number of such power series.

Though it is somewhat remarkable that our infinite product

$$F(z)=e^{g(z)}\prod_{n=1}^{\infty}\left(1-\frac{z}{a_n}\right)^{c_n}$$

may become zero even when $z\neq a_n$ (and really becomes e. g. if $(\arg a_n)c_n \neq 1$, § 7), which is contrary to the known theorem that an absolutely convergent infinite product vanishes when and only when some of the factors vanish i. e. $z=a_n$, and though this seems to offer an answer to the question proposed at the beginning of the introduction, yet this phenomenon seems rather inconvenient for application to other purposes. I shall therefore reform our infinite product so as to have the same property as the above theorem, by some change of c_n but keeping a_n as it stands.

All the above in this section relates to cases of positive index-series. It can be, however, quite similarly treated when all c_n are negative throughout. The only difference is that $\Re f(z)$ tends to $+\infty$ instead of $-\infty$, and $F(z)$ tends to $+\infty$ or $-\infty$ determinately instead of 0. $F(z)$ can not vanish at all.

Also the case where all c_n's are complex but with the real parts of same sign, may be considered similarly. Let $c_n=u_n+iv_n$, where both Σu_n, Σv_n should be absolutely convergent. Then

$$f(z)=\sum_{n=1}^{\infty}c_n(\log\rho_n+i\varphi_n) \qquad (-\pi<\varphi_n\leqq\pi)$$

$$=\sum_{n=1}^{\infty}(u_n\log\rho_n-v_n\varphi_n)+i\sum_{n=1}^{\infty}(v_n\log\rho_n+u_n\varphi_n).$$

Thus if all $u_n > 0$, the enunciation under theorem 4 still holds, because the contribution of $\Sigma v_n \varphi_n$ remains finite and determinate. $F(ra_p)$ tends to zero determinately, though oscillatory. If all $u_n < 0$, it is still similar in the convergent case. But in the divergent case $F(ra_p)$ may oscillate indefinitely by radial approaching, the amplitude increasing steadily and thus it becomes quite indeterminate.

III. Continued (Case of indices with altering signs).

11. Indices with different signs. In the case that c_n's are real constants but of different signs and that $\Sigma |c_n|$ is convergent, some similar assertion is possible if the point of approach z_0 is an isolated point of $\mathfrak{A}$. But when z_0 belongs to $\mathfrak{A}'$, it becomes quite difficult, owing to the variable contributions of factors.

Let

$$\sum_{n=1}^{\infty} c_n = \sum_{p=1}^{\infty} c'_p - \sum_{q=1}^{\infty} c''_q$$

where both of the summations on the right-hand side are positive convergent series since the left-hand side summation is absolutely convergent by hypothesis. Consider

$$f_1(z) = \sum_{p=1}^{\infty} c'_p \log\left(1 - \frac{z}{a_p}\right), \quad f_2(z) = \sum_{q=1}^{\infty} c''_q \log\left(1 - \frac{z}{a_q}\right).$$

They exist in the domain S' and S'' respectively (§§ 2–3). In the common domain S, we have

$$f(z) = f_1(z) - f_2(z),$$

in virtue of their absolute convergency in S.

When $z = re^{i\theta}$ tends to the boundary point $z_0 = e^{i\theta}$ which belongs to $\mathfrak{A}'$ but not to $\mathfrak{A}$,

$$\lim_{r=1-0} \Re f_1(re^{i\theta}) = -\infty \text{ or finite determinate,}$$

$$\lim_{r=1-0} \Re f_2(re^{i\theta}) = -\infty \text{ or finite determinate.}$$

Hence there are four possible cases:

(i) if both of them are finite, $\lim_{r=1-0} \Re f(re^{i\theta})$, finite determinate $= \Re f(re^{i\theta})$;

(ii) if only the first tends to $-\infty$, $\lim_{r=1-0} \Re f(re^{i\theta}) = -\infty$;

(iii) if only the second tends to $-\infty$, $\lim_{r=1-0} \Re f(re^{i\theta}) = +\infty$;

(iv) if both of them tend to $-\infty$, $\lim_{r=1-0} \Re f(re^{i\theta})$ has an apparently indeterminate form $\infty - \infty$, which needs further investigation.

It is to be noted that the simple convergency of $\Re f(e^{i\theta})$ does not mean the case (i), unless it is absolutely convergent. Further (iv) there occur, four cases:

(iv)$_1$ $\lim_{r=1-0} \Re f(re^{i\theta})$, finite determinate,

(iv)$_2$ $\lim_{r=1-0} \Re f(re^{i\theta}) = -\infty$,

(iv)$_3$ $\lim_{r=1-0} \Re f(re^{i\theta}) = +\infty$,

(iv)$_4$ $\lim_{r=1-0} \Re f(re^{i\theta})$ does not exist at all.

In every case, when the limit is determinate, still there occur two cases:

1 it coincides with $f(e^{i\theta})$ (for the meaning of this, cf. § 6),

2 it is different from $f(e^{i\theta})$.

I shall devote just a little space to some of these cases.

12. A convergent case. As a special case met with (iv), suppose $\mathfrak{A}(a_n)$ has a regressive (or progressive) limiting point $z_0 = e^{i\theta} \neq a_n$. It may have many limiting points or even become dense elsewhere, but all in finite distances from z_0. Also, assume $\theta = 0$, as can be done by a trivial transformation: $z \,||\, ze^{-i\theta}$. Thus we can divide $\mathfrak{A}$ into two subaggregates $\mathfrak{A}_0$ and $\mathfrak{A}_1$. The points of $\mathfrak{A}_0$ have arguments as follows:

$$(\delta \leqq) a_1^{(0)} > a_2^{(0)} > \cdots\cdots (> 0), \qquad \lim_{m=\infty} a_m^{(0)} = 0.$$

It is possible to arrange them thus in order of descending arguments since there is only an enumerably infinite number of isolated points; but now the old suffixes of given a_n's become confused, while the points of $\mathfrak{A}_1$ have arguments in $(\delta, 2\pi)$. Then inside the circle

$$(z) = \Sigma_0 + \Sigma_1 = g_0(z) + g_1(z)$$

where Σ_0 and Σ_1 relate to $\mathfrak{A}_0$ and $\mathfrak{A}_1$ respectively; and $g_1(z)$ being holomorphic in the vicinity of $z = 1$, we have only to consider $g_0(z)$. Let it be

$$\Re g_0(1) = \sum_{m=1}^{\infty} c_m^{(0)} \log |a_m^{(0)} - 1| = l, \text{ finite and determinate.}$$

Assume for the moment that

$$\lim_{r=1-0} \Re g_0(r) = \Re g_0(1).$$

Then $$\lim_{r=1-0} \Re f(r) = \lim_{r=1-0} [g_0(r) + g_1(r)] = l + g_1(1).$$

It should be noticed that $g_0(1)$ is only conditionally convergent. For

otherwise $g_1(1)$ being absolutely convergent, $g_0(1) + g_1(1)$ should be absolutely convergent, which contradicts the assumption that $f_1(1)$ and $f_2(1)$ both become $-\infty$.

Now to show that

$$\lim_{r=1-0} \Re\, g(r) = \Re\, g(1)$$

(dropping the suffix o for the sake of brevity), when the latter exists, we discuss as in § 9, but with some necessary modification. The relations

$$\left| \sum_C^D c_n \log|a_n - r| - \sum_C^D c_n \log|a_n - 1| \right|$$

$$< \left| \log(1 - \sqrt{1-r}) \right| \Sigma |c_n| = \epsilon_2(r)$$

and

$$\sum_C^A c_n \log|a_n - 1| = \epsilon_1(r)$$

still hold here. But in consequence of the different signs, the inequality

$$\sum_D^A c_n \log|a_n - r| < \left| \sum_D^A c_n \log|a_n - 1| \right|$$

is not evident, though for each term in this interval, we have

$$\left| \log|a_n - r| \right| < \left| \log|a_n - 1| \right|.$$

I make an additional assumption (without it, some ingeneous proof should be devised): Observing the convergency of

$$\Re\, g(1) = \sum_{n=1}^{\infty} c_n \log|a_n - 1|,$$

we have

$$\lim_{n=\infty} c_n \log|a_n - 1| = 0;$$

but it can tend to o after an infinite number of oscillations in signs and magnitude. To make the variation of signs determinative, assume that Σc_n is ultimately alternate as $c_n = (-1)^n b_n$ where $b_n < 0$; and thus

$$\lim_{n=\infty} b_n \log|a_n - 1| \equiv \lim_{n=\infty} \beta_n = +0$$

Yet β_n may tend to o after an infinite number of oscillations in magnitude. Hence we assume secondly that β_n becomes ultimately steadily decreasing after $n = n_0$, say. With these assumptions we are able to complete the above proof. For, making r sufficiently near to 1, the point D goes

sufficiently near to A, and thus beyond a_{n_0}. Then

$$\sum_{D}^{A}(-1)^n b_n \log|a_n - r| = \sum_{D}^{A}(-1)^n \beta_n \frac{\log|a_n - r|}{\log|a_n - 1|}.$$

Here the numerical coefficient of β_n being a proper fraction in $\widehat{DA}$, the above summand is certainly[1] steadily decreasing in magnitude. Hence

$$\left|\sum_{D}^{A} c_n \log|a_n - r|\right| < \beta_m \frac{\log|a_m - r|}{\log|a_m - 1|} < \beta_m,$$

where m denotes the index of the point a_n that lies on $\widehat{DA}$ and nearest to D (or it may coincide with D. Thus when r approaches to 1, i. e. $D(r)$ approaches to A, m tends to ∞, and β_m is a not increasing function of r with $\lim_{r=1} \beta_m = 0$. Combining all the above

$$\left|\sum_{C}^{A} c_n \log|a_n - r| - \sum_{C}^{A} c_n \log|a_n - 1|\right| < \epsilon_1(r) + \epsilon_2(r) + \beta_m(r).$$

Hence $$\lim_{r=1-0} \sum_{C}^{A} c_n \log|a_n - r| = \sum_{C}^{A} c_n \log|a_n - 1|. \qquad \text{Q. E. D.}$$

It is evident under our assumptions that $g_0(1)$ really exists, since it becomes ultimately $\Sigma(-1)^n \beta_n$, and β_n is a steadily decreasing positive function of n, with $\lim_{n=\infty} \beta_n = 0$. Thus it has been completely proved that there exists, under our assumptions,

$$\lim_{r=1-0} \Re f(r), \text{ finite and determinate.}$$

But it should be noted that this does not mean at all that

$$\lim_{r=1-0} \Re f(r) = \Re f(1)^2$$

---

1 It can be shown by a little calculation that, when $1 > r > 1 - e^{-1} = 0.63\ldots\ldots$,

$$\frac{\log|a-r|}{\log|a-1|} = \frac{\frac{1}{2}\log(1 + r^2 - 2r\cos\alpha)}{\log 2\sin\frac{\alpha}{2}}$$

decreases steadily with α, considering the logarithmic derivative with respect to α.

2 If our $f(z)$ be represented by a power series of z (§ 4), say $\mathfrak{p}(z)$, then

$$\lim_{r=1-0} \Re f(r) = \lim_{r=1-0} \Re \mathfrak{p}(r);$$

and by Littlewood's converse theorem on power series (§ 4), we have

$$\lim_{r=1-0} \Re \mathfrak{p}(r) = \Re \mathfrak{p}(1).$$

But this does not necessitate the existence of $\Re f(1)$ at all.

Really we have selected $\mathfrak{A}_0$ from $\mathfrak{A}$ and even changed the order of summands. Let

$$f(z) = f_0(z) + g_1(z)$$

where f_0 means the summation taken for the points of $\mathfrak{A}_0$ but in the ascending order of the original suffix n, while our $g_0(z)$ has been taken in the descending order of the argument of a_n. Thus though it is true in S that

$$f_0(z) = g_0(z) \quad \text{and} \quad \lim_{r=1-0} \Re f_0(r) = \lim_{r=1-0} \Re g_0(r),$$

yet it cannot be said that

$$f_0(1) = g_0(1)$$

even when the latter exists; because $g_0(1)$ being only conditionally convergent, it may possibly differ from $f_0(1)$. $f_0(1)$ itself may not exist and oscillates infinitely with n; e. g.
$g_0(1) = 1 - \frac{1}{2} + \frac{1}{3} - \ldots\ldots = \log 2$, while $f_0(1)$ may have a form such as $1 - \left(\frac{1}{2} + \frac{1}{4} + \frac{1}{6} + \ldots\ldots\right) + \left(\frac{1}{3} + \frac{1}{5} + \ldots\ldots\right) - \ldots\ldots$ and its partial sums may become nearly $1, -2, 3, -4, \ldots\ldots$ In this respect the above result resembles to the behaviour of the power series

$$\sum_{n=2}^{\infty} \frac{(\log n)^{\alpha}}{n} x^n, \quad (\alpha > 0)$$

which J.E. Littlewood[1] presented and after him A.E. Ingham generalized it.[2]

Particularly if $g_0(z) \equiv f(z)$,
i. e. if $\mathfrak{A}$ coincides with $\mathfrak{A}_0$, and the arguments of the old a_n are already ordered in descending magnitudes, then as a matter of course we have

$$\lim_{r=1-0} f(r) = f(1).$$

13. A divergent case. To treat a special one of the divergent cases, let us construct $g_0(z)$ as before. Assume

$$c_n = (-1)^n b_n \qquad (\text{now } b_n > 0)$$

and $$b_{n+2} = O(b_n), \qquad b_{2p+1} = o(b_{2p})$$

also $$\left|\log|a_n - 1|\right| = O\left(\left|\log|a_{n+1} - 1|\right|\right).$$

1. Loc. cit., 8.
2. Proc. London Math. Soc. Ser. 2, Vol. 23 (1924), p. 326.

Under these assumptions it is easy to prove that $g_0(1)=-\infty$. We shall prove that

$$\lim_{r=1-0} g_0(r) = -\infty.$$

Since $g_0(1)$ becomes $-\infty$ determinately, if we put (cf. Fig. 2)

$$-\sum_{C}^{D} c_n \log|a_n - 1| = \Omega(r),$$

$\Omega(r)$ becomes greater and greater with $\lim_{r=1-0} \Omega(r) = +\infty$.

But
$$\left|\sum_{C}^{D} c_n \log|a_n - r| - \sum_{C}^{D} c_n \log|a_n - 1|\right| = \left|\sum_{C}^{D} c_n \log\left|\frac{a_n - r}{a_n - 1}\right|\right|$$

$$< \sum_{C}^{D} |c_n| \cdot \left|\log(1 - \sqrt{1-r})\right|$$

$$< \left|\log(1-\sqrt{1-r})\right| \sum_{n=1}^{\infty} |c_n|$$

$$= \epsilon(r), \text{ with } \lim_{r=1-0} \epsilon(r) = 0.$$

Therefore $\Omega(r) - \epsilon(r) < -\sum_{C}^{D} c_n \log|a_n - r| < \Omega(r) + \epsilon(r)$. And we have only to show that $-\sum_{D}^{A} c_n \log|a_n - r|$ is bounded lowerly. Put, for the sake of brevity,

$$-b_n \log|a_n - r| = B_n (>0).$$

Then
$$-\sum_{D}^{A} c_n \log|a_n - r| = \sum_{D}^{A} (-1)^n B_n$$

where the summation begins from B_{2p} or else B_{2p-1}; thus we have for partial summations

$$\sum_{n=2p}^{m} = (B_{2p} - B_{2p+1}) + (B_{2p+2} - B_{2p+3}) + \cdots\cdots + B_{2q} \text{ or } +(B_{2q} - B_{2q+1})$$

or else

$$\sum_{n=2p-1}^{m} = \left(\frac{1}{2} B_{2p} - B_{2p-1}\right) + \left(\frac{1}{2} B_{2p} - B_{2p+1}\right) + B_{2q} \text{ or } +(B_{2q} - B_{2q+1}).$$

But these summands become all positive, if we make r sufficiently near to 1, and consequently p sufficiently great, so that we have, for all $p > q$,

$$\frac{B_{2p}}{B_{2p\pm1}} = \frac{b_{2p}\log|a_{2p}-r|}{b_{2p\pm1}\log|a_{2p\pm1}-r|} \asymp \frac{b_{2p}}{b_{2p\pm1}} > 2.$$

Hence $$-\sum_{D}^{A} c_n \log|a_n-r| > 0;$$

therefore $$-g_0(r) \equiv -\sum_{C}^{A} c_n\log|a_n-r| \geqslant \Omega(r),$$

and $$\lim_{r=1-0} g_0(r) = -\infty. \qquad \text{Q. E. D.}$$

Thus we have here again

$$\lim_{r=1-0} \Re f(r) = -\infty.$$

14. An indeterminate case. Allied Function $f(z, x)$.
Now we shall turn to an indeterminate case:

$$\Re g(1) = \sum_{n=1}^{\infty} c_n\log|a_n-1|, \text{ indeterminate.}$$

But it may have some sum, say, in Cesàro-Hölder's sense. Put for brevity

$$c_n\log|a_n-1| = \beta_n.$$

The Cesàro's sum of the k-th order is given by

$$s^{(k)} = \lim_{m=\infty} \frac{1}{A_m^{(k)}} \sum_{n=1}^{m+1} A_{m-n+1}^{(k)} \beta_n,$$

where $A_m^{(k)} = \dfrac{(1+k)(2+k)\ldots(m+k)}{\lfloor m}$, the coefficient of x^m in the expansion of $(1-x)^{-(1+k)}$. In our case $k>0$, for if otherwise, $s^{(0)}=s$ must exist, which contradicts the present hypothesis. Thus

$$s^{(k)} = l, \text{ finite and determinate.}$$

To consider the continuity of $\Re f(r)$, put

$$c_n\log|a_n-r| = \beta_n \frac{\log|a_n-r|}{\log|a_n-1|} = \beta_n\left\{1 + \left(\frac{\log|a_n-r|}{\log|a_n-1|} - 1\right)\right\}$$

$$= \beta_n\left\{1 + \epsilon_n(r)\right\}$$

where $|\epsilon_n(r)|$ ultimately decreases as r tends to 1, and $\lim_{r=1-0} \epsilon_n(r)=0$ for

all values of n. For, if a_n lies in $\widehat{CD}$ (Fig. 2),

$$0 > \log|a_n - r| - \log|a_n - 1| > \log(1 - \sqrt{1-r}),$$

so that $$0 < \epsilon_n(r) < \frac{\log(1-\sqrt{1-r})}{\log|a_n - 1|};$$

and if a_n falls on D, $\epsilon_n(r) = 0$;
and if a_n lies in $\widehat{DA}$, as it is

$$\epsilon_n(r) = \frac{\log|a_n - r|}{\log|a_n - 1|} - 1$$

which is a negative proper fraction but in absolute value steadily decreases as r tends to 1.
Since an ordinary sum (if it exists) gives still the same value as its Cesàro's sum, we have

$$\Re g(r) = \sum_{n=1}^{\infty} c_n \log|a_n - r| = \sum_{n=1}^{\infty} \beta_n \{1 + \epsilon_n(r)\}$$

$$= l + \lim_{m=\infty} \frac{1}{A_m^{(k)}} \sum_{n=1}^{m+1} A_{m-n+1}^{(k)} \beta_n \epsilon_n(r).$$

The last exists certainly because, considering $\beta_n\epsilon_n$ as the difference between $\beta_n(1+\epsilon_n)$, which is nothing but $c_n \log|a_n - r|$ and their sum becomes an ordinary sum, and β_n, the (C, K)-sum of which becomes l by hypothesis, we apply the known theorem[1] that if two series Σu_n, Σv_n are summable (C, K), then the series $\Sigma(u_n \pm v_n)$ shall be summable (C, K), and equal to the sum or difference of the respective Cesàro's sum of the former two.

Hence $$\lim_{r=1-0} \Re g(r) - l = \lim_{r=1-0} \lim_{m=\infty} \frac{1}{A_m^{(k)}} \sum_{n=1}^{m+1} A_{m-n+1}^{(k)} \beta_n \epsilon_n(r)$$

which gives the discrepancy. I endeavoured to find out if it becomes 0, but without success. It seems rather oscillatory in general. If it be so, has it nothing to do with l? To utilize it, let us consider $f(z, x)$ which has been defind in § 1 (rather to denote $g(z, x)$ here):

$$f(z, x) = \sum_{n=1}^{\infty} c_n x^n \log\left(1 - \frac{z}{a_n}\right),$$

1. Ford, Studies on divergent series and summability, p. 87

which exists for all z in S, if $|x| < \frac{1}{c}$, where $c = \overline{\lim_{n=\infty}} \sqrt[n]{|c_n|}$ and since Σc_n is absolutely convergent certainly $c \leqq 1$, and x may be conceived at least in the real interval $(0, 1^{-})$. Also when x goes to 1, since $f(z, 1)$ exists in S,

$$\lim_{x=1-0} f(z, x) = f(z, 1)$$

by Abel's continuity theorem on power series. Thus

$$\lim_{x=1-0} f(r, x) = g(r) = \sum_{n=1}^{\infty} c_n \log\left(1 - \frac{r}{a_n}\right).$$

On the other hand, since $\Re g(1)$ has the Cesàro's sum l, we have by Hölder's theorem[1]

$$\lim_{x=1-0} \Re f(1, x) = l.$$

Thus if we consider the limiting function $f(r, 1-0)$. it coincides with $g(r)$ except $r=1$, at which the former real part certainly exists and $= l$, while the latter's is indeterminate, and during the passage towards $r=1$, they are equal.

Let us try again to find the discrepancy. As usual, consider $l - \Re g(r) = [l - \Re f(1, x)] + [\Re f(1, x) - \Re f(r, x)] + [\Re f(r, x) - \Re g(r)]$. Or, the left-hand side being independant of x, we may consider as $x=r$: $l - \Re g(r) = [l - \Re f(1, r)] + [\Re f(r, r) - \Re g(r)] + [\Re f(1, r) - \Re f(r, r)]$. At first by Hölder's continuity theorem

$$l - \Re f(1, r) = \delta_1(r) \qquad \text{with } \lim_{r=1-0} \delta_1(r) = 0.$$

Secondly,

$$|\Re f(r, r) - \Re g(r)| = \left| \sum_{n=1}^{\infty} c_n (1 - r^n) \log |a_n - r| \right|$$

$$< (1-r) \left| \log (1-r) \right| \sum_{n=1}^{\infty} n |c_n|;$$

hence if we assume the convergency of $\Sigma n |c_n|$, we have

$$\Re [f(r, r) - g(r)] = \delta_2(r) \qquad \text{with } \lim_{r=1} \delta_2(r) = 0.$$

Thirdly divide the summation into two parts (Fig. 2)

$$\Re [f(1, r) - f(r, r)] = \sum_{C}^{D} + \sum_{D}^{A}$$

1. Math. Ann. **20**, S. 535.

where the summand $\equiv c_n r^n \log \frac{|a_n - 1|}{|a_n - r|}$, and in $\widehat{CD}$ its absolute value is less than $c_n \log(1 - \sqrt{1-r})$. Thus

$$\left|\sum_C^D\right| < \sum_C^D \left|c_n r^n\right| \cdot \left|\log(1-\sqrt{1-r})\right| < \left|\log(1-\sqrt{1-r})\right| \sum_{n=1}^{\infty} |c_n|,$$

and therefore

$$\sum_C^D = \delta_3(r) \quad \text{with } \lim_{r=1} \delta_3(r) = 0.$$

Let n_0 be the least suffix of a_n which falls in $\widehat{DA}$. The point D being really defined by r, n_0 is a non-decreasing function of r, with $\lim_{r=1-0} n_0(r) = \infty$. Thus

$$\sum_D^A \equiv \sum_{n=n_0}^{\infty} c_n r^n [\log|a_n - 1| - \log|a_n - r|]$$

$$= -\sum_{n=n_0}^{\infty} \beta_n r^n \epsilon_n(r).$$

Summing up all the above, we have

$$l - \Re\, g(r) = \delta(r) - \sum_{n=n_0}^{\infty} \beta_n r^n \epsilon_n(r)$$

where $\delta(r) = \delta_1(r) + \delta_2(r) + \delta_3(r)$ with $\lim_{r=1-0} \delta(r) = 0$. Hence the discrepancy is given by

$$\Re\, g(r) - l = \sum_{n=n_3(r)}^{\infty} \beta_n r^n \epsilon_n(r) - \delta(r).$$

When r tends to 1, not only $\delta(r)$ and $\epsilon_n(r)$ tend to 0, but also $n_0(r)$ tends to ∞, and indeed the interval $\widehat{DA}$ of the summands to be taken becomes smaller and smaller. Notwithstanding this, is it absurd to say that the discrepancy ultimately becomes zero? To my conjecture it seems true. Really we have assumed in the above that $\Sigma n c_n$ is absolutely convergent, which is more restrictive than before.

In the preceding paragraphs, it has been shown that

$$\lim_{r=1-0} g(r) = g(1)$$

if the latter exists. Thus the extension of the Abel-like theorem for our function was permissible. Now when $g(1)$, indeterminate, possesses some Cesàro-Hölder's sum, it seems probable that there exists some

Hölder-like theorem for our function at least under certain restricted conditions, though not in general. As the above proof is somewhat weak in the concluding point, some more delicate condition may be added if necessary.

If $g_0(1)$ is not summable at all, e. g. as $\Sigma(-n)^n$ or $\Sigma(-1)^n/n$, we have nothing to do.

There still remains the case where the point of approach $z_0 = a_p$, say belongs to $\mathfrak{A}$ and $\mathfrak{A}'$. Excepting the factor $c_p \log\left(1 - \frac{z}{a_\rho}\right)$, if the remaining summation becomes convergent at z_0, or else infinity but of the contrary sign to c_p, it is evident that

$$\lim_{r=1-0} f(re^{i\theta}) = \mp\infty \quad \text{according as} \quad c_p \gtrless 0.$$

But when the sign of infinity is the same as that of c_p, there occur grave difficulties. The orders of infinities must be compared, but I shall not carry the discussion of these circumstances any further in the present paper.

IV. Examples.

15. Examples.

Ex. 1. $f(z) = \sum_{n=1}^{\infty} \frac{1}{n^s} \log\left(1 - \frac{z}{a_n}\right)$ where $s \geqq 1+\delta$ ($\delta > 0$, however small but finite), and $\arg a_n = \alpha_n = 2\sin^{-1}\frac{1}{2} n^{-t}$ ($t \geqq 0$). Then $\lim_{n=\infty} a_n = 0$, but any $a_n \neq 0$; and the point $z=1$ is the only limiting point of $\mathfrak{A}$.

Now $$1 - e^{-i\alpha_n} = 2\sin\frac{\alpha_n}{2}\left(\sin\frac{\alpha_n}{2} + i\cos\frac{\alpha_n}{2}\right) = n^{-t} e^{\frac{\pi-\alpha_n}{2} i}.$$

Hence $$f(1) = \sum_{n=1}^{\infty} \frac{1}{n^s}\left(\log n^{-t} + \frac{\pi - \alpha_n}{2} i\right)$$

Since $s > 1$, the imaginary part is convergent; and

$$\Re f(1) = \sum_{n=1}^{\infty} \frac{-\log n}{n^{s-t}}, \text{ convergent or divergent } (-\infty)$$

according as $s - t \geqq 1 + \delta'$ ($\delta' > 0$, however small) or $\leqq 1$.

Hence if $s > 1 + t$, $f(1)$ is convergent and $\lim_{r=1} \exp f(r) = \exp f(1) \neq 0$; and if $1 + t \geqq s \geqq 1 + \delta$, $f(1)$ is divergent $(-\infty)$, and $\lim_{r=1} \exp f(r) = 0$. Thus the latter case is far rarer than the former.

Ex. 2. Let $c_n = \left(1 + \frac{1}{n}\right)^{-n^2}$, $\lim_{n=\infty} \sqrt[n]{c_n} = e^{-1} < 1$, so that Σc_n is convergent.

1° If $a_n = e^{-n^t}(t>0)$, $\lim_{n=\infty} a_n = 0$, as Ex. 1.

Now $\lim_{n=\infty} |\log a_n|^{\frac{1}{n}} = \lim_{n=\infty} n^{\frac{t}{n}} = 1 < e$ (§ 7); and therefore $f(1)$ is convergent for all values of $t>0$.

2° If $a_n = \exp(-e^{kn})$, $(k>0)$, $\lim_{n=\infty} a_n = 0$.

Now $\lim_{n=\infty} |\log a_n|^{\frac{1}{n}} = e^k \lesseqgtr e$ according as $k \lesseqgtr 1$. Thus if $0<k<1$, $f(1)$ is convergent, while if $k>1$ divergent. When $k=1$, taking Cauchy's condensation test for $r=1$, it is found that

$$\lim_{n=\infty} \frac{\log\{nc_n |\log a_n|\}}{\log n} = +\infty;$$ and therefore $f(1)$ is still divergent.

Ex. 3. $f(z) = \sum_{n=1}^{\infty} c_n \log(1 - ze^{-n^i})$ where Σc_n is any positive convergent series. When z tends to e^{n^i}, the corresponding term becomes $-\infty$; the real part of remaining summation becomes either $-\infty$ or finite and determinate by § 7; and $F(z) = \exp f(z)$ becomes 0, as z tends to e^{n^i}.

But with this it is not yet completed. What will be $\lim_{r=1-0} \Re f(r)$? If we make Σc_n a very rapidly convergent series, it seems that a convergent case occurs. Taking Σc_n to be a very slowly convergent series, is it impossible to make $\lim_{r=1-0} \Re f(r) = -\infty$? If it is possible, what is the index-series which divides these two categories?

At any rate, this example is shown because of the difficulty met by the author in applying Weirstrass's factor theorem. After his formation for the above case, we have

$$F(z) = \prod_{n=1}^{\infty} (1 - ze^{-n^i}) \cdot \exp\left[ze^{-n^i} + \frac{1}{2}(ze^{-n^i})^2 + \cdots\cdots + \frac{1}{n-1}(ze^{-n^i})^{n-1}\right]$$

$$= \exp - \sum_{n=1}^{\infty} \frac{z^n}{n}\left[e^{-n^i} + e^{-2n^i} + \cdots\cdots + e^{-n^2 i}\right], \text{ if } |z|<1,$$

which is holomorphic inside the unit circle. This attracts our attention because of the neatness of the expression, but nevertheless it is really inaccessible. To ask whether it tends to o when z tends to $z_0 = e^{n^i}$, we consider, as usual,

$$F(z) = \left[\prod_{n=1}^{m} (1 - ze^{-ni}) \exp \sum_{p=1}^{n-1} \frac{1}{p} (ze^{-ni})^p \right]$$

$$\exp\left[- \sum_{n=m+1}^{\infty} \sum_{p=n}^{\infty} \frac{1}{p} (ze^{-ni})^p \right]$$

and we have to show that the second factor remains finite. The real part of its index is

$$\Re \sum_{n=m+1}^{\infty} \sum_{p=n}^{\infty} \frac{1}{p} \left(\frac{z}{e^{ni}} \right)^p = \Re \sum_{p=m+1}^{\infty} \frac{z^p}{p} (e^{-p(m+1)i} + e^{-p(m+2)i} + \ldots\ldots + e^{-p^2 i})$$

Putting $z = re^{mi}$, it becomes

$$\sum_{k=m+1}^{\infty} \frac{r^p}{p} (\cos p + \cos 2p + \ldots\ldots + \cos(p - m)p)$$

$$= \sum_{p=m+1}^{\infty} \frac{r^p \cos\left(\frac{p-m+1}{2} p \right) \sin \frac{1}{2} p(p-m)}{p \sin \frac{1}{2} p}.$$

With this neat form, neither its value when $r = 1$, nor its limiting value for $r \to 1$, is clear to me though I attempted for a long time to find them. Thus even the proof of its vanishing at $z = e^{mi}$ is not yet completed. This gave me a motive to construct the function in this paper: i. e. a function which obviously vanishes at a given point.

Also Mittag-Leffler's generalized factor-theorem cannot be applied at all, since for our case the point aggregate $\mathfrak{A}(e^{ni})$ is not isolated. His formula merely reduces to unity if it be applied.

Ex. 4. $f(z) = \sum_{n=1}^{\infty} (-c)^{-n} \log(1 - ze^{-i\alpha_n})$, $\alpha_n = 2\sin^{-1} \frac{1}{2} b^n$, where $c > 1$ and $0 < b < 1$.

$$f(1) = \sum_{n=1}^{\infty} \frac{(-1)^n}{c^n} \left(\log b^n + i \frac{\pi - \alpha_n}{2} \right)$$

$$= \sum_{n=1}^{\infty} \frac{(-1)^n n}{c^n} \log b + i \sum_{n=1}^{\infty} \frac{(-1)^n}{c^n} \cdot \frac{\pi - \alpha_n}{2}.$$

Thus both the real and imaginary parts are absolutely convergent, and $f(r)$ is continuous at $r = 1$ (§ 11). Putting

$$f(z) = f_1(z) + f_2(z) = \Sigma' + \Sigma'',$$

$n = odd$ $n = even$

we see $\lim_{r=1} f(re^{i\alpha_n}) = +\infty$ or $-\infty$ determinately

according as n is odd or even.

Ex. 5. $f(z) = \sum_{n=1}^{\infty} \frac{(-1)^n}{n^s} \log\left(1 - \frac{z}{a_n}\right)$, $\arg a_n = \alpha_n = 2\sin^{-1}\frac{1}{2}e^{-n^t}$

where $s>1$, $t>0$.

When z tends to a_n radially, as before, $\Re f(z)$ tends to $+\infty$ or $-\infty$ according as n is odd or even. Now when $z=1$:

$$\Re f(1) = \sum_{n=1}^{\infty} \frac{(-1)^{n-1}}{n^{s-t}}.$$

Hence, (i) if $s-t>1$, it is absolutely convergent and by § 11, $f(r)$ is continuous at $r=1$.

(ii) If $0 < s - t \leqq 1$, it is still convergent but conditionally, and by § 12 $f(r)$ is cotinuous at $r=1$. But

(iii) if $s = t$, it becomes

$$\Re f(1) = 1 - 1 + 1 - 1 + \ldots\ldots$$

which is indeterminate, but summable $(C, 1)$ and $= \frac{1}{2}$. And it is this case that I suspected if

$$\lim_{r=1-0} \Re f(r) = \frac{1}{2},$$

but not without doubt. If my proof given in the latter half of § 14 is granted, i. e. under condition that not only Σc_n but also $\Sigma n c_n$ is absolute'y convergent, we have two sub-cases :

(iii) 1° When $s=t>2+\delta$, then $f(r)$ can be said to be continuous, if we assume the value of the function at $r=1$ to be $\frac{1}{2}$; for even if $r>1$, it tends to the same limiting value (§ 9).

(iii) 2° When $1<s=t<2$, the question remains unsolved. But at any rate it is certainly true that

$$\lim_{x=1-0} \sum_{n=1}^{\infty} \frac{(-x)^n}{n^s} \log\left(1 - \frac{1}{a_n}\right) = \frac{1}{2},$$

where $\arg a_n = 2\sin^{-1}\frac{1}{2}e^{-n^s}$.

(iv) When $s-t=$negative, similar propositions hold.

Ex. 6. $f(z) = \sum_{n=1}^{\infty} \frac{(-1)^n}{n^t} \log\left(1 - \frac{z}{a_n}\right)$, $\arg a_n = a_n = 2\sin^{-1}\frac{1}{2}\, n^{-t}$

$(t > 1 + \delta)$.

Now $$\Re f(1) = \sum_{n=1}^{\infty} \frac{(-1)^n}{n^t} \log n^{-n^t} = \sum_{n=1}^{\infty} (-1)^{n-1} \log n$$

which is indeterminate. If we take the partial sums:

$$S_{2p} = \log \frac{1.3.5.....(2p-1)}{2.4.6.....2p} = \log \frac{\lfloor 2p}{(2p\,\lfloor p)^2},$$

$$S_{2p+1} = \log \frac{\lfloor 2p+1}{(2p\,\lfloor p)^2};$$

$$S'_{2p-1} = \frac{S_1 + S_2 + ... + S_{2p-1}}{2p-1}$$

$$= \frac{1}{2p-1} \log \prod_{p=1}^{p-1} \frac{\lfloor 2p\ \lfloor 2p+1}{(2^p\,\lfloor p)^4}$$

$$= \frac{1}{2p-1} \log \frac{\lfloor 2\ \lfloor 3\ \lfloor 4 .....\lfloor 2p-1}{2^{2p(p-1)}(\lfloor 1\ \lfloor 2\ \lfloor 3 ...\lfloor p-1)^4}$$

But

$$\lfloor 0\ \lfloor 1\ \lfloor 2\ \lfloor 3 .....\lfloor n-1 = \frac{\lfloor n}{n} \cdot \frac{\lfloor n}{n(n-1)} .....$$

$$\times \frac{\lfloor n}{n(n-1) .....2\cdot 1} = \frac{\lfloor n^n}{1^1\, 2^2\, 3^3 .....n^n}.$$

We have to find $1^1 2^2 3^3 .....n^n$ or its logarithm.
Using the Euler-Maclaurin's formula,[1] we have

$$\sum_{n=1}^{N} n \log n = \frac{1}{2} N \log N + \int_1^N x \log x\, dx \left[\frac{B_2}{\lfloor 2} \frac{d(x \log x)}{dx} \right.$$

$$\left. + \frac{B_4}{\lfloor 4} \frac{d^3(x \log x)}{dx^3} + ... \right]_1^N$$

$$= \frac{1}{2} N \log N + \frac{N^2}{2}\left(\log N - \frac{1}{2}\right) + \frac{1}{4}$$

1. E.g. Wirtinger, Acta Math., **26**, p. 255.

$$+ \frac{B_2}{2} \log N + \frac{B_4}{4}\left(1 - \frac{1}{N^2}\right) + \cdots\cdots$$

$$= \frac{1}{2}\left(N^2 + N + \frac{1}{6}\right)\log N - \frac{1}{4}N^2 + o(\log N).$$

Thus

$$\log 1^1 2^2 3^3 \cdots\cdots n^n \sim \log n^{\frac{1}{2}\left(n^2+n+\frac{1}{6}\right)} e^{-\frac{1}{4}n^2}.$$

Hence

$$\underline{|1}\ \underline{|2}\ \underline{|3}\cdots\cdots\underline{|n-1} \sim \frac{(n^n e^{-n}\sqrt{2\pi n})^n}{n^{\frac{1}{2}\left(n^2+n+\frac{1}{6}\right)} e^{-\frac{1}{4}n^2}}$$

$$\sim n^{\frac{1}{2}n^2 - \frac{1}{12}} e^{-\frac{3}{4}n^2} \sqrt{2\pi}^n.$$

Applying this asymptotic formula, we obtain

$$S'_{2p-1} \sim \frac{1}{2p-1} \log \frac{(2p)^{2p^2-\frac{1}{12}} e^{-3p^2}\sqrt{2\pi}^{2p}}{2^{2p(p-1)}\left(p^{\frac{1}{2}p^2-\frac{1}{12}} e^{-\frac{3}{4}p^2}\sqrt{2\pi}^p\right)^4}$$

$$\sim \frac{1}{2p-1} \log p^{\frac{1}{4}}\left(\frac{2}{\pi}\right)^p.$$

Hence $$\lim_{p=\infty} S'_{2p-1} = \log\sqrt{\frac{2}{\pi}}.$$

But $$S'_{2p} = \frac{1}{2p}\left\{(2p-1)S'_{2p-1} + S_{2p}\right\}$$

and $$\lim_{p=\infty} \frac{S_{2p}}{2p} = \lim_{p=\infty} \frac{1}{2p} \log \frac{1}{\sqrt{\pi p}} = 0,$$

so that $$\lim_{p=\infty} S'_{2p} = \lim_{p=\infty} S'_{2p-1} = \log\sqrt{\frac{2}{\pi}}.$$

Thus $\Re f(1) = \sum_{n=1}^{\infty}(-1)^{n-1}\log n$ is summable $(C, 1)$ and it is equal to $\log\sqrt{\frac{2}{\pi}}$ (< 0).

This value has, at least, the following meaning: If $a_n =$

$\exp 2i \sin^{-1} \frac{1}{2} n - n^t$,

$$\lim_{x=1-0} \Re \sum_{n=1}^{\infty} \frac{(-x)^n}{n^t} \log\left(1 - \frac{1}{a_n}\right) = \log \sqrt{\frac{2}{\pi}}.$$

Ex. 7. $f(z) = \sum_{n=1}^{\infty} \frac{(-1)^n}{n^2} \log\left(1 - \frac{z}{a_n}\right)$,

$$\arg a_n = \alpha_n = 2 \sin^{-1} \frac{1}{2} e^{-n^2} \underline{|n-1}.$$

Now $$\Re f(1) = \sum_{n=1}^{\infty} \frac{(-1)^n}{n^2} \log e^{-n^2} \underline{|n-1} = \sum_{n=1}^{\infty} (-1)^{n-1} \underline{|n-1}.$$

This is not summable in Cesàro's sense at all. With Borel's method, constructing his associated function

$$\phi(z) = \sum_{n=0}^{\infty} \frac{(-1)^n \underline{|n}}{\underline{|n}} z^n = \sum_{n=0}^{\infty} (-1)^n z^n = (1+z)^{-1},$$

we cannot build up the equality

$$\Re f(1) = \int_0^{\infty} e^{-t} (1+t)^{-1} dt.$$

16. Example with a conditionally convergent index-series.

Hitherto it has been assumed that the index-series Σc_n is absolutely convergent. If it be only conditionally convergent, what shall be our $f(z)$ or $F(z)$? Let e. g.

$$F(z) = \left(1 - \frac{z}{a_1}\right)^{-1} \left(1 - \frac{z}{a_2}\right)^{\frac{1}{2}} \left(1 - \frac{z}{a_3}\right)^{-\frac{1}{3}} \cdots\cdots,$$

$$f(z) = \sum_{n=1}^{\infty} (-1)^n \frac{1}{n} \log\left(1 - \frac{z}{a_n}\right).$$

Put

$$z = re^{i\theta}, \quad a_n = e^{i\alpha_n}, \quad \zeta_n = 1 - \frac{z}{a_n} = 1 + re^{(\pi+\theta-\alpha_n)i}$$

$$= \rho_n e^{i\varphi_n};$$

we have $$f(re^{i\theta}) = \sum_{n=1}^{\infty} (-1)^n \frac{1}{n} (\log \rho_n + i\varphi_n),$$

where $$\rho_n = \sqrt{1 - 2r\cos(\theta - \alpha_n) + r^2}$$

$$\left.\begin{aligned}\rho_n\cos\varphi_n &= 1 - r\cos(\theta - a_n)\\ \rho_n\sin\varphi_n &= \quad - r\sin(\theta - a_n)\end{aligned}\right\} \quad (-\pi < \varphi \leqq \pi).$$

In order that $f(re^{i\theta})$ may be convergent, we must have

$$-\log\rho_1 + \frac{1}{2}\log\rho_2 - \frac{1}{3}\log\rho_3 + \cdots\cdots, \text{ convergent,}$$

and $$-\varphi_1 + \frac{1}{2}\varphi_2 - \frac{1}{3}\varphi_3 + \cdots\cdots\cdots, \text{ convergent.}$$

They are convergent if both of $\log\rho_n$, φ_n decrease with n. To secure it we make some choice about a_n: Let

$$\frac{\pi}{3} \geqq a_1 > a_2 > \cdots\cdots, \qquad \lim_{n=\infty} a_n = 0.$$

Make, as usual, fundamental loops. Consider the domain $S_1: z = re^{i\theta}$ of which r, θ satisfy the conditions: $\cos\theta < r \leqq 2\cos\theta$, $0 < \delta_1 < \theta < \frac{\pi}{2} - \delta_2$ (where δ_1, $\delta_2 > 0$ however small); besides if $r \geqq 1$, θ must not be

Fig. 3.

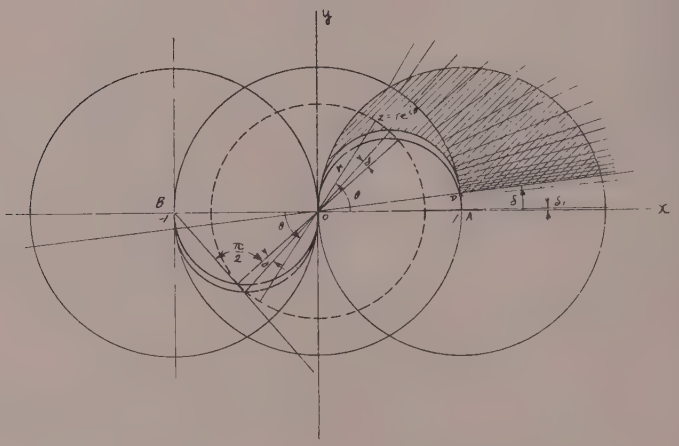

equal to a_n. In S_1 it is easy to observe geometrically that both $\log\rho_n$ and φ_n are negative and ultimately decreasing in absolute values (Fig. 3), and consequently $f(re^{i\theta})$ is convergent, though not uniformly. To make it uniformly convergent, take a point $D(=e^{i\delta})$ between a_{N-1} and

a_N, thus $a_{N-1}>\delta>a_N$, and describe a circle with OD as diameter. Excluding from S_1 the region common to this circle and S_1 as well as the region $\theta<\delta$, call the remaining domain S_0 (the shaded domain in Fig. 3; of course, every circle of the loop about a_n must have a finite radius $\epsilon>0$). Then for all points in S_0, both $\log\rho_n$ and φ_n are ultimately negative and dereasing in absolute values after $n=N$, and really

$$\rho_n > \sin(\delta - a_N), \quad \text{for all } n \geqq N.$$

Hence the rest after $(n'-1)$ terms of $f(re^{i\theta})$ is, when $n'>N$,

$$\left| \sum_{n=n'}^{\infty} \frac{(-1)^n}{n} (\log\rho_n + i\varphi_n) \right| < \frac{1}{n'} \sqrt{(\log\rho_{n'})^2 + \varphi_{n'}^2}$$

$$< \frac{1}{n'} \sqrt{[(\log\sin(\delta - a_N)]^2 + \pi^2};$$

and consequently $< \sigma$ (a prescribed small quantity),

if $n' \geqq n_0$, uniformly for all z in S_0. Thus $f(re^{i\theta})$ is uniformly convergent (though not absolutely), and therefore it defines a holomorphic function in S_0 which can be made to coincide with S_1 as nearly as we please. Whence it follows that its behaviour toward $z_0=a_n$ (isolated point of $\mathfrak{A}$) should be quite similar as the case Σc_n is absolutely convergent.

Also let $\pi<\varphi_n'<3\pi$ (adding 2π to φ_n), we shall still obtain a regular domain S': $0 < r \leqq \cos\theta$, $0 < \delta_3 < \theta < \frac{\pi}{2} - \delta_4$. For, in S', $\log\rho_n$ (<0) ultimately decreases in absolute value with n, while φ_n', now determined, is positive and also decreasing.

Also in domain S'': $-\delta_5>\theta>-\pi+\delta_6$ (δ_5, $\delta_6>0$ however small) and outside of the circle $(x-1)^2+y^2=1$, we see that $\log\rho_n$ ultimately becomes positive and monotonously decreasing, while φ_n is positive, if it is confined in $(-\pi, \pi)$, and increasing with n. Put $\varphi''=\varphi_n-2\pi$, then φ_n'' (<0) decreases in absolute value.

Thus a certain branch of $f(re^{i\theta})$ is holomorphic in S' and S'' respectively. But it is by no means meant that the whole Gauss plane is thus divided into several distinct defining domains; the domains above determined may possibly be extended.

Let us investigate Σ more closely.

$$\Re f(re^{i\theta}) = \sum_{n=1}^{\infty} \frac{(-1)^n}{n} \log\rho_n, \ (r \gtrless 1).$$

Since a_n decreases monotonously, the change of $\rho_n=\sqrt{1+r^2-2r\cos(\theta-a_n)}$ should be ultimately monotonous, with the limit $\sqrt{1+r^2-2r\cos\theta}=\rho$, say. Thus putting $\rho_n=\rho+\epsilon_n$, the error ϵ_n should be ultimately of the same sign and decreasing in absolute value. Hence

$$\sum_{n=1}^{\infty}\frac{(-1)^n}{n}\log\rho_n=-\log 2\log\rho+\sum_{n=1}^{\infty}\frac{(-1)^n}{n}\log\left(1+\frac{1}{\rho}\epsilon_n\right);$$

really the second summation is convergent, since the summands become of alternate signs, approaching to 0.

When $r=1$,

$$\Re f(e^{i\theta})=\sum_{n=1}^{\infty}\frac{(-1)^n}{n}\log 2\sin\left|\frac{\theta-a_n}{2}\right|;$$

and $\lim_{n=\infty}\rho_n=\rho=2\sin\left|\frac{\theta}{2}\right|>0$, except $\theta=0$ (or $2m\pi$). As before, putting $\rho_n=\rho+\epsilon_n$, we may show the convergency though not uniformly.

As to the imaginary part, a similar analytical proof may be given. Or geometrically we see that it is convergent in the upper half-plane, except the region S' of the upper semicircle described with OA as diameter, but the lower half region S_2, say of the same circle being inclusive. In S', however, if $\varphi_n'=\varphi_n+2\pi$ be considered, $\Sigma\frac{(-1)^n}{n}\varphi_n'$ is still convergent, and thus

$$\Sigma\frac{(-1)^n}{n}\varphi_n=\Sigma\frac{(-1)^n}{n}\varphi_n'-2\pi\log 2.$$

In the lower half-plane, except S_2, if $\varphi_n''=\varphi_n-2\pi$ be considered, it is still convergent, and thus

$$\Sigma\frac{(-1)^n}{n}\varphi_n=\Sigma\frac{(-1)^n}{n}\varphi_n''+2\pi\log 2.$$

After all, keeping the convention initially made $-\pi<\varphi_n\leqq\pi$, the given summation defines a one-valued function even in the domain S of § 2, though the holomorphism or even the continuity is not yet asserted.

17. Example with a divergent index-series.

An ordinary infinite product such as

$$\prod_{n=1}^{\infty}\left(1-\frac{z}{a_n}\right),\quad\text{where}\quad|a_n|=1,$$

is divergent throughout ($z \neq 0$). But if we consider

$$F(z, x) = \prod_{n=1}^{\infty} \left(1 - \frac{z}{a_n}\right)^{x^n}, \text{ where } x \text{ is real,}$$

it is convergent in S as long as $|x| < 1$, as shown already. Furthermore, considering

$$f(z, x) = \sum_{n=1}^{\infty} x^n \log\left(1 - \frac{z}{a_n}\right), \quad (z \neq 0)$$

is it always that

$$\lim_{x=1-0} \Re f(z, x) \text{ does not exist?}$$

The answer is in the affirmative.[1] For example, let $a_n = \arg a_n$ be such that

$$2 \sin \frac{1}{2} a_{2p-1} = \frac{2p}{p+1} \quad \text{and} \quad 2 \sin \frac{1}{2} a_{2p} = \frac{p+1}{2p}$$

($p = 1, 2, 3, \ldots\ldots$), Then even when $z = 1$, the sum

$$\Re f(1, 1) = \sum_{n=1}^{\infty} \log |a_n - 1| = \sum_{n=1}^{\infty} \log\left(2 \sin \frac{a_n}{2}\right),$$

although indeterminate at first sight has, for Cesàro-Hölder's sum, the value $\frac{1}{2} \log 2$. Really we have

$$S_{2p} = 0, \quad \lim_{p=\infty} S_{2p} = 0,$$

while

$$S_{2p-1} = \log \frac{2p}{p+1} \quad \therefore \quad \lim_{p=\infty} S_{2p-1} = \log 2.$$

But taking the second partial sums, evidently we have

$$\sum_{n=1}^{2p} S_n = \sum_{n=1}^{2p-1} S_n = \log \prod_{p=1}^{p} \frac{2p}{p+1} = p \log 2 - \log(p+1).$$

Hence as the mean partial sum we obtain

---

1. Though generally it does not exist as e.g. when all $a_n = 1$

$$f(z, x) = \frac{x}{1-x} \log(1 - z)$$

and $\lim_{x=1-0} f(z, x) = \infty$, for all values of $z (\neq 0)$.

$$S'_{2p} = \frac{p\log 2 - \log(p+1)}{2p}, \quad S'_{2p-1} = \frac{p\log 2 - \log(p+1)}{2p-1}.$$

Hence $\lim_{p=\infty} S'_{2p} = \lim_{p=\infty} S'_{2p-1} = \frac{1}{2}\log 2.$

Thus, analogous to the so-called mean sum, we may conceive as *the mean product*

$$\prod_{n=1}^{\infty} \left| 1 - \frac{1}{a_n} \right| = e^{\frac{1}{2}\log 2} = \sqrt{2}.$$

This conception may be utilized in general. For the aim[1] to lower the rank ν_n of the Weirstrass' prime factor in

$$\prod_{n=1}^{\infty} \left(1 - \frac{z}{a_n}\right) \exp \sum_{k=1}^{\nu_n} \frac{1}{k} \left(\frac{z}{a_n}\right)$$

and thus to make the reining effect, so to speak, as little as possible, the above mean product seems to be at the extremity.

Returning to the preceding example, by Hölder's theorem, we have

$$\lim_{x=1-0} \Re f(1, x) = \frac{1}{2}\log 2,$$

and $$\lim_{x=1-0} \left| 1 - \frac{1}{a_n} \right|^{x^n} = \sqrt{2}.$$

It is rather more important, when the indices are of alternate signs. In general, let $\sum_{n=1}^{\infty} d_n$ be a divergent series but with $\overline{\lim_{n=\infty}} \sqrt[n]{|d_n|} = 1$. [The case where this superior limit becomes >1 is not under investigation at present; also when it is <1, Σd_n cannot be divergent.] Consider

$$\prod_{n=1}^{\infty} \left(1 - \frac{z}{a_n}\right)^{d_n} \quad \text{and} \quad \sum_{n=1}^{\infty} d_n \log\left(1 - \frac{z}{a_n}\right).$$

They cannot exist in general. But certainly

$$f(z, x) = \sum_{n=1}^{\infty} d_n x^n \log\left(1 - \frac{z}{a_n}\right)$$

exists in S, if $|x| < 1$, since now $\sum_{n=1}^{\infty} d_n x^n$ should be absolutely convergent.

1. E. g. D. Mordouhay-Boltovsky, Sur les facteurs primaires de la fonction entière, C. R. Paris, **180** (1925), p. 191.

Hence making $x \to +1$, we define $f(z)$:

$$f(z) = \lim_{x=1-0} f(z, x)$$

if it exists. It is the same thing as the Cesàro's sum of the given summation.

Assuming, as in the last paragraph, that $\mathfrak{A}(a_n)$ has only one regressive limiting point at $z=1$, consider the sum in Cesàro's sense:

$$\Re f(z) = \sum_{n=1}^{\infty} (-1)^n \log \rho_n = \sum_{n=1}^{\infty} (-1)^n \log(\rho + \epsilon_n),$$

where $$\rho = \lim_{n=\infty} \rho_n = \lim_{n=\infty} \sqrt{1 + r^2 - 2r\cos(\theta - a_n)}$$

and ϵ_n shall be ultimately of the same sign and monotonously decreasing in magnitude (§ 16). Thus

$$\Re f(z) \cong -\frac{1}{2}\log\rho + \sum_{n=1}^{\infty} (-1)^n \log\left(1 + \frac{\epsilon_n}{\rho}\right);$$

the latter summation is already summable in itself, because the summand with alternating signs becomes ultimately monotonously decreasing in magnitude, and

$$\lim_{n=\infty} \log\left(1 + \frac{\epsilon_n}{\rho}\right) = 0.$$

Hence, as usual, when $\theta = a_p$, excluding the term $(-1)^p \log(1-r)$, we see the remaining summation remains finite when r tends to 1. Thus the behaviour toward the given point a_p is just the same as before.

There is some difficulty to approach to $z=1$.

As another example, consider

$$f(z) = \sum_{n=1}^{\infty} (-1)^n n^s \log\left(1 - \frac{z}{a_n}\right), \quad a_n = \arg a_n = \cos^{-1} n^{-t} > 0,$$

where $s, t > 0$; thus $\mathfrak{A}$ has the limiting point $a = \frac{\pi}{2}$. To show, at any rate, its existence [of course in the sense of (C, K)], consider

$$\Re f(r) = \sum_{n=1}^{\infty} (-1)^n n^s \log\sqrt{1 + r^2 - 2r\cos a_n}, \quad (0 < r < 1)$$

$$= \sum_{n=1}^{\infty} (-1)^n n^s \left[\log\sqrt{1+r^2} + \log\left(1 - \frac{2r}{1+r^2}\frac{1}{n^t}\right)^{\frac{1}{2}}\right].$$

If the Cesàro's sum of $\Sigma(-1)^n n^s$ be d,[1] considering as in § 14, we obtain

$$\Re f(r) \cong d \log \sqrt{1+r^2} + \frac{r}{1+r^2} \sum_{n=1}^{\infty} (-1)^n n^{s-t} \log \left(1 - \frac{1}{N_n}\right)^{N_n}$$

where

$$N_n = \frac{1+r^2}{2r} n^t,$$

and, therefore, if $t > s+1$, the last summation is already summable in itself, and so also even when $t > s$ simply, because

$$\lim_{N=\infty} N \log \left(1 - \frac{1}{N}\right) = -1$$

and it tends so, monotonously decreasing in magnitude. Thus $\Re f(r)$ exists certainly.

---

1. Cesàro, Sur la multiplication des séries, Bull. sci. math. 2 sér. t. 14, p. 119.

"The Reversal-Like Phenomena" of the Secondary and the Tertiary Discharge-Figures impressed on Photographic Plates

By

Tatsumi Terada

(Received May 21, 1928)

Abstract

1. The reversal-like phenomena occur also in the secondary and the tertiary discharge-figures similarly as in the primary ones.

2. The phenomena in the secondary figures corresponding respectively to the primary negative and the primary positive figures are similar to those of the primary positive and the primary negative figures respectively; and the phenomena in the tertiary figures corresponding respectively to the primary negative and the primary positive figures are similar to those of the primary negative and the primary positive figures respectively. Therefore, the tertiary figure corresponding to the primary negative, and the secondary figure corresponding to the primary positive are of a negative nature.

Introduction

In the arrangement shown in Fig. 1, P_1 and P_2 are two photographic plates, which are in contact with each other on their plain glass sides; and P_3 is another photographic plate. The shaded portions of these photographic plates represent the film-covered sides of the plates. M, which is just beneath the photographic plate P_3, is an earthed metal-plate; and s is an air-space.

Now, one of the electrodes of a charged condenser is connected to the terminal E which is laid on the sensitive film of the photographic plate P_1, and the other electrode to the earth, and if a momentaneous brush discharge takes place on the sensitive film of the photographic

plate P_1, we shall see the beautiful discharge-figures impressed on the photographic plates after development. The discharge-figures impressed on the photographic plates P_1, P_2 and P_3 are called respectively the primary, the secondary and the tertiary figure by Mikola,[1] Pedersen,[2] and Yoshida and Tanaka.[3] According to these investigators when the positive terminal of the charged condenser is connected with the terminal *E* on the photographic plate P_1, the figure impressed on it is called "the primary positive figure," that on the plate P_2 "the secondary negative figure" and that on the plate P_3 "the tertiary positive figure." When the negative terminal of the charged condenser is connected with the terminal *E*, the discharge-figures are named "the primary negative figure," "the secondary positive figure" and "the tertiary negative figure" respectively.

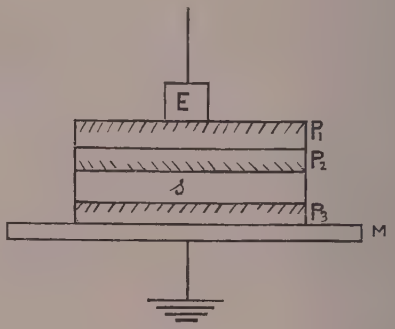

Fig. 1

The secondary positive figure consists of two parts: one the concentric lines running in the direction perpendicular to the branches of the primary negative figures, and the other the short brushes radiating outward or inward from the concentric lines. The secondary negative figure consists of an assemblage of many diffuse lines running in a direction nearly perpendicular to the branches of the primary positive figure.

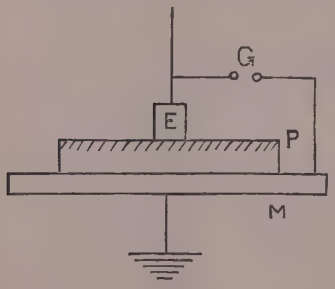

Fig. 2

As shown in Fig. 2, if a spark gap *G* is inserted between the electrode *E* and the earthed metal-plate M, then when a brush discharge from the electrode *E* takes place on the sensitive film of the photographic plate P simultaneously with a direct spark at the spark gap *G*, an interesting phenomenon occurs in each of the primary negative and positive figures. This interesting phenomenon was first ob-

1 Mikola, Phys. Z.S. **18**, 158, (1917).
2 Pedersen, K. Danske. Vidensk. Selsk. **1**. No. II, (1919).
3 U. Yoshida and S. Tanaka, Mem. Coll. Sci. Kyoto, **5**, 145, (1921).

served by Prof. Yoshida.[1] In the negative figure, an enveloping margin comes out at the ends of the negative branches as shown in Fig. 1a, Plate I; and in the positive figure, each branch is enveloped separately with a diffused margin of stronger intensity as shown in Fig. 1b, Plate I. According to Prof. Yoshida, these phenomena are not explained by a mere photographic reversal, so the writer will hereafter call this interesting phenomenon "The reversal-like phenomenon" for convenience' sake.

Now, it is interesting to see whether or not this reversal-like phenomenon will occur with the secondary and the tertiary figures as with the primary one, since it may enable us to learn the real nature of this phenomenon. The experimental arrangements and the results are described below.

Experimental Arrangements and Results

The electrical circuit used is shown in Fig. 3. This circuit is similar to those used by Max Toepler,[2] Przibram,[3] Pedersen,[4] Peters[5] and Paul Heymans.[6]

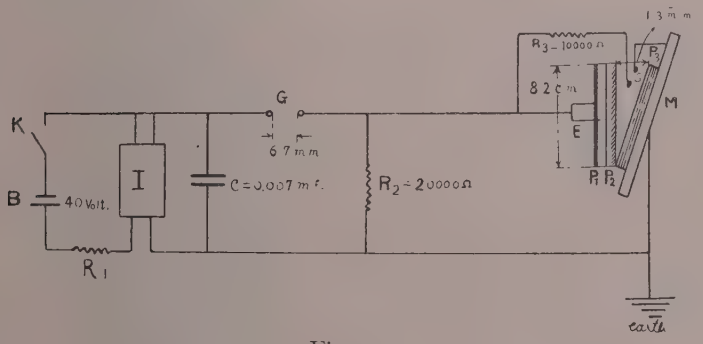

Fig. 3

In Fig. 3, K is a key, B a 40-volts battery, I an induction coil of which the maximum needle-plate-spark-gap is 40 cms. with the primary electric source of 40 volts, R_1 an electric resistance as the regulator of the primary current, C a condenser whose electric capacity is 0·007

1 U. Yoshida. Mem. Coll. Sci. Kyoto, **2**, 315, (1917).
2 Toepler. Phys. Z. S., **8**, 743, (1907).
3 Przibram. Phys. Z. S., **21**, 480, (1920).
4 Pedersen. Ann. d. Phys. **69**, 205, (1922), Ann. d. Phys. **71**, 315, (1923).
5 Peters. Elec. Wld. **83**, 769, April 19, (1924).
6 Heymans and Frank. Phys. Rev. **25**, 865, (1925).

microfarad, G a spark gap, E the cylindrical terminal whose diameter is 1·27 cm., R_2 a water resistance of about 20,000 Ω, R_3 another water resistance of about 10,000 Ω, and S is a short spark gap. This illuminating spark gap S is laid on an insulating plate P_3. The plate P_1 is a black glass plate obtained by developing a photographic plate of 1·2 mm. in thickness, which had previously been exposed to the sunlight for some seconds. By means of this black glass, the writer prevented the light, which is emitted by the primary discharge at the terminal E, from coming toward the photographic plate P_2. The secondary figures, Fig. 2a, Fig. 2b in plate I, and Fig. 3a, Fig. 3b, Fig. 4a in plate II are obtained by the use of this black glass P_1 and the insulating glass plate P_3, which is 1·2 m.m. in thickness. The tertiary figures, Fig. 2c in Plate I and Fig. 3c and Fig. 4b in Plate II are obtained on a photographic plate in the position of P_3 in Fig. 3, the glass side of which had been brought into contact with the earthed metal-plate M.

In the first place, the electric resistance R_1 and the lengths of the spark gaps G and S are so adjusted that the electric sparks take place simultaneously at these two spark gaps, when the key is broken. In that case, when the electric impulse resulting from a spark at the gap G reaches the electrode E and the gap S, the secondary and the tertiary figures are impressed respectively on the plates P_2 and P_3, at the same time as the formation of a spark at S; and the light emitted by this spark illuminates the plates P_2 and P_3.

The brushes of the secondary figure corresponding to the primary negative one grow from the system of concentric rings outwards or inwards according to the thickness of the insulating plate P_3 in Fig. 1, as was pointed out by Yoshida and Tanaka.[1] Fig. 2a in Plate I, was obtained when the thickness of insulating plate P_3 was 1·2 mm., Fig. 2b in the same plate was secured when its thickness was 0·2 mm. In these cases, the brushes of the former grow inwards, and those of the latter outwards. With the arrangement in Fig. 3, if the illuminating spark appears at the same time as the impression of the discharge-figures, each of the brushes causes the reversal-like phenomenon as shown in Figs. 3a and 3b in Plate II, and it may be easily seen in these figures that the reversal-like phenomenon is of the nature characteristic of the positive one.

Fig. 2c in Plate I is the tertiary figure corresponding to the primary negative one, and it will easily be seen that this figure consists of regular

1 U. Yoshida and S. Tanaka, Mem. Coll. Sci. Kyoto. **5**, 145, (1921).

negative and irregular positive-like brushes. Fig. 3c in Plate II, is the tertiary negative figure obtained with the arrangement in Fig. 3, by illuminating the plate with the spark at S. In this figure, we can see clearly the enveloping margin which is characteristic of the negative figure. Again, the same phenomenon was obtained with a celluloid film instead of a photographic plate.

As to the secondary figure corresponding to the primary positive one, Yoshida and Tanaka[1] say "……it was observed by the writers that these diffuse lines in the secondary figure, on some of photographs taken with a sufficiently thick air space, had fine structures characteristic of the regular primary negative figure. Judging from this, the secondary figure corresponding to a primary positive one seems to be of a negative nature, and it may be called 'the secondary negative figure, after Mikola and Pedersen."

The writer undertook to observe the reversal-like phenomena of this secondary figure by using an insulating glass plate P_3 as shown in Fig. 3, which was 1·2 mm. in thickness; but the result was negative, probably owing to the weakness of the impression of the secondary figure. Next, he used a thin celluloid film 0·2 mm. in thickness as an insulator instead of the glass plate P_3 in Fig. 3; and the expected phenomenon appeared on the photographic plate P_2 in Fig. 3 as reproduced in Fig. 4a, Plate II. The enveloping margin in this photograph was clearly of a negative nature as was seen in the primary negative one.

The reversal-like phenomena of the tertiary figure corresponding to the primary positive one was observed by the writer on a photographic plate placed in the position of the insulating plate P_3 in Fig. 3, by putting the film-side of the photographic plate against the spark gap S in this figure. In some dozens of photographs taken, the reversal-like phenomena characteristic of the primary positive figure always happened as shown in Fig. 4b, Plate II. The same phenomenon was also obtained with a celluloid film instead of a photographic plate.

In conclusion, the author wishes to express his hearty thanks to Professor U. Yoshida of the Kyoto Imperial University for the deep interest he has taken in this research.

Physics Laboratory,
Imperial Naval College, Etajima

1 U. Yoshida and S. Tanaka, loc. cit.

Plate I

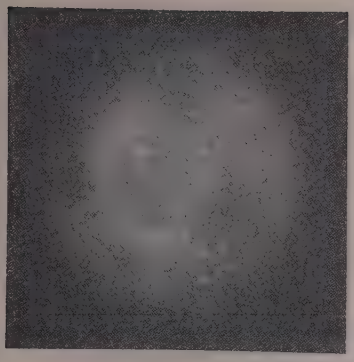

Fig. 2a

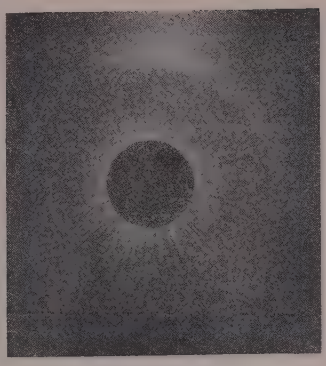

Fig. 1a

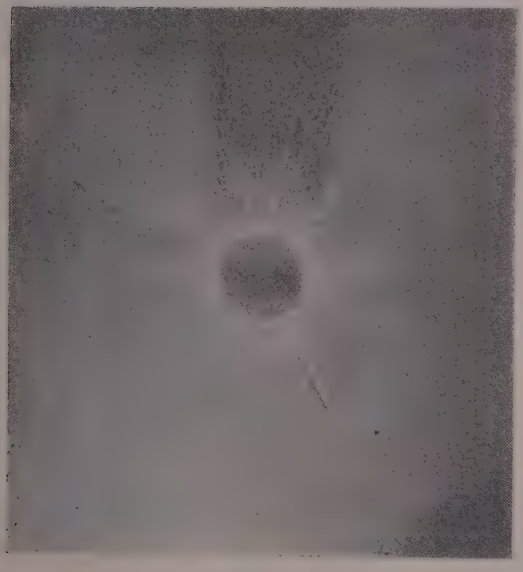

Fig. 1b

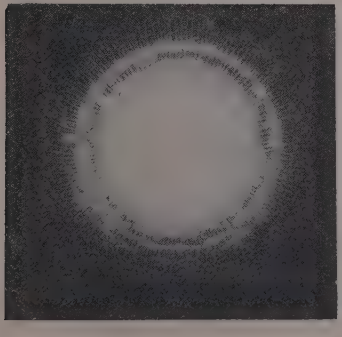

Fig. 2b

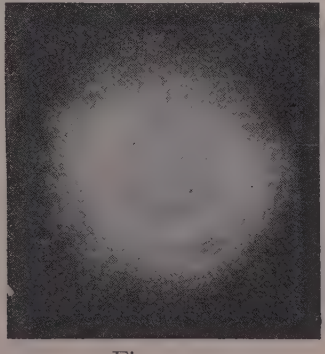

Fig. 2c

Plate II

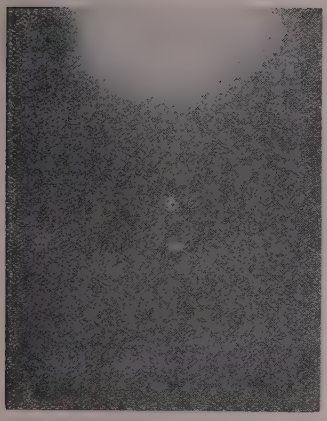

Fig. 3a

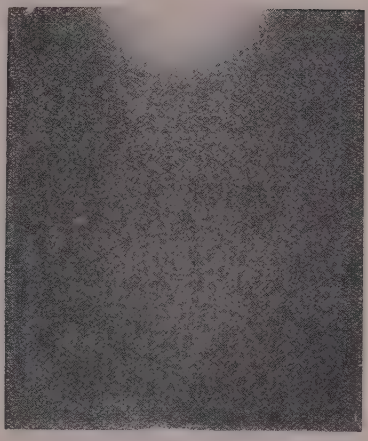

Fig. 3b

Fig. 3c

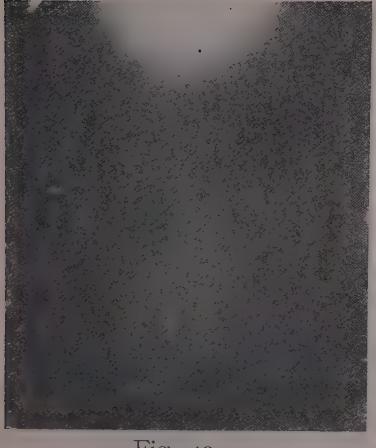

Fig. 4a

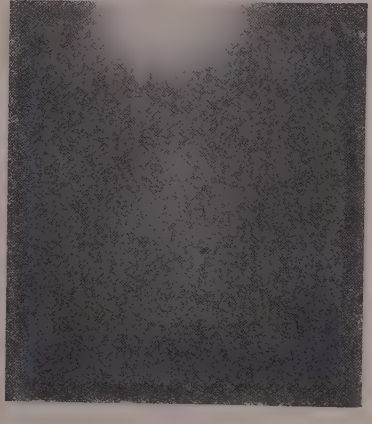

Fig. 4b

The Orientation of Single-Crystals of Zinc

By

Kenzo Tanaka

(Received June 4, 1928)

Abstract

The orientations of many single-crystals of zinc, formed under various conditions, are examined to see whether they depend upon the conditions under which the crystals are formed or not; and some peculiarities in their orientation are found in some cases.

Whether the orientations of the single-crystals of metals, formed under various conditions, have some relations with these conditions or not has not yet been satisfactorily investigated. In a previous paper[1], the writer reported some regularities in the distribution of the orientations of the single-crystals of aluminium, which are due to the conditions under which they were formed. In the present paper are reported the results of a further investigation carried out on 119 different pieces of the single-crystals of zinc. The method of determining the orientation of the crystal by means of X-rays was essentially the same as before, and it was very much facilitated by the use of the globe and the spherical scale devised by Prof. U. Yoshida[2]. The orientations of the axes of the test-piece of a single-crystal of zinc, in reference to the crystallographic axes of the hexagonal crystal of zinc, were represented in a stereographic projection, by taking the three crystallographic axes [0001], [11$\bar{2}$0] and [10$\bar{1}$0] as the reference directions.

Fig. 1 shows the orientations of large crystals formed in the test-pieces of plates; which were prepared from commercial zinc plates of 1.5 mms. thickness, by first rolling the plates to about a 20—70% reduction

1 Jap. J. Phys., **4**, 137 (1927).
2 Jap. J. Phys., **4**, 133 (1927).

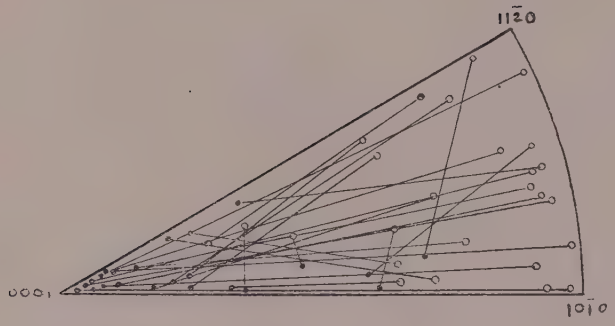

Fig. 1.

in thickness and then by annealing at 400° C for one day. In Fig. 1 the direction of the surface normal of the plate and that of the rolling are represented respectively by a dot and a small circle, and the line joining a dot and a small circle indicates that they belong to the same specimen of one single-crystal. It can be seen from the figure that the rolled plane or the plane of the plate of most of the crystals is nearly parallel to the base of the hexagonal crystal of zinc. Fig. 2 shows the results obtained with similar test-pieces of plates as in the case of Fig. 1; the test-pieces in this case were prepared by being extended, instead of being rolled, before annealing. The dot and the small circle in this figure represent respectively the direction of the surface normal of the plate and the direction of pulling of the plate. The single-crystals thus obtained show almost the same distribution of their orientations as in Fig. 1.

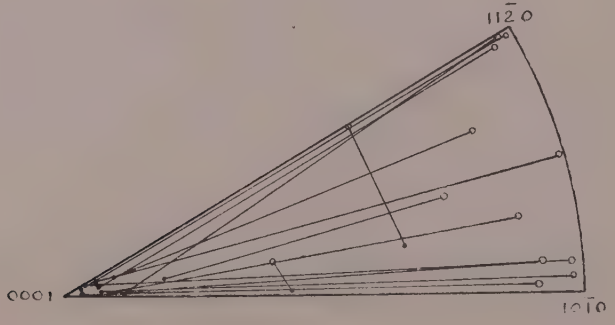

Fig. 2.

In Fig. 3, commercial zinc-wires of 1.5 mm. diameter were drawn to about 0.5mm. through dies, and then they were subjected to the same heat-treatment as the plate. In this figure, the axis of the wire is represented by a dot; and it will be seen from the figure that the $[11\bar{2}0]$ axes of most of the *Zn*-crystals take a direction nearly parallel to the axis of the wire. A rather random distribution of the orientations of the crystals shown in Fig. 4 is of the crystals formed in the test-pieces of 1.5 mm. wires, which were subjected to pulling for an elongation of a very small percentage before annealing.

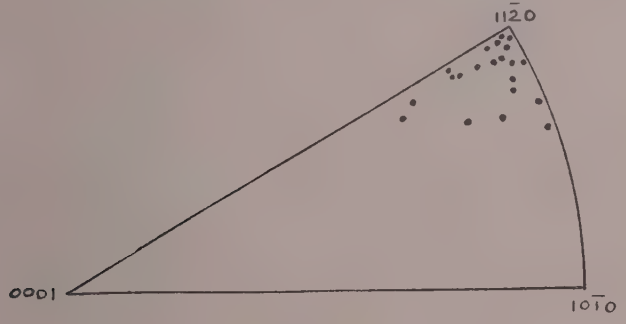

Fig. 3.

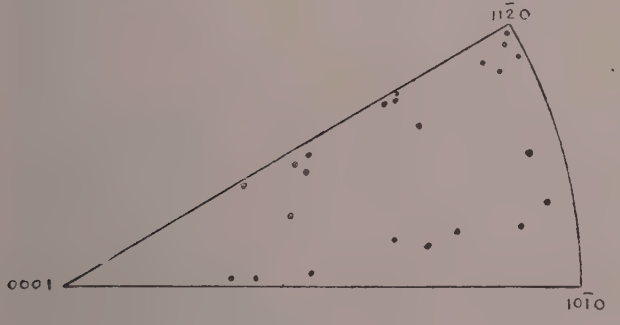

Fig. 4.

When a circular zinc plate is melted and cooled gradually from the peripheral part toward the center of the plate, there grow some large crystals from the periphery as the process of cooling proceeds toward the central part. By etching the surface thus obtained with some proper

Fig. 5.

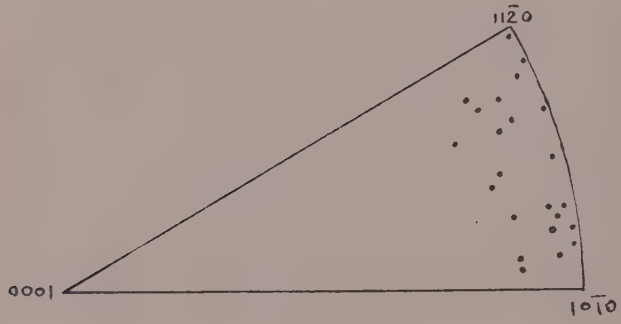

Fig. 6.

reagent, we can detect clearly that many large crystals have grown toward the center of the specimen, and that the plate is divided into many sectors with these crystals of different orientations. The orientations of these crystals are shown in Fig. 5, where the dot and the small circle represent roughly the direction of the surface normal and the radial direction or the direction of the process of cooling in the specimen respectively. Fig. 5 shows that most of the crystals grow in a direction nearly parallel to the plane of the base of the hexagonal crystal. This result is confirmed by the results shown in Fig. 6. In this case, metallic zinc was melted in a thin and long glass tube, and then it was cooled gradually and slowly from one end of the tube to the other end. Comparatively large crystals of zinc in the wire were obtained by this process. The direction of the growth of the crystals must be the same, in this case, as that of the progress of cooling along the axis of the specimen. Thus

the axis of the wire of the zinc-crystal was taken as the direction of the growth of the crystal and it was represented by the dot in Fig. 6. The fact stated in connection with Fig. 5, that the crystals of zinc grow in a direction nearly parallel to the base of the hexagonal crystal of zinc, is also seen in Fig. 6.

These results stated above show that the orientations of zinc-single-crystals formed by various treatments, depend to some extent upon the manner of the heat-treatment and also upon the history before the heat-treatment.

In conclusion, the writer wishes to express his sincere thanks to Prof. U. Yoshida for his kind guidance in the research.

On Paradoxes and Definitions.

By

Toshizô Matsumoto.

(Received June 5, 1928)

---

1. When a thing has two names, it must be made clear that the two names signify the one and the same thing. If the two names given to a thing should not at once make clear that they signify the one and the same thing, some confusion would occur. Such confusion is often met in our daily life. Quite in the same way, if we give two definitions to a mathematical thing, we must make sure that the definitions point out the one and the same thing. No contradiction will occur if and when such verification is possible. When such verification is possible, we shall say that the two definitions are *congruent*.

The locus of points equidistant from a fixed point in a plane is called a circle. (Def. A) The circle may also be defined as the intersection of a sphere and a plane. (Def. B) Thus we have given two definitions to the circle. Now we must prove that the definitions A and B are congruent. To do it we prove under the definition A that the intersection of a sphere and a plane is a circle and conversely under the definition B that the locus of points equidistant from a fixed point in a plane is a circle. If it be done, the figures defined by the definitions A and B are identical.

So far as I know, it seems that in several antinomies or paradoxes in Cantor's theory of sets, such verifications are often forgotten. In this paper I intend to discuss from the point of view of the definitions, those antinomies given in Frenkel's books[1].

---

1. Einleitung in die Mengenlehre (1923).
Zehn Vorlesungen uber die Grundlegung der Mengenlehre (1927).

2. Richard's paradox. All the decimal numbers which may be defined by a finite number of words (including signs) are countably infinite in number. But the decimal number a defined by Cantor's diagonal method applied to those decimal numbers already defined is not contained in them. Hence the decimal number a must not be defined by a finite number of words. But the number a is already completely defined. This is a contradiction.

According to Russel, the definition of the decimal number a is not *predicative*. That which is defined by all elements of a set cannot be an element of the set. It explains that the decimal number a is not contained in the set of the decimal numbers used to define a.

According to my consideration, if the decimal number a be contained in the set, the number a will have two definitions. For since we have assumed that the number a is contained in the set whose decimal numbers are already defined, it has a definition. (Def. A) On the other hand the number a has been defined by the diagonal method. (Def. B) Consequently we must prove that those two definitions are congruent. If these definitions be congruent, the decimal number a must be contained in the original set of the decimal numbers. If otherwise we cannot identify the number a with a number of the set. Cantor's proof on the power of the continuum says that the definitions A and B are not congruent. Thus the decimal number a is not contained in the original set of the decimal numbers.

In the above paradox, the newly defined decimal number a is not contained in the original set. But paradoxes may occur in some cases where the newly defined thing belongs to the original set.

Let $a, b, c, \ldots\ldots$ be positive integers which can be defined by one hundred words. Then there is necessarily a minimum integer, Let a be the minimum integer. Thus the integer a is defined by less than one hundred words. This is a contradiction. Let us consider the definitions more closely.

Since the integer a is an element of the set of positive integers defined by a hundred words, the integer a was already defined. (Def. A)

Next, we have defined the integer a as the minimum of the original set of positive integers. (Def. B) Thus two definitions are given to an integer a. If these definitions be congruent, assuredly there is a contradiction. But a close inspection of these two definitions will show us that they are not congruent. To prove it, at first efface the definition A, then the definitions B loses its sense. For without the aid of the definition A, the element a of the set $a, b, c, \ldots\ldots$ is undefined. Consequently, the word minimum among elements partly defined and partly

undefined loses its meaning. Therefore the definition B comes to contain two unknowns namely a and *minimum*. Thus without the definition A, the definition B does not define completely the minimum integer a.

After Poincaré's consideration[1], the integer a with the definition B will cease to be the positive integer definable by exactly one hundred words. Therefore the classification of the positive integers definable by a hundred words will be changed. Then I think the integer a will leave the original set. But if it do so, the number a will lose definition A. Therefore, a will become meaningless and the essential point of the explanation of our paradox seems to be the incompleteness of definition B.

3. To prove the existence of a root of the algebraic equation $f(x) = 0$, we employ the property that $|f(x)|$ becomes minimum at a point of any circle of the complex plane. In the polemic between Poincaré and Zelmero, the latter noticed that the definition of the above minimum is not predicative. Poincaré so refuted it that instead of the minimum of $|f(x)|$, we have only to consider its lower limit for all rational values of the variable x. It is clear that the minimum of $|f(x)|$ and its lower limit for the rational values of x are equal. Now let a be the minimum of $|f(x)|$. (Def. A) a may be defined also as the lower limit of $|f(x)|$ for any rational x. (Def. B) Hence the definition A and B are congruent. As we have seen above, in Richard's paradox, the definitions A and B were not congruent, while in the present case, they are congruent. Consequently the impredicative definition is not necessarily contradictory. On the other hand, it is known that the term *impredicative* is contradictory to itself. For any logical criticism, it seems reasonable to avoid such a word which is contradictory to itself.

4. Tertium non datur. It has been explained by the intuitionists represented by Brower that many mathematical theorems are related to *tertium non datur*. By tertium non datur, I think the existence of the thing with a given property E will be ascertained, while the possibility of its constructing is not proved. In mathematics it is generally difficult to construct a thing having a given property E. If the existence and the possibility of its constructing be the same, among theorems which are considered to have been rigorously proved, there are many uncertain ones. De Loor gave the following example:

Let k be the number of the decimal places of π from which for the first time seven 7 continuously occur. Next, if such an integer k does not exist, put $\rho \equiv \pi$ or else put $\rho \equiv \pi + 10^{-k}$ or $\rho \equiv \pi - 10^{-k}$ according as

1. Dernières Pensées, 104.

k is odd or even. Then the discriminant D

$$D=-108(\pi^6-\rho^6)$$

of the equation

$$x^3-3\pi^2x+2\rho^3=0$$

is not known to be zero or not. Hence by aid of tertium non datur, the discriminant cannot determine the multiplicity of the roots of the equation.

We have defined ρ as π, $\pi+10^{-k}$ or $\pi-10^{-k}$ according as the case may be. (Def. B) But we do not know what number ρ is. If we assume ρ to be a definite number, that number is already defined, (Def. A), since we are working under the hypothesis that all numbers are well defined. Consequently we must prove the congruence of these two definitions A and B. Before we prove it, it is a matter of-course that we may not discuss the value of the discriminant D.

The mathematics of to-day cannot determine what number ρ is. In other words, we cannot prove whether the definitions A and B are congruent or not. As we have said above tertium non datur ascertains that ρ is *a number*. That ρ is a number is nothing but that ρ is *a constant*.

The example where the discriminant of an equation cannot determine the multiplicity of its roots may be given independently of tertium non datur. Consider the quadratic equation

$$x^2+ax+b=0,$$

where a and b are certain numbers (i. e. constants). It cannot be settled whether this equation has a double root or not.

Brower has pointed out the uncertainty of the theorem determining the ordering of the set of all real numbers[1]. Let the decimal expansion of π be

$$\pi=3\cdot d_1d_2\ldots d_md_{m+1}\ldots d_{m+9}\ldots,$$

where $d_1=1$, $d_2=4,\ldots\ldots$ Suppose for the first time

$$d_m=0,\ d_{m+1}=1,\ldots\ldots,\ d_{m+9}=9.$$

Now put

$$c_\nu\equiv\left(-\frac{1}{2}\right)^m,\quad \text{if}\quad \nu\geqq m,$$

1. Crelle J. 3, **154** (1924).

or

$$c_\nu \equiv \left(-\frac{1}{2}\right)^\nu, \quad \text{if} \quad \nu < m.$$

Then $c_1, c_2, c_3, \ldots\ldots$ tend to a real number r, though we do not know whether $r>0$, $r<0$ or $r=0$. Therefore, real numbers are not ordered.

By tertium non datur m is an integer yet undetermined. Hence m is a constant. In other words, tertium non datur ascertains only that m is a constant. Consequently it is natural that r may not be ordered. But if r be a definite number, it will have two definitions, since we are assuming that all numbers are well defined. Therefore we should prove their congruence.

Here I want to insert Borel's interesting example[1].

Consider a sequence of numbers $a_1, a_2, \ldots\ldots, a_n, \ldots\ldots$ such that its general term a_n is

$$a_n = 0 \quad \text{or} \quad a_n = 1.$$

Put

$$x_n \equiv 1 + |a_1 - a_2| + \ldots\ldots + |a_{n-1} - a_n|,$$

$$x \equiv \lim \frac{1}{x_n}.$$

Next, we define a function $y(x)$ such that

$$y = 1, \quad \text{if} \quad x \neq 0,$$

or

$$y = 0, \quad \text{if} \quad x = 0.$$

Then though the series

$$y + a_1 y + (a_2 - a_1) y + \ldots\ldots + (a_n - a_{n-1}) y + \ldots\ldots$$

is convergent, its sum is zero if the sequence $a_1, a_2, \ldots\ldots, a_n, \ldots\ldots$ tends to no limit, while the sum will be 1 or 2 according as the limit of the sequence be 0 or 1.

The contradiction occurs since there is an infinite number of constants $a_1, a_2, \ldots\ldots, a_n, \ldots\ldots$

5. Russell's antinomy. According to Russell all sets of elements are divided into two classes by the condition whether a set contains itself as an element or not. All sets none of which contains itself as an

1. Méthode et problèmes de théories des fonctions, 17 (1922).

element, form a set M by Cantor's definition. This set M is contradictory. For we can neither assume that the set M contains itself as an element nor that the set M does not contain itself.

Now in general consider a set N which contains itself as an element. We may take the set into consideration since it has been defined by a certain definition. (Def. B) On the other hand, since the set N is contained in itself as an element, and all elements are well defined, the element N has already been defined. (Def. A) Therefore the set N has two definitions A and B. We must prove their congruence.

Let us return to Russell's antinomy. We have defined the set M. (Def. B) If the set M contains itself as an element, then M is already defined. (Def. A) On the contrary, even when the set M does not contain itself as an element, yet the set M has already been defined, (Def. B), since we are assuming that all sets none of which contains itself as an element are already well defined. In any case we have two definitions A and B for the set M. How can we prove the congruence of these two definitions?

Let us compare this antinomy with Richard's paradox explained in § 2. When the definition B loses its meaning without the definition A, it seems that the thing defined by the definition B exists *relative* to the thing defined by the definition A. The relativity of higher infinities has been remarked by Skolem[1]. But here we cannot give the same explanation to Russell's antinomy, since we are considering *all possible sets* none of which contains itself as an element and no sets higher than those are allowed to be considered.

Relativity in mathematics means nothing but that mathematics undergoes *creative evolution*. It is known that the cardinal number of the set of all possible sets is contradictory. But if we could conceive all possible sets, we might consider their totality. The totality is a newly created idea. This is the stand-point of the axiomatists of to-day.

The theory of sets is strongly explained by Hilbert[2] to be the study of actual infinity, ∞. The infinitesimal, its sign being o, has already been closely studied. o has another meaning, i. e., *nothing*. Everyone knows o, nothing, after which the idea of the infinitesimal has been evoluted by the discovery of the infinitesimal calculus. At the same time the potential ∞ i. e., $\lim x \to \infty$ has become known. To speak from my

1. Wissenschaftliche Vorträge, fünften Kongress der Skandinavischen Mathematiker, 222 (1922).
2. Math. Annalen, 161, **95** (1926).

present state of recognition, I can scarcely understand the actual ∞ in so far as it does not mean *all* things. Russell's antinomy relates to *all* sets. If the theory of sets be the study of *all*, it is not weakened by Russell's antinomy. On the contrary, it is a theme of our study. Russell's antinomy loses its meaning by the axiomatic study of the theory of sets. By axioms I understand those propositions which enable us to objectify the objects of individual persons. *All sets* in Russell's antinomy is not yet completely objectified.

6. Finally I wish to remark briefly on the relation of the tertium non datur to the equally like occurrence of events in probability. Suppose a coin is tossed. The event that the head will appear is equally likely as the event that the tail will appear. To assume that the head or the tail must appear is only reasonable from the point of view of experiments. But if we desire the theory of probability to be regarded as a mathematical theory, then since exact mathematics is independent of any experiments, we must consider the following possibilities:

(1) The head will appear.

(2) The tail will appear.

(3) No reason to ascertain (1) and (2).

Only in such a case, events are said to occur equally likely and their probability is $\frac{1}{2}$. This idea is different from those of Jacob Bernoulli, Laplace and v. Kries[1].

---

1. Cf. Czuber, Wahrscheinlichkeitsrechnung, 1. Bd.

The Arrangement of the Micro-Crystals in Compressed Magnesium and Aluminium Plates

By

Shogo Tsuboi

(Received June 8, 1928)

Abstract

When a circular plate of magnesium is compressed the micro-crystals of which the metal is composed, tend to direct the principal axis of the hexagonal crystal in the direction of compression. The fibrous arrangement of the micro-crystals obtained by compressing a circular plate of aluminium takes the [110] axis of the crystal of aluminium as the axis of the fibre in the direction of compression, and corresponds to that of the complete rotation of micro-crystals. In the case of the compression of a long elliptic plate of aluminium it is a little different. In the neighbourhood of the minor axis of the ellipse, where the metal flows in the direction of this axis, the axis of the fibre becomes now the [112] axis of the specimen in a direction parallel to the minor axis of the specimen; and one of the (110) planes tends to be nearly perpendicular to the direction of compression. While at the end of the major axis of the ellipse the structure is the same as in the case of the compressed circular plate. Thus the fibrous structure depends both on the direction of compression and on the direction of the flow of the metal by compression.

A. Magnesium

A test piece of magnesium in the form of a circular plate of 2.4 mm. thickness and of 3 mm. diameter was cut out from a cast magnesium block, and this test piece was compressed down to a thickness of 0.4 mm. The Laue-photographs with this specimen, were taken by sending a narrow beam of x-rays from a molybdenum target, in the following two directions:

(1) a direction normal to the surface of the specimen (Fig. 1 Plate I), and

(2) a direction parallel to the surface of the specimen (Fig. 2 Plate I).

The normal incidence of the x-rays gave the ordinary Debye-Hull's rings. Comparing the Hull data with the observed lattice constants of various atomic planes of the hexagonal crystal of magnesium, which were obtained from the values of the radii of the concentric rings on the photograph, we know that there are lacking the reflections of the x-rays from the atomic planes, of the crystal of magnesium, which have the indices (0001) (lattice constant d=2.59 A. U.), ($10\bar{1}2$) (d=1.90 A. U.) and ($10\bar{1}3$) (d=1.48 A. U.) as shown in Table I. The reason for this will be given later.

Table I.

lattice const. (obs.)	Hull's data	
—	2.59	(0001)
2.42	2.44	($10\bar{1}1$)
—	1.90	($10\bar{1}2$)
1.59	1.60	($11\bar{2}0$)
—	1.48	($10\bar{1}3$)
1.34	1.38	($10\bar{1}0$)

In the case of the parallel incidence of the x-rays to the surface of the specimen, the Laue-photograph shows that most of the micro-crystals of the compressed magnesium are nearly arranged fibrously. Fig. 1 shows the curves calculated, as will be described below; and as this figure represents well the general features of Fig. 2, Plate I, it may be looked upon as a simplified sketch of Fig. 2, Plate I, for convenience' sake. In order to explain Fig. 1 the writer takes, for the present, the principal axis (the [0001] axis) of the hexagonal crystal of magnesium as the common axis of the fibre. This suggestion is obtained from the consideration that the axis of the fibre will be in the direction of compression and the fact that though the impression of the 0001 ring is absent in the case of a normal incidence it appears intensely in the case of the parallel incidence, which is marked No. 1 in Fig. 1. If the micro-crystals of magnesium are arranged exactly in the fibrous arrangement considered above, we ought to obtain sharp bands radiating outwards from the centre of the direct image on the photograph. But this is not actually so, and the bands are diffused on the photograph reproduced in Fig. 2, Plate I. This shows that the micro-crystals are not arranged exactly in the fibrous manner: and the writer supposed that the crystallographic axis [0001] of the

fibrous arrangement of the micro-crystals were scattered to some extent from a direction perpendicular to the surface of the compressed specimen. If so the angular breadth of any radiating band, which is to be measured in reference to the centre of the direct image, will represent the degree of scattering of the crystallographic axis [0001] of the fibrous arrangement of the micro-crystals from a direction perpendicular to the surface of the specimen. This degree of scattering was measured by the angular breadth of the radiating band in Fig. 2, Plate I, which corresponds to the spectrum No. 1, in Fig. 1, in the position of the K_α spectrum of molybdenum on it, and the maximum angle of this scattering from a direction perpendicular to the surface of the specimen was estimated to be about 23°. Then the angle α which the direction AB in Fig. 1, drawn parallel to the surface-normal of the specimen on the photograph, makes with the line connecting the central spot with either of the two ends of the K_α spectrum-line on any radiating band, will be given by the expression

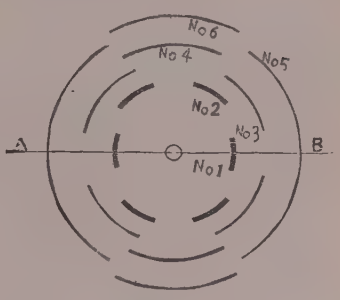

Fig. 1.

$$\cos \alpha = \frac{\cos (\beta \pm 23^\circ)}{\cos \theta} .$$

Where β is the angle between the crystallographic axis of the fibrous arrangement and the direction representing the normal of the atomic plane to which is due the radiating band under consideration; and θ is the glancing angle of the K_α radiation of molybdenum to that atomic plane. The values of α thus calculated are shown in Table II; and the calculated curves with these values of α are shown in Fig. 1, the general features of which are in fine accordance with the photograph reproduced in Fig. 2, Plate I. This accordance seems to indicate the appropriateness of our previous consideration about the arrangement of the micro-crystals.

Table II.

Indices		$\alpha_{min.}$	$\alpha_{max.}$
No. 1	0001	0°	23°
No. 2	10$\bar{1}$1	38°	85°
No. 3	10$\bar{1}$2	17°	66°
No. 4	11$\bar{2}$0	66°	90°
No. 5	10$\bar{1}$3	0°	59°
No. 6	1010	66°	90°

Let us now again consider the case of the normal incidence of the specimen. If the above consideration is correct the K_α radiation of molybdenum will be reflected only towards the photographic plate from the atomic planes for which the following two conditions are satisfied:

(1) $\beta-23^\circ<\frac{\pi}{2}-\theta<\beta+23^\circ$,

(2) all or at least some of the values between $2(\beta-23^\circ)$ and $2(\beta+23^\circ)$ are greater than 90°.

Table III.

Indices	θ	β	β−23°, 90°−β, θ+23°	2(β−23°), 2(β+25°)		Remarks
0001	7°50′	0°	−23° 82°10′ 23°	−46°	46°	—
$10\bar{1}1$	8°20′	62°	39° <81°40′< 85°	78°	170°	appeared
$10\bar{1}2$	10°50′	43°20′	20°20′ 79°10′ 66°20′	40°20′	132°40′	—
$11\bar{2}0$	12°50′	90°	67° <77°10′<113°	134°	226°	appeared
$10\bar{1}3$	13°50′	32°	9° 76°10′ 55°	18°	110°	—
$10\bar{1}0$	14°50′	90°	67° <75°10′<113°	134°	226°	appeared

The atomic planes satisfying these relations are $(10\bar{1}1)$, $(11\bar{2}0)$ and $(10\bar{1}0)$ as shown in Table III; and the reflections from these planes were actually observed as was stated before.

B. Aluminium

The results obtained by the writer on the compressed circular plate of aluminium are the same as those of Prof. Ono[1] of the Imperial University of Kyushu. The common axis of the fibrous arrangement of the micro-crystals is the [110] axis of the cubic crystal of aluminium in the direction of the compression of the plate, and the structure corresponds to that of a complete rotation of the micro-crystals.

Prof. Ono's results and also those of the writer show that the arrangement of the micro-crystals in a compressed circular plate of aluminium depends only upon the direction of compression, and no particular relation

1 Memoirs of the College of Eng., Kyushu Imp. Univ., III, 1923—25.

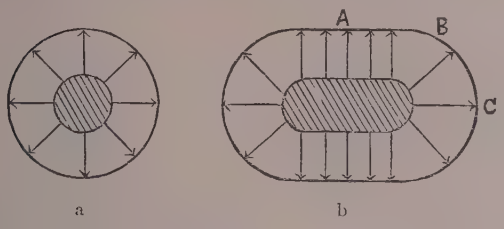

Fig. 2.

of it was found as regards the direction of the flow of metal by compression, which is schematically shown by Fig. 2 a. But actually the arrangement of the micro-crystals must depend, directly or indirectly, upon the manner of the flow of the metal by compression, and this point was examined by compressing a long elliptic plate of aluminium.

A specimen of the shape shown in Fig. 2 b by the shaded portion, was cut out from a commercial plate of aluminium; and its thickness was reduced from 1.8 mm. to 0.13 mm. by compression. A rough sketch of the direction of the flow of the metal by compression is shown by the arrows in Fig. 2 b.

First, the minor axis of the compressed elliptic plate was set in a vertical direction and a narrow beam of the x-rays was made to strike the specimen horizontally, at the portion denoted by A in Fig. 2 b, in a direction normal and then parallel to the surface of the specimen. The Laue-photographs thus obtained are reproduced in Figs. 3 and 4, Plate I. Here Fig. 3, Plate I is the photograph obtained by the normal incidence, and Fig. 4, Plate I is that obtained by the parallel incidence of the x-rays on the surface of the specimen. Here it must be remarked that in examining the various portions of the specimen by x-rays, the small portion of the specimen which is to be examined is separated from the remainder of the specimen by etching the specimen carefully and very slowly with some dilute acid. This method of excising a small specimen was also utilized with the plate of magnesium.

These two photographs show the presence of the fibrous structure of what is often seen in the case of the rolled foils of some ordinary metals such as Pt, Ag, etc. The axis of the fibre, in this case, the [112] axis of the cubic crystal of aluminium, which is arranged parallel to the direction of the flow of the metal by compression; and the photographs seem to be explainable as such fibrous arrangement of the micro-crystals with incomplete rotation. In Fig. 3, the assemblage of the dots

and the small circles represents the K_α spectra of *Mo*, which are to be impressed on the photographic plate, when the micro-crystals of aluminium are arranged in the fibre above mentioned with complete rotation. However, in Fig. 3, Plate I, only one set of the spots represented by the dots in Fig. 3 appear; and the other sets of spots represented by the small circles in Fig. 3 appear in Fig. 4, Plate I. In the case of the latter photograph, where the x-ray-beam illuminated the specimen in the direction parallel to the surface of the specimen and perpendicular to the direction of the minor axis, two spots due to the atomic plane (110) appear on the horizontal line AB in Fig. 3, which was drawn parallel to the surface-normal of the specimen on the photographic plate, so as to pass through the centre of the direct image. This fact teaches us that one of the atomic planes (110) of the micro-crystals takes an orientation roughly parallel to the surface of the specimen. In the case of Fig. 3, Plate I, where the x-ray-beam illuminated the specimen in a direction both perpendicular to the surface of the specimen and the direction of the minor axis, two spots due to the atomic plane (111) appear on the horizontal line AB in Fig. 3. This indicates the presence of one of the atomic planes (111) of the micro-crystals in an orientation roughly perpendicular to the surface of the specimen. Considering these facts, the ideal orientation of the micro-crystals in the specimen seems to be such as is represented in Fig. 4. The crystallographic axis [112] runs parallel to the direction of the minor axis, which is the direction of flow of the metal by compression; the atomic plane ABC (110) is parallel to the surface of the specimen. This is, of course, an ideal arrangement of the micro-crystals as stated above; and the real one will be such that their orientations are scattered, within a certain limit away from the ideal one. The photographs Figs. 3 and 4, Plate I seem to be explainable on the consideration that the micro-crystals take the orientations rotated around the axis [112], which is the axis of the fibre, with some angles smaller than about 30° in two opposite senses from the

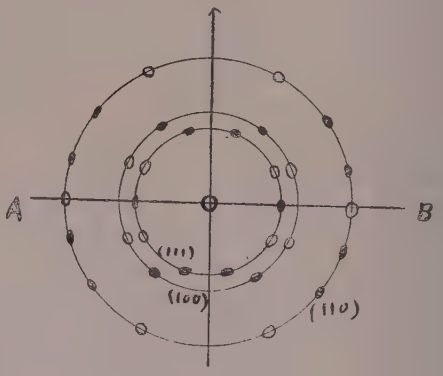

Fig. 3

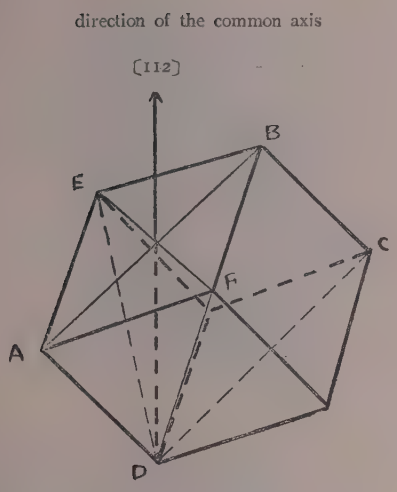

Fig. 4.

ideal orientation,

Next, the arrangement of the micro-crystals in the portion denoted by *C* in Fig. 2 b was examined, which is in the vicinity of the end of the major axis of the compressed elliptic plate. All the Laue-photographs taken of this portion of the specimen were the same respectively as those obtained with the compressed circular plate, as was to be expected from the similarity of the flow of metal by compression in both cases (Figs. 5, 6, 7, Plate I). The common axis of the fibrous structure was found to be [110] axis lying parallel to the direction of compression of the specimen and the micro-crystals showed complete rotation.

Lastly, sending the x-ray-beam normally to the surface of the specimen, the various portions near the edge of the compressed elliptic plate were examined successively by taking the Laue-photographs. When we come from the portion B to C in Fig. 2 b, the K_α lines of molybdenum on the photograph increased successively in their lengths, and, finally, become an ordinary Debye-Hull ring at the portion denoted by C in Fig. 2 b, which is in the vicinity of the end of the major axis. This fact teaches us that there is an intimate connection between the two different arrangements of the micro-crystals in the neighbourhood of the minor axis, and at the end of the major axis of the compressed elliptic plate. The ideal arrangement of the micro-crystals in the neighbourhood of the minor axis is stated already to be such that their atomic planes (110) are parallel to the surface of the specimen, and their [112] axis run in the direction of flow of the metal by compression. When we come from the portion A to C in Fig. 2 b, the lines representing the direction of the flow of the metal become gradually divergent; and the axes [112] of the micro-crystals will also become divergent at the same time, by keeping the orientation of the planes (110) unaltered. This means that the micro-crystals are rotated a little around the axis [110], which is in the direction of the surface-normal of the specimen. The angle of such rotation of the micro-crystals increases gradually as we proceed from the portion B

to C in Fig. 2 b, and finally the rotation becomes complete in the portion C. This final state of rotation is nothing but the ideal arrangement of the micro-crystals in the compressed circular plate of aluminium. Thus the arrangement of the micro-crystals in a compressed aluminium plate depends not only on the direction of compression of the specimen, but also on the direction of the flow of the metal by compression.

In conclusion, the writer wishes to express his sincere thanks to Professor U. Yoshida of the Kyoto Imperial University for his kind guidance and encouragement during this research.

Shiga Normal School.

Plate I

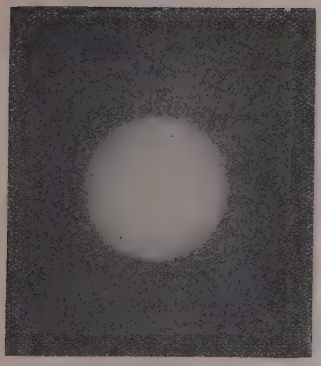

Fig. 1

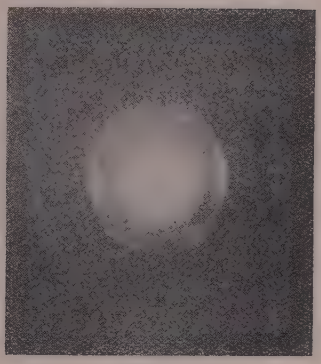

Fig. 2

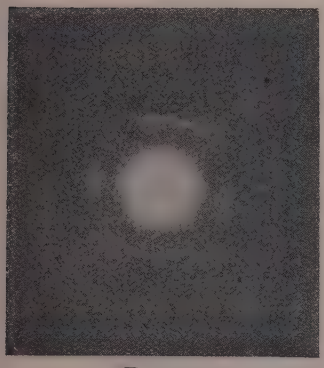

Fig. 3

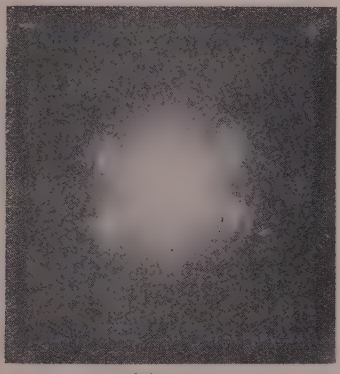

Fig. 4

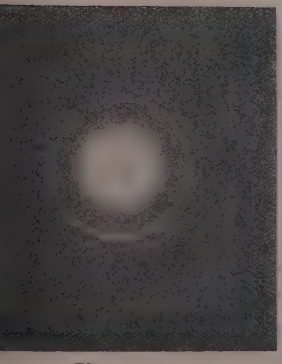

Fig. 5
(normal incidence)

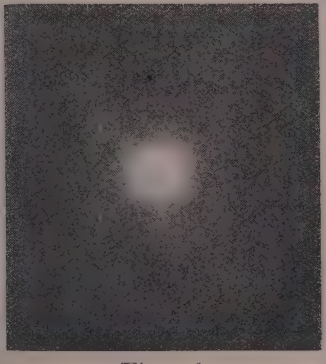

Fig. 6
(parallel incidence)

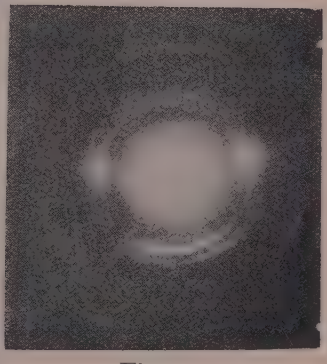

Fig. 7
(45° incidence)

The Electrolytic Oxidation of Alcohols, III. Electrolytic Oxidation of Benzylalcohol.

By

Shunzo Koidzumi

(Received June 23, 1928)

Among investigations into electrolytic oxidation reactions of the hydrocarbon sidechains attached to the benzene ring, that on toluene has been already attempted by H. D. Law and F. M. Perkin[1], Merzbacher and Smith[2], and Renard[3], etc. The oxidation products which varied according to the conditions of electrolysis consisted chiefly of benzaldehyde, and the formation of benzoic acid was scarcely to be noticed while the maximum current yield was reported to be 14 percent, and the yield in material 15 percent for benzaldehyde. Later on, Fichter and Stocker[4] have pointed out that by the electrolytic oxidation of toluene, hydroquinone and toluhydroquinone are formed side by side with benzaldehyde, thus showing a difference in progress of reaction of the electrolytic oxidation from that of the purely chemical oxidation of benzene derivatives. In 1920 Fichter[5] investigated the electrolytic oxidation of benzaldehyde and benzoic acid, and attempted an elucidation of the mechanism of reaction in the electrolytic oxidation of toluene.

Notwithstanding this, there is not yet any record found of any experimental study of the electrolytic oxidation of benzylalcohol which is considered to be the first oxidation stage in the progress of the electro-

1 Chem. News, **91** (1904), 54; Ibid., **92** (1905), 69; Trans. Farad. Soc., **1** (1905), 31.
2 J. Am. Chem. Soc., **22** (1900), 723.
3 Compt. rend., **91** (1880), 175.
4 Ber., **47** (1914), 2003.
5 Helv, Vol. III (1920), 22.

lytic oxidation of toluene. If in electrolytic oxidation toluene changes to benzaldehyde through the stage of benzylalcohol thus:

$$C_6H_5CH_3 \rightarrow C_6H_5CH_2OH \rightarrow C_6H_5CHO$$

then the electrolytic oxidation of benzylalcohol may also be expected chiefly to stop at the stage of benzaldehyde without so far proceeding as to give benzoic acid. To see if such really be the case the present investigation was undertaken.

Material used: Benzylalcohol B. P. 204°–206° C., Sp. Gr. 1.0445 $\frac{25^\circ}{25^\circ}$

I. Reaction in an Acid Electrolytic Solution

Since it was found by a preliminary experiment, that the oxidation efficiency was increased by stirring the electrolytic solution while the decomposition was accelarated by the rise of temperature, the solution was always stirred and the temperature kept at or below the room temperature.

As to the stirring device, a porous cylinder containing the cathode solution was immersed into the anode solution and made to rotate, and it was found to work very effectively. As is shown in the illustration, the porous cylinder was tightly stoppered with a rubber stopper through which a stout glass tube carrying a wire connected with a cathode passes, and this glass tube served as a rotating shaft. A little mercury was poured into this rotating shaft and a conducting wire from a cathode terminal was dipped into it. Two slender glass rods were attached to the wall of the cylinder to make the stirring effective.

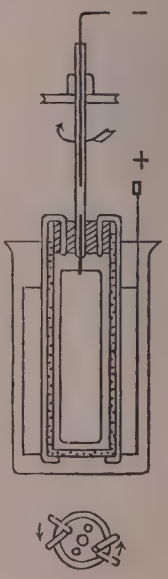

Treatment after Electrolysis:

The brown-colored electrolyzed solution, acid with sulphuric acid, was saturated with sodium sulphate and repeatedly extracted with ether. To the ether extract a conc. solution of sodium sulphite (prepared by dissolving 20 gr. in 60 cc. of water) was added and the mixture set aside for 24 hours with occasional shaking. The addition product of benzaldehyde and acid sodium sulphite $C_6H_5CH(OH)SO_3Na$ which separated out was then filtered and the acid sodium sulphite solution remaining below the

ether solution was separated, and, after neutralization with sodium carbonate, was subjected to steam distillation. If the aldehyde appeared in the distillate in an oily form, it was dissolved by addition of a small volume of alcohol and made up to 1 litre. Out of the total volume of 1 litre, 100 cc. were taken out for precipitating the aldehyde with phenylhydrazine. From the weight of the benzylidenephenyl-hydrazine (m. p. 153°) thus obtained, the total weight of the aldehyde in the whole distillate was calculated. To this amount of the aldehyde the amount calculated from the addition product of acid sodium sulphite was added and the grand total was taken as the final yield of the benzaldehyde.

The ether extract from which the benzaldehyde was separated was now shaken with a sodium carbonate solution in order to isolate the acidic products in it. When the sodium carbonate solution was separated and acidified with sulphuric acid, benzoic acid (m. p. 120°) was liberated.

Finally, the residual ether extract was evaporated and a small quantity of a brown liquid was obtained which sometimes contained, beside the original benzylalcohol that escaped the reaction, a small quantity of benzyl-benzoic acid, distilling between 320° and 340°. There was always found a small quantity of a tarry residue after distillation.

(1) Anode: Lead peroxide (12 × 18.5) 222 sq. cm.
Anode solution: 300 cc. of 0.5 N-H_2SO_4 to which 20 g. of the sample were added.
Cathode: Iron plate.
Cathode solution: 0.5 N-H_2SO_4
Temperature: 14° ± 1°.

Current quantity	Current density amp/sq. cm.	Sample used	Sample recovered	Benzaldehyde		Benzoic acid	
				Current yield	Material yield	Current yield	Material yield
24 amp. hours	0.009	20 g	1.0 g.	4.18 g.		7.50 g.	
				8.79%	22.39%	27.45%	34.94%
do.	0.018	20	1.5	3.62		8.01	
				7.62	19 94	29.30	38.32
do.	0.027	20	2.4	3.66		7.2	
				7.71	21.18	26.34	36.21
18 amp. hours	0.0135	20	2.8	7.32		5.50	
				30.53	43.34	26.83	28.31

From the above results it may be concluded that the variation of current density does not exert any great influence upon the yield of the reaction product, while the variation of current quantity exerts a rather considerable influence upon it. Thus while the yield of the aldehyde decreases with the increase of current quantity, the yield of the acid does not show any corresponding increase, showing that, above a certain limit of current quantity, the current is expended not simply for the oxidation of the aldehyde into acid but for the oxidation of the benzene nucleus, or some destructived oxidation, thus resulting in the decrease of its oxidation efficiency. When, for 20 g. of the material, a far greater quantity of current was used than the amount calculated as necessary, the yield of benzoic acid was about 8 g. With a still greater excess of current, there was found, besides the nuclear and destructive oxidation, the formation of a phenol derivative which gave a purple color reaction with ferric chloride.

(2) The Influence of the Electrodes.

Anode solution: 300 cc. of 1 N$-H_2SO_4$ with 20 g. of the material added.

Cathode: Lead.

Cathode solution: Similar to the anode solution.

Temperature: $15^\circ \pm 1^\circ$.

Anode	Current	Sample used	Sample recovered	Benzaldehyde		Tarry residue	Fraction 210°—260°
				Current yield	Material yield		
Platinum foil 7.1×5.1=36.21 sq. cm.	0.0829 amp./sq. cm. 24amp. hours	20 g.	14.2 g.	3.924 g.		about 1 g.	about 0.5 g.
				8.26%	68.93%		
Platinum gauge 5.0×11.0=55 sq. cm.	0.0545 amp./sq. cm. 9 amp. hours	20	13.1	4.276		„ 1	„ 1
				24.01	63.14		
Platinum gauge 5.0×11.0=55 sq. cm.	0.0545 amp./sq. cm. 24amp. hours	20	12.9	4.121		„ 1.5	„ 0.5
				10.92	59.13		
Gold foil 8×7.5 =60 sq. cm.	0.0667 amp./sq. cm. 24amp. hours	20	13.3	3.329		„ 1	„ 0.7
				6.97	50.31		

As may be seen from the above table, when platinum and gold electrodes are used, the oxidation efficiency of the current is far lower than when the lead peroxide electrode is used. Moreover, in the former cases, there is hardly any formation of benzoic acid noticeable even with the

expenditure of 24 ampere-hours of the current. The fractions boiling at 210°—260° being very small in amount were gathered and subjected to repeated fractionation, but no substance giving a constant boiling-point was separated except that a little more benzylalcohol was recovered. The tarry residue, though small in amount, was always found even when the fractionation was carried on under diminished pressure or in a current of carbon dioxide gas.

(3) The Influence of the Concentration of Sulphuric Acid.

Anode: Lead peroxide, 222 sq. cm.

Cathode: Iron plate.

Cathode Solution: The same as the anode solution.

Temperature: 15°±2°

Current density: 0.01802 amp./sq. cm.

Current quantity; 24 amp.—hours.

Anode Solution 300 cc. H_2SO_4	Current quantity amp.-hours.	Material used	Material recovered	Benzaldehyde		Benzoic acid		Tarry resid.
				Current yield	Material yield	Current yield	Material yield	
0.5 N	24	20 g.	1.5 g.	3.62 g.		8.01 g.		
				7.62%	19.94%	29.30%	38.32%	
1—N	24	20	0.8	3.58		8.21		
				7.53	19.00	30.03	37.85	less than 1 g.
2—N	24	20	—	5.661		8.15		
				11.92	28.84	29.82	36.08	
2—N	18	20	2.0	5.633		7.20		
				15.81	31.88	35.12	35.41	

In the neighborhood of the sulphuric acid concentration of 2—N, the total oxidation efficiency is greatest, while the decomposition is correspondingly great and the electrolytic solution is colored a deep brown. In the electrolysis of sulphuric acid solutions phenol derivatives are found only when a great excess of current is passed, and as is shown by the instances given above, the passage of a current of 24 ampere-hours against the calculated quantity of 19.84 am.-hours does not induce the formation of any phenol derivatives detectable by the ferric chloride reaction. Yet even in these cases, it sometimes happens that a minute quantity of a coloring matter giving a distinct purple colour by an alkali is contained in the tarry matter produced to a more or less extent. It

may be conjectured that the coloring matter[1] here mentioned is formed by the condensation of the phenol produced in minute quantity in the electrolytic solution with benzaldehyde by the action of the accumulated sulphate ions on the anode surface.

II. Reactions in an Alkaline Electrolytic Solution.

Treatment after electrolysis.

The alkaline solution after electrolysis was repeatedly extracted with ether. The ether extract was completely dehydrated by means of anhydrous sodium sulphate and then the ether distilled off. The remaining liquid was subjected to fractional distillation in a carbon dioxide atmosphere to prevent the oxidation of benzaldehyde.

The electrolyzed alkaline solution, thus deprived of benzaldehyde and benzylalcohol by ether extraction, was now completely neutralized with sulphuric acid and concentrated by the low temperature distillation under diminished pressure. From the resulting liquid benzoic acid was liberated by acidification.

(1) Anode: Platinum gauge, 55 sq. cm.
Anode solution: To 300 cc. of 2N−NaOH solution were added 20g. of benzylalcohol. The mixture was well stirred in a closed anode chamber.
Cathode: Nickel gauge.
Cathode solution: The same as the anode solution.
Current density: 0.07273 amp./sq. cm.
Temperature: 25°±2°.

Current	Material		Benzaldehyde		Benzoic acid	
	taken	recovered	Current yield	Material yield	Current yield	Material yield
24 amp.-hours	20. g.	0.8 g.	12.5 g.		2.85 g.	
			26.31%	66.33%	10.42%	13.14%
28.8 amp.-hours	20	—	9.8		2.9	
			17.19	49.93	8.84	12.83

In this case as in the case of electrolysis in an acid solution, the increase of current quantity does not practically accompany the increase of the yield of the acid while that of the aldehyde actually decreases.

1 Melzer, Zeit. f. anal. Chem., **37** (1898), 345.

Thus the current efficiency in oxidizing the aldehyde into benzoic acid is very slight, and not only does it decrease beyond a certain quantity of current, but it even induces a decomposition reaction at the same time. If the volume of the gas evolved in the tightly sealed anode chamber is examined the evolution of oxygen is found to increase in proportion to the duration of the electrolysis. The carbonic acid formed by the decomposition reaction is completely absorbed by the alkaline electrolytic solution. In 500 cc. of the anode gas collected under the above-mentioned condition, the presence of hydrogen could not be detected.

(2) All the conditions were made the same as the above, except that the temperature was kept at 0°.

Current	Material		Benzaldehyde		Benzoic acid	
	taken	recovered	Current yield	Material yield	Current yield	Material yield
24 amp.-hours	20 g.	1 g.	10.8 g.		2.7 g.	
			22.74%	57.90%	9.88%	12.58%

As may be seen from the results, even when the solution is cooled down to 0° during the electrolysis, it gradually assumes a brown colour accompanied by a destructive oxidation and the yield of the products remains unchanged.

(3) The Influence of the Concentration of Alkalis.

i) The temperature was kept at $25° \pm 2°$ and the electrodes, current density, current quantity etc. remained the same as before.

Anode solution	Material		Benzaldehyde		Benzoic acid	
	taken	recovered	Current yield	Material yield	Current yield	Material yield
0.5 N NaOH	20 g.	0.8 g.	9.10 g.		2.9 g.	
			19.15%	48.28%	10.61%	13.38%
1 N NaOH	20	0.5	10.8		2.87	
			20.74	56.43	10.50	13.03
2 N NaOH	20	1.5	11.0		2.85	
			23.16	60.57	10.42	13.63

ii) The anode solution consisted of 300 cc of $2N-Na_2CO_3$ solution mixed with 20 g. of the material. Current quantity and the other con-

ditions all remained the same as before.

2−N Na_2CO_3	20 g.	2 g.	12.50 g.		Benzoic acid could not be separated.
			26.31%	70.74%	

In the electrolysis of alkaline solutions, the yield of benzaldehyde is greatest when a sodium carbonate solution is used as the anode solution and its material yield reaches 70.74% while the formation of benzoic acid is scarcely noticed.

When the electrolyzed solution was completely extracted with ether and the benzoic acid liberated was filtered off, the solution still retained a deep brown colour. Although various organic solvents were tried in order to obtain some further electrolytic products from this coloured solution, their extraction was found to be a difficult matter. However, a mixture of amylalcohol and ether repeatedly shaken with the deep brown solution, extracted almost completely the colouring matter from it. When this alcohol-ether extract was separated and subjected to distillation under a diminished pressure, a black tarry residue weighing about 1 g. was obtained, the nature of which has not yet been made clear.

From the experimental results so far described it may be concluded that the electrolytic oxidation of benzylalcohol generally takes place so as to produce benzoic acid as well as benzaldehyde, and differs from that of toluene which, as was stated before, does not proceed further than the aldehyde formation. In an acid solution when platinum is taken as the anode, and also in a sodium carbonate solution, benzylalcohol is, however, not oxidizable to benzoic acid, benzaldehyde being the final oxidation product.

The present investigation was carried out under the guidance of Professor M. Matsui with the expenses defrayed from a fund granted to him by the Imperial Academy of Japan. It is therefore the pleasant obligation of the author to acknowledge his indebtedness to Professor Matsui and to the Imperial Academy.

The Electrolytic Oxidation of Alcohols, IV. Electrolytic Oxidation of Propylalcohol in Alkaline Solutions

By

Shunzo Koidzumi

(Received July 3, 1928)

According to Habermann[1] and E. Müller[2] when methylalcohol, the lowest member of the aliphatic alcohols, is subjected to electrolytic oxidation in a concentrated solution of caustic soda, hydrogen is evolved in great quantities at the anode; whereas if ethylalcohol is subjected to the same treatment there are evolved at the anode hydrogen and methane as the chief products in addition to a small quantity of ethane. As to the mechanism of the above reaction different explanations have been proposed by E. Müller[3] on the one hand and Fr. Fichter[4] on the other; the latter assumes the intermediate formation of a peroxide, while the former considers it more probable that alcoholate ions change temporarily to the compounds containing a pentavalent carbon atom, such as $RCH_2:O$.

Both of these explanations have, however, received no confirmation yet and as the elucidation of such a mechanism may lead to the clearing up of the real nature of the Kolbe reaction, the present writer has attempted to investigate the electrolytic oxidation of the higher alcohols

1 Monatsh., **7** (1886), 540.

2 Zeit. f. Elekt. Chem., **20** (1914), 367; Ann., **420** (1920), 241; Zeit. f. Elekt. Chem., **27** (1921), 54; **27** (1921), 563.

3 Zeit. f. Elekt. Chem., **27** (1921), 54; **27** (1921), 563; **28** (1922), 101.

4 Helv. Chem. Acta, 1 (1918), 146; Zeit. f. Elekt. Chem., **27** (1921), 489.

with the expectation to get some insight into the above stated relation. Furthermore, a perusal of the literature of a similar experimental study of the aliphatic alcohols reveals the fact that there are, regarding monatomic alcohols higher than propylalcohol, only the experiments made by Müller, which rather negate the previous reactions. According to him, the evolution of anodic hydrogen was extremely small, and no reaction similar to that of methyl or ethyl alcohol could be recognized, and he came to the conclusion that it was impossible to realize a reaction leading to the anodic formation of a combustible gas from monatomic alcohols higher than propylalcohol by means of the electrolysis. It is conceivable, however, that this fact is caused by the inadequacy of concentration of the higher alcohol in the anode solutions due to the scantiness of its solubility in the caustic soda solutions. Starting from this conception, the present writer attempted to examine the anodic reaction of the higher monatomic alcohols, taking methylalcohol as the solvent for increasing their concentration. Propylalcohol was first subjected to the operation and the evolution of a fairly large quantum of combustible gases such as ethane and ethylene, etc., besides hydrogen, was clearly recognized, and conclusive evidence for the production of a similar reaction to that of the lower alcohols was secured.

Methylalcohol used as the material for experiment was of B. P. 65°—66°, and sp. gr. $0.797\frac{15^\circ}{15^\circ}$. It was prepared by redistillation of Merck's sample.

n-Propylalcohol used as the material was of B. P. 97°—98° and sp. gr. $0.807\frac{15^\circ}{15^\circ}$. It was prepared by redistillation of Kahlbaum's sample.

Apparatus used for Electrolysis.

The electrolyzing apparatus as shown in the figure was thus contrived. The bell jar A carries a tube closed at one end into which a small quantity of mercury is poured and a thermometer inserted. The anode plate stands within the jar upon a glass tube bent in U-form to which its stem is firmly sealed. The jar and the anode are sunk into a porous earthenware cylinder filled with the anode solution. By filling the jar completely with the anode solution, by application of suction at the three-way cock C_1, and then beginning the electrolysis, it is possible to collect all the gases evolved at the anode in an uncontaminated state in the bell jar. The gas burette B and the gas reservoir D and all the capillary tubes connecting them with the cock C_1 were completely filled

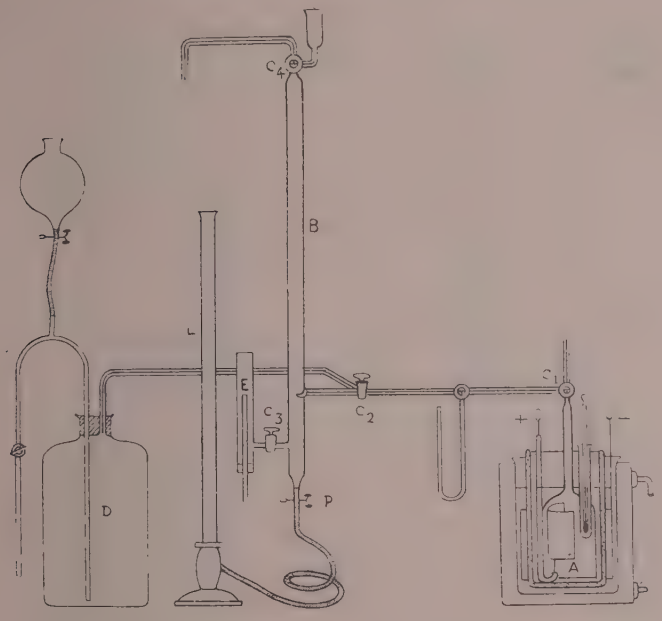

with water saturated with the anode gas before acutal measurement was commenced. From time to time during the electrolysis, the anode gas evolved in the jar was transferred to the burette and the volume read off. The levelling tube E is provided for the purpose of regulating the gas pressure when it is led into the burette B. D is a provisional gas reservoir. The volume of the gas in the burette B is measured by closing the three-way cock C_2 and the stop cock C_3, opening the pinch cock P, and adjusting the pressure to the prevalent atmospheric pressure by moving the levelling tube L up and down. The gas is then transferred to an ordinary gas-burette to be subjected to analysis.

I. Methylalcohol.

Anode:	Platinum plate 36.21 sq. cm. (7.1 × 5.1), active surface 72.42 sq. cm.
Anode solution:	175 cc. of 8 N−NaOH mixed with 175 cc. of CH_3OH.
Cathode:	Nickel gauge.
Cathode solution:	4 N−NaOH.
Temperature:	15°−17° C.
Current:	1 amp.
Current densito:	0.0138 amp./sq. cm.

Table I.

Duration of electrolysis	Anode gas cc./hour	CO_2	O_2	CO	H_2
0— 1	25.5	0	19.5	1.2	79.0
1— 2	23.9	0	19.0	1.0	79.5
2— 3	22.6	0	17.0	1.5	81.1
3— 4	24.7	0	16.4	1.2	82.0
4— 5	25.0	0	16.0	1.6	82.0
5— 7	23.5	0	14.5	1.3	83.7
7— 9	23.3	0	14.2	1.3	84.3
9—11	23.0	0	13.8	1.4	84.5
11—13	22.8	0	14.4	1.3	84.0
13—15	21.9	0	14.1	1.5	84.1
15—17	21.5	0	16.2	2.6	81.0
17—19	21.0	0	17.6	2.2	79.8
19—21	20.9	0	17.5	—	—
21—23	21.0	0	15.1	2.0	82.6
23—25	19.5	0	17.9	2.1	79.0
25—27	17.7	0	17.4	2.6	79.8
27—29	14.5	0.2	18.0	6.1	75.6
29—31	14.0	9.1	19.1	15.5	56.1
31—51	21.5	18.6	15.0	54.5	11.7
51—55	22.0	25.2	23.8	35.9	14.8

The above results may be represented in curves for the individual constitute gases in the figure on the next page.

As can be clearly seen from the curves, in the neighborhood of 30 hours after the commencement of electrolysis, the evolution of anode hydrogen diminishes rapidly and that of carbon monoxide increases equally rapidly, while carbon dioxide begins to be freshly formed. This change is probably an indication of the ending of the characteristic reaction, and the sudden increase of carbon monoxide and the new evolution of carbon dioxide is due to the destructive oxidation of aldehyde and acid.

By the experiments above described it was ascertained that the particular gases evolved at the anode during the electrolytic oxidation of methylalcohol consisted of hydrogen and a small quantity of carbon-monoxide alone and that there was no production of hydrocarbons. Steps were therefore taken to examine the reactions of the anodic oxidation of

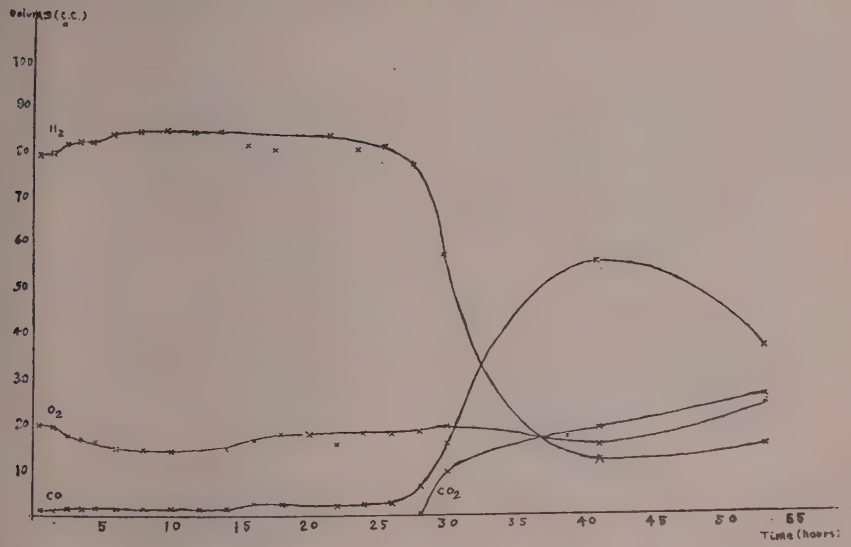

higher monoatomic alcohols in a caustic soda solution with methylalcohol as solvent.

II. Normal Propylalcohol.

Anode :	Platinum plate 72.42 sq. cm. (active surface)
Anode solution :	150 cc. of 8 A—NaOH mixed with 75 cc. of CH_3OH and 75 cc. of $CH_3CH_2CH_2OH$
Cathode :	Nickel gauge.
Temperature :	20°—25°.
Current density :	0.0138 amp./sq. cm.

Table II.

Gas employed	100.0 cc.		
After absorption with conc. KOH soln.	73.8	26.2%	CO_2
" " " Bromine water	61.7	12.1	C_nH_{2n}
" " " Alkaline pyrogallic acid soln.	54.5	7.2	O_2
" " " Ammoniacal Cu_2Cl_2	45.4	9.1	CO
20cc. of the remaining gas were mixed with oxygen to	99.2		
After explosion	65.7		
Contraction by explosion (C_X)	33.5	37.7%	H_2
After absorption with conc. KOH soln.	58.8		
Contraction by absorption with KOH (C_{KOH})	6.9	7.8%	C_2H_6

By the electrolysis extending over 30 hours there were collected about 800 cc. of anode gases. Analysis of a portion thereof gave the results as is seen in the table II.

As the presence of saturated as well as unsaturated hydrocarbons was ascertained by the results of the analysis, the following qualitative examinations were carried out.

(1) Unsaturated Hydrocarbons.

Table III.

Gas employed	100.0 cc.		
After absorption with conc. KOH soln.	73.9	26.1%	CO_2
" " " $Hg(CN)_2$ reagent	73.5	0.4	
" " " $Hg(NO_3)_2$ reagent	62.6	10.9	C_2H_4
" " " Bromine water	61.7	0.9	

Table IV.

Gas employed	100.0 cc.		
After absorption with conc. KOH soln.	74.0	26.0%	CO_2
" " " H_2SO_4 (sp. gr. 1.84)	72.0	2.0	
" " " $Hg(NO_3)_2$ reagent	61.8	10.2	C_2H_4
" " " Bromine water	61.6	0.2	

As is clear from Table III, among the unsaturated hydrocarbons there is almost none that is absorbed by the mercuric cyanide reagent[1], the special absorbent for acetylene. The greater part is absorbed by the mercuric nitrate reagent[2], the special absorbent for ethylene. When finally tested with bromine water for any remaining heavy hydrocarbons there was almost none detectable. As the mercuric nitrate reagent, however, absorbs propylene besides ethylene, in the experiment shown in Table IV a conc. sulphuric acid reagent[3] was used as the absorbent for propylene, and it was found that a small percentage was absorbed by the reagent. The bulk of the gas, however, was absorbed by the mercuric nitrate reagent, showing that the unsaturated hydrocarbons formed in the electrolysis consist principally of ethylene.

1, 2. Treadwell u. Tauber, Helv. Chim. Acta. **2** (1919); 601.

3 Sutton, Volumetric Analysis p. 533.

(2) Saturated Hydrocarbons.

Table V.

Gas employed	100.0 cc.		
After absorption with conc. KOH soln.	73.9	26.1 %	CO_2
" " " Bromine water	61.7	12.2	C_2H_4
" " " Alkaline pyrogallic acid soln.	54.4	7.3	O_2
" " " Ammoniacal Cu_2Cl_2	45.2	9.2	CO
After factional combustion with Pd-black	7.8	37.4	H_2
7.8 cc. of the remaining gas were mixed with oxygen to	40.8		
After explosion	24.1	$C_x = 16.7$	$\frac{C_x}{C_{KOH}} = 1.205$
After absorption with Conc. KOH	10.9	$C_{KOH} = 13.2$	

Table VI.

7 cc. $(C_n H_{2n+2}) + O_2$ =	85.0		
After explosion	73.9	$C_x = 11.1$	$\frac{C_x}{C_{KOH}} = 1.233$
After absorption with KOH	64.9	$C_{KOH} = 9.0$	

Table VII.

10 cc. $(C_n H_{2n+2}) + O_2$ =	85.8		
After explosion	63.3	$C_x = 22.5$	$\frac{C_x}{C_{KOH}} = 1.257$
After absorption with KOH	45.4	$C_{KOH} = 17.9$	

Table VIII.

13 cc. $(C_n H_{2n+2}) + O_2$ =	95.6		
After explosion	67.7	$C_x = 27.9$	$\frac{C_x}{C_{KOH}} = 1.1$
After absorption with KOH	42.4	$C_{KOH} = 25.3$	

In the experiments shown in Tables VI, VII and VIII definite quantities of the gas mixture were first treated step by step with the necessary absorbents completely to remove CO_2, C_2H_{2n}, O_2, and CO. Hydrogen was now absorbed with palladium black at 80°—90° and the remaining gas was then mixed with oxygen and the mixture subjected to fractional combustion of the residual hydrogen by means of palladium black. After thus removing hydrogen completely, the gas, consisting of saturated hydrocarbons mixed with air in the palladium tube, was subjected

to explosion, and the contraction by explosion was compared with the contraction by subsequent absorption with a solution of caustic potash. This ratio in the case of ethane is represented in the following equation: $C_2H_6+3.5\ O_2=2CO_2+3\ H_2O$; $C_x/C_{KOH}=1.25$. From the figures obtained for C_x/C_{KOH}, it was concluded that the saturated hydrocarbon formed in the present instance was chiefly ethane.

(3) Change of Composition of the Anode Gas with Temperature.

Electrolysis at 25°, other conditions kept the same as before,

Table IX.

Duration of electrolysis	Anode gas cc./hour	CO_2	C_2H_4	O_2	CO	H_2	C_2H_6
0—19 hours	24.7	1.9	4.0	10.1	1.4	81.2	1.0
19—21	20.0	2.2	5.9	10.8	1.0	75.3	4.3
21—23	19.3	2.3	9.5	10.6	1.2	69.2	6.8
23—25	17.1	2.1	12.4	9.7	2.1	68.2	7.4
25—27	16.8	2.1	18.4	9.2	1.5	60.0	9.8

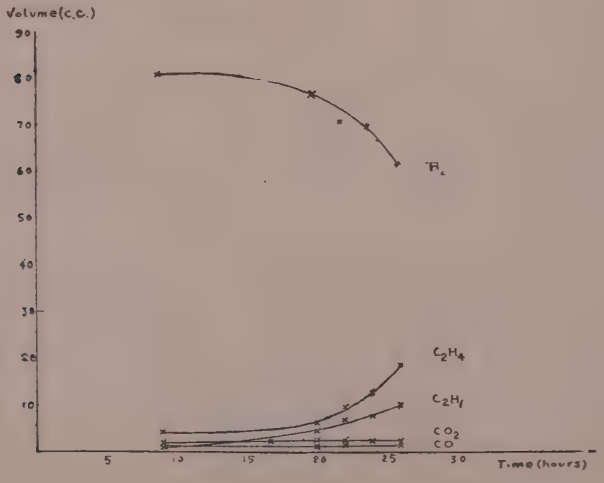

Electrolysis at 15°—18°.

Table X.

Duration of electrolysis	Anode gas cc./hour	CO_2	C_2H_4	O_2	CO	H_2	C_2H_6
0—3.5 hours	30.7	0.0	7.5	7.9	3.2	70.3	5.9
3.5—10.5	27.8	2.8	7.4	5.2	4.2	67.7	12.5
10.5—14.5	25.2	3.2	11.8	6.2	6.2	48.5	23.5

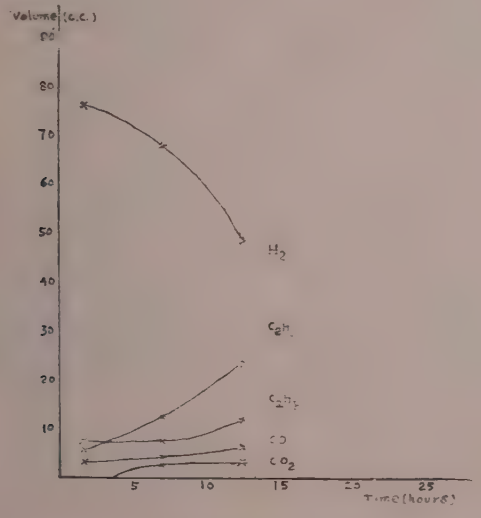

From the experiments here reported the fact becomes evident that by the electrolytic oxidation of propylalcohol in a caustic alkali solution ethylene and ethane are produced together with hydrogen, and the yield of such saturated and unsaturated hydrocarbons are greatly increased by lowering the electrolysing temperature. More especially, the fact that such an unsaturated hydrocarbon as ethylene is evolved here must be intimately related to the fact that an unsaturated hydrocarbon is produced in the Kolbe reaction, for instance, ethylene from salts of propionic acid. The above phenomenon is therefore a question full of importance in considering the mechanism of the Kolbe reaction. Although there must be many more experimental explanations for the elucidation of this mechanism, the reaction is presumed to proceed through the following stages in the case of propylalcohol:

$$CH_3CH_2CH_2ONa + OH' + F \rightarrow CH_3CH_2CH_2O + NaOH$$

$$CH_3CH_2CH_2O \rightarrow \begin{cases} CH_3CH_2CHO + H \rightarrow H_2 \\ HCHO + CH_3CH_2 \rightarrow CH_3CH_3 \\ \qquad\qquad \xrightarrow[+F]{} CH_2=CH_2 + H \end{cases}$$

The Kolbe reaction of the salts of propionic acid may be deemed to take place just analogously as follows :

$$CH_3CH_2COO' + H_2O + F \rightarrow CH_3CH_2COOH + OH$$

$$CH_3CH_2COONa + OH \rightarrow NaOH + CH_3CH_2COO$$

$$CH_3CH_2COO \rightarrow CO_2 + CH_3CH_2 \xrightarrow[+F]{} CH_2=CH_2 + H$$

In the Kolbe reaction of the salts of propionic acid, contrary to that of propylalcohol, there is no evolution of hydrogen and the reason for the non-appearance of ethane is, therefore, self-evident.

This investigation was carried out under the direction of Professor Motooki Matsui with the aid of the fund granted to him by the Imperial Academy of Japan. The author wishes, therefore, to acknowledge his obligations to the Imperial Academy of Japan and to Prof. M. Matsui.

An Examination of the Micro-Crystals of Calcium Carbonate in Molluscan Shells by means of X-Rays, Part II.

By

Jinzo Tsutsumi

(Received July 2, 1928)

Abstract

By means of X-rays it is confirmed that the micro-crystals of calcium carbonate in the nacreous layer of *Atrina japonica* Reeve are in the form of an aragonite instead of a calcite, and it is also found that they are arranged fibrously, the orthorhombic *c*-axes of its crystals being arranged parallel to the direction perpendicular to the surface of the nacreous layer.

After the determination of the crystal-form and the arrangement of the micro-crystals of calcium carbonate in the *prismatic layer* of the *Atrina japonica* Reeve, the result of which has already been reported in Part I,[1] the writer continued the same examination of the micro-crystals with the *nacreous layer* of the same shell, by using the same X-ray tube and the apparatus as in the former experiment. That the micro-crystal of calcium carbonate in the nacreous layer of the shell of *Atrina japonica* Reeve is in the form of an aragonite is already known, having been suggested by the observations by various means of many previous investigators.

This fact was stillmore confirmed in the present experiment by taking a powder-photograph with X-rays.

The photograph reproduced in Fig. 1, Plate I, was obtained with the nacreous layer of the *Atrina japonica* Reeve, by setting the surface of the nacreous layer perpendicular to the incident X-ray beam, and by

1 These Memoirs, A, II, (1928).

placing the photographic plate at right angles to the direct X-ray beam at a distance 4.7 cm. behind the specimen. In the accompanying figure, Fig. 1, the diffraction-pattern in Fig. 1, Plate I is shown diagrammatically. In this figure the line AOA′ represents the direction on the surface of the photographic plate, which is parallel to the surface-normal of the nacreous layer, and the lines COC′, DOD′ etc. represent the positions of the radiating bands. In this figure we see the radiating bands arranged symmetrically about the horizontal and the vertical lines BOB′, AOA′. Fig. 2, Plate I was taken with the incident beam of the X-rays proceeding perpendicularly to the surface of the layer; and it consists of concentric rings without any radiating band as seen in Fig. 1, Plate I. These facts indicate that the micro-crystal in the nacreous layer is arranged fibrously and that the axis of the fibre is nearly in a direction perpendicular to the surface of the nacreous layer.

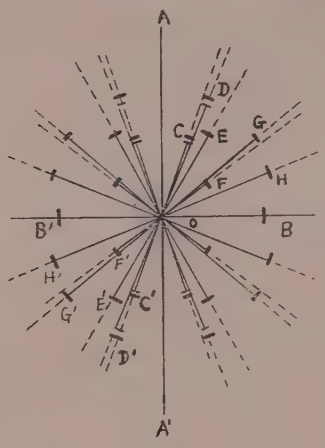

Fig. 1.

An arragonite-crystal belongs to the orthorhombic system, and its lattice-structure was investigated by W. L. Bragg[1] and other investigators[2]. According to Bragg, the dimensions of its elementary cell containing four molecules of calcium carbonate is:

$a = 4.94$A.U.; $b = 7.94$A.U.; $c = 5.72$A.U.

In order to know the crystallographic axis of the fibrous arrangement of the micro-crystals, we must determine the indices of the atomic planes by which the radiating bands in Fig. 1, Plate I, are caused. This was done by measuring the distance r between the centre of the central spot and the position of an intense spot on any radiating band. As such intense spot on a radiating band is nothing but the spectrum of the K-radiation of the Mo-target of the X-ray tube, the value of the spacing d between two consecutive atomic planes, and, consequently, the indices of that atomic plane, which is responsible for the radiating band under consideration, will be obtained from the wave-length of the K-radiation of molybdenum.

1 Proc. Roy. Soc. CV, 16, (1924).
2 Huggins: Phys. Rev. (2)19, 354, (1922), S. I. Tomkeieff: Min. Mag. XX, 408, (1925).

Table I.

spots	r in cm.	θ (obs.) in degrees	spacing (obs.) in A. U.	Bragg's data		d (calc.) in A. U.	indices of reflecting planes
				d in A. U.	indices of planes		
F	1.00	6°. 06′	3.38	—	—	3.38	111
B	1.40	8°. 18′	2.45	2.47	100	2.47	100
C	1.27	7°. 30′	2.70	—	—	2.69	012
E	1.40	8°. 18′	2.45	2.47	102	2.47	102
G	1.85	10°. 45′	1.89	1.86	101	1.87	101
H	1.70	9°. 55′	2.06	—	—	2.04	211
D	1.97	11°. 23′	1.79	—	—	1.78	103

The values of the spacings d, thus obtained, between two consecutive atomic planes for various radiating bands, are given in the fourth column in Table I.

F, B, C, etc., in the first column of the same table correspond respectively to the spots F, B, C. etc., in Fig. 1. In comparison Bragg's data for the values of d for three different atomic planes are given in the fifth column. The values of d for many atomic planes were also calculated by the writer from the Bragg data given before, and are placed down in the seventh column of the table. From the agreement between the calculated and the observed values of d, as shown in the Table, the indices given in the last column are assigned for various radiating bands respectively.

Table II.

radiating bands	indices of the atomic planes	α (obs.)
COC′	012	19°
DOD′	103	21°
EOE′	102	30°
FOF′	111	53°
GOG′	101	50°
HOH′	211	68°
BOB′	100	90°

In Table II, the indices of the atomic planes which caused the radiating bands and the angle α which the line AOA′ in Fig. 1 makes with the line connecting the centre of the central spot and the intense spot on a radiating band are tabulated. From these values of α for various atomic planes, the angles β which the normals to various atomic planes make with the direction of the axis of the fibre can be calculated readily, by taking the angle between the axis of

the fibre and the incident X-ray beam as 90°, so as to fit in our case. The values of β thus calculated for various radiating band and the indices of the corresponding atomic planes are tabulated in Table III.

Table III.

indices of atomic planes	001 axis or *c*-axis	β
111	53°. 45′	52°. 55′
100	90°. 00′	90°. 00′
012	19°. 45′	18°. 00′
101	49°. 10′	48°. 30′
102	30°. 00′	29°. 30′
103	20°. 55′	20°. 10′
211	69°. 08′	67°. 57′

These of β must be respectively the same with an angle between the normals to various atomic planes tabulated in Table III and the crystallographic axis arranged in the direction of the axis of the fibre. Taking this fact into consideration, the crystallographic axis, which is the axis of the fibre, was reached with the aid of the globe and the spherical scale devised by Prof. U. Yoshida; and it was found that the angular relation shown in Table III could only be accounted for by taking the *c*-axis of the orthorhombic crystal of aragonite as the axis of the fibre. The angles between the *c*-axis and the normals to various atomic planes are given in the second column of Table III. The agreement between the values of these angles and those of β is remarkable.

In Fig. 2, the curve drawn in full lines and the spots on these curves show respectively the radiating bands and the positions of the spectrum of the K-radiation of Mo on these bands, which are expected to appear on the photographic plate from ths above consideration; and the shaded parts represent the portions actually observed on the photograph as shown in Fig. 1, Plate I. The agreement between the calculation and the observation is found again to be satisfactory.

Thus we are enabled to conclude that unmistakably the calcium carbonate in the nacreous layer of *Atrina japonica* Reeve is an aggregate of the micro-crystals of aragonite, which are arranged in a fibrous manner; and that the orthorhombic *c*-axis of the micro-crystals of aragonite are arranged in a direction perpendicular to the nacreous layer of

Fig. 2.

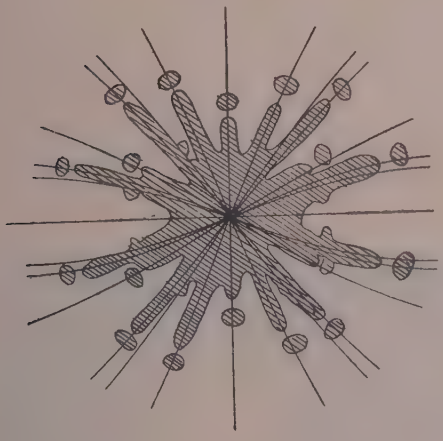

the shell, which is at the same time the direction of the axis of fibre.

The writer is now planning to examine the molluscan shells belonging to various genera and species and a general conclusion is hoped to be attained in the near future.

In conclusion, the writer's sincere thanks are due to Professors U. Yoshida and T. Kawamura for their kind guidance and encouragement throughout this research.

Plate I

Fig. 1

The direction parallel to the surface-normal of the nacreous layer.

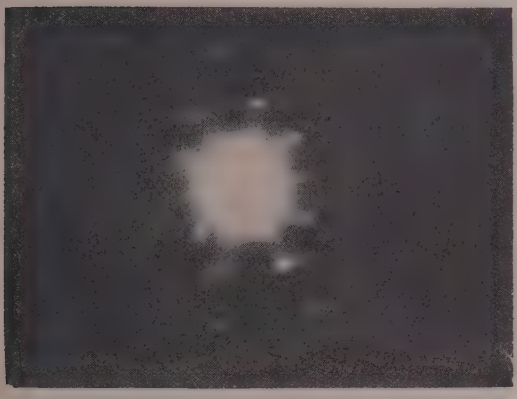

Fig. 2

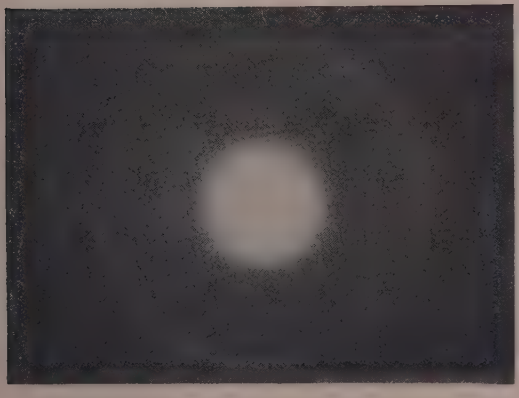

On the Electrolytic Reduction of Aldehydes. Part III.

Ortho- and Para- Oxybenzaldehydes

By

Goro Shima

(Received July 5, 1928)

Ortho-Oxybenzaldehyde.

Regarding the electrolytic reduction of *o*-oxybenzaldehyde, or salicylaldehyde, there are found in the literature only two papers by Law and Schepps. Law[1] tried his electrolytic reduction of aldehydes by using an alcoholic sulphuric acid solution as catholyte with copper as cathode and although he generally succeeded in reducing them to alcohol and hydrobenzoin as principal products, yet with salicylaldehyde he reports that the entire substance was changed to a resinous substance.

Schepps[2] carried out his electrolytic reduction of the aldehydes in alcoholic sulphuric acid solution with cadmium as cathode. Although he generally succeeded in getting a tolerably good yield of the corresponding hydrocarbons, yet with salicylaldehyde he reports, in confirmation of Law's results, that *o*-cresol was not obtained, and the greater part of the material was converted into a resinous substance.

From these results it has been found unsuitable to use as the electrolytic solution for the reduction of salicylaldehyde so strong a mineral acid as sulphuric acid. Presumably in this case salicylaldehyde forms at

1 J. Chem. Soc., **91**, 754 (1907).
2 Ber., **46**, 2564 (1913).

first oxybenzyl alcohol, or saligenin, and this latter substance is easily polymerised by the mineral acid into such a substance as saliretin.

When, in the catholyte, an alkali is used, instead of sulphuric acid, most of the aldehydes are changed principally to hydrobenzoin, and, according to Law[1], the carbonyl compounds, first reacting with alkali, form an intermediate product as shown in the following equation

$$X-CO-Y + NaOH = X-\overset{\overset{OH}{|}}{\underset{|}{C}}-ONa \quad (Y)$$

and this latter product is then reduced to form hydrobenzoin as follows:

$$2\,X-\overset{\overset{OH}{|}}{\underset{|}{C}}-ONa \quad (Y) + 2\,H = X-\overset{\overset{OH}{|}}{\underset{|}{C}}-\overset{\overset{OH}{|}}{\underset{|}{C}}-X + 2\,NaOH \quad (Y\ Y)$$

With salicylaldehyde, Law obtained, by using nickel or platinum plate as cathode, oxyhydrobenzoin with a yield of 70 per cent:

$$2\,OH \cdot C_6H_4 \cdot CHO + 2\,H = HO \cdot C_2H_4 \cdot CHOH \cdot CHOH \cdot C_6H_4 \cdot OH$$

Moreover, at the same time as the above, there is produced 9–10–dioxyphenanthrene.

With the purpose of preparing o-oxybenzyl alcohol by the electrolytic reduction of salicylaldehyde, I first made experiments with an alkaline solution as the catholyte. As nickel and platinum cathodes had already been tried by Law, besides those I also used copper, lead, zinc, and mercury, which have a greater over-voltage, as cathodes. With each of these no alcohol was obtained, the chief product consisting of oxyhydrobenzoin with a yield of 70 to 80 per cent. The reduction efficiency was small with platinum and nickel which have a small over-voltage, and it was greater in proportion to the rise of the over-voltage as with mercury zinc, and lead.

As I had learned from the above experiments, that for preparing o-oxybenzyl alcohol by electrolytic reduction of salicylaldehyde a strong mineral acid or a free alkali cannot be used, I performed the reduction

1 Law, J. Chem. Soc., **89**, 1512 (1906); Kaufmann, Z. Elek. Chem., **2**, 365 (1895); Elbs and Brand, Z. Elek. Chem., **8**, 784 (1902).

with the electrolytic solution constantly kept only weakly alkaline by using as catholyte a solution of sodium bicarbonate into which a stream of carbon dioxide was kept passing throughout the electrolytic process for the purpose of neutralizing the free alkali as it formed. Thereupon, quite to my expectation, no resinous substance or condensation product such as hydrobenzoin was formed, and salicyl alcohol was produced with current and material yields of 80 to 90 per cent:

$$OH \cdot C_6H_4 \cdot CHO + 2\,H = OH \cdot C_6H_4 \cdot CH_2OH$$

Moreover, when such a very weakly acid solution as sodium acetate solution acidified with acetic acid is used in place of the sodium bicarbonate solution, the yield of salicyl alcohol was found to be just as good.

Although each of the metals, mercury, zinc, copper, lead, and nickel, forms alcohol when used as cathode, the current efficiency is highest with mercury and decreases regularly with the decrease of over-voltage in the order of zinc, lead, copper, and nickel.

Experimental.

When zinc, lead, copper, and nickel were used as cathodes, the electrode was inserted into the cell and the solution was vigorously stirred

Fig. 1.

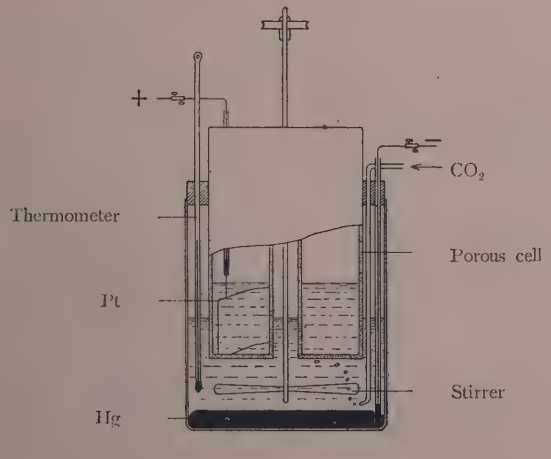

during the electrolysis. When mercury was employed as cathode the outside of the cell was used as the cathode compartment, and a specially constructed cell having double walls served as the anode compartment. The stirrer was made to rotate in the centre of the cell as is shown in figure 1. By this device, not only a small volume of the cathode solution suffices for the purpose, and it can be easily and vigorously agitated, but also the process of reduction can be watched from outside.

I. Experiment with an alkaline solution.

Catholyte : 100 cc. of a 5% sodium hydroxide solution with 5 gr. of salicylaldehyde.
Anode : Lead.
Anolyte : 5% sodium hydroxide solution.
Temperature : 16°—18°
Current density : 1.5 amp./100 sq. cm.

The volumes of hydrogen evolved at the cathode and at the coulometer were compared and the reduction efficiency of different cathodes was estimated by the usual method. This result is shown in figure 2 which shows that the efficiency is large in proportion to the amount of the over-voltage, and that in the case of zinc it gives a value closely approximating the theoretical. On the contrary, nickel with its slight over-voltage is found to cause no reduction at all under the same conditions.

Table I.

Zinc		Lead amalgam		Lead		Copper	
Time (mins.)	Reduction efficiency (%)	Time (mins.)	Reduction efficiency (%)	Time (mins.)	Reduction efficiency (%)	Time (mins.)	Reduction efficiency (%)
4	100.0	2	92.6	2	93.4	2	82.7
15	97.2	20	91.6	15	91.9	10	73.7
25	95.5	40	86.3	25	91.0	20	65.3
35	94.6	50	85.3	37	88.8	40	60.4
48	90.0	60	79.2	45	84.1	50	55.8
55	81.2	70	72.3	55	78.2	65	53.8
65	66.8	80	65.6	67	54.6	75	50.4
74	56.1	90	60.2	75	23.0	90	42.5
85	44.8	100	52.9	85	11.3	100	37.4

The efficiency curve for zinc and lead first shows a sudden fall after the passage of electricity of one ampere-hour which is just the quantity of current required for converting salicylaldehyde into oxyhydrobenzoin. Still, the fact that the reduction does not cease at this point but that hydrogen continues to be absorbed indicates that a portion of the oxyhydrobenzoin is further reduced.

Fig. 2.

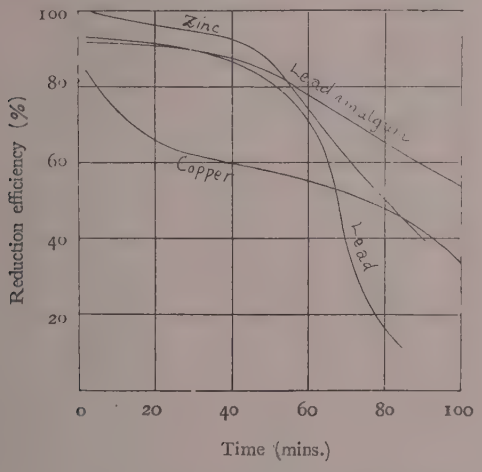

The catholyte was treated, under cooling, with about 5 gr. of hydrogen sodium carbonate and then neutralized with dilute acetic acid to the acid degree of carbonic acid.

This was done to avoid the danger of changing the precipitate formed into a dark brown substance by an acidity stronger than that of carbonic acid. The precipitate thus obtained is oxyhydrobenzoin or a mixture of its isomers, and forms a white amorphous mass which is filtered by the aid of suction, and well washed with water. It is with difficulty soluble in water, and, although soluble in alcohol and ether, does not crystallize out from these solutions. It was, therefore, dissolved in a dilute sodium hydroxide solution and then precipitated with acetic acid and thoroughly washed. About 2 gr. of the purified product were thus obtained.

The product soluble in the carbonic acid solution was repeatedly extracted with ether and subjected, after dispelling the ether, to steam distillation. On cooling the distillate there appeared some white needle crystals insolube in alkali. When recrystallized from alcohol, the substance

melted at 112° (according to Law 113°) and gave on analysis the following result:

Substance, 0.1065 gr.	CO_2= 0.3117 gr.	H_2O=0.0502 gr.
	C =79.75%	H =5.27%
Substance, 0.0931 gr.	CO_2= 0.2742 gr.	H_2O=0.0466 gr.
	C =80.34%	H =5.60%
Calculated for $C_{14}H_{12}O_2$,		
	C =79.21%	H =5.71%

The substance is, therefore, 9–10–dioxyphenanthrene formed by the reduction of oxyhydrobenzoin as indicated in the following equation:

$$OH \cdot C_6H_4 \cdot CHOH \cdot CHOH \cdot C_6H_4 \cdot OH + 2H = \text{ 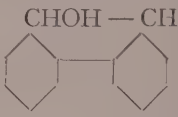 } + 2H_2O$$

The residue after steam distillation was twice extacted with ether, and the extract dehydrated with anhydrous sodium sulphate. After dispelling the ether, the resinous residue obtained was allowed to stand for one or two days, when it crystallized out in small wart like masses. This substance is soluble in alcohol, ether, and warm water. When decolorized with charcoal and recrystallized from water, it forms white shining crystals softening at 136° and melting at 142°. The result of the elementary analysis of it is as follows:

Substance, 0.1073 gr.	CO_2= 0.2698 gr.	H_2O=0.0566 gr.
	C =68.58%	H =5.90%
Substance, 0.1111 gr.	CO_2= 0.2777 gr.	H_2O=0.0610 gr.
	C =68.17%	H =6.14%
Calculated for oxyhydrobenzoin,	C=68.28%	H =5.73%

It is, therefore, oxyhydrobenzoin. The present yield was about 1.5 gr. and the total yield 70—80 per cent.

II. Experiments with a sodium bicarbonate solution.

Cathode: Mercury, 50 sq. cm.

Catholyte: 100 cc. of a saturated sodium bicarbonate solution containing 5 gr. of salicylaldehyde.

Anode : Lead,
Anolyte : 5 % solution of sodium hydroxide.
Current density : 4 amperes/100 sq. cm.
Current : 4 ampere-hours.
Temperatures : 16°—18°

As salicylaldehyde is insoluble in a sodium bicarbonate solution, it was suspended in the solution and electrolyzed under strong agitation. Moreover, throughout the electrolysis, a constant stream of carbon dioxide was passed through the catholyte to neutralize the free alkali and to keep the solution always weakly alkaline.

The electrolytic solution which was yellow at first gradually got decolorized and was perfectly colorless at the completion of reduction. It was treated in the same manner as before. When, however, it was neutralized with acetic acid to the degree of acidity of carbonic acid, there was no precipitation of hydrobenzoin and the solution remained clear. It was now repeatedly extracted with ether, and the extract dehydrated with anhydrous sodium sulphate and, after dispelling the ether, subjected to steam distillation for the purpose of removing any volatile substance such as aldehydes. The residue in the flask was cooled, filtered from the insoluble substance, and extracted with ether. The ether extract was dehydrated with anhydrous sodium sulphate. When the ether was evaporated off, the substance in the residue crystallized out immediately in a colorless rhombic plate soluble in alcohol, ether, warm benzene, and water. After recrystallizing from a large quantity of ligroin the substance melted at 82° and weighed 4.2 gr., corresponding to 85 per cent of the theoretical yield. The result of the elementary analysis is as follows :

Substance, 0.1429 gr.	CO_2= 0.3524 gr.	H_2O=0.0848 gr.
	C =67.25%	H =6.64%
Substance, 0.1009 gr.	CO_2= 0.2511 gr.	H_2O=0.0621 gr.
	C =67.90%	H =6.89%
Calculated for oxybenzyl alcohol ($C_7H_8O_2$) :		
	C =67.70%	H =6.50%

Saligenin, first obtained by Piria[1] by the decomposition of salicin, was reported as melting at 86°, but according to later literture its true melting-point is 82°, with which my result agrees well.

1 Ann. **56**, 37 (1845).

Influence of Temperature.

All the conditions of electrolysis were kept the same as in the previous experiment, except that the weight of the salicylaldehyde taken was 2 gr., and the quantity of the current somewhat less than that necessary for the electrolysis in question: viz. it was only 0.7 ampere-hour. The influence of temperature upon the current efficiency was thus examined.

Table II.

Temperature °C	Current Efficiency for Saligenin (%)
5°—10°	69
16°—18°	85
22°—26°	82

In the neighborhood of 16° the current efficiency is highest, reaching to 87 per cent of the material yield. At lower temperatures the current yield is low, although there is no change in the material yield, which reaches to more than 85 per cent. A small rise of temperature shows no considerable influence, while too high a temperature causes the formation of condensation products, and a diminution both of current and of material yields.

III. Experiments with acetic acid - sodium acetate solution.

All the conditions of electrolysis were the same as in the preceding experiments, except that the catholyte consisted of 5 cc. of glacial acetic acid, 10 gr. of sodium acetate, 100 cc. of water, and 2 gr. of salicylaldehyde. Again in this case, as the aldehyde was insoluble in the solution mixture, it was electrolyzed in a state of suspension with vigorous stirring of the solution. After completion of the electrolysis, the solution was neutralized with sodium bicarbonate to the acidity of carbonic acid and then subjected to the same treatment as before.

A. Influence of Cathode.

Temperature: 16°—18°
Current density: 4 amperes/100 sq. cm.
Current quantity: 0.7 ampere-hour.

Table III.

Cathode	Current efficiency for Saligenin (%)
Mercury	90
Zinc	65
Lead	61

Besides mercury, zinc, and lead, copper and nickel also give the alcohol as the principal product; and the current efficiency is highest with mercury which is highest in over-voltage, giving a material yield of 93 per cent under this condition. Although the current efficiency decreases step by step from mercury to zinc and lead, there is found no great change in the material yield.

B. Influence of Current Density.

All the experimental conditions were the same as before except that mercury was used as cathode.

Table IV.

Current density ampere/100 sq. cm.	Temperature °C	Current quantity ampere-hour	Current yield %
2	12°—13°	0.75	57
4	16°—18°	0.70	90
6	18°—23°	0.70	76
8	18°—30°	0.73	70

For the formation of saligenin, the best result is obtained by the use of 4 amperes/100 sq. cm, of current density. The lower yield at the higher current densities is, however, presumed to be due to the rise of the temperature.

C. Influence of Temperature.

All the experimental conditions were the same as before except that the current density was maintained at 4 amperes/100 sq. cm.

Table V.

Temperature °C	Current efficiency in saligenin (%)
5°– 8°	54
16°–18°	90
28°–35°	51

The influence of the temperature is, in this case, much greater than when sodium bicarbonate solution is used. The rise of temperature leads to the easy formation of condensation products such as oxyhydrobenzoin and resins, resulting in a great diminution of current and of material efficiency for salicyl alcohol.

D. Influence of the Anode Solution.

All the experimental conditions were the same as before except that the temperature was maintained at from 16° to 18°.

Table VI.

Anode solution (5%)	Current efficiency for saligenin (%)
Sulphuric acid	69
Sodium hydroxide	90

When a strong acid such as sulphuric acid is used in the anode solution, its diffusion into the cathode chamber increases, with the progress of the electrolysis, the hydrogen ion concentration in it, and accelerates the formation of the condensation products, diminishing at the same time the yield of saligenin. When a saturated solution of sodium carbonate was used as anode solution, the material yield was raised to 94 per cent although the current efficiency remained the same as when caustic alkali was used.

Summarising the results described above, the optimum conditions for the production of saligenin by the electrolytic reduction of salicylaldehyde can be formulated as follows:

Cathode: Mercury.

Catholyte: Although a neutral solution is the ideal, it is impossible to get such a solution, and it is advisable to use as nearly neutral a solution as possible, such as either a weakly acid solution like acetic acid - sodium acetate solution, or the saturated sodium bicarbonate solution, which is kept weakly alkaline by constantly passing carbon dioxide throughout the electrolysis.

Anolyte: Saturated solution of sodium carbonate.

Temperature: 16°—18°.

Current density: 4 amp./100 sq. cm.

As salicylaldehyde is not soluble in such a catholyte and has to be electrolyzed with constant agitation, if a great quantity is used at one time there is danger not only of incurring loss by spattering or volatilizing, but also of easily producing resins under the electric strain, and it is advisable to add small quantities of it in separate portions.

Para-oxybenzaldehyde.

As I obtained by electrolysis of salicylaldehyde, so excellent an amount of saligenin as 94 per cent of material yield, and 90 per cent of current yield, I also tried the electrolytic reduction of p-oxybenzaldehyde under the same conditions and obtained p-oxybenzyl alcohol with the same favourable yield.

P-oxybenzyl alcohol can be obtained by electrolytic reduction of p-oxybenzoic acid[1], by a purely chemical reduction of p-aldehyde with sodium amalgam in a dilute alcoholic sulphuric acid solution[2], or by reduction of p-oxybenzamide with sodium amalgam in an alcoholic sulphuric acid solution[3], I have, however, succeeded under a simple handling of the electrolytic method, in attaining the favourable result of more than 90 per cent of current and material yield, without the formation of various by-products.

The best electrolytic conditions given above were adopted and the catholyte consisted of 10 cc. of glacial acetic acid, 10 gr. of sodium acetate, 100 cc. of water and 5 gr. of p-oxybenzaldehyde, which was added in three instalments instead of being added all at once. Acetic

1 Mettler, D. R. P. 177490; C. II, 1790 (1906).

2 Biedermann, Ber., **19**, 2374 (1886).

3 Hutchinson, J. Chem., Soc., **57**, 957 (1890); Ber., **24**, 175 (1891); Auwer, Daecke, Ber., **32**, 3374 (1899).

acid was added in such a way as just to prevent the anolyte from getting alkaline. When three ampere-hours of current had passed the solution was tested with nitrophenylhydrazine for the aldehyde and it was found to have completely been reduced. The current was then cut off, and the anode solution was neutralized with sodium bicarbonate to the acidity of carbonic acid, repeatedly extracted with ether, and dehydrated with anhydrous sodium sulphate. When the ether was evaporated off there remained white needle crystals. This substance was dissolved in water, filtered from insoluble matter, and extracted with ether. The ether extract was dehydrated and evaporated when nearly pure p-oxybenzyl alcohol separated out to a yield of 4.6 gr., corresponding to 92 per cent of the theoretical. It is almost insoluble in chloroform, benzene, and ligroin, and soluble in water, alcohol, and ether. When it is heated to about 100° it changes to a transparent vitrious mass insoluble in water.

P-oxybenzyl alcohol obtained by Auwer and Daecke melted at 124.5° —125.5°. The substance obtained as above described, when once recrystallized from water, and dissolved in warm chloroform, and precipitated with ligroin, melted at 110° and agreed with the substance obtained by Biedermann, Hutchinson, and Mettler.

The result of an elementary analysis was as follows:

Substance, 0.1278 gr.	CO_2 = 0.3169 gr.	H_2O = 0.0743 gr.
	C = 67.65%	H = 6.51%
Substance, 0.0898 gr.	CO_2 = 0.2214 gr.	H_2O = 0.0545 gr.
	C = 67.23%	H = 6.79%
Calculated for p-oxybenzyl alcohol ($C_6H_8O_2$):		
	C = 67.70%	H = 6.50%

With the expectation that, besides the oxyaldehydes, substances that are easily changeable to resins such as vanillin, heliotropin, the halogen-aldehydes and cinnamic aldehyde and some other unsaturated aldehydes can be smoothly reduced by the above described reduction method, I am continuing this investigation further.

The present writer wishes to express his sincere thanks to Professor M. Matsui under whose kind guidance and encouragement this work was carried out.

On the Electrolytic Reduction of Aldehydes. Part IV. Vanillin and Piperonal

By

Goro Shima

(Received July 5, 1928)

In the preceding report I stated that even the substances that are easily changeable to resins, such as o- and p- oxybenzaldehyde can be changed to alcohol by electrolytic reduction in nearly neutral solutions, at the favourable result of more than 90 per cent current and material yield, while the formation of condensation products like hydrobenzoin and resins is avoided. By performing under the same conditions the electrolytic reduction of vanillin and piperonal, substances easily convertible to resins, I have also obtained with a yield approximating the theoretical value vanillic alcohol and piperonyl alcohol respectively.

$$CH_3O{\cdot}C_6H_3(OH){\cdot}CHO + 2H = CH_3O{\cdot}C_6H_3(OH){\cdot}CH_2OH$$

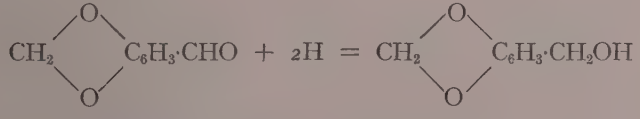

Herewith, it is proposed to report on the results.

I. The Reduction of Vanillin.

Of the purely chemical reduction of vanillin there is a report of an investigation by Tiemann[1] in which he obtained hydrovanilloin and

1 Ber., **9**, 415 (1876); Ber., **18**, 1123 (1885); Ber., **18**, 1599 (1885).

vanillic alcohol by reduction of vanillin with sodium amalgam, although nothing is mentioned of any yield. The vanillic alcohol thus obtained melted at 103,° indicating that it was not pure. Later on, however, he obtained by decomposing glucovanillic alcohol by means of emulsin glucose and vanillic alcohol the latter of which was ascertained to have a melting point of 115°.

On the electrolytic reduction of vanillin, there are only two investigations reported so far. The one is by Law,[1] who has shown that by using copper as cathode in an alcoholic sulphuric acid solution vanillin is completely changed to resin in a similar manner to salicylaldehyde. In alkaline solutions, he has obtained in addition to much resin hydrovanilloin with a yield of 45%.

$$2\,CH_3O{\cdot}C_6H_3(OH){\cdot}CHO + 2\,H = CH_3O{\cdot}C_6H_3(OH){\cdot}CHOH{\cdot}CHOH{\cdot}C_6H_3(OH){\cdot}CH_3O$$

The other report originates from Schepps[2] who has obtained by using cadmium as cathode in an alcoholic sulphuric acid solution creosol with a yield of 28% as the result of a reductton at a comparatively high temperature and high current density.

$$CH_3O{\cdot}C_6H_3(OH){\cdot}CHO + 4H = CH_3O{\cdot}C_6H_3(OH){\cdot}CH_3 + H_2O$$

Experimental

I. Experiments in a weak acid solution

The apparatus used was the same as in the reduction of salicylaldehyde. Mercury was made the cathode and 10 gr. of sodium acetate dissolved in 100 cc. of water were made the catholyte in which 5 gr. of vanillin were suspended. This catholyte was kept during the electrolysis as neutral as possible or very weakly acid by adding from time to time small quantities of acetic acid. The anode consisted of a platinum plate, and the anolyte of the saturated solution of sodium carbonate. The whole apparatus was immersed in ice water, and the temperature of the catholyte was maintained at 8°–10°. The current density was 4 amp./100 sq. cm.

With the progress of the electrolysis, the vanillin dissolved to a light yellow solution at first; it slowly became colorless separating at the same time a fine white crystalline precipitate. After the passage of about 4 ampere-hours of current (nearly double the calculated quantity),

1 J. Chem. Soc., **89**, 1512 (1906); **91**, 754 (1907).
2 Ber., **46**, 2564 (1913).

the mercury was separated from the catholyte by means of a separating funnel and was repeatedly washed with water. The precipitate thus produced was filtered and washed with water and dried in a desiccator. The quantity obtained amounted to 0.5 gr.

This substance is insoluble in ordinary organic solvents such as toluol, ligroin, benzene, ether, and chloroform. It is only slightly soluble in boiling water, and in alcohol. When recrystallized from alcohol, it forms fine white needle crystals melting at 222°–223° decomposing at the same time to a brown-coloured substance. The result of the elementary analysis is as follows:

Substance, 0·1098 gr. CO_2=0·2503 gr. H_2O=0·0583 gr.
C = 62·15% H = 5·94%
Substance, 0·1282 gr. CO_2=0·2934 gr. H_2O=0·0676 gr.
C = 62·56% H = 5.90%
Theoretical for hydrovanilloin
C = 62·74% H = 5.88%

The substance is thus nothing but hydrovanilloin, and its yield was 10 per cent.

The filtrate from hydrovanilloin, which was nearly colorless, was neutralized to the acidity of carbonic acid by the addition of sodium carbonate and extracted with ether. The ether extract was dehydrated with anhydrous sodium sulphate, and evaporated to remove the ether, when the residue was immediately changed to fine needle crystals. This substance was dissolved in hot water, filtered from insoluble matter, treated with acid sodium sulphite, and again extracted with ether. When the ether was removed by evaporation after a thorough drying, the crystals that were obtained consisted of almost pure vanillic alcohol, weighing altogether 4·1 gr., corresponding to nearly 82 per cent of the theoretical value.

Vanillic alcohol does not distill with steam. It is soluble in alcohol, ether, and water, but insoluble in cold benzene, ligroin, and toluol. When recrystallized from benzene it forms beautiful needle crystals melting at 115° and giving the following result of elementary analysis:

Substance, 0·1089 gr. CO_2=0·2476 gr. H_2O=0.0631 gr.
C = 62·00% H = 6·48%
Substance, 0·1205 gr. CO_2=0·2749 gr. H_2O=0·0722 gr.
C = 62·23% H = 6·70%
Theoretical for vanillic alcohol
C = 62·29% H = 6·54%

Influence of Temperature

Generally speaking, when the aldehydes are reduced electrolytically the lower the temperature is, the better is the yield of the alcohols, and proportionally with the rise of temperature there is an increase of hydrobenzoin and other condensation products. The same general rule holds true also in the case of vanillin. The experimental results under the same electrolytic conditions as above but with varying temperatures are shown in the following table:

Temperature	Hydrovanilloin (%)	Vanillic alcohol (%)
8°–10°	10	82
25°–30°	52	34
45°–48°	24	32

With the rise of the temperature, the yield of alcohol decreases and that of hydrovanilloin increases. When, however, the temperature rises too high there is a decrease not only of the alcohol but also of the hydrovanilloin, resulting in the sole increase of resin. The formation of creosol was not noticed under the above conditions.

Experiments were also performed with a cadmium electrode in slightly acid solutions at high temperatures and high current densities. However, the reduction down to the utmost stage of hydrocarbons was not to be attained by this means.

II. Experiments in slightly acid alcoholic solutions.

Starting from the consideration that by electrolytically reducing vanillin insoluble in water in an alcoholic solution instead of in suspension there might be obtainable a better result, I took as the catholyte 60 cc. of alcohol containing 5 gr. of vanillin, and mixed it with 70 gr. of water containing 10 gr. of sodium acetate. During the electrolysis the solution was kept weakly acid by adding small quantities of acetic acid from time to time. The temperature was maintained at 10°–15° and all the other conditions were the same as in previous experiments. The result was as follows:

Hydrovanilloin	Vanillic alcohol
16%	72%

The material yield of vanillic alcohol was not much different from that in which the suspension of vanillin was electrolyzed.

III. Experiments in slightly alkaline solutions.

The apparatus and electrolytic conditions were made the same as in the preceding experiments.

The catholyte consisted of 100 cc. of the saturated sodium bicarbonate solution containing 5 gr. of vaniline as suspension. By vigorously agitating the solution and passing carbon dioxide through it, it was kept as weakly alkaline as possible.

Temperature	Hydrovanilloin (%)	Vanillic alcohol (%)
8°–10°	–	92
25°–30°	8	80

With the rise of temperature the formation of hydrovanilloin and of the resin increased although the influence was not so strong as with the acid solution. The yield of vanillic alcohol was much more favourable in the weakly alkaline solution than in the weakly acid solution, reaching to 92% of the material yield and 85% of the current yield.

IV. Experiments in a weak alkaline alcoholic solution.

As vanillin is only slightly soluble in a sodium bicarbonate solution, it was electrolyzed in an alcoholic solution. The catholyte consisted of 70 cc. of the saturated sodium bicarbonate solution and 50 cc. of alcohol, containing 5 gr. of vanillin, through which carbon dioxide was passed during the whole of electrolysis, The catholyte consisted of a 5% caustic soda solution while the other conditions remained the same as before.

Hydrovanillion	Vanillic alcohol
10%	36%

The yield of vanillic alcohol was strikingly small and the greater part was changed to resin.

The use of an alcoholic solution for the reduction of the aldehydes makes condensation easier and is unsuitable for reduction to the stage of the alcohol.

V. Experiments in an acid sulphite solution.

Vanillin was made soluble with acid sulphite and was electrolyzed in a weak alkaline solution. The catholyte consisted of 5 gr. of vanillin and 4 gr. of acid sodium sulphite dissolved to make up 100 cc, and after being saturated with sodium bicarbonate it was treated with carbon dioxide throughout the electrolysis. The other conditions remained the same as before.

Hydrovanilloin	Vanillic alcohol
8%	76%

The benzoyl derivative of vanillic alcohol.

There is none of the benzoyl derivatives yet known of vanillic alcohol. I have added benzoyl chloride to the caustic soda or pyridine solution of vanillic alcohol resulting from the above electrolysis. The mixture was well shaken and allowed to stand for some time at room temperature, and then acidified with well-cooled dilute sulphuric acid, when an oily substance separated out and solidified within a few hours. It was filtered, pressed on a porous plate, and recrystallized from methyl alcohol, when it came out as white crystalline scales melting at 120°.

The result of the elementary analysis was as follows:

Substance, 0·1067 gr. CO_2=0·2788 gr. H_2O=0·0498 gr.
C = 71·01% H = 5·22%
Substance, 0·1265 gr. CO_2=0 3264 gr. H_2O=0·0574 gr.
C = 70·36% H = 5·08%
Theoretical for vanillic alcohol dibenzoate,
C = 70·99% H = 5·37%

It was saponified by the method of Meyer and Hartmann[1] and its molecular weight was estimated by titration. The hydrolysis was performed with a methyl alcoholic solution of caustic soda, and the resulting

1 Ber., **38**, 3956 (1905)

mixture was acidified with phosphoric acid and subjected to steam distillation, The benzoic acid thus separated was titrated with a barium hydroxide solution.

Substance, 0·5612 gr. required $Ba(OH)_2$ solution (0·0946 N) 33·35 cc.

Molecular weight 355

Calculated for vanillic alcohol dibenzoate: 362

Vanillic alcohol dibenzoate is soluble in alcohol, benzene, and acetone, but insoluble in water and in ligroin.

II. The Reduction of Piperonal

Fittig and Remsen[1] had obtained hydro- and isohydro-piperoin as well as piperonyl alcohol by the purely chemical reduction of piperonal with sodium amalgam.

Law[2] has stated that by the electrolytic reduction in an alcoholic sulphuric acid solution piperonal is completely changed to resin in a similar manner to salicylaldehyde and vanillin.

He has also stated that by using an alkaline solution it produces like other aldehydes a theoretical yield of hydro- and of iso-hydropiperoin

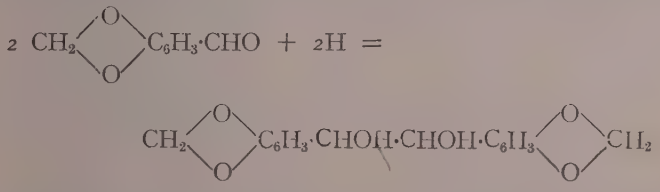

Schepps[3] obtained, by using a cadmium cathode in an alcoholic sulphuric acid solution, and electrolyzing at a comparatively high temperature and high current density, besides small quantities of the alcohol (7–8%) and of hydropiperoin (3–8%), homopyrocatechin methyl ether with a yield of 33%

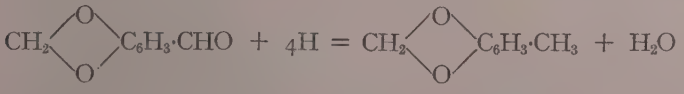

I carried out the electrolytic reduction of piperonal with mercury as the cathode in a sodium bicarbonate solution in the same manner as in the case of vanillin. The electrolytic conditions were exactly the same

1 Ann., **159**, 129 (1871).

2 J. Chem. Soc., **89**, 1512 (1906); **91**, 754 (1907).

3 Ber., **46**, 2564 (1913).

as stated above in II. The temperature was kept at 10°–12°, and 5 gr. of piperonal were used.

After employing about 5 ampere-hours of current the catholyte was separated from the mercury by means of a separating funnel, extracted with ether, and dehydrated with anhydrous sodium sulphate.

After expelling off the ether the residue was thoroughly treated with a concentrated solution of acid sodium sulphite to remove the remaining aldehyde, extracted with ether, dehydrated, and the ether evaporated off. The residue crystallized out in needle form in a few minutes. It weighed 4·5 gr. corresponding to about 90% of the theoretical. If in this case the original aldehyde was not thoroughly removed beforehand the ethereal residue took oily form and did not easily crystallize out.

Piperonal is more insoluble in sodium bicarbonate solution than vanillin. When the reduction was attempted in an alcoholic solution the yield of piperonyl alcohol was strikingly small, as was found in the case of vanillin, and the greater part changed to hydropiperoin and resin.

The reason for the easy production of the hydrobenzoin due to the presence of alcohol in a weakly alkaline solution, can probably be ascribed to the fact that the aldehyde first forms an intermediate substance by reacting upon the alcohol,

$$R-\underset{H}{\overset{|}{C}}=O + C_2H_5OH = R-\underset{H}{\overset{OH}{\overset{|}{C}}}-OC_2H_5$$

and the intermediate substance is then reduced:

$$2\,R-\underset{H}{\overset{OH}{\overset{|}{C}}}-OC_2H_5 + 2H = R-\underset{H}{\overset{OH}{\overset{|}{C}}}-\underset{H}{\overset{OH}{\overset{|}{C}}}-R + 2\,C_2H_5OH$$

According to Fittig and Remsen piperonyl alcohol is soluble in ether and alcohol, but only slightly soluble in hot water. It was not, however, obtained from its aqueous solution as crystals, but separated out in oily form. This oily substance was reported to form, when left for a long time in a sulphuric acid desiccator, colourless needle crystals melting at 51°.

Nevertheless, the substance obtained by me by electrolysis is comparatively easily soluble in water and also soluble in ether, alcohol, benzene, methyl alcohol and chloroform, but insoluble in cold ligroin. When its solution in warm ligroin is allowed to stand aside for a few

days, large prismatic crystals separated out, melting at 56°.

The result of its elementary analysis is as follows:

Substance, 0·1694 gr. CO_2=0·3899 gr. H_2O=0·0836 gr.
C = 62·75% H = 5·52%
Substance, 0·1446 gr. CO_2=0·3337 gr. H_2O=0·0701 gr.
C = 62·92% H = 5·42%
Theoretical for piperonyl alcohol
C = 63·16% H = 5·26%

It thus agrees well with piperonyl alcohol.

The substance obtained by Fittig and Remsen, judged from its low melting-point, was perhaps impure on account of the incompleteness of the removal of the original aldehyde.

The benzoyl derivative of piperonyl alcohol.

Fittig and Remsen had reported that by the action of benzoyl chloride upon piperonyl alcohol, a thick oil is formed, the composition of which was not determined due to insufficiency of the material. I have however treated with benzoyl chloride, in the same manner as in the case of vanillin, the piperonyl alcohol obtained by electrolysis as described above, and found that the oily substance that separated out at first, quickly solidified into a crystalline mass, which, recrystallized with dilute methyl alcohol, formed shining needle crystals, melting at 66°.

The result of its elementary analysis was as follows:

Substance, 0·1205 gr. CO_2=0·3112 gr. H_2O=0·0528 gr.
C = 70·45% H = 4·86%
Substance, 0·1178 gr. CO_2=0·3035 gr. H_2O=0·0503 gr.
C = 70·25% H = 4·78%
Theoretical for piperonyl alcohol bezoate
C = 70·29% H = 4·76%

This ester was hydrolysed with a methyl alcoholic solution of caustic soda, acidified with phosphoric acid, and subjected to steam distillation. The benzoic acid thus separated was titrated with a barium hydroxide solution for determining its molecular weight.

Substance, 0·4729 gr. required $Ba(OH)_2$ solution (0·947 N) 19·7 cc.
Molecular weight 253

Calculated for $C_{15}H_{12}O_4$ 256

In concluding, the author wishes to express his grateful appreciation to Professor Motooki Matsui for his kind guidance in carrying out this investigation.

On the Arrangements of the Micro-Crystals in Bismuth and Antimony deposited by Electrolysis[1]

By

Hideki Hirata

(Received July 9, 1928)

Abstract

The arrangements of the micro-crystals in electrolysed specimens of bismuth and antimony, deposited under various conditions, were examined with X-rays, by the so-called "transmission method." The diffraction-patterns thus obtained were seen to be explainable by the following considerations:- (1) The formation of the regular arrangements of bismuth crystals seems to be influenced at least by two factors: i.e., the current density and the concentration of the electrolyte. The smaller current density and the lower concentration of the electrolyte seem to be the favorable conditions for the formation of regular arrangement. (2) The non-metallic cloddy deposits found on the cathode by the electrolysis of bismuth or antimony, are composed mainly, at least, of the micro-crystals having the same space lattices respectively as those of bismuth or antimony. (3) The micro-crystals of bismuth in its fibrous specimen are so arranged that the crystal-axis[2] of the indices [211] is parallel to the axis of the fibre. Not only in the fibrous specimens, but also in the single crystals of bismuth obtained in an acicular form, the same crystal-axis is parallel to the direction of the acicular axis.

Introduction

Up to now, a number of investigations have been carried out in connection with the crystalline structures of electrodeposited metals, by making use of the diffraction phenomena of X-rays. As the results of these researches, it has generally been accepted that the micro-crystals

1 This was read in part at the meeting of the Chemical Society of Japan, April, 1927.

2 Following Niggili, the indices of a direction in the crystal are represented by its direction ratios h k l with respect to the three rhombohedral edges of the crystal of bismuth. This direction is called, in this paper, the crystal-axis bearing the indices [h k l].

of an electrolytically deposited metal have the tendency to arrange themselves in a fibrous form, on the one hand,[1] while, on the other, they precipitate without any regularity under certain circumstances.[2] Quite recently it has however been found that the formation of single crystals by electrolysis is also possible in a certain condition.[3]

Thus, in the present investigation of crystal structures, it seems to be of vital importance to distinguish the conditions, under which the different arrangements of the micro-crystals are produced. It may also be suggestive to compare the orientations of crystal-axes in various electrodeposited metals for the furtherance of investigations.

Only a few experimental data are however available for our consideration. Especially, with regard to electrodeposited metals belonging to some peculiar lattice-forms such as bismuth and antimony, no datum has as yet been obtained up to the present time. So, the writer was induced to start the experiments with electrolytic bismuth and antimony. The procedure of obtaining the specimens is described below.

Experimental Part

Specimen. The specimens used in this experiment were deposited on a thin electrolytic sheet copper 14 cm.^{2} in area as the cathode. A cast plate of bismuth or antimony of the same size served as the anode. Two electrodes were suspended parallel to each other at a distance of about 2·5 cm., and the potential difference applied to them was 2 volts for bismuth and 4 volts for antimony.

The specimens were deposited, usually, in a cloddy form like platinum black, but in a few special cases, where the current density and the concentration of electrolyte were small, the specimens with the proper metallic lustre of bismuth or antimony in very minute acicular or lamellar forms (0·7—1·2 mm. in diameter) came to appear mixed with the cloddy specimens.

Let us designate the metallic specimen as Specimen-A, and the cloddy one as Specimen-B, and for their sub-classes with different numerical suffixes, as A_1, A_2, B_1, B_2, etc.

1 R. Glocker u. K. Kaupp: Z. S. f. Phys., **24**, 121 (1924).
Richard M. Bozorth: Phys. Rev., **26**, 390 (1925).

2 R. Glocker u. K. Kaupp: Loc. cit.
Richard M. Bozorth: Loc. cit.

3 G. Asahara and T Sasahara: Scientific Papers of the Institute of Physical and Chemical Research, **5**, 79 (1926).

The conditions, under which these specimens were obtained, are given below :–

Bismuth.

Specimens A_1 and B_1

Electrolyte : 42 ccs. of HCL, 178 ccs. of H_2O, and 18 grams of No_3 (OH_2) Bi.

Current density : 0·07 amp./cm.^{2}

Specimens A_2 and B_2

Electrolyte : 84 ccs. of HCL, 356 ccs. of H_2O, and 18 grams of NO_3 (OH_2) Bi.

Current density : 0·036 amp./cm.^{2}

In the above two cases, the most part of the deposit was the cloddy Specimen B, the metallic Specimen A being very scarce.

Specimens A_3 and B_3

Electrolyte : 84 ccs. of HCL, 356 ccs. of H_2O, and 9 grams of NO_3 (OH_2) Bi.

Current density : 0·025 amp./cm.^{2}

The specimens obtained were mostly of the metallic Specimen A.

Specimen B_4

Electrolyte : The same as with A_1 and B_1.

Current density ; 0·036 amp./cm.^{2}

In this case, the specimen with the metallic lustre could hardly be detected.

Antimony.

Specimens A_2 and B_2.

Electrolyte : 113 grams of K_2CO_3, 54 grams of Sb_2S_3, and 1 litre of H_2O.

Current density : 0·036 amp./cm.^{2}.

In this case the electrolyte was prepared according to the following procedure :

The mixture described above was boiled about one hour. Its concentration was kept unchanged during the boiling by adding now and then as much water as was lost by evaporation. The filtrate obtained from the boiled solution was left to cool gradually, and then used as its electrolyte.

Specimen B_1: In this case the electrolyte was prepared in the same way as with Specimen A_2 and B_2, and kept boiling during the process of the electrolysis,

What has been described above, can be summarized as follows : with respect to bismuth and antimony, a specimen represented by a

smaller numerical suffix corresponds generally to a larger current density and to a larger concentration of the electrolyte. The only exception to the above is the Specimen B_4 of Bi. In this case, the current density and the concentration of the electrolyte were larger than those corresponding to Specimen–B_3 and Specimen–A_3 of Bi.

The micro-photographs of various specimens are reproduced in Plate I.

Outline of the Experimental Method. In the present experiment the writer adopted the ordinary "transmission method", and it was essentially the same as that previously employed by H. Komatsubara and the present writer[1] to examine electrolysed silver.

The heterogeneous X–rays emitted from the molybdenum–anticathode of Coolidges U–type tube were confined to a narrow circular beam by letting them pass through narrow circular holes in two lead diaphragms. And the specimen to be tested was illuminated by this narrow beam of X–rays. To obtain the diffraction figure, a photographic plate was always placed perpendicularly o the incident beam in a position 3·2 cms. behind the specimen, unless otherwise stated. The maximum voltage applied to the tube was about 50–80 K.Vs., and the current through it was 4–5 milliamperes.

By the electrolysis of bismuth and antimony, it was very difficult to get a good specimen of moderate size and of a suitable thinness for X–ray examination. A slight increase in its thickness would considerably reduce the intensity of the diffracted rays. Thus, most of the specimens gave very diffuse, sometimes too diffuse to be reproduced, diffraction figures.

So, it seems to be of fundamental importance to select specimens profitable for our experiments. This selection was made by taking preliminary diffraction figures, and the profitable specimens were chosen for further experiments.

Experimental Results.

I. Bismuth

(i) Specimen–A. A piece of Specimen–A_1 (0·7 mm. in diameter), with which the experiment was first performed, was pasted on a sheet of paper, so that its lamellar face became parallel to the surface of the paper. When this lamellar face, which coincided with the surface of

1 H. Hirata & H. Komatsubara: These Memoirs, **10**, 85 (1926); or Z. S. f. Anorg. u. Allgem. Chem., **158**, 137 (1926).

the paper, was set perpendicular to the incident beam, then the diffraction figure reproduced in Fig. 11, Plate II, was usually obtained on the photographic plate.

In this figure, the prominent part or "intensity maxima", consists of a number of concentric circular rings and several radiating bands which have many intense spots on them. Thus we can conclude, from Fig. 11, that the Specimen-A_1 is partly composed of a fibrous structure, but considerable portion of it consists perhaps of an irregular aggregation of the micro-crystals.

Fig. 12, Plate II, is the diffraction figure taken with the Specimen-A_2, in a similar way as Fig. 11, plate II. In this case a piece of the lamellar specimens (0·8–1·2 mm. in diameter) was used. The diffraction pattern obtained, as can be seen in Fig. 12, Plate II, consists of a number of radiating bands; but no concentric circular rings can be detected. The absence of concentric circular rings in this case shows us without doubt, that the growth of fibrous structure is complete in Specimen-A_2: i. e., the specimen does not contain any considerable irregular aggregation of the micro-crystals, but that it is mostly made up of the fibrous crystalline arrangements.

Next, the writer extended his investigation to Specimen-A_3. The specimens belonging to this group came to appear mostly in an acicular form; and a few lamellar mixtures could also be found among these aciculae. With a lamellar fragment of Specimen-A_3, the interference figure was taken in a similar way as Figs. 11 and 12, Plate II; while to take the interference figure with an acicular specimen, the acicular axis was placed perpendicularly to the direction of the incident ray. The diffraction figure obtained in the former case, (not reproduced) was of the pattern consisting not only of a number of radiating bands, but also of an irregular assemblage of many Laue's spots; while, in the latter case, we obtained the figure reproduced in Fig. 13, Plate II. The prominent part of this figure consists of a set of Laue's spots, which seem to be produced by a single crystal, as will be considered later.

Thus we may conclude, from the presence of Laue's spots in both figures above-mentioned, that Specimen-A_3 is composed of crystals of considerable dimensions. Especially, in the acicular specimen, which gave rise to Fig. 13, Plate II, the growth of the crystal of bismuth is so complete that the trace of fibrous or irregular aggregations of the micro-crystals can no more be detectable.

Here, it must be remarked that the foregoing statement is rather a general, or so to speak, a statistical one, obtained from many specimens

belonging to every sub-class. Here and there occasionally a few exceptions were detected: e. g., some of the specimens belonging to Specimen-A_1 (in the ratio of 1 to 4) gave rise to a diffraction figure which was essentially the same as that obtained with Specimen-A_2. The prominent part of this figure consisted of several radiating bands of the same angular distribution as that in Fig.12, Plate II, without any concentric circular rings.

Conversely to the case above stated, the same diffraction figure Fig. 14, Plate II, as with Specimen-A_1 was sometimes obtained with Specimen-A_2 (in the ratio of 1 to 4).

It was confirmed, however, that such an interchange of the corresponding figures between two different specimens occurred only when their suffix numbers differed by one; i.e., the two specimens which interchanged their corresponding diffraction figures, were always those deposited under the nearest conditions. From this fact, we may suppose that the exceptions above stated are due probably to some accidental causes, such as the variation of the local current density.

The argument which has hitherto been advanced with respect to Specimen-A, leads us to the following conclusions:-

When the current density and the concentration of the electrolyte are comparatively large, the micro-crystals of bismuth have no remarkable tendency to deposit themselves in a fibrous form. But, this tendency becomes the more remarkable with a smaller current density and smaller concentration of the electrolyte, and a perfect fibrous arrangement is realizable under such conditions as will produce Specimen-A_2.

In an extreme case, when the current density and the concentration of the electrolyte are so small as to produce Specimen-A_3, the electrodeposit tends to form single crystals of considerable dimensions.

(ii) Specimen B. The specimens belonging to this group, as already stated, were of apparently non-metallic amorphism with an appearance like platinum black. Among the specimens of this category, Specimens B_1, B_2, and B_3 came to appear in a very brittle cloddy form, while Specimen B_4 was of a lamella deposited on the surface of the cathode.

All of these specimens have no proper micro-structure of metallic bismuth. Consequently, it was questionable whether they were composed of metallic bismuth, or of its compound.

Now, to investigate the crystalline structure of those specimens, the diffraction figures were taken in two different ways. With a cloddy specimen such as Specimens B_1, B_2, and B_3, a diffraction figure was taken by transmitting the incident beam of X-rays to a small clod of

the specimen, which had been pasted on a sheet of paper. Next, with Specimen-B_4, which was a lamellar aggregation of numerous fine grains, the writer investigaetd the interference phenomena obtained in the following two orientations of the sample: one when the surface of the lamella was set perpendicular to the direction of the incident beam, and the other when it was rotated by about 20° around an axis perpendicular to the direction of the incident beam. In this way, it should be possible to detect regular structures, if any, in the specimen.

From these results of the investigation, it became clear that the same diffraction figure is obtainable with all the specimens belonging to Specimen-B. In this figure, the prominent part of the diffraction-pattern consisted of a number of concentric circular rings as shown in Fig. 17, Plate III, which was produced by the normal incidence of X-ray-beam on the lamellar surface of Specimen B_4. It will be shown later that the radii of these concentric circular rings agree fairly well with the results of calculation, carried out from the experimental data of metallic bismuth given by James[1] and Ogg,[2] and from the wavelength of the K_α radiation of molybdenum.

As a consequence of such calculation, it was seen that the concentric rings $I'_{1,2}$, II′, $III'_{1,2}$, I_1'', I_2'', II″, IV_1', and I_2''' in Fig.17, Plate III were produced by the prominnt atomic planes of the indices[3] $(111)_I$ and $(\bar{1}11)_I$, $(100)_I$, $(110)_I$ and $(\bar{1}10)_I$, $(111)_{II}$, $(\bar{1}11)_{II}$, $(100)_{II}$, $(211)_I$, and $(\bar{1}10)_{III}$ respectively. Here, it must be understood that the numerical suffixes used in the symbols $(\quad)_I$, $(\quad)_{II}$, and $(\quad)_{III}$ denote the order of the spectrum.

From these facts, it can be inferred that the so called amorphous deposits under consideration, or some part of them at least, are not amorphous, but composed mainly of the irregular aggregation of the micro-crystals of metallic bismuth. Moreover, as was stated before, the diffraction-figure was essentially the same as Fig.17, Plate III, even when Specimen-B_4 was tilted from its normal position against the incident beam. This shows that the micro-crystals in the specimen are irregularly orientated with respect to any direction.

---

1 Phil. Mag., **42**, 193 (1921).

2 Phil. Mag., **42**, 163 (1921).

3 To represent the family of atomic planes in bismuth or antimony, the notation is used in the same way as by James & Tunstall.[4]

4 Phil. Mag.. **40**, 233 (1920)

II. Antimony.

(i) Specimen A. Fig.15, Plate III is the diffraction figure taken with a piece of Specimen-A_2. To obtain this figure, the face of this lamellar specimen was set perpendicular to the incident beam, as was done with a lamellar specimen of bismuth.

The prominent part of Fig.15 in Plate III consists of a set of Debye-Hull's rings I_2'', II'', IV_1', I_1''', III_1'' and II''', which were found, from the results of calculation, described later, to be produced by the reflection from the prominent atomic planes of the indices $(11\bar{1})_{II}$, $(100)_{II}$, $(211)_I$, $(111)_{III}$, $(110)_{II}$, and $(100)_{III}$ respectively.

It can also be expected that the rings corresponding to $(\bar{1}11)_I$, $(100)_I$, $(110)_I$ and $(\bar{1}10)_I$ would come to appear in the figure. But they are considered to fall inside the broad central spot, because their radii are smaller than that of the central spot. No clear evidence of the fibrous structure was detected in this case, as in the case of Bi.

Specimen B: As Specimen B_4 of Bi, Specimen B_1 of Sb was also a black cloddy lamella formed on the cathode. To examine this specimen, the writer took the diffraction figures in two orientations of the sample, as was the case with Specimen B_4 of Bi: i.e., one when its lamellar face was set perpendicular to the direction of the incident beam, and the other when it was rotated by about 20° around an axis perpendicular to the direction of the incident beam. Fig.16, Plate III is the diffraction figure obtained in the former orientation. The prominent part of this figure consists, as with Specimen B of Bi, of a number of concentric circular rings. The same figure as Fig.16 Plate III was also obtained in the latter orientation.

Consequently, we may conclude that the majority of the micro-crystals in Specimen B_1 of Sb is irregularly orientated with respect to any direction.

The same calculation as with Specimen A of Sb applies well to the present instance. As its results, it became clear that the rings II', $III'_{1,2}$, I_1'', I_2'', II'', IV_1', I_1''' and I_2''' in Fig.16 Plate III were due to the reflections of the X-rays from the prominent atomic planes of the indices $(100)_I$, $(110)_I$ and $(\bar{1}10)_I$, $(111)_{II}$, $(\bar{1}11)_{II}$, $(100)_{II}$, $(211)_I$, $(111)_{III}$, and $(\bar{1}11)_{III}$ respectively.

The facts so much as were confirmed, lead us to the same conclusion as in the case of the Specimen B of Bi: i.e., the most part, if not the whole, of the apparently amorphous Specimen B of Sb, is not amorphous, but composed of an irregular aggregation of the micro-

crystals of antimony.

Discussion of the Experimentat Results. In the preceding chapter, rather qualitative arguments were advanced with respect to the crystalline structure of each specimen. The further arguments we now attempt to make in this chapter, aim at the quantitative explanation of our experimental facts. In the first place, the indices of the atomic planes which gave rise to the intense spots on the radiating bands and to the Debye-Hull's rings observed, will be determind by calculation. Secondly will be investigated what direction of the fibrous axis would produce the angular distribution of radiating bands, as was observed with Specimen-A_2 of Bi. The last part of the arguments will deal with the mechanism of the formation of Laue's Figure as was observed with some specimens belonging to Specimen-A_3 of Bi.

Now, before entering into detail, it would be well to find out the formulae from which the numerical values of an angle between two atomic planes and the spacing of each one of these planes in the crystal are derived. By making use of these numerical values, Yoshida's "globe and spherical scale"[1] which facilitates the troublesome calculations, can be made available to our present investigation.

Fig. 1 Antimony Type Space-Lattice

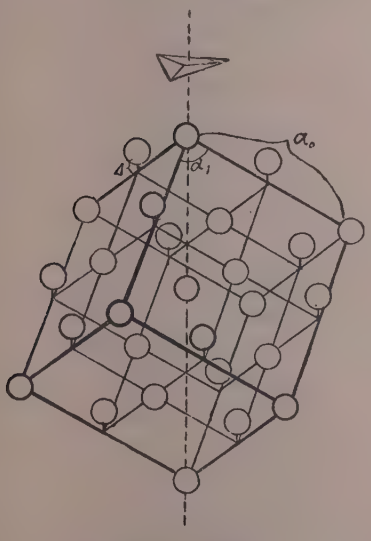

From the researches of James,[2] [4] Tunstall[2], Ogg[3] and others,[5] it is known that the crystals of both metals under consideration, as are represented diagrammatically in Fig.1, consist of two interpenetrating face-centred rhombohedral lattices, which have a trigonal axis in common. Moreover it is already known that the rhombohedral angles α_1 of bismuth and antimony crystals are 87°34′ and 86° 58′ respectively. While, two rhombohedral lattices which form the bismuth or antimony crystal are considered to

1 U. Yoshida: Japanese. J. Phys., 4, 133 (1927).
2 Loc. cit.
3 Loc. cit.
4 Loc. cit.
5 L. W. Mc Keehan: Journ. Franklin Institute, Jan., (1923).

be displaced to each other by $\triangle=0{\cdot}027\ t_0$ and $\triangle=0{\cdot}04\ t_0$ respectively, along the common trigonal axis, where t_0 is the length of this common trigonal axis of the unit cell. If we represent the length of the rhombohedral edge of the unit cell by a_0, it amounts to $6{\cdot}20\times10^{-8}$ cm. in antimony. As to the numerical value of a_0 in bismuth, James and others gave $6{\cdot}56\times10^{-8}$ cm., while, according to Ogg, it amount to $6{\cdot}52\times10^{-8}$ cm. Thus, let us use their mean value $6{\cdot}53\times10^{-8}$ cm. in our further calculation.

Now, let us take the three rhombohedral edges which incline with the angle α_1 with each other as the axes of an oblique co-ordinate system, and the corner atom situated at the intersecting point of these axis as the origin. If we temporarily suppose that the crystals are of the simple rhombohedral lattice, then the equations of the atomic planes with the indices h k l and h′ k′ l′ will respectively be given by

$$\left.\begin{aligned} hx+ky+lz&=a_0 \qquad (1a)\\ h'x+k'y+l'z&=a_0 \qquad (1b)\end{aligned}\right\}$$

Now, let ξ, η, ζ, and ξ', η', ζ' be the two sets of the angles between the co-ordinate axes and the normals of these two atomic planes respectively, then the perpendicular distances d_{hkl} and $d_{h'k'l'}$ from the origin to these planes should be expressed respectively by

$$\frac{\cos\xi}{h}=\frac{\cos\eta}{k}=\frac{\cos\zeta}{l}=\frac{d_{hkl}}{a_0}$$

$$\frac{\cos\xi'}{h'}=\frac{\cos\eta'}{k'}=\frac{\cos\zeta'}{l'}=\frac{d_{h'k'l'}}{a_0}$$

$\cos\xi$, $\cos\eta$, $\cos\zeta$ and $\cos\xi'$, $\cos\eta'$, $\cos\zeta'$ in the above expressions being respectively the direction cosines of the same straight line, the following relations (3) and (4) should hold good in the present case.

$$\begin{vmatrix} 1 & \cos\alpha_1 & \cos\alpha_1 & \cos\xi \\ \cos\alpha_1 & 1 & \cos\alpha_1 & \cos\eta \\ \cos\alpha_1 & \cos\alpha_1 & 1 & \cos\zeta \\ \cos\xi & \cos\eta & \cos\zeta & 1 \end{vmatrix}=0 \qquad (3)$$

$$\begin{vmatrix} 1 & \cos\alpha_1 & \cos\alpha_1 & \cos\xi' \\ \cos\alpha_1 & 1 & \cos\alpha_1 & \cos\eta' \\ \cos\alpha_1 & \cos\alpha_1 & 1 & \cos\zeta' \\ \cos\xi' & \cos\eta' & \cos\zeta' & 1 \end{vmatrix}=0 \qquad (4)$$

Moreover, the angle β_1 between the two atomic planes (h_1 and h_2) should be given by

$$\begin{vmatrix} 1 & \cos\alpha_1 & \cos\alpha_1 & \cos\xi' \\ \cos\alpha_1 & 1 & \cos\alpha_1 & \cos\eta' \\ \cos\alpha_1 & \cos\alpha_1 & 1 & \cos\zeta' \\ \cos\xi' & \cos\eta' & \cos\zeta' & \cos\beta_1 \end{vmatrix} = 0 \qquad (5)$$

Consequently, from (2), (3), (4), and from the above expression (5), we get

$$\cos\beta_1 = \frac{\Sigma hh' \sin\alpha_1 + \Sigma kl' (\cos^2\alpha_1 - \cos\alpha_1)}{\sqrt{\{\Sigma h^2 \sin^2\alpha_1 + 2\Sigma kl' (\cos^2\alpha_1 - \cos\alpha_1)\}\{\Sigma h'^2 \sin^2\alpha_1 + 2\Sigma k'l' (\cos^2\alpha_1 - \cos\alpha_1)\}}} \qquad (6)$$

$$\left.\begin{aligned} d_{hkl} &= \frac{a_0\sqrt{1 + 2\cos^3\alpha_1 - 3\cos^2\alpha_1}}{\sqrt{\Sigma h^2 \sin^2\alpha_1 + 2\Sigma kl (\cos^2\alpha_1 - \cos\alpha_1)}} \\ d_{h'k'l'} &= \frac{a_0\sqrt{1 + 2\cos^3\alpha_1 - 3\cos^2\alpha_1}}{\sqrt{\Sigma h'^2 \sin^2\alpha_1 + 2\Sigma k'l' (\cos^2\alpha_1 - \cos\alpha_1)}} \end{aligned}\right\} \qquad (7)$$

As was stated before, the above expressions (6) and (7) represent respectively the angle between the normals of two atomic planes and the spacings of these planes in a simple rhombohedral lattice. These expressions can easily be modified as to be applicable to a face-centred rhombohedral lattice, as is the case in bismuth or antimony. In the following articles, the experimental results will be compared with the consequence of calculations which are founded on the above two expressions.

The angles between any crystal axis and the normals to various atomic planes of the crystals may be calculated similarly as above.

(i) On the Formation of Debye-Hull's Rings:

The expression (7) represents the spacing between two consecutive atomic planes having the indices $h\ k\ l$ in a simple rhombohedral lattice. Thus, if we modify the expression (7) so that it be applicable to a face-centred rhombohedral lattice, and substitute the proper numerical values for a_1 and a_0, the spacing of each atomic plane in bismuth or antimony crystal should immediately be found.

In each of the first columns of Tables 1 and 2, the indices of the prominent atomic planes of bismuth and antimony are represented. The numerical values of the corresponding spacing d, thus calculated from expression (7), are given in the second columns of the same Tables.

From these numerical values of d, the radii of Debye-Hull's rings on the photographic plate will be calculated. For this purpose a calculation was carried out, by making use of the following two well known relations :—

$$2a \text{ Sin } \theta = n\lambda \qquad (8)$$

$$L \text{ Tan } 2\theta = r \qquad (9)$$

where n is a positive integer representing the order of the spectrum, θ the glancing angle of the incident X-ray, λ the wavelength of the incident X-rays, and L the distance of the photographic plate from the specimen. The value of L was 3.2 cm. in the present experiment.

The values of γ thus calculated are given in the fourth columns of

Table 1 *Bi*

Calculated Values						Observed Values			
Indices of the Reflecting Planes			d in 10^{-8} cm.	n	r in. cm.	r in cm.			No. of Rings
						Fig. 11	Fig. 14	Fig. 17	
1	1	1	3.934	1 2 3	0.58 1.22 1.95	1.23	1.23	1.23	— I_1'' —
1	1	$\bar{1}$	3.719	1 2 3	0.62 1.29 2.10	1.29 2.10	1.31	1.28 2.10	— I_2'' I_2'''
1	1	0	2.357	1 2 3	1.00 2.25 4.36	*	0.97	*	III_1' — —
1	$\bar{1}$	0	2.264	1 2 3	1.04 2.37 4.77	*	1.05	* 2.39	III_2' III_2'' —
1	0	0	3.265	1 2 3	0.69 1.50 2.51	* 1.50	* 1.50	* 1.49	— II'' —
2	1	1	1.381	1	1.83		1.80	1.80	IV_1
2	1	$\bar{1}$	1.341	1	1.89				—
$\bar{2}$	1	1	1.306	1	1.96				—

Table 2 *Sb*

Calculated Values						Observed Values		
Indices of the Reflecting Planes			d in 10^{-8} cm.	n	r in cm.	r in cm. Fig. 15	r in cm. Fig. 16	No. of Rings
1	1	1	3.770	1	0.61			—
				2	1.27		1.25	I_1''
				3	2.06	2.06		I_1'''
1	1	$\bar{1}$	3.517	1	0.65			—
				2	1.38	1.38	1.41	I_2''
				3	2.26		2.26	I_2'''
1	1	0	2.299	1	1.03	*	*	—
				2	2.40	2.39		III_1''
				3	4.85			—
1	$\bar{1}$	0	2.135	1	1.11	*	1.11	III_2'
				2	2.58			—
				3	5.50			—
1	0	0	3.096	1	0.75	*	0.75	II'
				2	1.60	1.62	1.65	II''
				3	2.71	2.79		II'''
2	1	1	1.321	1	1.94	1.92	1.94	IV_1'
2	1	$\bar{1}$	1.254	1	2.07			—
$\bar{2}$	1	1	1.223	1	2.14			—

Tables 1 and 2. To calculate these numerical values of γ, we have assigned to λ the value of the wavelength of the K_α line of molybdenum. Though it may be possible that the K_β line of molybdenum will also appear, yet as the intensity of this line is very feeble compared with that of the K_α line, the latter line has only been taken to our consideration. For the value of the wavelength of the K_α line, we have given the mean value of the $K_{\alpha 1}$ and $K_{\alpha 2}$ lines, which is equal to $\lambda_\alpha = 709.73 \times 10^{-11}$ cms.

The numerical values of γ can also be obtained by measuring the radii of the rings in the figures. These observed values of γ are represented in the fifth, sixth and seventh columns of Table 1, and in the fifth and sixth columns of Table 2. The Roman numerals in the last columns of Table 1 and 2 denote the numbers of the rings from which these numerical values of γ are measured.

As was to be expected, each one of these observed values of γ agrees fairly well with one of the calculated values in the fourth column of the Tables.

In these two Tables, the rings marked with an asterisk were expected to be so intense, that they would be detectable in the figures. But, this did not come out sight, owing to their radii being smaller than that of the broad central spot.

As the consequence of the foregoing arguments, we may legitimately assign the indices of the atomic planes and the order of the spectra as given in the first and third columns to each concentric ring which is represented in the last columns of the Tables.

In the Tables 1 and 2, the indices of the atomic planes and the order of the radiation were attributed to each Debye-Hull's ring, which was obtained with the Specimens of *Bi* and *Sb*. Such a correspondency between the indices of the atomic plane and the concentric rings was found to exist not only with respect to Figs. 11, 14, 15, 16, and 17, but to all the diffraction figures obtained in this experiment. Consequently, it seems to be legitimate to consider that each concentric ring in these figures was produced by the reflection of a prominent atomic plane in the bismuth or antimony crystals.

(ii) On the Formation of the Radiating Bands:

Next, let us determine the direction of the fibrous axis which will produce an angular distribution of radiating bands as in Figs. 12 and 14, Plate II. For this purpose the following relation was used:—

$$\mathrm{Cos}\,\beta = \mathrm{Cos}\,\gamma\,\mathrm{Cos}\,\alpha + \mathrm{Sin}\,\gamma\,\mathrm{Sin}\,\alpha\,\mathrm{Cos}\,\varphi \qquad (10)$$

where α is the angle between the incident ray and the fibrous axis of the crystals, β the angle between the normal of a certain reflecting plane and the fibrous axis of the crystals, $\gamma = \frac{\pi}{2} - \theta$ the angle between the incident ray and the normal of the reflectiong plane, and φ the azimuth of a point on a radiating band measured on the photographic plate from the line of intersection of the photographic plate with the plane containing the incident X-rays and the fibre, by taking the central spot as the pole.

From the above relation (10) and equation (9), each radiating band will be traced out, for definite values of α and β, by giving various values to γ and by finding the numerical relations between φ and γ. Especially when $\alpha = \frac{\pi}{2}$ the radiating bands become nearly straight in the vicinity of the central spot, and the values of φ will be nearly equal to β. Thus, if the value of β is found by measuring the angles between

Table

k k l	1 0 0	0 1 0	0 0 1	1 1 0	1 0 1	0 1 1	1 1 0	1 0 $\bar{1}$	0 $\bar{1}$ 1	1 1
1 0 0	0°	87° 40′	87° 40′	46° 10′	46° 10′	86° 37′	44° 53′	44° 53′	90°	56°
0 1 0	87° 40′	0°	87° 40′	46° 10′	86° 37′	46° 10′	44° 53′	90°	44° 53′	56°
0 0 1	87° 40′	87° 40′	0°	86° 37′	46° 10′	86° 37′	90°	44° 53′	44° 53′	56°
1 1 0	46° 10′	46° 10′	86° 37′	0°	62° 47′	62° 47′	90°	55° 40′	55° 40′	36°
1 0 1	46° 10′	86° 37′	46° 10′	62° 47′	0°	62° 47′	55° 40′	90°	55° 40′	35°
0 1 1	86° 37′	46° 10′	46° 10′	62° 47′	62° 47′	0°	55° 40′	55° 40′	90°	36°
1 $\bar{1}$ 0	44° 53′	44° 53′	90°	90°	55° 40′	55° 40′	0°	60°	60°	90°
1 0 $\bar{1}$	44° 53′	90°	44° 53′	55° 40′	90°	55° 40′	60°	0°	60°	90°
0 $\bar{1}$ 1	90°	44° 53′	44° 53′	55° 40′	55° 40′	90°	60°	60°	0°	90°
1 1 1	56° 24′	56° 24′	56° 24′	36° 57′	36° 57′	36° 57′	90°	90°	90°	0°
$\bar{1}$ 1 1	51° 58′	55° 17′	55° 17′	88° 5′	88° 5′	34° 40′	34° 43′	34° 43′	90°	71°
1 $\bar{1}$ 1	55° 17′	51° 58′	55° 17′	88° 5′	34° 40′	88° 5′	34° 43′	90°	34° 43′	71°
1 1 $\bar{1}$	55° 17′	55° 17′	51° 58′	34° 40′	88° 5′	88° 5′	90°	34° 43′	34° 43′	71°
2 1 1	33° 14′	68° 13′	68° 13′	31° 20′	31° 20′	57° 36′	73° 40′	73° 40′	90°	20°
$\bar{2}$ 1 1	33° 36′	65° 24′	65° 24′	72° 30′	72° 30′	53° 3′	29° 59′	29° 59′	90°	90°
2 $\bar{1}$ 1	35° 49′	62° 56′	67° 7′	75° 7′	29° 59′	87° 16′	29° 37′	72° 59′	54° 11′	63°
2 1 $\bar{1}$	35° 49′	67° 7′	62° 56′	29° 59′	75° 7′	87° 16′	72° 59′	29° 57′	54° 11′	63°
1 2 1	68° 13′	33° 14′	68° 13′	31° 20′	57° 36′	31° 20′	73° 40′	90°	73° 40′	20°
1 2 1	62° 56′	35° 49′	67° 7′	75° 7′	87° 16′	29° 59′	29° 37′	54° 11′	72° 59′	63°
1 $\bar{2}$ 1	65° 24′	33° 36′	65° 24′	72° 30′	53° 3′	72° 30′	29° 59′	90°	29° 59′	90°
1 2 $\bar{1}$	67° 7′	35° 49′	62° 56′	29° 59′	87° 16′	75° 7′	72° 59′	54° 11′	29° 37′	63°
1 1 2	68° 13′	68° 13′	33° 14′	57° 36′	31° 20′	31° 20′	90°	73° 40′	73° 40′	20°
$\bar{1}$ 1 2	62° 56′	67° 7′	35° 49′	87° 16′	75° 7′	29° 59′	54° 11′	29° 37′	72° 59′	63°
1 $\bar{1}$ 2	67° 7′	62° 56′	35° 49′	87° 16′	29° 59′	75° 7′	54° 11′	72° 59′	29° 37′	63°
1 1 $\bar{2}$	65° 24′	65° 24′	33° 36′	53° 3′	72° 30′	72° 30′	90°	29° 59′	29° 59′	90°

of β_1

2 $\bar{1}$ 1	2 1 $\bar{1}$	1 2 1	$\bar{1}$ 2 1	1 $\bar{2}$ 1	1 2 $\bar{1}$	1 1 2	$\bar{1}$ 1 2	1 $\bar{1}$ 2	1 1 $\bar{2}$
35° 49′	35° 49′	68° 13′	62° 56′	65° 24′	67° 7′	68° 13′	62° 56′	67° 7′	65° 24′
62° 56′	67° 7′	33° 14′	35° 49′	33° 36′	35° 49′	68° 13′	67° 7′	62° 56′	65° 24′
67° 7′	62° 56′	68° 13′	67° 7′	65° 24′	62° 56′	33° 14′	35° 49′	35° 49′	33° 36′
75° 7′	29° 59′	31° 20′	75° 7′	72° 30′	29° 59′	57° 36′	87° 16′	87° 16′	53° 3′
29° 59′	75° 7′	57° 36′	87° 16′	53° 3′	87° 16′	31° 20′	75° 7′	29° 59′	72° 30′
87° 16′	87° 16′	31° 20′	29° 59′	72° 30′	75° 7′	31° 20′	29° 69′	75° 7′	72° 30′
29° 37′	72° 59′	73° 40′	29° 37′	29° 59′	72° 59′	90°	54° 11′	54° 11′	90°
72° 59′	29° 37′	90°	54° 11′	90°	54° 11′	73° 40′	29° 37′	72° 59′	29° 59′
54° 11′	54° 11′	73° 40′	72° 59′	29° 59′	29° 37′	73° 40′	72° 59′	29° 37′	29° 59′
63° 20′	63° 20′	20° 37′	63° 20′	90°	63° 20′	20° 37′	63° 20′	63° 20′	90°
60° 2′	60° 2′	62° 28′	19° 5′	61° 41′	88° 56′	62° 28′	19° 5′	88° 56′	61° 41′
19° 5′	88° 56′	87° 45′	60° 2′	18° 24′	60° 2′	62° 28′	88° 56′	19° 5′	61° 41′
88° 56′	19° 5′	62° 28′	88° 56′	61° 41′	19° 5′	87° 45′	60° 2′	60° 2′	18° 24′
48° 52′	48° 52′	35° 31′	82° 58′	79° 51′	61° 21′	35° 31′	82° 58′	61° 21′	79° 51′
47° 31′	47° 31′	79° 51′	32° 24′	60°	80° 17′	79° 51′	32° 24′	80° 17′	60°
0°	71° 37′	82° 58′	57° 18′	32° 24′	80° 4′	61° 21′	80° 4′	34° 1′	80° 17′
71° 37′	0°	61° 21′	80° 4′	80° 17′	34° 1′	82° 58′	57° 18′	80° 4′	32° 24′
82° 58′	61° 21′	0°	48° 52′	69° 23′	48° 52′	35° 31′	61° 21′	82° 58′	79° 51′
57° 18°	80° 4′	48° 52′	0°	47° 31′	71° 37′	61° 21′	34° 1′	80° 4′	80° 17′
32° 24′	80° 17′	63° 29′	47° 31′	0°	47° 31′	79° 51′	80° 17′	32° 24′	60°
80° 4′	34° 1′	48° 52′	71° 37′	47° 31′	0°	82° 58′	80′ 4′	57° 18′	32° 24′
61° 21′	82° 58′	35° 31′	61° 21′	79° 51′	82° 58′	0°	48° 52′	48° 52′	69° 23′
80° 4′	57° 18′	61° 21′	34° 1′	80° 17′	80° 4′	48° 52′	0°	71° 37′	47° 31′
32° 24′	80° 4′	82° 58′	80° 4′	32° 24′	57° 18′	48° 52′	71° 37′	0°	47° 31′
80° 17′	32° 24′	79° 51′	80° 17′	60°	32° 24′	69° 23′	47° 31′	47° 31′	0°

the bands, the axis of the crystal arranged in the direction of the axis of the fibre will be known immediately.

In Figs. 12 and 14, Plate II, all the radiating bands are nearly straight. This indicates that the axis of the fibre was nearly perpendicular to the incident beam of the X-rays, and is in a direction nearly parallel to the lamellar surface of the specimens in these cases. Thus from the relation stated above the value of φ may be taken to be equal to that of β in these cases.

Now let us provisionally suppose that the normal to one of the atomic planes in bismuth-crystals is arranged parallel to the direction of the fibrous axis. If our consideration be correct, the calculated values of β_1, whice represent the angles between the normals to various atomic planes and the direction of the fibrous axis, should agree well with the numerical values of β measured in the vicinity of the central spot on the photographic plates.

Table 3 represents the numerical values of β_1, obtained from the expression (6). All these numerical values of β_1, were confirmed to be correct by using the Yoshida globe and sphericals scale[1].

Thus the fundamental problem is to find out the direction, on the photographic plate, which is parallel to the direction of the fibrous axis. This was accomplished by trial by taking successively the various directions on the photographic plate as the direction of the fibrous axis and by examining the agreement between the observed values of β and the calculated values of β_1 for various atomic planes by taking a certain atomic plane as a reference plane.

With respect to Fig. 12, Plate II, the direction represented by an arrow in that figure was found, in the manner above stated, to be the best one for the direction parallel to the fibrous axis of the specimen. The values of β for various radiating bands in Fig. 12, Plate II, which were measured from the direction represented by the arrow, are given in the third, fourth, fifth, and sixth columns of Table 4. The value of β for each radiating band the number of which is denoted in the seventh column of Table, was measured each quadrant of the figure.

Here it can be noticed that these observed values of β are nearly equal to the calculated values of β_1, in the vertical rows corresponding to the indices 2 1 1, 1 2 1 and 1 1 2 in Table 3. Thus it will not be unnatural to consider that the atomic planes of the indices (2 1 1) are

---

1 Loc. cit.

Table 4.

Calculated Values		Observed Values						
Indices of Pls. h k l	β_2	β 1st Quadrant	β 2nd Quadrant	β 3rd Quadrant	β 4th Quadrant	No. of Rad Bds.	Indices of Family of Pls.
1 1 1	18° 20′	19°	18°	19°	18°	I_1	(1 1 1)
1 1 0 1 0 1	31° 28′	—	—	31°	—	III_1	(1 1 0)
1 0 0	38° 2′	38°	38°	38°	38°	II	(1 0 0)
0 1 1	55° 21′	—	—	—	—	III_1	(1 1 0)
1 $\bar{1}$ 1 1 1 $\bar{1}$	63° 21′	63°	63°	63°	63°	I_2	(1 1 $\bar{1}$)
0 1 0 0 0 1	66° 48′	66°	66°	—	66°	II	(1 0 0)
1 1 0 1 0 $\bar{1}$	74° 9′	74°	74°	76°	75°	III_2	(1 1 0)
0 1 1 1 1 1	90°	88°	90°	90°	92°	$I_2 III_2$	(1 1 $\bar{1}$) (1 $\bar{1}$ 0)

arranged nearly, though not exactly, parallel to the direction of the fibrous axis in this case.

Next, in expressing the direction of the crystal, which is arranged parallel to the direction of the axis of the fibre, it is more natural to take a crystallographic axis than to take the normal of an atomic plane of the crystal. These two directions are slightly different in the case of bismuth and antimony. As the angle between the crystallographic axis [2 1 1] and the normal to the corresponding atomic plane 2 1 1 is only 2° 27′ in the case of the bismuth-crystal, the writer preferred the crystallographic axis [2 1 1] as the axis of the fibre.

The values of β_2 calculated and tabulated in Table 4 are the angles between the crystallographic axis [2 1 1] and the normals to various atomic planes, whose indices are given in the first column of the same table. A fair agreement between the values observed for β and those calculated for β_2 will be seen in the table.

In Fig. 12, Plate II, we can detect the appearance of the intense spots on some of the radiating bands. These intense spot are certainly caused by the reflections of the K_α radiation of molybdenum from various

atomic planes. The indices of each one of these atomic planes were founded from the value of the spacing between two consecutive atomic planes, which was calcutated from the wavelength of the K_α line of molybdenum and the distance of the corresponding intense spot from the centre of the central spot. The indices thus determined experimentally are given in the last column of Table 4, and they are in fair accordance with those given in the first column of that table.

Next, as to the problem whether or not another crystallographic axis may be taken as the axis of the fibre, it was confirmed also by means of the globe and spherical scale devised by U. Yoshida that no other axis than [2 1 1] could account for the distribution of the radiating bands in Fig. 12, Plate II.

The full lines in the annexed Fig. 2 represent diagrammatically the prominent radiating bands, traced out with the calculated values given in the second column of Table 4; and the short lines crossing these radiating bands express the calculated positions of the impression of the K_α line of *Mo* on the photographic plate. The shaded part in the same figure is the copy of the diffraction pattern in Fig. 12, Plate II.

Fig. 2.

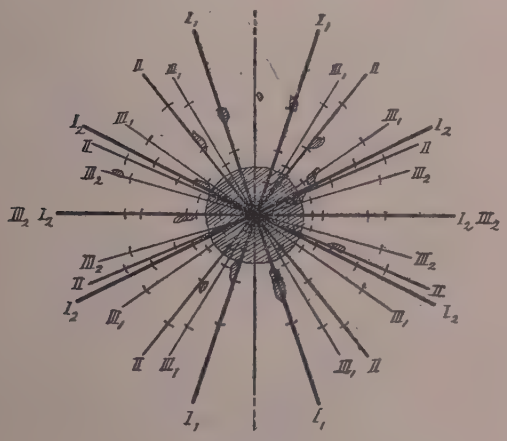

As may be seen from the figure, not only with respect to the angular distribution of the radiating bands, but also with respect to the positions of the intense spots, the agreement between the calculated curves and the obrerved ones is rather satisfactory. Moreover, this agreement was

found to hold good also not only in Fig. 12 but in all the figures consisting of several radiating bands, as Figs. 11 and 14. The arrow in these figures represents the direction of the fibrous axis.

Thus our consideration having been confirmed as above, we may legitimately conclude that the micro-crystals of bismuth have a tendency to deposit themselves in a fibrous from with the crystal-axis [2 1 1] arranged parallel to the direction of the fibrous axis.

Next, to confirm the above consideration still further, the writer investigated the interference phenomena obtained in two orientations of the samples, one when it was rotated 22° around the direction parallel to the axis of the fibre, and the other when it was rotated 22° around an axis perpendicular to the axis of the fibre.

In both cases, the interference figures were photographed with the same lamellar fragment as was used in the case of Fig. 12, Plate II. The distance between the photographic plate and the specimen was 3.5 cm. If our consideration be correct, the figure in the former case should remain unaltered; while in the latter case the symmetry of the figure should be violated. As was expected, the interference figure, essentially the same as Fig. 12, Plate II, was obtained in the former case, but in the latter the interference figure was quite different from the former one. Fig. 18, Plate III is the photograph taken when the axis of the fibre was tilted from its vertical position toward the incident ray.

The full lines in Fig. 3 represent the radiating bands calculated from the consideration stated above, and the shaded part in this figure is the copy of the diffraction pattern in Fig. 18, Plate III (Fig. 3 in the position rotated about 80° in the plane of the paper). In these figures

Fig. 3.

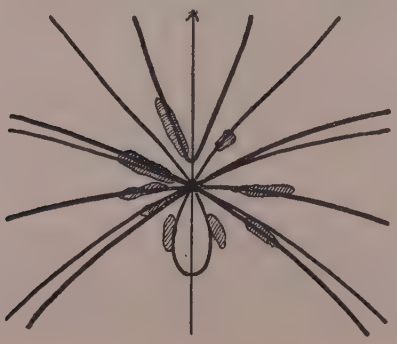

the direction represented by the arrow indicates the line of intersection of the surface of the photographic plate with the plane containing the incident X-ray-beam and the direction of the axis of the fibre in the specimen. The thick full lines in Fig. 3 are the calculated curves corresponding to $\beta = 18^\circ\ 20'$, $\beta = 63^\circ\ 21'$ and $\beta = 90^\circ$. These lines are to be caused by the reflection from the most prominent atomic planes of the indices (1 1 1) and (1 1 $\bar{1}$), and they correspond to the strongest bands marked by I_1 and I_2 in the case of the normal incidence of the X-rays to the lamellar surface of the specimen. The thin full lines are the calculated curves corresponding to $\beta = 38^\circ\ 2'$ and $\beta = 66^\circ\ 48'$, and they correspond to the bands marked by II in the case of normal incidence, whose intensities are next to those marked by I_1 and I_2. As may be seen from Fig. 3, the agreement between the calculated curves and the observed ones is satisfactory.

Accordingly, our foregoing consideration is again confirmed, and we may conclude that a crystal-axis of the indices [2 1 1] is arranged in a direction parallel to the axis of the fibre.

(iii) On the Formation of Laue's Spots:

It was already stated that the acicular specimen belonging to Specimen A_3 of *Bi* is supposed to be an aggregation of crystals of considerable size. The further arguments we now attempt to make, aim to determine the orientation of each crystal in this specimen, with respect to the direction of the acicular axis. This determination was easily carried out from the positions of Laue's spots as in Fig. 13, Plate II, by making use of the Yoshida globe and spherical scale; and it was found in the case of Fig. 13, Plate II, that only when the direction of the incident beam inclines 48°, 27° and 18° respectively to the normals to the atomic planes 0 1 1, 0 0 1, and 1 0 $\bar{1}$, was the distribution of Laue's spots found to agree well with that of Fig. 13, Plate II. This relation is shown in Fig. 4. Considering this to be correct, and if we take into account the atomic planes of a small glancing angle only (less than 20°), it can be expected that each one of the atomic planes 1 1 1, 1 0 1, and 1 $\bar{1}$ 1, will give rise to a very intense spot. As was expected, three spots represented respectively by a, b, and c in Fig. 13, Plate II, came to appear just at the positions where the reflected beams from the atomic planes 1 1 1, 1 0 1, and 1 $\bar{1}$ 1 were to be registered. Thus, we may conclude that the direction of the incident beam is parallel to the direction $\overrightarrow{PQO}$ in Fig. 4.

Fig. 4.

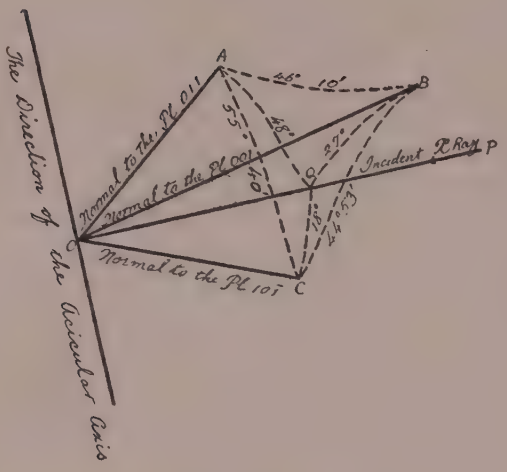

Here, it should be noticed that this direction $\overrightarrow{PQO}$ is normal to the crystal-axis of the indices [2 1 1], and that Fig. 13, Plate II is a diffraction figure produced by the normal incidence of the X-ray-beam to the acicular axis of the specimen. Accordingly, if the azimuth of the acicular direction measured from a certain standard line (e. g., the line *Oa*) in Fig. 13, be equal to that measured on the globe by taking the direction $\overrightarrow{PQO}$ in Fig. 4 as the pole, then it can be concluded that the crystal axis of the indices [2 1 1] is orientated parallel to the direction of the acicular axis. As was observed from Fig. 13, Plate II, the angle between the direction of the acicular axis which is represented by an arrow and that of the line *Oa* amounts to 18°, while on the globe the azimuth of the axis [2 1 1] measured from the point corresponding to the atomic plane 1 1 1 on the globe is also 18°.

Accordingly, it may be concluded that in Specimen A_3 of *Bi* the crystal axis of the indices [2 1 1] are arranged parallel to the direction of the acicular axis, and that the diffraction figures Fig. 13, Plate II was produced by the normal incidence of the X-ray beam to the acicular axis.

Hitherto we have treated the diffraction pattern in Fig. 13, Plate II as an ordinary Laue's figure But, strictly speaking, it is not exactly so; and a slight elongation of each Laue's spots indicates the presence of a fibrous nature of weak degree.

To make clearer this point, it would be advisable to reconsider our argument which has previously been made in connection with Specimen A_2 of *Bi*. As was stated before, two different figures Figs. 12 and 14, Plate II were obtained with the samples belonging to this specimen. The former figure consists of several radiating bands; while in the latter not only several radiating bands, but a number of concentric rings are detectable. This shows us that the micro-crystals in the sample, with which the latter figure Fig. 14, Plate II was produced, is rather irregularly arranged compared with the other sample which is responsible for the former figure, Fig. 12, Plate II.

Furthermore, it can be noticed that the radiating bands themselves are of different nature in both figures; in Fig. 14, a number of long radiating bands come to appear symmetrically with respect to the direction of the fibrous axis. On the other hand, it is observed that the radiating bands are comparatively short and the symmetry of their angular distribution is violated to some extent in the case of Fig. 12, Plate II. This shows us that, in the case of Fig. 12, II, the rotation of the micro-crystals of bismuth around the axis of the fibre is less than in the case Fig. 14, Plate II.

This tendency is more remarkable in the acicular Specimen A_3 of *Bi*, which gave rise to Fig. 13, Plate II. The rotation of the micro-crystals around the axis of the fibre became so small, in this case, that the specimen can be looked for almost as a single crystal. The angle of rotation of the micro-crystals around the axis [2 1 1] was obtained by means of the Yoshida globe and spherical scale; and it was estimated to be within 10° in this case.

Summary.

From our foregoing argument in connection with electrolysed bismuth and antimony, we arrive at the following conclusions:—

(1) The smaller current density and the lower concentration of the electrolyte seem to be the more favourable conditions for the formation of a regular arrangement of bismuth crystals.

When the current density and the concentration of the electrolyte are comparatively large, the micro-crystals of bismuth have not a remarkable tendency to deposit themselves in a fibrous form. But, this tendency becomes more remarkable with a smaller current density and with a smaller concentration of the electrolyte; and a perfect fibrous arrangement

is at last obtained, when both of them are reasonably small. In the extreme case, when the current density and the concentration of the electrolyte are very small, the micro-crystals tend to form a crystal of considerable size, having not only a certain crystal-axis but all the crystal-axes coinciding with each other.

(2) The non-metallic cloddy deposits found on the cathode by the electrolysis of bismuth or antimony, are at least mainly composed of substances having the same crystal-lattices as those of bismuth or of antimony.

(3) The micro-crystals of bismuth in the fibrous specimens are so arranged that their crystal-axis of the indices [2 1 1] is parallel to the fibrous axis. In the case of the bismuth-single-crystals of acicular form, the same crystal axis [2 1 1] is also parallel to the direction of the acicular axis. Thus it may be said that the axis [2 1 1] of the rhombahedral crystal of bismuth has a distinct physical nature.

In conclusion, the writer wishes to express his best thanks to Prof. M. Chikashige for his kind suggestions and interest and to Professor U. Yoshida for his efficacious guidance during the progress of the experiment. His thanks are also due to Mr. J. Tsutsumi, by whose kind advice some of the specimens were prepared.

Plate I

Fig. 5, Bi. Specimen A_2

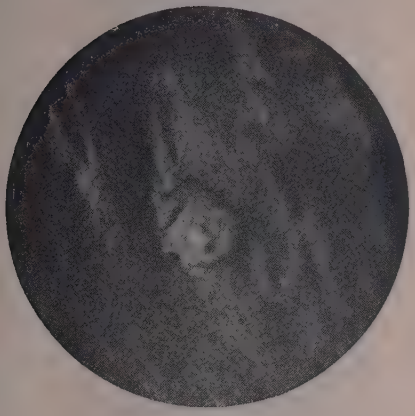

×75

Fig. 6, Bi. Specimen A_1

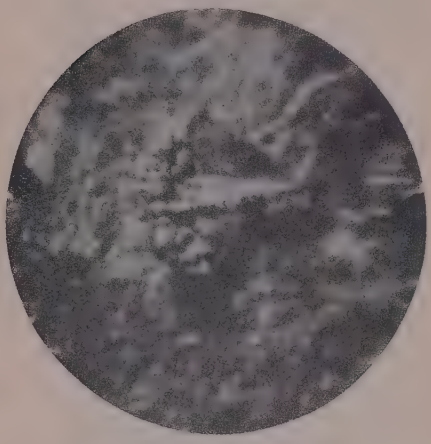

×75

Fig. 7, Sb. Specimen B_2

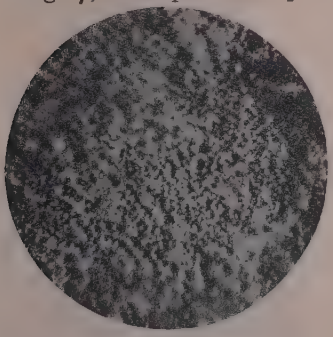

×140

Fig. 8, Sb. Specimen A_1

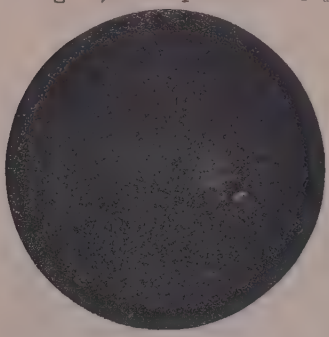

×75

Fig. 9, Bi. Specimen B_1

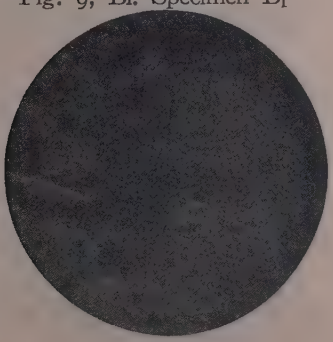

×40

Fig. 10, Bi. Specimen A_3

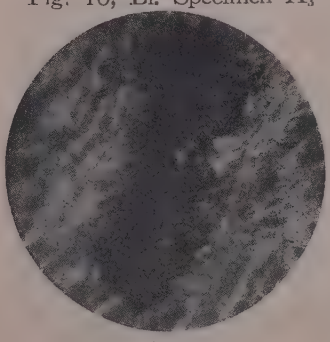

×75

Plate II

Fig. 11, Bi. Specimen A_1

Fig. 12, Bi. Specimen A_2

Fig. 13, Bi. Specimen A_3

Fig. 14, Bi. Specimen A_2

Plate III

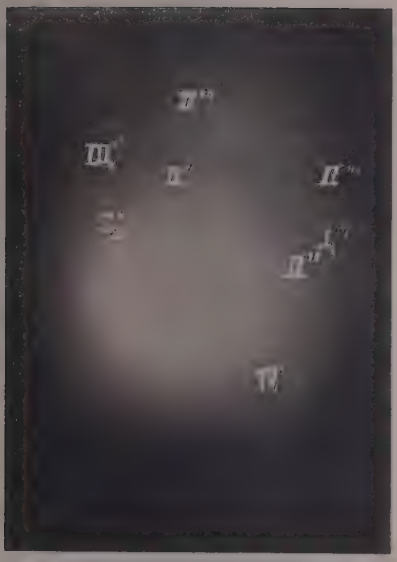

Fig. 15, Sb. Specimem A_2

Fig. 16, Sb. Specimen B_1

Fig. 17, Bi. Specimen B4

Fig. 18, Bi. Specimen A_2

Vol. XI, No. 5, Published September 25, 1928

Price - - - Yen 2·00

These Memoirs are on sale at

MARUZEN COMPANY, LTD.

TOKYO, OSAKA, KYOTO, NAGOYA, YOKOHAMA, FUKUOKA
& SENDAI

昭和三年九月二十日 印刷
昭和三年九月廿五日 發行

編纂兼發行者 京都帝國大學理學部

印刷者 須磨勘兵衞
京都市下京區北小路通新町西入

印刷所 內外出版印刷株式會社
京都市下京區西洞院七條南

賣捌所 丸善株式會社
東京、大阪、京都、名古屋、横濱、福岡、仙臺

CONTENTS

Some Notes on Solar Research
By Issei Yamamoto... 303
On some Functions defined by certain Infinite Products
By Yoshikatsu Watanabe....311
"The Reversal-like Phenomena" of the Secondary and the Tertiary Discharge-Figures impressed on Photographic Plates
By Tatsumi Terada....355
The Orientation of Single-Crystals of Zinc
By Kenzo Tanaka....361
On Paradoxes and Definitions
By Toshizô Matsumoto....367
The Arrangement of the Micro-Crystals in Compressed Magnesium and Aluminium Plates
By Shogo Tsuboi....375
The Electrolytic Oxidation of Alcohols, III. Electrolytic Oxidation of Benzylalcohol
By Shunzo Koidzumi....383
The Electrolytic Oxidation of Alcohols, IV. Electrolytic Oxidation of Propylalcohol in Alkaline Solutions
By Shunzo Koidzumi....391
An Examination of the Micro-Crystals of Calcium Carbonate in Molluscan Shells by means of X-Rays, Part II
By Jinzo Tsutsumi....401
On the Electrolytic Reduction of Aldehydes, Part III. Ortho- and Para-Oxybenzaldehydes
By Goro Shima....407
On the Electrolytic Reduction of Aldehydes, Part IV. Vanillin and Piperonal
By Goro Shima....419
On the Arrangements of the Micro-Crystals in Bismuth and Antimony deposited by Electrolysis
By Hideki Hirata....429

The Probability of Lightning Strokes

By

Usaburo Yoshida, Hidehiko Fukushima and **Megumu Iso**

(Received July 15, 1928)

Abstract

The density distribution of the hits of imitated lightning sparks on a wide circular metallic disc with or without a lightning needle, is examined for the sparks starting from a fixed point above the surface of the disc. The results of the experiment are shown to agree nearly with those obtained by calculation based upon the consideration of the probability.

Some years ago Peek[1] made a laboratory experiment on the distribution of lightning strokes under various conditions in imitating the lightning-strokes from cloud to earth. Recently the writers repeated a similar experiment, and a calculation based upon the consideration of probability has been tried and found to be successful to some extent in explaining the results.

Experiment

The experimental arrangement employed is illustrated schematically in Fig. 1. C is a metal ball of 22 mms. diameter, on whose lower surface is attached a small metallic protuberance, so as to make electric sparks start always from this protuberance. E is an earthed circular metal disc of 31 cms. diameter, which is provided with a small hole of about 1 mm. diameter at its center. This large circular disc, which corresponds to a flat surface of the earth vis à vis the lightning, is placed horizontally in

1 F. W. Peek: J. Franklin Inst., **199**, 14 (1925)

such a position that the central hole of the disc is situated precisely below the protuberance of the spherical electrode C. In examining the effect of the lightning rod, the writers inserted a sharp needle through the central hole of the circular disc at various heights above the surface of the disc. The circular disc E is covered with a thin black paper of 0.1 mm. thickness, so that the hits of the lightning flashes on the circular disc are recorded on this black paper; and the density of the lightning strokes on the disc can be measured by counting the hit-marks on the paper. For the excitation of the sparks between the electrode C and the circular disc electrode E, a small influence machine is employed. The spark-length between the electrode C and the circular disc E, with which the experiment is carried out, is 9 cms. when the electrode C is charged positively. The positively charged electrode C corresponds to the positively charged cloud, as is common in nature. The value of the spark-length above mentioned is of course too short to imitate the actual lightning; but as it seemed to the writers that the essential features of the distribution of the lightning strokes would still be retained with short sparks, they have carried out their experiment with these short sparks and tried to find out some laws governing the distribution of the lightning strokes. When the electrode C is charged negatively the maximum spark length, attainable with the small influence machine employed by the writers, between the electrode C and the disc E is much shorter than when the electrode C is charged positively; and the present experiments were performed only with the electrode C charged positively. With the influence machine employed by the writers the sparks occur in slow succession one after another between the electrodes, so that we could count without any difficulty the number of the sparks which passed by listening to the sound they made. By so counting the number of the sparks which passed, the number of the hit-marks on the black paper placed on the upper surface of the circular disc is checked in every case. When the hit-marks on the black paper are over crowded, the number of the hit-marks is always smaller than that counted by listening to the sound, due to the overlapping of the hit-marks. In examining the density of the hit-marks, this overlapping of the hit-marks must be avoided as much as possible. For this purpose, the writer always confined the total number of the sparks below 200 on one sheet of black paper; and the density determination of the

Fig. 1

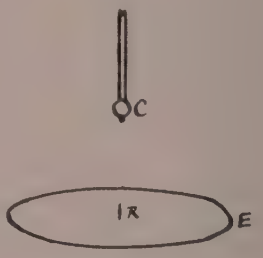

Fig. 2

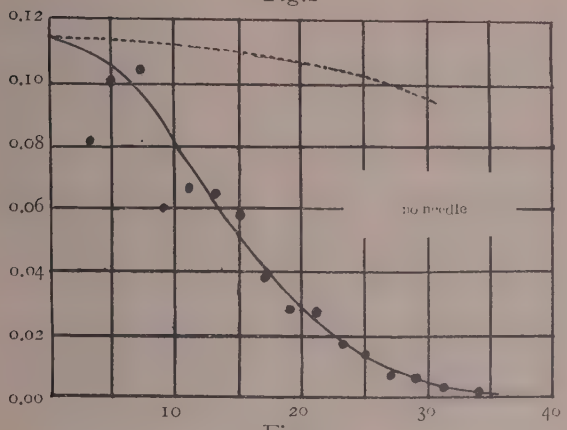

Fig. 3

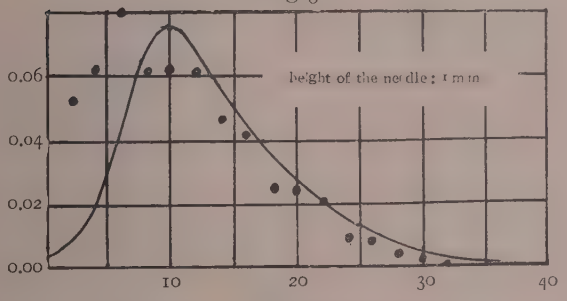

Fig. 4

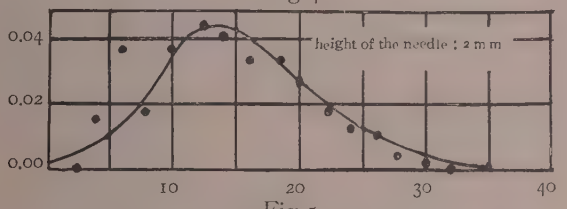

Fig. 5

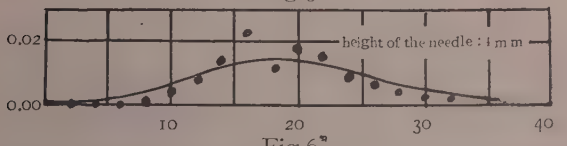

Fig. 6

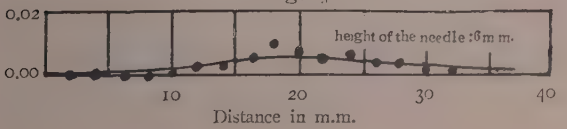

Density of the lightning strokes

Distance in m.m.

lightning strokes was made on about 1000 hit-marks impressed on five or six different sheets of black paper. With sparks less than 200 in number on one sheet of black paper the overlapping of the hit-marks was confirmed to be negligible. The results of the experiments are shown in Figs. 2, 3, 4, 5 and 6. In these figures the abscissa represents the distance of a point on the surface of the circular disc E from the central hole on it in mm. This central hole is situated just below the protuberance on the surface of the electrode C. In examining the effect of the lightning rod, a sharp needle is inserted in this central hole as stated before; consequently the abscissa in the figures of these cases is nothing but the distance between the needle and a point on the surface of the circular disc. The ordinate in the same figures represents the density of the hits of the sparks per square millimetre of the surface of the circular disc expressed in a percentage of the total hits on the whole surface of the circular disc. In the figures, the dots represent the observed densities of the hits of the sparks at various points on the circular disc, and the curves drawn in unbroken and broken lines represent those calculated; the manner of this calculation will be described later. In Fig. 2, the sparks were made to hit the flat surface of the circular disc which was unprovided with any needle; and in Figs. 3, 4, 5 and 6, the sharp needle, which corresponds to the lightning rod, was made to protrude at various heights above the surface of the circular disc; and the heights of this protrusion are written in each figure. As shown in these figures, the density of the lightning strokes, without any lightning rod, is roughly maximum at a point just below the starting point of the spark on the surface of the electrode C. By inserting a lightning rod at this point, the density of the lightning strokes in its vicinity diminishes with the height of the rod as expected.

Theoretical Consideration

If the electrical property of the air were entirely homogeneous the spark would pass along the line of force of the strongest field-intensity; thus with the arrangement described in the preceding chapter the spark should strike the circular disc E at the point just below the protuberance on the surface of the spherical electrode C. But this is not actually so, and the hit-marks of the sparks on the circular disc are scattered in a comparatively wide area. This fact is, of course, to be expected from the irregular zigzag shape of the spark. It was pointed out before by

Mr. H. Hirata and one of the writers[1] that the shape of the spark was different according as the spark occurred along the preliminary negative brush or along the preliminary positive brush. It is also known that the elongation of the irregular positive brush is much longer than that of the rather regular negative brush. Thus unless special care is paid to prevent the appearance or the development of the positive brush, the spark will pass, for the most part of its path, along the positive preliminary brush of mush longer extension. This seems to be the reason why the branches of the lightning from the positively charged could to the earth are toward the earth, and why the irregular zigzag shape of the lightning is similar to that of the positive brush. Considering in such a way it seems not to be unnatural to suppose that the spark in the present experiment occurred, for the most part of its path, along the way formed by the preliminary positive brush starting from the protuberance on the surface of the spherical electrode C. If so the irregular zigzag paths of the sparks as seen in Figs. 1 and 2 in Plate I must be due to the irregular branches of the positive brushes. As to the formation of these irregular branches of the positive brush, an explanation based on the consideration of an irregular and random distribution of the free ions in the air, was given by Mr. Hirata and one of the writers[2]. If such explanation be correct, the irregular and zigzag path of the spark will be also explained by the irregular distribution of the free ions in the air. The calculation, based on the consideration of probability, of the distribution of the density of the lightning strokes, which will be given below, owes its origin to the idea mentioned above.

Considering in the above way, we can suppose that a spark consists of an irregular continuation of a large number of very short and straight sparks, the lengths and the inclinations to the vertical direction of these short sparks being different for every one, due to the irregular distribution of the free ions in the air, and the intensities of the electric fields near the ends of the branches of the preliminary positive brush at the moment of its development. Now let Δz be the mean value of the vertical components of all the short sparks forming a spark, and let Δr be the mean value of the horizontal components of all the short sparks forming the same spark. Then the value of $\Delta r/\Delta z$ will be pretty small compared with unity in the present case, where the vertical component of the intensity of the electric field is strongly predominant; and the value of Δz will be nearly the same as the average value of the lengths of all the

1 U. Yoshida and H. Hirata; These Memoirs, **4**, 89 (1919)

2 ibid.

short sparks forming the same spark. Thus the value of Δz will solely be determined by the density of the free ions in the air and it will nearly be independent from the actual length and the shape of the spark in the present case, where nearly all sparks pass roughly in the vertical direction. Considering in such a way, when a spark passes between a point and a horizontal plane, the total number n of Δz for this spark will be nearly proportional to the height h of the point above the horizontal plane, irrespective of the actual shape and the inclination of the path of the spark, and h may be put equal to $n\Delta z$.

For the mean value Δr of the horizontal components of all the short sparks forming a spark, it will also depend upon the density of the free ions in the air. But for a given value of this density the value $\Delta r/\Delta z$ will not be affected much by the actual path of the spark for the sparking electrodes of given shape and dimensions.

Considering in the above way we may suppose that a spark in our case consists of n short and straight sparks, the vertical and the horizontal components of each of these short sparks being respectively equal to Δz and Δr for every one; and consequently that a spark starting from a point arrives at a horizontal plane, separated at a vertical distance h from the point, by a zigzag continuation of such n short sparks. During the development of the preliminary positive brush, the horizontal components of the electric field in the immediate neighbourhood of the end of every branch of the positive brush may be looked for as nearly symmetrical, on an average, about the vertical line passing through the end point of every branch, for the major part of the the path of spark. In conjunction with this fact, the random distribution of the free ions in the air compels us to consider that the directions of the mean horizontal components Δr of the short sparks forming a spark is at random for all directions in a horizontal plane.

Fig. 7

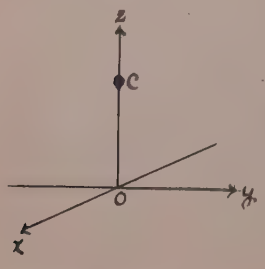

Let us imagine that a spark starts from the point C in Fig. 7 and arrives at a horizontal plane xoy, which is situated at a distance h below the point C. Let O be the point of intersection of the plane xoy with the vertical line passing through the point C. Then take the direction OC as the z-axis, and the directions ox and oy in the horizontal plane under consideration as the x- and the y- axes respectively of the rectangular co-ordinates system. Next, resolve the mean value Δr of the horizontal

components of the short sparks into x and y components, and let Δx and Δy be respectively the means of the absolute values of these two components, then Δx and Δy will respectively be equal to $\frac{2}{\pi}\Delta r$; because the direction of Δr is considered to be entirely at random in all directions in a horizontal plane.

Now let us consider, for the sake of rough calculation, that a spark passes between the point C and the horizontal plane xoy by the continuation of n short sparks, and roughly that Δx or Δy may have the positive and the negative values with equal probability; then the probability, for a spark, of hitting the plane xoy at a certain distance from the origin O will be calculated by the combination of certain numbers of the positive and the negative values of Δx and Δy, similarly as in the calculation of the probability of errors. Thus if we represent by P the probability per unit area, for a spark, of its hitting a point distant from O by r on the plane xoy, then P will be given by

$$P = \frac{1}{\pi k^2} e^{-\frac{r^2}{k^2}},$$

in which k^2 has been written to represent the quantity $2n\left(\frac{2}{\pi}\right)^2(\Delta r)^2$, and is a constant for a given experimental condition. Thus when N lightning flashes come from the point C to the plane xoy, the density of the lightning strokes at a point on the plane xoy will be

$$NP = \frac{N}{\pi k^2} e^{-\frac{r^2}{k^2}}. \quad \ldots\ldots\ldots\

that the density of the sparks is roughly proportional to that of the lines of force, then the density of the lightning strokes on the plane surface must be proportional to the density of the induced charge on it. If we imagine approximately that a point charge is situated in the protuberance on the surface of the spherical electrode C in Fig. 1, then the surface density of the induced charge and consequently the density of the lightning strokes at a point on the plane surface E in that figure will be nearly proportional inversely to the cube of the distance between the point charge and the point on the plane surface E. This relation is shown by the broken line in Fig. 2, and which resulted in a clear disagreement with the experiment.

Fig. 8

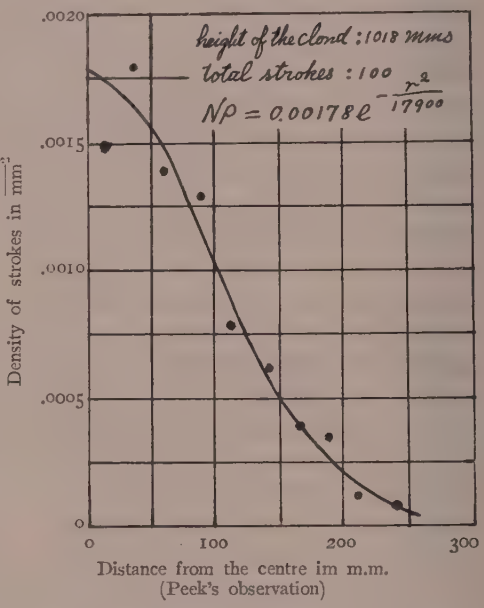

In the present experiment, the spark-length between the spherical electrode and the circular disc electrode was only 9 cms. as was stated before; while Peek[1] made a similar experiment with a much longer spark-length. His result with a spark-length of about 1 metre is shown by the dots in Fig. 8, and the curve in the same figure is drawn by equation (1) by giving proper values to N and k^2, which are written in the figure. Here again we see a fair agreement between the observation and the calculation.

Lightning strokes on a plane surface with a lightning rod. The function of the lightning rod in absorbing the lightning flashes may be roughly understood by the photographs reproduced in Plate I. These are the photographs in profile of an assemblage of many sparks, which passed one after another between the upper spherical electrode C and the lower circular disc electrode E in Fig. 1 when the latter was provided with a needle in a position just below the protuberance on the surface of

1 Peek: loc. cit.

the spherical electrode C. The height of this needle above the surface of the electrode E are respectively 6 and 8 mms. in Figs. 1 and 2, as is written respectively in these figures; and the vertical distance between the circular disc electrode E and the protuberance on the surface of the upper electrode is 9 cms. in both cases. In either of these figures, the protuberance on the surface of the upper electrode is placed in a position in the upper part of the figure, where the ends of most of the sparks meet together; and the point in the lower part of the figure, where the ends of most of the sparks meet together corresponds to the top of the sharp needle. The circular disc electrode is in a position a little lower than the top of the needle, the presence of which will be imagined in these figures by the somewhat diffuse reflection of light emitted by the sparks.

From the figures in Plate I, we can detect that the outer boundary of the sparks, which are absorbed by the needle, forms nearly a circular conical surface in the region near the top of the needle, by making that top its vertex. Considered thus it seems not to be unnatural that there should exists a conical protecting region just above the top of the needle, its semi-vertical angle and the height of its vertex from the circular base being a constant for a given height of the needle; and that the sparks which arrive at the base of this protecting cone are all absorbed by the needle.

In Fig. 9, let h be the vertical distance between the protuberance on the surface of the spherical electrode C and the circular disc E, which distance is 9 cms. in the present experiment; and let h_n be the height of the needle, h_c the height of the cone and b the radius of the circular base of the cone. If we represent h_n+h_c by h_2, then the vertical distance h_1 between the base of the cone and the protuberance on the surface of the spherical electrode C will be equal to $h-h_2$.

Fig. 9

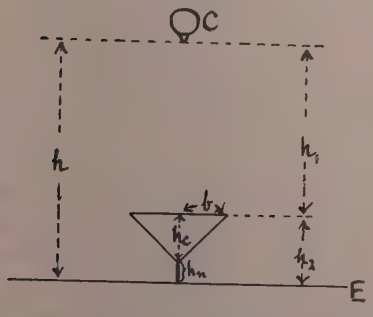

Now let us roughly suppose that the sparks from the electrode C pass through the horizontal plane passing through the base of the cone with the distribution given by equation (1). Among these sparks, those which pass through the base of the cone will all be absorbed by the needle, and the remaining ones will shoot down upon the circular disc electrode E, according to the same law of probability as was stated

before, and which will give rise to the observed distribution of the density of the lightning strokes on the circular disc E. Actually the calculation is made in the following manner. First, the density distribution of the hits of the fulguration on the circular disc electrode, which fulguration have passed through the base of the cone, is calculated on the supposition that there is no needle and that these sparks flash down to the circular disc according to the same law of probability as was stated before; and then the densities of the strokes of these sparks at various points on the circular disc are subtracted respectively from those of the lightning strokes which have occurred in the case of no needle, and which is calculated as was described before.

Here we shall consider about the constant k^2 in equation (1), which has been written to represent the quantity $2n\left(\frac{2}{\pi}\right)^2(\Delta r)^2$. We can express this quantity in another form: i. e.

$$2\left(\frac{2}{\pi}\right)^2 n\Delta z\left(\frac{\Delta r}{\Delta z}\right)\Delta r = 2\left(\frac{2}{\pi}\right)^2 h\left(\frac{\Delta r}{\Delta z}\right)\Delta r;$$

which shows that this quantity is roughly proportional to the vertical distance h between the protuberance on the surface of the spherical electrode and the circular disc electrode, provided that the value of $\frac{\Delta r}{\Delta z}$ and Δr are roughly constant. Thus for the paths of the sparks between the electrode C and the horizontal plane passing through the base of the cone we take $2\left(\frac{2}{\pi}\right)^2 h_1\left(\frac{\Delta r}{\Delta z}\right)\Delta r$ as the probability constant k_1^2 corresponding to k^2 in equation (1); and for the paths of the sparks between the plane passing through the base of the cone and the circular disc electrode, we take $2\left(\frac{2}{\pi}\right)^2 h_2\left(\frac{\Delta r}{\Delta z}\right)\Delta r$ as the probability constant k_2^2, for the sake of rough calculation.

Let D_c be the density of the paths of the sparks at the plane passing through the base of the cone, when N sparks start from the upper electrode C; then D_c will be given by

$$D_c = \frac{N}{\pi k_1^2} e^{-\frac{r^2}{k_1^2}} \quad \text{.....(2)}$$

Among these sparks, those which pass through the base of the cone will all be absorbed by the lightning needle. If this lightning needle should be absent, then these sparks will hit the circular disc; and the

distribution of the strokes of these sparks will be governed also by the law of probability as was stated before.

Now take the vertical direction passing through the lightning needle as z-axis, as shown in Fig. 10; and take the x- and y-axes, and x'- and y'-axes of the rectangular coordinates-system respectively in the plane of the circular disc and in that of the base of the cone, by making respectively x- and x'-axes and y- and y'-axes parallel to each other. Let us consider a surface element $dx'dy'$ at a point (x', y') on the surface of the base of the cone, then the number of the paths of the sparks which pass through this surface element will be

Fig. 10

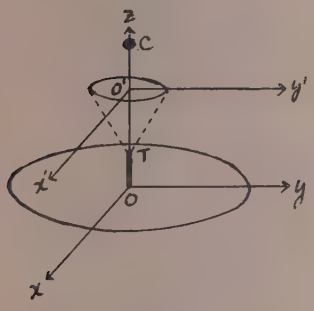

$$D_e dx'dy' = \frac{N}{\pi k_1^2} e^{-\frac{r'^2}{k_1^2}} dx'dy', \quad \ldots\ldots\ldots\ldots\ldots\ldots\ldots\ldots\ldots\ldots (3)$$

where $r'^2 = x'^2 + y'^2$. Now consider a surface element at a point (x, o) on the surface of the circular disc, then the surface density of the sparks which have passed through the surface element $dx'dy'$ and arrive at this surface element is

$$\frac{N}{\pi^2 k_1^2 k_2^2} e^{-\frac{r'^2}{k_1^2}} e^{-\frac{(x-x')^2+y'^2}{k_2^2}} dx'dy'.$$

By putting $x' = r' \cos\theta'$, and $y' = r' \sin\theta'$, the above expression becomes to

$$\frac{N}{\pi^2 k_1^2 k_2^2} e^{-\frac{r'^2}{k_1^2}} e^{-\frac{r'^2 - 2xr'\cos\theta' + x^2}{k_2^2}} r'dr'd\theta' = \frac{N}{\pi^2 k_1^2 k_2^2} e^{-\frac{x^2}{k_2^2}} \times$$

$$e^{-\left(\frac{1}{k_2^2}+\frac{1}{k_1^2}\right)r'^2} e^{\frac{2xr'\cos\theta'}{k_2^2}} r'dr'd\theta'. \quad \ldots\ldots\ldots\ldots\ldots\ldots (4)$$

This expression, when integrated over the whole surface of the base of the cone, will give the density of the hits of the sparks at the point (x, o) on the surface of the circular disc, if the lightning needle should be absent. Thus if we represent this density by D_E, it will be

$$D_E = \frac{N}{\pi^2 k_1^2 k_2^2} e^{-\frac{x^2}{k_2^2}} \int_0^b e^{-\left(\frac{1}{k_1^2}+\frac{1}{k_2^2}\right)r'^2} r'dr' \int_0^{2\pi} e^{\frac{2xr'\cos\theta'}{k_2^2}} d\theta'.$$

The integration with respect to θ' is made by expanding $e^{\frac{2xr'\cos\theta'}{k_2^2}}$ into a power series of $\left(\frac{2xr'\cos\theta'}{k_2^2}\right)$, and this gives

$$\int_0^{2\pi} e^{\frac{2xr'\cos\theta'}{k_2^2}} d\theta' = 2\pi\left\{1+\frac{1}{(1!)^2}\frac{x^2r'^2}{(k_2^2)^2}+\frac{1}{(2!)^2}\frac{x^4r'^4}{(k_2^2)^4}+\frac{1}{(3!)^2}\frac{x^6r'^6}{(k_2^2)^6}+\cdots\cdots\right\},$$

and consequently, by putting $k_i=\frac{1}{k_1^2}+\frac{1}{k_2^2}$,

$$D_E=\frac{2N}{\pi k_1^2k_2^2}e^{-\frac{x^2}{k_2^2}}\left\{\int_0^b e^{-k_ir'^2}r'dr'+\frac{1}{(1!)^2}\left(\frac{x}{k_2^2}\right)^2\int_0^b e^{-k_ir'^2}r'^3dr'+\frac{1}{(2!)^2}\left(\frac{x}{k_2^2}\right)^4\int_0^b e^{-k_ir'^2}r'^5dr'+\cdots\cdots\right\}$$

which becomes, on integration and by putting $\frac{k_1^2}{k_1^2+k_2^2}=g$, to

$$D_E=\frac{N}{\pi(k_1^2+k_2^2)}e^{-\frac{x^2}{k_2^2}}\left\{B_0+\frac{1}{1!}\left(\frac{x^2}{k_2^2}\right)gB_1+\frac{1}{2!}\left(\frac{x^2}{k_2^2}\right)^2g^2B_2+\frac{1}{3!}\left(\frac{x^2}{k_2^2}\right)^3g^3B_3+\cdots\cdots\right\}, \quad \cdots\cdots(5)$$

where B_0, B_1, B_2, etc. represent respectively

$$\left.\begin{aligned}
B_0&=1-e^{-k_ib^2},\\
B_1&=1-e^{-k_ib^2}\left\{1+(k_ib^2)^1\right\},\\
B_2&=1-e^{-k_ib^2}\left\{1+(k_ib^2)^1+\frac{1}{2!}(k_ib^2)^2\right\},\\
B_3&=1-e^{-k_ib^2}\left\{1+(k_ib^2)^1+\frac{1}{2!}(k_ib^2)^2+\frac{1}{3!}(k_ib^2)^3\right\},
\end{aligned}\right\} \quad \cdots\cdots(6)$$

etc.

If we represent by r the distance between a point on the plane xoy and the origin O, then we can write r for x in equation (5), because the direction of the x-axis has nothing to do with the density-distribution of the strokes of sparks in the present case.

Fig. 11

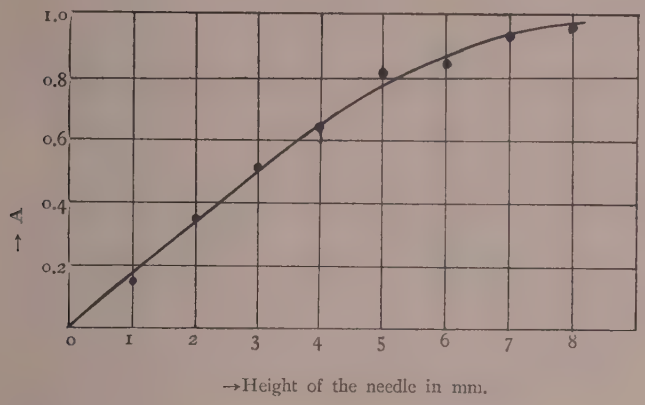

Fig. 12

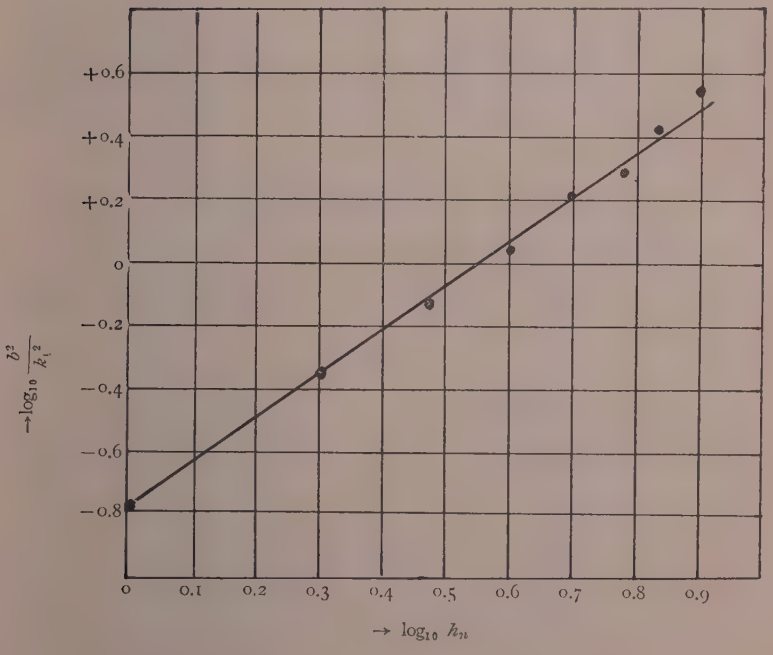

For the numerical calculation of D_E in equation (5), we must know the values of b and k_1^2 for various heights of the needle. For this purpose the ratio of the number of sparks absorbed by the needle to the total number of sparks passed between the electrodes, serves in giving us the values of b^2/k_1^2. If we denote this ratio by A, then we have the following relation:

$$A=\frac{\int_0^b \frac{N}{\pi k_1^2} e^{-\frac{r'^2}{k_1^2}} 2\pi r' dr'}{\int_0^\infty \frac{N}{\pi k_1^2} e^{-\frac{r'^2}{k_1^2}} 2\pi r' dr'}=1-e^{-\frac{b^2}{k_1^2}} \quad \cdots\cdots\cdots(7)$$

Thus when A is known from the observation, the value of b^2/k_1^2 will be obtained readily by equation (7). The observed values of A for various heights of the needle is shown in Fig. 11. The relation between the value of b^2/k_1^2 thus obtained and the height h_n of the needle is shown in Fig. 12, by taking the logarithms of these quantities in ordinate and abscissa. As seen in this figure the observed points denoted by the dots lie nearly on a straight line; and from this linear relation the writers obtained the following empirical formula representing the relation between b^2/k_1^2 and h_n:

$$\frac{b^2}{k_1^2}=0.162\, h_n^{1.4}, \quad \cdots\cdots\cdots(8)$$

where h_n represents the height of the needle.

Table I

h_n in mm.	$b_{calc.}$	$b_{obs.}$ on curves	$b_{obs.}$ on photos.	k_1^2	k_2^2
0	0	—	—	278	0
1	6.56	7	—	266.2	11.8
2	10.34	11	—	249.3	28.7
3	13.21	15	—	231.0	47.0
4	15.51	17	9	213.7	64.3
5	17.42	18	12	197.0	81.0
6	18.92	19	15	182.3	95.7
7	20.35	20	18	167.5	110.5
8	21.45	23	19	155.0	123.0

For the values of b we can make a rough estimate in two ways: one, by measuring the conical outer boundary of the sparks absorbed by the needle, as seen in Figs. 1 and 2 in Plate I; and the other, by measuring the distance between the centre and the point of maximum density of the strokes of sparks in the curves as shown in Figs. 3, 4, 5 and 6. Of these two estimates, the former will give a somewhat smaller value, because the bulging of the conical outer boundary of the sparks absorbed by the needle is still to be expected by increasing the number of sparks; and the latter estimate will give us a somewhat greater value, because the point of the maximum density of the strokes of sparks was found, by actual calculation, to be displaced to a point a little farther apart, from the vertical axis passing through the needle, than the circle forming the outer boundary of the protecting cone considered before. The values of b estimated in such a way are tabulated in the 3rd and 4th column in Table I.

Taking the circumstances above mentioned into consideration, the writers tried to get an empirical formula representing the relation between b and h_n, and the formula was so selected as to satisfy the following three conditions:

1) b must be zero when $h_n=0$.

2) b must tend to a certain finite value when h_n becomes very large.

3) k_1^2 must be equal to 278 when h_n is equal to zero; this value of k_1^2 is that found for the circular disc electrode without any needle.

The first two conditions are satisfied by the formula

$$b^2=\frac{c\,h_n^{1.4}}{a+d\,h_n^{1.4}}, \qquad \cdots\cdots\cdots\cdots\cdots\cdots\cdots\cdots\cdots\cdots(9)$$

when a, d, and c are constants; and these constants can be chosen, so as to fulfil the 3rd condition. From equations (8) and (9) we have

$$k_1^2=\frac{b^2}{0.162h_n^{1.4}}=\frac{ch_n^{1.4}}{0.162h_n^{1.4}(a+dh_n^{1.4})}=\frac{c}{0.162\,a\left(1+\frac{d}{a}h_n^{1.4}\right)}.$$

By putting $h_n=0$ and $k_1^2=278$, the above equation becomes

$$\frac{c}{a}=0.162\times 278=45;$$

and by putting this value into equation (9), we get

$$b^2 = \frac{45\, h_n^{1.4}}{1 + \frac{d}{a} h_n^{1.4}} \quad \cdots\cdots\cdots\cdots\cdots\cdots\cdots\cdots\cdots\cdots\cdots\cdots (10)$$

For the value of d/a in the above equation, the writers took the value of 0.0433 by trial, so as to fit the observation most closely. By using this value of d/a, equation (10) becomes

$$b^2 = \frac{45\, h_n^{1.4}}{1 + 0.0433 h_n^{1.4}} \quad \cdots\cdots\cdots\cdots\cdots\cdots\cdots\cdots\cdots\cdots\cdots\cdots (11)$$

This is the empirical formula used by the writers for the calculation of the radius b of the base of the cone. The values of b thus calculated for various heights of the needle are tabulated in the second column of Table I. By comparing the values of b thus calculated with those observed we know that the calculated ones are not unreasonable; and consequently the writers utilized the values calculated by equation (11) for further calculation.

Next, the values of k_1^2 are calculated with equation (8) by using the values of b calculated, and they are given in the 5th column of Table I. The values of k_2^2 given in the last column of the same table are obtained from the values of k_1^2 by making use of the relation $k_1^2 + k_2^2 = k^2 = 278$.

With the values of b, k_1^2 and k_2^2 obtained in the manner stated above, we can get the values of g and k_i in equations (5) and (6) immediately; and thus the values of D_E for various points on the surface of the circular disc electrode and for various heights of the needle will be calculated by equations (5) and (6). If D_E thus found is subtracted from NP in equation (1), which is the density of the strokes of sparks without any needle, then the remainder represents the density of the strokes of sparks, when the lightning needle is present. The curves drawn in unbroken lines in Figs. 3, 4, 5 and 6 are calculated in this way. As shown in these figures, the general features of the density distribution of the strokes of sparks seem to be well represented by the calculated curves. This fact seems to support conversely our consideration, described before, on the mechanism of the development of the spark, and on the protecting cone of the lightning rod.

Here it must be noted that the convergency of the infinite series in equation (5) is not good, and consequently that very many terms (sometimes about 20 terms) have to be taken into account; which fact accompanies a laborious numerical calculation.

Up to now we have treated the case of the lightning starting at a point just above the lightning needle. But this is not the case with actual lightning in nature; and the random distribution of the starting-points of the lightning in a high altitude will be rather suited to the case of the natural lightning. This random distribution of the starting-points of the lightning in a high altitude will give a uniform density of the paths of the lightning in the region above the lightning rod; and this uniform density of the paths of the lightning will be given also by a fixed starting point of the lightning when its altitude becomes immense. With this consideration the writers calculated the density of the lightning strokes on the circular disc, in the neighbourhood of a lightning needle of 4 mms. in height. The calculation was made with equations (5) and (6) by putting $h_1 = \infty$, and consequently by putting $k_1^2 = \infty$; from which follows that $k_i = \frac{1}{k_1^2} + \frac{1}{k_2^2} = \frac{1}{k_2^2}$, and $g = \frac{k_1^2}{k_1^2 + k_2^2} = 1$. As to the constants b and k_2^2 of the lightning needle the writers employed the values given in Table I for the needle of 4 mms. height; and for the value $\frac{N}{\pi(k_1^2 + k_2^2)}$ in equation (5) it was taken to be unity, which means that the density of the lightning strokes is one per mm^2. on the circular disc if the needle be absent. The density of the lightning hits thus calculated for various points on the circular disc are shown by the curve in Fig. 13, where the value of the radius of the circular base of the protecting cone is represented by the position of the broken line.

Fig. 13

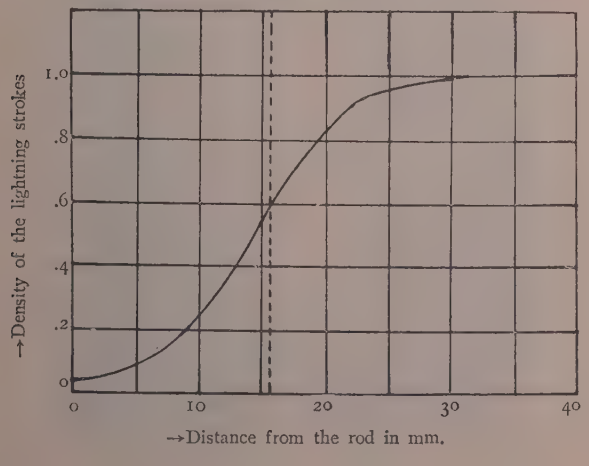

The scale of the experiments made by the writers is too small to extend the results obtained to the case of the natural lightning and of the real lightning-rod. A further experiment with a longer spark length and a longer lightning needle is expected to be carried out in the near future.

Plate I

Fig. 1

Height of the needle: 6 mm.s

Fig. 2

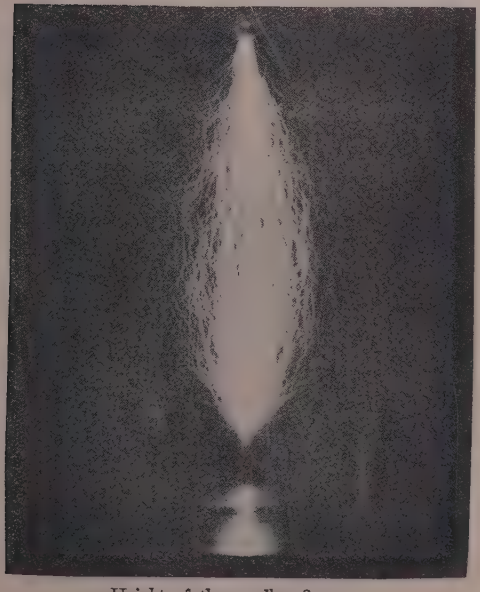

Height of the needle: 8 mm.s

A Method of Determining the Orientation of Crystal-Axes by X-Rays

By

Setsuzo Takeyama

(Received August 17, 1928)

Abstract

A simple method of determining the orientation of crystals with the X-rays is described. In an ordinary rotating crystal spectrometer a V-shaped frame of lead wires was inserted between the crystal and the photographic plate, and was rotated with the crystal. From the positions of the shadows cast by the lead wires on the spectral lines the angle through which the crystal should be rotated to reflect these spectral lines, can be calculated. Therefore, if the wave length of the illuminating X-rays be known, the orientation of the crystallographic axes can be determined. The method is especially convenient for the thick crystal and for the crystal which has grown on the surface of a thick substance. The method is also applicable to the investigation in the arrangement of the micro-crystals on the surface of metals which have been subjected to some regular cold workings. The arrangement of the micro-crystals on the polished surface of copper was examined, and it was observed that the greater part of them were so arranged that their (111) or (100) plane is nearly parallel to the polished surface.

Introduction

For determining the orientation of crystal axes by means of X-rays the methods hitherto proposed by many investigators may be divided into two types: the Laue-spots method and the rotating crystal method. The orientation is determined from the Laue-spots pattern produced by white X-rays, with the aid of "the globe and the spherical scale" according to the method of U. Yoshida[1], and by means of the stereographic projection employed by Schiebold and Sachs[2]. If the illuminating rays contain the characteristic radiation of the target of the X-ray tube and

1 U. Yoshida; Jap. J. Phys., **4**, 133 (1927).

2 Schiebold u. Sachs; Z. S. f. Krist., **63**, 34 (1927).

if their spectra appear in the spots, they also serve as a clue for the determination, as has been experienced by T. Fujiwara[1], and by U. Yoshida and K. Tanaka[2]. Of the rotating crystal methods, those devised by Weissenberg[3], by Dawson[4], and by Davy[5] consist in rotating the crystal continuously through a certain range of angle, and in those devised by Müller[6], and by Aston[7] the crystal is made to rotate in a step-wise manner with a small step-angle. In any case the essential point is to know the angle through which the crystal should be rotated to bring forth the reflection of the characteristic radiation from a certain atomic plane of the crystal.

The present paper gives a rotating crystal method, using a new device to measure the angle to be rotated which would call forth the reflection of the characteristic radiation from a certain atomic plane of the crystal. With this method the writer has determined the orientation of the crystallographic axes of a thick single crystal of copper. The method is also employed to investigate the arrangement of the micro-crystals on the surface of a rolled platinum foil and on the polished surface of a thick copper block.

Description of Apparatus

The arrangement used is depicted diagrammatically in Fig. 1. A specimen to be tested is so mounted at C on the table of a rotating spectrometer as to have its surface to be tested in a vertical direction. The X-rays emitted from a point source T on the target of an X-ray tube pass through a long and narrow vertical slit at S; and the X-rays thus diverged in a vertical plane illuminate the surface of the specimen to be tested in a plane parallel to the axis of rotation ACB. Behind the specimen a V-shaped frame PVQ of lead wires is so fixed to the table and is made to rotate with it that the plane containing the frame is perpendicular to the surface of the specimen to be tested, and that the bisector of the angle PVQ is always perpendicular to the rotating axis during the rotation. The X-rays reflected from the crystal are

1 T. Fujiwara; Mazda Kenkyu Jiho, Tokyo Elect. Co., **1**, 182 (1926).
2 U. Yoshida and K. Tanaka; Nature, **118**, 912 (1926).
3 Weissenberg; Z. S. f. Physik, **23**, 229 (1924).
4 Dawson; Phil. Mag., **5**, 756 (1928).
5 Davy; Phys. Rev., **23**, 764 (1924).
6 Müller; Proc. Roy Soc., **105**, 500 (1924).
7 Aston; Cambr. Phil. Soc., **23**, 561 (1927).

Fig. 1

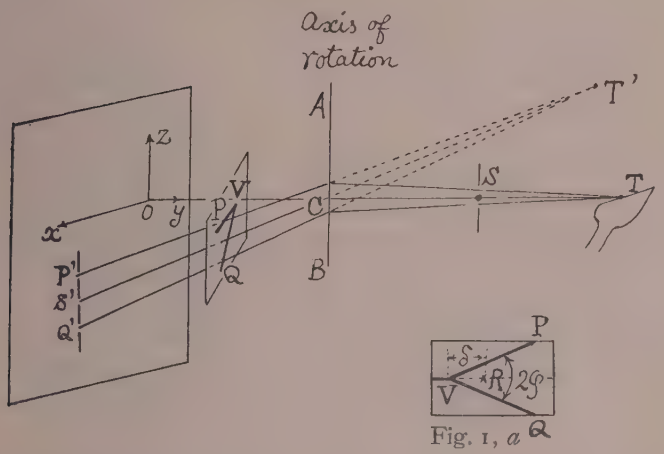

Fig. 1, *a*

absorbed by the lead wires VP and VQ on their way to a fixed photographic plate placed parallel to and behind the rotating axis, and the shadows P′ and Q′ of the lead wires are cast on the image of the spectral line on the photographic plate.

Further, a lead wire S is stretched across the long slit so as to cut off the incident ray running perpendicularly to the axis of rotation, and the shadow S′ of this lead wire is also cast on the spectral line on the photographic plate placed perpendicular to the central ray TS.

In this method, an X-ray tube with a sharply focussed target is preferable, in order to get distinct shadows of the lead wires. This purpose is, however, accomplished even with a tube the focus of which is not quite sharp, by setting it in such an orientation that the surface of its target is nearly, but not exactly, at right angles to the slit.

Calculation

From the positions of the shadows P′ or Q′ and S′ cast by the lead wires VP or VQ and S respectively on the photographic plate the angle, say ϕ, through which the crystal should be roatated in order to reflect the characteristic radiation of the target from a certain atomic plane, can be calculated as follows:— Consider a rectangular coordinates system, as shown in Fig. 1, where the foot of the central incident ray TS on the photographic plate is taken as the origin O, and the three orthogonal directions: one perpendicular to the axis of rotation of the

crystal on the photographic plate, next, one parallel to the axis of rotation of the crystal on the photographic plate, and third, the direction of the central incident ray ST, are taken as the x-, z- and y-axis respectively. Let the coordinates of the two shadow points S′ and P′ be (x_0, o, z_0) and (x, o, z) respectively, and the distances of the focus T on the target, of the photographic plate and of the plane of the lead wire V-shaped frame PVQ, from the axis of rotation be a, b and d respectively.

Before the specimen is made to rotate, the frame of lead wires PVQ is so adjusted that the central beam TSC is perpendicular to the plane of the frame and intersects the bisector of its angle PVQ at the point R, as shown in Fig. 1, *a*. If we represent the distance between V and R by δ, then, at the moment when the frame is rotated through ϕ, the direction consines of the lead wire VP are $\cos\varphi\cos\phi$, $\cos\varphi\sin\phi$ and $\sin\varphi$, where φ is the half of the angle PVQ; and the coordinates of the vertex V of the frame of lead wires are $d\sin\phi - \delta\cos\phi$, $b - d\cos\phi - \delta\sin\phi$, and zero. If T′ is the average position of the image of the focus T with respect to a reflecting atomic plane, then the condition that the two straight lines T′P′ and VP may intersect is given by

$$\begin{vmatrix} x - d\sin\phi + \delta\cos\phi & \cos\varphi\cos\phi & x + A x_0 \\ b - d\cos\phi - \delta\sin\phi & -\cos\varphi\sin\phi & b(1+A) \\ z & \sin\varphi & z + Az_0 \end{vmatrix} = 0,$$

where $A = \dfrac{a}{\sqrt{x_0^2 + b^2 + z_0^2}}$.

Since x is nearly equal to x_0 we get from the above equation

$$\{(d x_0 + b\delta)P - bQ\}\cos\phi = \{(bd - \delta x_0)P + x_0 Q\}\sin\phi + R,$$

where

$$P = (1+A)\tan\varphi,$$

$$Q = A(z - z_0),$$

$$R = d(z + Az_0).$$

This equation gives the value of the angle ϕ.

On the other hand, if the wave length of the characteristic radiation used is known, the indices of the reflecting atomic plane of the crystal, which is responsible for the spectral line appearing on the photograph, can easily be determined from the relation

$$\tan 2\theta = \frac{\sqrt{x_0^2 + z_0^2}}{b},$$

and Bragg's equation

$$2d \sin\theta = n\lambda.$$

Next, take a rectangular coordinate C-XYZ fixed to the specimen as shown in Fig.2, where the X-, Y- and Z-axes are to be taken as parallel respectively to the x-, y- and z-axes when the specimen is not rotated. Let the direction of the central beam of the X-rays be SC, then the direction cosines (l, m, n) of the normal to the atomic plane whose indices are above determined are given as follows:

$$\begin{cases} l = \cos\beta_1 = \cos\gamma \sin\phi + \sin\gamma \cos\phi \sin\alpha, \\ m = \cos\beta_2 = \cos\gamma \cos\phi - \sin\gamma \sin\phi \sin\alpha, \\ n = \cos\beta_3 = \sin\gamma \cos\alpha; \end{cases}$$

where $\alpha = \arctan x_0/z_0$,

and $\gamma = \frac{\pi}{2} - \theta$: is the angle of incidence of the X-ray beam to the atomic plane under consideration.

Fig. 2

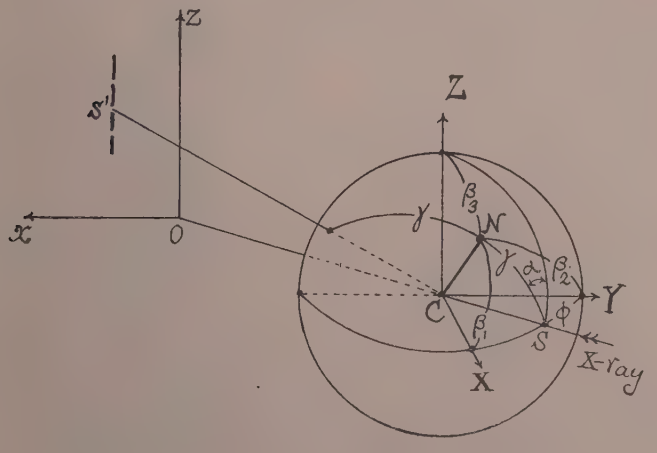

Thus, from a spectral line appearing on the photograph, the direction of the normal to an atomic plane referred to the axes fixed to the specimen will be determined together with its indices. Therefore, if two spectral lines, at least, appear on the photograph, the orientation of the crystal in the specimen will be perfectly determined.

Experiments

In the arrangement employed, a Müller spectrometer was utilized; and the specimen rotated, by means of clock-work, forward and backward through about twenty degrees. The distance, d, from the axis of rotation to the plane of the V-shaped frame of lead wires, and the angular opening of this frame are 17 cm. and 38° respectively. As a source of X-rays a Coolidge tube of molybdenum anticathode was used. The perpendicular distance, a, between the source point on the target and the axis of rotation was estimated as follows:— A lead plate of a given breadth was illuminated normally with the X-rays from the focus point of the target, and its shadow cast on a photographic plate placed parallel to and at a certain distance behind it; and the distance a is determined from the breadth of the lead plate and that of the shadow, the distance between the lead plate and the photographic plate and that between the photographic plate and the axis of rotation of the specimen. The value of a thus determined is 220 cm.

Table I $\left(\begin{matrix} b=4.0 \text{ c. m. s} \\ \delta=0 \end{matrix}\right)$

No. of spectral lines	x_0 in c.m.	z in c.m.	Glaning angle, θ			Order of spect. lines	ϕ
			$\theta=\frac{1}{2}\tan^{-1}\frac{x_0}{b}$ (obs.)	$\theta=\sin^{-1}\frac{n\lambda}{2d}$ (calc.)			
1	.85	.076	6°	6°10′	$K\alpha$	3	5°20′
2	1.16	.098	8°10′	8°10′	$K\alpha$	4	7°40′
3	1.30	.107	9°	9°10′	$K\beta$	5	8°40′
4	1.48	.123	10°10′	10°20′	$K\alpha$	5	9°30′

As a preliminary experiment the reflection from a mica sheet was examined, and the photograph taken is reproduced in Fig. 1 of Plate I;

the result of the measurements from this photograph is shown in Table I. The values of the glancing angle given in the fifth column are calculated from Bragg's equation by taking 0.710 and 0.630 Å. U. respectively as the wave lengths of K_α and K_β lines of molybdenum and 9.91 Å. U. as the lattice constant of the mica. The lines and the orders assigned to the spectral lines which appeared on the photograph are given respectively in the sixth and the seventh columns of the Table.

Since X-rays are reflected from the cleavage surface of the mica in this case the values of ϕ should be taken to be equal to those of the glancing angle, because the cleavage surfase of the mica is set parallel to the plane $\phi=0$ initially. The Table shows that the agreement between the values of θ and ϕ is roughly within the limit of experimental error.

Table II $\left(\begin{matrix}b=3.8 \text{ c.m.s} \\ \delta=0\end{matrix}\right)$

No. of spectral lines	x_0 in c.m.	z_0 in c.m.	z in c.m.	Indices of reflecting atomic planes	ϕ
1	1.41	.76	.59	(100) $K\alpha$	3°
2	1.21	.69	.52	(100) K_β	3°30′
3	2.13	−2.08	−1.46	(113) $K\alpha$	13°

Fig. 3

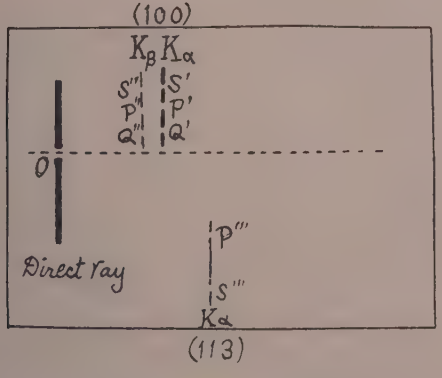

Next, the orientation of the crystallographic axes of a single crystal of copper was determined. The single crystal of copper used here was

obtained by the stress-annealing-method. An annealed copper plate was elongated by about one per cent., and then it was again annealed at about 900° C. for a day or two in an evacuated furnace. By this method the writer was able to obtain copper crystals of about 1 cm. square. The orientation of one of the crystals thus prepared was determined by the above method. The photograph reproduced in Fig.2 of Plate I was taken with such crystal of copper, and it is represented diagrammatically in Fig.3. Table II shows the result of the measurements from this photograph. The two spectral lines on the photograph are confirmed as due to the reflection from the (100) and (113) planes. The orientation of their normals referred to the coordinate axes fixed to the specimen is calculated and shown in Table III. The stereographic representation of the orientation of the surface normal and of the axis of rotation of the specimen referring to the crystallographic axes is shown in Fig. 4.

Table III

Crystallographic axis	Angle from surface normal of specimen	Angle from axis of rotation
100	29° (28°)	62° (62′)
113	44° (46°)	133° (131°)

Fig. 4

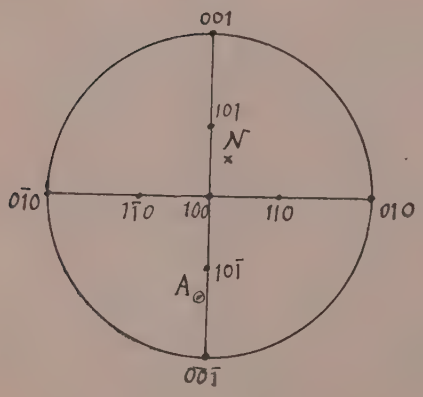

× N: normal of the surface.
⊙ A: axis of the rotation

The orientation of the crystallographic axes of the same specimen was also determined from the Laue-spots pattern by using U. Yoshida's[1] "globe and spherical scale," and the result, which agrees well with that acquired above, is shown by the figures in parentheses in Table III. Fig.3 of Plate I is the reproduction of the Laue-spots pattern taken with the normal incidence of the X-ray beam upon the surface of the copper plate, the distance of the photo-

1 U. Yoshida; loc. cit.

graphic plate from the specimen being 2.9 cm. in this case.

Arrangement of the Micro-Crystals on the Surface of Rolled Platinum Foil and of Polished Copper

An X-ray analysis of the arrangement of the micro-crystals on the surface of metals which were subjected to some regular cold workings has been reported by Professor S. Tanaka[1] and W. H. Bragg[2]. In Professor Tanaka's method, divergent X-rays are projected on the surface of a rolled platinum foil wound on the surface of a cylindrical wooden rod and the spectra produced by reflection from an atomic plane are obtained. By this method only is it possible to examine such a specimen as has, or can be formed into, the shape of a cylindrical surface. W. H. Bragg has also obtained sharp spectral lines reflected from certain atomic planes of platinum, gold and copper foils. But by this method it is quite impossible to know at what angular position during the rotation the specimen has reflected the spectral line. The method described before serves to fill up this defect in the method of rotating crystal. The photograph taken with a platinum foil prepared by rolling and with the polished surface of a copper block are reproduced in Fig.4 and Fig.5 of Plate I.

The platinum foil used here was the same specimen as that examined before by Professor S. Tanaka[1]; and the polished surface of copper was prepared as follows :— A rectangular block of pure copper was annealed at about 800° C. for about 10 hours in an evacuated furnace. One face of thus annealed block was polished successively with grind-stones of different grain-sizes : first with that of coarse grain, and then with those of successively finer grains; and lastly, the surface was polished with rouge on a flat surface of pitch. All these processes of polishing were made by hand slowly and reversely in the same direction.

As may be seen in Figs. 4 and 5, Plate I, we have the spectral lines containing the shadows cast by the lead wires. The result of the measurement from the photographs are represented in Tables IV and V. The values of ϕ and θ for each corresponding line in these Tables are nearly equal within the limit of experimental error. As the surface of

1 S. Tanaka; These Memoirs, **8**, 319 (1925).
2 W. H. Bragg; Nature, **113**, 639 (1924).

Table IV

Rolled Platinum Foil ($b=4.0$ c.m.s, $\delta=0$)

No. of spectral lines	x_0 in c.m.	z in c.m.	Indices of reflecting atomic planes	Glancing angle, θ		ϕ
				$\theta=\frac{1}{2}\tan^{-1}\frac{x_0}{b}$ (obs.)	$\theta=\sin^{-1}\frac{\lambda}{2d}$ (calc.)	
1	2.24	.205	(110) $K\alpha$	14°30′	14°50′	13°30′
2	1.94	.175	(110) K_β	12°30′	12°30′	12°

the specimen, which is examined, is set parallel initially to the plane $\phi=0$ in both cases, the agreement between the values of ϕ and θ indicates that the atomic plane of the crystal under consideration is parallel to the surface of the specimen. Thus it may be concluded from the result obtained that the majority of the micro-crystals are so arranged that the (110) plane in the case of the rolled platinum foil and the (111) and (100) planes in the case of the polished surface of copper are almost parallel to the examined surface of the specimens.

Table V

Polished Surface of Copper ($a=21.0$ c.m.s, $b=4.0$ c.m.s, $\delta=0.2$ c.m.s)

No. of spectral lines	x_0 in c.m.	z in c.m.	Indices of reflecting atomic planes	Glancing angle, θ		ϕ
				$\theta=\frac{1}{2}\tan^{-1}\frac{x_0}{b}$ (obs.)	$\theta=\sin^{-1}\frac{\lambda}{2d}$ (calc.)	
1	1.35	.210	(111) $K\alpha$	9°	9°50′	10°
2	1.59	.215	(100) $K\alpha$	11°	11°20′	12°

The result obtained with the rolled platinum foil is entirely the same as that obtained by Professor S. Tanaka. As to the examination of the polished surface of copper it is entirely of a preliminary nature; and though the final conclusion on the effect of polishing is still far from the scope of the present experiment, yet the result obtained suggests, at least, that we must be very cautious in examining microscopically the crystalline structure of the polished surface of metals.

Lastly, it must be noted that the method described before is especially preferable for the examination of the crystalline arrangement near the surface of a heavy substance.

In conclusion the writer wishes to express his sincere thanks to Prof. U. Yoshida under whose kind guidance and encouragement the present experiment was carried out.

Plate I

Fig.1

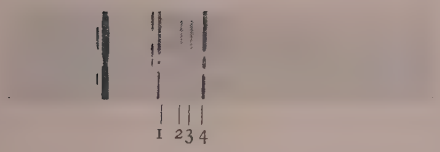

Fig.3

Axis of rotation

Fig.2

Fig.4

Rolled Pt foil

Fig.5

Polished Cu surface

Biochemical Studies on Pityrol, I.
Introduction to the Biochemistry of Pityrol

By

Shigeru Komatsu

(Received September 12, 1928)

It was said, in Japan, that a brownish-black tarry substance which was formed from rice bran by burning a small quantity slowly on a piece of Japanese paper strectched across the mouth of a teacup, and the tar which allowed to drop into the cup through the scorched paper, has been used as an infallible remedy for certain skin diseases such as eczema.

Dr. Matsuura, a former Professor of the Department of Medicine of our University, investigated in a clinical experiment the rice bran tar named "Pityrol" by him, which was obtained, according to tradition, by dry distillation of rice bran in a retort, and the value of this product as an important remedy for skin diseases began to be admitted by every body, and much attention has been paid to a study of the effect of the crude drug upon patients. However, nothing was yet known concerning the active principle of the crude drug, the relation between the chemical constituents of the tar and their pathological action, and also the chemical changes which take place in the constituents of the rice bran during the process of distillation, and these problems of the rice bran tar awake the interest of the present writer, and started him on this study, in connection with the pathological investigation by Professor Matsumoto of the Dermatological Institute of the Department of Medicine, the successor of Professor Matsuura. The writers' biochemical investigations into pityrol are, therefore, of value only when taken together with the pathological study by Professor Matsumoto.

U. Matsuura: Japan. Zeit. f. Dermat. u. Urologie **16**, 573

The rice bran which was prepared by means of a milling machine designed by Mr. Tsuge, from the rice named "Shinriki", grown near Osaka, was subjected to dry distillation in Fischer's aluminum retort. It was noticed that a colourless oil begins to distil with some water at about 200°, the colour of the distillate becoming darker as the amount increases, and the temperature rises. The main reaction which takes place between 350° and 400° with the formation of a dark brown-coloured tar and large quantities of a combustible gas, and at 450° the reaction is completed. The yield of tar, coke, aqueous liquor and gas was 24%, 28%. 36% and 12% respectively.

The tar, thus obtained, was a dark brown viscous liquid containing some carbon particles and having a peculiar odour, and soluble in alcohol, acetone and benzene. In order to learn in the chemical nature of the tar, it was divided into two parts-volatile and non-volatile, and each part was further divided into acidic, basic and neutral parts with the results (A) shown in Table I.

To attain our purpose, the pityrol obtained through the courtesy of Mr. S. Ichinose, Director of the Shinyaku Kaisha, Kyoto, was meticulously investigated as to its chemical constituents.

Table I.

		A	B	C
Tar		24 %	15 %	—
Coke		28 „	31 „	—
Aqueous liquor		36 „	40 „	—
Gas		12 „	14 „	—
Tar	Volatile part	13 „	17 „	12 %
	Non-volatile part	87 „	83 „	88 „
Tar	Neutral part	67 „	50 „	57 „
	Acidic „	29 „	37 „	37 „
	Basic „	4 „	13 „	6 „
Volatile part	Neutral	66 „	44 „	89 „
	Acidic	30 „	39 „	6 „
	Basic	4 „	16 „	5 „
Non-volatile part	Neutral	68 „	55 „	52 „
	Acidic	29 „	55 „	41 „
	Basic	3 „	10 „	7 „

The percentage of the various fractions (C) in commercial pityrol, as investigated by Mr. Sakami, seems to differ slightly from that obtained on a laboratory scale (A) by Dr. Fujita.

According to the pathological study of the tar and its constituents which was carried out in the laboratory of Professor Matsumoto,[1] these substance being applied repeatedly to the skin of a rabbit's ear, the degree of inflammation and the evidence of irritation differed according to the differing constituents of each substance: the larvae of mosquitoes, and maggots were affected by the acidic fraction most strongly, while the neutral fraction proved to be most mild. Differing symptoms of intoxication due to the differing nature of fraction were also noticed when these fractions were administered to mouse or snake subcutaneously or by inhalation. The most interesting symptom of the non-volatile neutral fraction which boiled at above 250° under 10 mm., was that when applied repeatedly to the inner surface of a rabbit's ears, malignant epithelioma was produced, which then terminated in true cancer. However, such a terrible disease on animal skin has never before been observed by applying the pityrol itself.

Hence, certain questions naturally arose in the writer's mind whether other tars produce similar pathological effects on animals and whether the constituents of tar from any substance would be affected by the external conditions under which the materials are subjected to distillation.

Now, it was a well-known fact that a terrible disease has arisen out of the development of the tar industry, and it was said that the tars from coal or vegetable materials have been noticed by many investigators to be a cancer producing factor for the workers in the factories where tars were manufactured or treated to derive useful materials from them. The tar cancer study has been the subject of study by investigators, since the experimental research by Yamagiwa and Ishikawa in producing malignant epithelioma by application of coal tar on a rabbit's ear.[2]

E. L. Kennaway's investigations[3] indicate that the fractions of the coal tars, except blast furnace tar, whish boils above 270°, has the cancer producing principle, and accordingly it seems true that the active principle which produces epithelioma on an animal skin will occur in certain tars produced by distilling coals and other vegetable materials under certain conditions, though our knowledge concerning the cancer-producing factor in tars is exceedingly scant.

1 Acta Dermato. **5**, 228; **9**, 383; **10**, 325, 393, 485; **11**, 45, 86.
2 Mit. d. Med. Ges., J. Tokyo, **30**, 1.
3 British Med. J. 564 (1924).

The neutral substances which compose the major part of pityrol perform certain pathological actions on the skin of the rabbit ear, and the chemical constituents of those substances were investigated by Sakami in the following manner.

The volatile neutral part of pityrol was treated with conc. sulphuric acid and fuming sulphric acid successively on the one hand, and on the other, with liquid sulphur dioxide[1] to separate it into saturated and unsaturated fractions. and it was confirmed as composed of about 80% of unsaturated hydrocarbons; and the percentage of the hydrocarbons of paraffin, an unsaturated and aromatic series, was estimated by the treatment above-mentioned.

In order to isolate the hydrocarbons of the paraffin series only, the oily residue which had been unaffected by the treatment with the sulphuric acids above mentioned, was passed on reduced nickel heated at 300° to remove the polymethylene hydrocarbons, and the reaction product was subjected to fractional distillation after being treated with con. sulphuric acid to remove any aromatic hydrocarbons which would formed from hexamethylenes by the catalytic oxidation. By repeated fractional distillation, the hydrocarbons C_8H_{18}. C_9H_{20}, $C_{10}H_{22}$, $C_{11}H_{24}$, $C_{12}H_{26}$, $C_{13}H_{28}$, $C_{14}H_{30}$ and $C_{15}H_{32}$ were isolated in a state of purity, among which the hydrocarbons of the carbon atoms C_{10}, C_{11}. C_{12}, & C_{13} were noticed to compose the major part of the neutral volatile oil. The unsaturated hydrocarbons which were supposed to be transformed by the sulphuric acid treatment partly into alcohols,[2] and partly polymerised into hydrocarbons of high molecular weight,—both of these reaction products were investigated separately—& alcohols of the carbon atoms C_{10}, C_{11}, C_{13}, C_{14} & C_{15} and the hydrocarbons $C_{16}H_{26}$, $C_{18}H_{30}$, $C_{21}H_{35}$, $C_{24}H_{38}$, $C_{28}H_{46}$ were actually comfirmed as occurring in the reaction products by isolating them in a fairly pure state by fractional distillation.

When our assumption was admitted to be correct that alcohols will form by treating olefine hydrocarbons with sulphuric acid as a result of the hydrolysis of the alkyl sulphuric acid esters formed by the direct interaction of two substances, and polymerization was the principle result of high unsaturated hydrocarbons by the treatment, though the tendency to form alcohols from olefines decreases with increasing molecular weight, while with increasing molecular weight polymerization becomes the principal result,[2] and consequently it was concluded that the unsaturated

1 Edeleanu; Z. angew. Chem, **32**, 175 (1919).
2 Michael & Brunel. Am. Chem. J. **41**, 118 (1909).

hydrocarbons which make up the volatile part of the pityrol should be homologues of the series, C_nH_{2n}, & C_nH_{2n-2}, having the carbon atoms C_8, C_9, C_{10}, C_{12} & C_{14}.

As to the nature of the neutral compounds in the non-volatile part of the tar, the fractions which separated from each other by distillation, were assumed from the determination of the physical constants and analysis, to be composed of hydrocarbons of the polymethylene series of high molecular weight such as $C_{20}H_{41}$ with some hydrocarbons of the aromatic series.

	Fraction	Yield	d_4^{25}	n_D^{25}	C%	H%
1	to 130° (10 mm.)	10 %	0.8804	1.4837	85.6	11.5
2	130°–180° „	23 „	0.8616	1.4750	85.6	12.4
3	180°–230° „	24 „	0.8999	1.4870	82.3	12.0
4	230°–300° „	13 „	0.9445	1.5270	84.3	11.4

Pityrol, so far as studied, is similar in the nature of its constituents especially of the hydrocarbons to Russian or Japanese Petroleum and the low-temperature coal tar, but not coal tars resulting from high temperature carbonization[1].

The basic part of pityrol though the amount of it was very scanty compared to the other constituents, has an important relation with its physiological actions; the offensive odour of the tar and the decline of appetite of the workers in the laboratory where the tar is treated was frequently noticed, and these facts are due to the presence of the basic compounds.

Suzuki's experiment on the isolation of the basic compounds, indicates that they are composed of tertiary amines with some primary and secondary amines. By repeated fractional distillation, the basic part was divided into fractions, and each fraction was then converted into the double salts of mercuric chloride or picrates. By fractional crystallisation in their aqueous or alcoholic solution, 2–methyl pyridine, 3–methyl pyridine, 2–4–dimethyl pyridine, 2–6–dimethyl pyridine, 2–4–6–trimethyl pyridine, aniline and quinoline were isolated in a pure free state. The fact that the methyl derivatives of pyridine, aniline and quinoline occur in pityrol and probably also in coal tars, aroused the present writer's interest since

1 C. Engler u. H, v. Höfer: Das Erdöl II. (1909). S. Komatsu & S. Kusumoto: These Memoirs, **7**, 77 (1924); A. R. Warnes: Coal tar distillation 1923.

the occurence of these compounds in tars would have some intimate relation with the chemical transformation which takes place during distillation in the retort, of the organic compounds which are to be found in the raw materials.[1]

The acidic part of pityrol, has a connection with some pharmacological action of the tar, was investigated by Masumoto to learn its chemical nature.

The volatile acidic part of pityrol, according to the report made by T. Shimoda[2], has a highly irritative effect on the rabbit ear, the cutaneous connective tissue being affected most intensely by this compared with other constituents of the tar.

The volatile acidic fraction of the tar, which was isolated by means of a 5% caustic soda solution, was fractionated after being converted into methyl derivatives by means of dimethyl sulphate and caustic soda to avoid their oxidation. Although the pure compound could not be isolated by Masumoto's efforts, the existence of a compound of the molecular formula $C_{10}H_{18}O=C_9H_{15}OCH_3$ in the region of a B.p. 70°–75° under 7 mm. was assumed by referring to the physical constants and also by the analysis of the fractions resulting by repeated fractional distillation of the methylated oil, but such a compound has never been observed to occur in coal tars.

An interesting comparative study of coal-tars and pityrol by cutaneous injection into rabbit's ears was carried out by Dr. Shimoda[2] in Professor Matsumoto's laboratory. The experiments indicate that the hyperkeratotic change of the epithelial new-growth due to coal tar is evident, proliferation into the deeper layer being also marked, while both these changes are only slight in the case of pityrol application, and also the proliferative change of the subcutaneous tissue or of the cartilaginous plate of the ear due to the injection of coal-tar is far more evident than that due to pityrol in both cases. Such difference in the pathological action between coal tar and pityrol should be attributed to the difference in quality and quantity of the chemical constituents of the tars, and the hypothesis for the explanation will be granted when the analytical results by Sakami, Suzuki, and Matsumoto on pityrol are compared with those of the coal tars mentioned in the literature.[3]

The difference in the chemical constituents of both coal and rice

1 A. E. Tschitschibabn: J. p. Chem. **107**, 109, 122 (1924).
2 Acta Dermat. **10**, 500, 578 (1927).
3 A. R. Warnes: Coal tar distillation, 1923.

bran tars will account for the differentiation of the constituents of the raw material and also the external conditions under which the material was subjected to distillation.

Although the development of the chemistry of synthetic colours and drugs brought on a great advance in the coal-tar chemistry, the actual details of the chemical transformations occurring in the distillation of the coal material in the retort are still only known in part; the view proposed by Berthelot[1] that many of the aromatic hydrocarbons in coal tar resulted from high temperature carbonisation, which originated from acetylene by a process of condensation and polymerisation, is now opposed by the "bound" molecular theory[2] proposed by Jones & Wheeler, in which the hydrocarbons of coal tar can be produced by brerking down the "bound" condition present already in coal of a "bound" molecule which is attached chemically or physically to the non-alkyl groups.

The birth and development of the low temperature carbonization of coals, which has been going on during the decade of this century facilitate the recognition by chemists of the idea that the chemical composition and physical properties of tars are influenced to a wide extent by external conditions such as pressure and temperature under which the destructive distillation of the materials are performed.

Dealing first with physical constants, the lower specific gravity tars of coals are generally produced when low carbonisation temperatures are used, or coals are carbonized in vertical retorts, while the high temperature carbonisation in horizontal retorts usually produces tars of high specific gravity[3]. The vacuum tar, according to the investigation by Pictet and Bouvier[4], is composed of a mixture of saturated and of unsaturated hydrocarbons, but with an entire absence of aromatic hydrocarbons, which usually occur abundantly in high-temperature tar. It wrs, therefore, supposed that most of the compounds found in the high-temperature tars were produced by the thermal decomposition of the compounds previously formed from coals, which were similar or of the same character as the low-temperature tar or the vacuum tar compounds.

It will be of interest to study from this stand point the nature of the distillates obtained from various kinds of coal when they are submitted to destructive distillation under the same conditions; according to the experiment by F. Fischer and W. Glund[5], the low-temperature tar from lignite

1 M. Berthelot: Les carbures d'hydrogène I, 92 (1901).
2 J. Chem. Soc., **105**, 140 (1914).
3 P. E. Spielmann: The Const. of coal tar. 2 (1924).
4 C. R., **157**, 1436 (1913); **160**, 629 (1914).
5 *Z.* angew. Chem., **32**, 337 (1919).

is semi-solid, and from bituminous coal is liquid, and the essential difference between these low-temperature tars, the former tar being composed chiefly of paraffin hydrocarbons, should account for the difference of the chemical constituents of the raw materials from which the tars were obtained.

The experimental results[1], cited here, indicate that the raw material, and the temperature and the pressure of the carbonisation in the retort will greatly affect the quantity & quality of the reaction products-gas, tar and coke.

Material.	Condition.			
	Reduced pressure		Ordinary pressure	
			400°	1000°
Cellulose	tar	45 %	23 %	4 %
	aqueous liquor	32 „	33 „	36 „
	gas	13 „	25 „	10 „
	coke	10 „	17 „	40 „
Lignine	tar	15 „	13 „	—
	aqueous liquor	21 „	12 „	—
	gas		18 „	—
	coke	52 „	57 „	—

Various points of interest emerge from these researches; cellulose or allied substances which occur in natural substances in a free state or as a compound, furnishes an acidic substances in the tar, while basic compounds are derived from proteins and other nitrogenous matter. Lignine and resinous substances by destructive distillation will result in the forming of aromatic compounds. However, the relation of the composition of coal to the products of the distillate is rendered difficult by the lack of a true knowledge of the composition of coal, though there is now no need of any discussion as to the vegetable theory of the origin of coal. The problem should be solved in the near future and a solution of the problem, which will be awaited with interest, in dealing with natural substances of known constitution on the one hand, and on the other, by the endeavour to ascertain the chemical nature of coal substances.

The fact that the rice bran yields much more tar in comparison with the quantum derived from peat and wood—a fact obtained from statistics compiled from the results of the experiments of many chemists,—should

1 Strache—Lant: Kohlenchemie (1924)

be ascribed to the occurrence of protein and fatty substances in a greater amount in the bran than in the other natural substances in which carbohydrates and lignine predominate.

	H_2O	Ash	Protein	Fat	Carbohydrates		Lignine
					Simple & disacharides	Poly-sacharides	
Rice bran	15	9	13	23	12	20	—
Fat-free rice bran	14	12	17	0.7	15	26	—
Woods	—	—	1	1—3	10—25	43—56	20—29
Peats	—	—	—	6—13	10—16	9—18	8—12

	Coke	Aqueous distillate	Tar	Gas
Peat[1]	31—40	36—30	6—10	19—28
Wood[2]	38	33	9	20
Rice bran	28	36	24	12

From the analytical figures shown in the table, it was anticipated that the rice bran which had its fatty substance removed by extraction with petroleum ether would yield coke in greater quantum and tar in less degree than the ordinary bran, and the assumption was realized by Fujita's experiment shown in the table. These facts correspond with the hypothesis that tarry matter would have its origin mostly in the open chain carbon compounds, such as fatty and protein substances, and that coke, on the contrary, would be derived from lignine or other closed chain carbon compounds.

The organic matters in the whole rice bran by distillation in the retort were distributed in a ratio of 12.8 : 29.6 : 38.4 : 18.2 to aqueous liquor, coke, tar and gas respectively, while the distribution ratio of the organic matters in extracted bran was altered to 10 : 5 : 8.

The percentage of volatile and non-volatile parts and also that of

1 P. Hoering: Moornutzung u. Torfverwertung (1915), 265.

2 L. F. Hawley & L. E. Wise: The Chemistry of Wood (1926) 195, 201, 304.

the acidic, basic and neutral fractions in both parts were different in two cases (A & B), and we noticed especially a marked difference in the content and properties of the neutral oil, which, according to our theory, would owe its origin principally to the fatty substances in the raw material.

The difference which was noticed in the chemical constitution between the pityrols prepared on technical and laboratory scales, should be attributed to that in the material of the retort and the external conditions, such as temperature, under which the tar was produced.

In order to settle the assumption that the saturated and unsaturated aliphatic hydrocarbons which occur in pityrol were derived from fatty substances in the bran, palmitic and oleic acids which are the chief constituents (20% and 80% respectively) of the fatty acids of the oil, were isolated from the "Haze tallow" and the "Tsubaki oil" in a pure state respectively, and subjected to distillation of their sodium salts in Fischer's aluminium retort.

Professor Pictet[1] has reported sodium stearate gives rise by distillation under reduced pressure to a mixture of liquid or solid hydrocarbons of the series C_nH_{2n+2}; while Kawai's experimental results as will be seen from the table, differ from the former[2].

According to the experiment by Shoyama, sodium palmitate by distillation in a retort under ordinary pressure, yielded tar, coke and gas in the following proportions:—

	Tar	Coke	Gas & loss
Stearate			
(Pictet)	70	20	10
(Kawai)	72	15	13
Palmitate			
(Shoyama)	70	24	6
Oleate			
(Pictet)	70	24	6
(Kawai)	63	28	9
(Ogata)	65	17	18

Sodium oleate, under the same conditions as palmitate, was noticed by Ogata to decompose into tar, coke and gas with the yield shown in the table.

1 Hel. Chim. Acta, **2**, 501 (1919)
2 J. Soc. Chem. Ind., (Japan) **27**, 56 (1924)

Although there is no marked difference among the experimental results of the organic acids by different investigators into the yield of tar, coke and gas, as shown in the table, the relative proportions of volatile and non-volatile parts, and of saturated and unsaturated compounds in the tars will be noticed to differ from each other owing to the difference in the conditions under which the acids were distilled.

	V. p.	N-v. p.	Saturat.	Unsaturat.
Stearate (Pictet)	—	—	100	—
(Kawai)	—	—	40	60
Palmitate (Shoyama)	45	55	38	62
Oleate (Pictet)	—	—	—	100
(Kawai)	—	—	37	63
(Ogata)	47	53	20	80

S. Kawai has reported that by distillation under ordinary pressure of the calcium salts of stearic and oleic acids, saturated and unsaturated hydrocarbons were obtained in both cases, though the pure hydrocarbons could not be isolated from the tars, while Pictet and his coworkers had described the hydrocarbons of the series C_nH_{2n+2} from stearic acid and those of the series C_nH_{2n} from oleic acid as being only reaction products.

Shoyama has endeavoured to isolate pure hydrocarbons from the distillation product and has succeeded in the isolation of the saturated and unsaturated hydrocarbons of the carbon atoms from C_6 to C_{14}, in a fairly pure state from the volatile part of the tar, and those of $C_{13}-C_{30}$ from the non-volatile part. The main constituents of the neutral part of the tar were the hydrocarbons of the C_nH_{2n} series, C_8H_{16}, $C_{10}H_{20}$, $C_{11}H_{22}$, $C_{13}H_{26}$, $C_{15}H_{30}$, $C_{20}H_{40}$, $C_{30}H_{60}$, and also those of the C_nH_{2n+2}, series C_8H_{18}, C_9H_{20}, $C_{12}H_{26}$, $C_{14}H_{30}$, $C_{18}H_{38}$, $C_{20}H_{42}$, and the results agree fairly well in their statement of the constant of the hydrocarbons with those announced by Sakami from the neutral part of pityrol.

Under the same conditions as the palmitic acid, sodium oleate was noticed to yield of the hydrocarbons of the carbon atom C_7, C_8, C_9, C_{10}, C_{11}, C_{15}, C_{16}, C_{17}, of the C_nH_{2n} series as a principal constituent of the distillate with some saturated hydrocarbons C_9H_{20}, C_8H_{18} & C_7H_{16}, and these unsaturated hydrocarbons were previously isolated by Pictet from

the distillation product of sodium oleate under reduced pressure, and were also comfirmed by Sakami to occur in the neutral volatile part of pityrol.

As to the fate of pentosan, cellulose and other soluble carbohydrates in the rice bran during the distillation in the retort, we have at present no exact knowledge as to the products therefrom. However, as it was stated by Klason, Heuser & Scherer[1] that the pentosans are obviously the source of the volatile acids, furfural and other furane products, and cellulose would be transformed under similar treatment as that of the pentosans into the acidic substances and, furfural & its derivatives.[2] Simple sugars and sucrose which would undergo analogous chemical changes by distillation as cellulose and hemicellulose, and are supposed to yield compounds mentioned above.

However, the alkali-soluble constituents of the tars which are obtained from woods and coals, are largely composed of phenolic compounds which are assumed by many chemists to be derived partly from the lignine and partly from carbohydrates, since these compounds and their degradation products occur in these neutral substances, and such an assumption was proved, partly by experiments, to be true. The acidic compounds which were isolated by Masumoto in an impure state from pityrol, should have their origin in the carbohydrates or the protein in the rice bran, since the bran usually lacked lignine and its allied substances.

As a matter of fact, pityrol from commerce and laboratory contains acidic substances in measurable quantity, and this accords with the hypothesis that carbohydrates and protein mostly give rise to acidic substances by distillation.

The distillation of sucrose was undertaken by Hidaka in connection with the explanation of the origin of the alkali-soluble constituents of pityrol.

Sucrose by dry distillation yields tar, an aqueous distillate, charcoal and gas, and the yield of these substances is shown in the table with the results of cellulose as comparison.

	Sucrose	Cellulose[3]
Tar & aqueous distillate	25 %	37 %
Charcoal	45 „	34 „
Gas & loss	30 „	29 „

1 Brenstoff. Chem., **4**, 24 (1924)

2 Evdnaun & Schaefer: Ber. D. Chem. Ges., **43**, 2398 (1910)

3 P. Klason, G von Heidenstan, & E. Norlin, Z. angew. Chem., **22**, 1205 (1909)

Furfural, methyl furfural & oxymethyl furfural, were found in the distillate and the results are similar to the case of cellulose & glucose.[1]

The basic constituents of pityrol which are derived solely from proteins, occur in the bran in according with Pictet's suggestion[2] that protein by dry distillation furnishes the basic compounds together with some organic acids.

According to the experiment by Suzuki, the methyl derivatives of pyridine, quinoline and some aniline were isolated from the basic fraction of pityrol, and it is remarkable that the basic compounds in pityrol are entirely absent from pyrrol & its derivatives, and these facts will suggest that the pyridine bases in the tar would have their origin in pyrrol and its derivatives, and that the former are formed by the pyrogenic reaction from the latter compounds during the destructive distillation.

When rice bran is subjected to dry distillation in a retort, 38% and 30% of the organic substances in the bran were transformed into tar and coke respectively, while with bituminous coal by distillation at 500°, 7% of its organic matter was converted into tar and 70% remained as coke. The yield of the tar from lignine and cellulose which are the chief constituents of wood, was estimated to be 30% and 70% respectively. These facts indicate that the open chain carbon compounds such as fat, & the carbohydrates, give rise to tar in a large amount; and close-chain carbon compound on the contrary yield tar in less quantity than the former compounds.

With regard to the chemical changes which take place in the fatty constituents of rice bran in retort, we can picture to ourselves the probable course as follow:—the primary effect of heat on the fatty acids is to cause an elimination of CO_2 from the molecule in both ways:

(1) $RCH_2CO_2H \rightarrow (RCH_2)_2CO + CO_2 + H_2O$

(2) $RCH_2CO_2H \rightarrow RCH_3 + CO_2$.

Ketones which are formed from acids by splitting off CO_2 & H_2O, being of unstable nature toward heat[3], and will in turn eliminate CO by loosening or dissolving the bonds between the carbon atoms, together with a simultaneous dissociation of hydrogen, giving rise to residues such as RCH_2 or RCH, which may subsequently either form unsaturated compounds by intra-molecular rearrangement or polymerize to form high

1 E. von Lippmann: Die Chemi d. Zuckerarten. I (1904) 301

2 Hel. Chim. Acta, **2**, 188 (1919) and refer the distillation of silk fibroin by Johnson. J. Am. Chem. Soc., **41**, 1147 (1919)

3 P. Sabatier: La Catalyse en chimie organique, 327 (1920)

molecular compounds as indicated below:

(3) $(RCH_2)_2CO \rightarrow RCH + CO + H_2$; $2RCH \rightarrow (RCH)_2$.

(4) $(RCH_2)_2CO \rightarrow (RCH_2)_2 + CO$.

Experimental facts accord well with the hypothesis indicated above, in isolating palmitone, saturated & unsaturated hydrocarbons by Shoyama from the distillate of palmitate. The gas evolved from the retort in which palmitic or oleic acids are carbonized at a temperature of 500°, contains equal quantities of CO and CO_2 in both cases, and the result supports the correctness of our hypothesis for the transformation of fatty substances by distillation.

It is, however, surprising that the composition of the gas from rice bran carbonized in the retort, not only differs qualitatively from that of the acids, but quantitatively also, containing comparatively little CO, still less hydrogen and lower members of saturated hydrocarbons, although the CO_2–content is as high as 32 per cent. Thermal decomposition of carbohydrates & other substances, except of fatty substances occurring in rice bran may account for such an unexpected result.

Gas–Analysis

Yield	Rice Bran		Palmitate	Oleate	Wood
	A 12%	B 14%	6 %	18%	—
C_nH_{2n+2} & H	2	3	36	46	7
C_nH_{2n}	26	18	29	23	2
CO	17	21	12	15	24
CO_2	32	32	12	16	67

As a consequence, in the case of rice bran, the thermal reaction of its organic substances resulted in the percentage of the olefines in the gaseous product being found to be much higher than the percentage of paraffin & hydrogen, while the decomposition phase of the paraffin hydrocarbons formed from the fatty acids by the primary reaction, which has been described previously, would be the same in both the fatty acids & the rice bran in forming hydrocarbons of low molecular weight.

As a matter of fact, the paraffin hydrocarbons C_9H_{20}, $C_{10}H_{22}$, $C_{15}H_{33}$, $C_{30}H_{62}$ are found in pityrol and also in tars from the fatty acids as a main reaction product, and the facts harmonize with the idea proposed by G. Egloff & R. I. Moore with regard to the thermal stability of the

paraffin hydrocarbons that the hydrocarbons $C_{12}H_{26}$ & $C_{15}H_{32}$ are most stable[1] & those of fewer and of more carbon atoms less stable. Keeping the relative thermal stability of hydrocarbons, which depends on the molecular weight and configuration of the molecule in mind, the thermal changes—decomposition & polymerisation—of the hydrocarbon residue derived by the splitting of the CO_2 from the palmitic & oleic acids, will be interpreted in the following scheme:

$C_{15} \rightarrow C_{10} + C_5$ ..... decomposition.

$2C_{10} \rightarrow C_{20}$ .....
$2C_{15} \rightarrow C_{30}$ ..... } polymerisation.

To our astonishment, the pathological actions of the constituents of pityrol are quite different in some cases from those of pityrol itself, for instance, the pathological behaviour of the high fraction of the neutral oil from pityrol, which effects on the animal skin to produce cancer is never observed of pityrol or of any fraction of tar derived from palmitic acid.

We are reminded in this connection that Kennaway has expressed his opinion concerning cancer-producing tars, the tar cancer is caused by a very small quantity of an unstable compound that exists in the high-boiling fraction (250° to 500°) of a high temperature coal tar, which will be removed from tar-constituents by purification, as purified anthracene, which, like all other pure compounds does not produce cancer. The cancer-producing principle of the tars, therefore, seems to stand in this respect, in a similar relation as vitamines to food materials.

Such mysterious examples are sometimes noticed in the pharmacological investigations of crude drugs, the action of a crude drug will sometimes diminish markedly or be entirely destroyed on purification or concentration of the active principle by chemical or physical means, due to its partial destruction, disappearance or some other unknown reason by the treatments. The difficulty which has often been encountered in isolating an essence such as an enzyme or a vitamine in a pure state, from natural substances, and the statements which have just been reviewed, give strong support to the belief that the behavior particullarly of the biological actions of a compound occurring in nature and isolated in a pure state, towards living organs or substances would not be the same in every respect when it is employed in association with other substances which occur together in nature.

---

1 Met. Chem. Eng., **16**, 47 (1917)

Biochemical Studies on Pityrol, II. Distillation of Rice Bran

By

Shinzaburo Fujita

(Received September 12, 1928)

1. Analysis of Rice Bran

The rice bran which was used in the preparation of the tar was obtained from the rice named Shinriki which is grown near Osaka, and was taken to the laboratory immediately after being milled in a milling machine designed by Mr. Tsuge. The bran was subjected to a dry heat of about 80°C for one hour to destroy any enzymes in it.[1] It was divided into two parts, and the one part (B) was treated with petroleum ether in an oil extractor[2] of Wegelin and Huebner A–G, Hall, to extract the rice oil, and dried in the open air, and both samples were analysed with the following results:

1. Water-content.

A sample taken in a weighing-bottle was kept at 105° to a constant weight, the loss in weight is the assumed water-content.

2. Ash-content.

Crude ash prepared by burning in a porcelain crucible with an alcohol lamp, and then incinerated at about 400°C in an electric oven, and weighed.

3. Elementary analysis.

The dried sample was analysed and the results, calculated on ash-free and dry bases, are shown in the table.

4. Crude fat.

1 C. A. Browne: J. Am. Chem. Soc., **25**, 948 (1903)

2 Ullmann: Encyclopedia Bd. **5**, 375 (1914)

Table I

	A	B
C	46.2	39.9
H	7.4	6.0
N	2.4	3.0
S	1.5	2.0
Water	14.7	14.1
Ash	9.3	12.0
Crude fat	22.4	0.7
Protein	12.9	16.5
Cellulose	11.4	14.6
Pentosans	8.7	11.1
Reducing sugar	1.3	1.5
Sucrose	10.6	13.6

The fatty substance in the sample was extracted with ether in Soxlet's extractor, and the residue obtained by expelling the solvent by distillation, was estimated of itsacid and iodine values in the usual manner: A.V.=160; I.V.=118.

5. Crude protein.

The total nitrogen content was estimated by Kjeldahl's method and the crude protein was calculated by multiplying the total nitrogen by 6.25.

6. Pentosan.

The content of pentosans was estimated by Tollens aud Kruger's method as usual.

7. Sucrose.

According to Dr. S. Hirai[1], reducing and non-reducing sugars which occur in the bran were composed mostly of d-glucose, and sucrose, respectively, and were isolated from the aqueous extract.

The bran, after being deffated, was treated with 50% hot ethyl alcohol in presence of calcium carbonate, and the content of d-glucose and sucrose in the extracted solution was estimated by means of Fehling's solution.

8. Cellulose.

The cellulose content was determined of the dried sample by Cross-Bevan's method modified by Renker.[2]

1 Acta Scholae Medi. Univ. Imp. Kyoto, **7**, 463 (1925)

2 J. Soc. Chem. Ind., **28**, 1269 (1910)

2. Dry Distillation

30 grm. each of samples (A and B), were distilled in Fischer's aluminium retort, and the tar with aqueous distillate was condensed in a flask connected directly with the retort, which carried a delivery tube by which the generated gas was permitted freely into the gas holder. The apparatus used in this experiment is similar in arrangement to the low temperature assay apparatus for coal of the Fuel Research Board[1].

The gas began to evolve at 200°, a tarry substance of a light yellow colour distilled and at 350° the generation of gas and tar of a dark colour increased equally with the temperature rise, a violent decomposition of the contstituents of the rice bran taking place at about 400° and the reactions as will be seen in the temperatures-volume curve of the gas, were completed at 450°.

Repeating the same operation, 2500 grm. of one or the other samples (A and B) were distilled and the following results were obtained:

Table II

	A	B
Tar	600 grm.	375 grm.
Coke	700 „	775 „
Aqueous liquor	900 „	1000 „

The yields of these reaction products are shown in percentage.

The yield of the reaction products, as may be seen in the foregoing table, will vary with the chemical composition of the raw material, though the conditions under which the sample were treated were the same in both cases.

In order to see what difference in chemical and physical properties will be found between the reaction products-gas and the tar, which was obtained from the two materials, the tar was divided into two portions—volatile, and non-volatile by steam distillation and each fraction was then subdivided into acidic, basic and neutral parts. The oil-containing bran yields, as may be seen in Table IV, a neutral tarry matter in a greater amount than the other, while the content of the basic and acidic parts is greater in the tar from the oil-free material. The physical constants

1 C. H. Lander and R. F. McKay: Low temperature carbonisation (1924), P. 61

Table III

	A	B
Tar	24 %	15 %
Coke	28 „	31 „
Aqueous liquor	36 „	40 „
Gas	12 „	14 „

	Tar	
	A	B
d_4^{25}	0.967	0.981
Volatile part	13 %	17 %
	d_4^{27}=0.871	d_4^{25}=0.919
Non-volatile	87 „	83 „

	Aqueous liquor	
	A	B
Density	1.021	1.035
Organic matter	22	19

	Coke	
	A	B
Moisture	0.80	1.23
Ash	32.67	34.56
Volatile carbon	19.42	19.06
Non-volatile carbon	47.11	45.15
Elementary analysis		
C	49.79	51.73
H	2.82	3.24
N	3.58	3.74
S	0.02	0.03
Ash	33.46	35.30

	Gas	
	A	B
Bases	22 %	23 %
C_nH_{2n}	25.4 „	17.4 „
C_2H_4	0.4 „	0.4 „
C_nH_{2n+2}	2 „	3 „
CO	17.3 „	20.6 „
CO_2	31.8 „	31.6 „

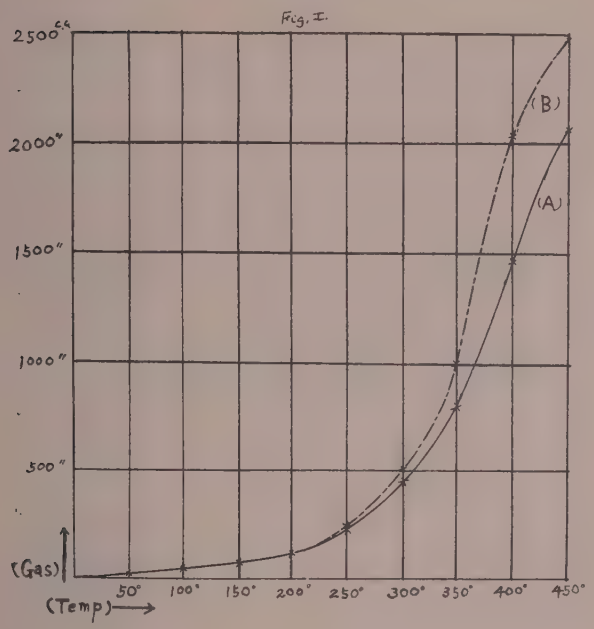

Table IV

		A	B
	Neutral part	68 %	53 %
	Acidic „	29 „	35 „
	Basic „	3 „	11 „
	Neutral part	66	46
V. part	Acidic „	30	39
	Basic „	4	16
	Neutral part	68	55
N. V. part	Acidic „	29	35
	Basic „	3	10

and the analytical results of the aqueous liquor and coke are similar in both cases, while the chemical composition of the tar and the gas is different as may be seen from the table IV.

The neutral oil from bran A. is lower in density and index of refraction than the oil from B, the difference in the physical properties

Table V

	Fraction (5–10 mm)	A	B
Neutral Oil.	60°—100°	1.9 grm (25%)	2.3 (37%)
	d_4^{25}	0.8021	0.8377
	n_D^{25}	1.4476	1.4617
	I.V.	201	200
	C.	83.48	82.28
	H.	11.86	11.11
	100°—150°	3.1 grm (41%)	2.3 grm. (37%)
	d_4^{25}	0.8486	0.8889
	n_D^{25}	1.4715	1.4893
	I.V.	167	202
	C.	83.60	82.25
	H.	11.94	10.98
	150°—180°	1.1 grm (14%)	0.6 grm. (10%)
	d_4^{25}	0.8516	0.8935
	n_D^{25}	1.4734	1.4912
	I.V.	164	183
	C.	83.21	82.55
	H.	12.44	11.06
	Residue	1.5 grm.	1.1 grm.
Acidic Oil.	60°—100°	1.1 grm (22%)	2.1 grm. (38%)
	d_4^{25}	0.9757	0.9949
	n_D^{25}	1.4892	1.5020
	C.	71.03	72.20
	H.	9.05	8.41
	100°—150°	1.5 grm (31%)	1.8 grm. (32%)
	d_4^{25}	0.9785	1.006
	n_D^{25}	1.4863	1.5073
	C.	69.93	72.30
	H.	9.35	9.13
	Residue	1.3 grm.	1.7 grm.

	760 mm.	A	B
Basic Oil.	100°—200°	0.5 grm (17%)	0.6 grm. (14%)
	d_4^{25}	0.9981	0.9785
	n_D^{25}	1.4853	1.4791
	C.	66.00	66.25
	H.	8.46	8.83
	N.	8.51	7.05
	200°—255°	0.9 grm. (31%)	1.6 grm. (38%)
	d_4^{25}	1.0265	1.0470
	n_D^{25}	1.5241	1.5292
	C.	71.03	71.00
	H.	7.78	7.30
	N.	7.73	6.60
	Residue	1.4 grm.	2.0 grm.

indicates that of the chemical nature in both tars. The lighter oil should be saturated in chemical structure, and the analytical results of carbon, & the hydrogen content of the fractions, show a fair agreement with the indication of the physical constants. The relation in the physical and the chemical natures, which was observed in the natural oils, was also noticed in the acidic oils from the two different origins, but not in the two basic oils, and the explanation for the difference in the properties of the neutral and the acidic oils from two different origins would be learned when we take the difference in the constituents of the brans into consideration.

Biochemical Studies on Pityrol, III. Neutral Constituents of Pityrol

By

Saburo Sakami

(Received September 12, 1928)

The tar obtained by the dry distillation of rice bran, which was named "Pityrol" by Professor Matsuura, was a dark-brown viscous liquid of a peculiar unpleasant odour, with some carbon particles. 50 kg. of the tar manufactured in the Shinyaku Kaisha, Kyoto, were kindly presented to us by Mr. Ichinose, Director of the company. It was subjected to steam distillation to separate into two parts-volatile and non-volatile and each part was subdivided into neutral, acidic and basic fractions by treating with a 7% caustic soda solution and 10% sulphuric acid successively.

Table I

Fraction	Yield	
Volatile part	12. %	10.8 kg.
Non-volatile part	88. „	89.2 „

Fraction	tar	volatile part	non-volatile part
Neutral substance	57 %	89 %	52 %
Acidic „	37 „	6 „	41 „
Basic „	6 „	5 „	7 „

NEUTRAL SUBSTANCES

1.5 kg. of the volatile neutral substances of the dark-brown light oil mentioned above were treated with a 5% solution of sulphuric acid, and then with a dilute caustic soda solution to remove completely the basic and acidic substances from the neutral one, and the light brown residual oil was subjected to fractioned distillation after being dried with anhydrous sodium sulphate.

Table II

	Fraction	Yield		d_4^{25}	n_D^{25}	C	H
1	to 150°	160 gr.	10.3 %	0.8131	1.5578	84.4	11.4
2	150°—180°	369 „	23.8 „	0.8215	1.4547	85.5	11.5
3	180°—210°	524 „	33.8 „	0.8338	1.4615	85.1	11.8
4	210°—240°	359 „	23.1 „	0.8425	1.4683	86.7	12.1
5	240°—270°	140 „	9.0 „	0.8326	1.4620	86.9	13.1

The analytical results of the fractions indicate that the hydrocarbons which composed almost entirely the neutral substance of the pityrol, were of unsaturated nature as indicated in their physical constants.

1. Action of Fuming Sulphuric Acid on Hydrocarbons.

In order to remove the unsaturated hydrocarbons from the fractions

Table III

	Fraction	Yield		d_4^{25}	n_D^{25}
1	to 150°	2.5 c.c.	10 %	0.7115	1.3962
2	150°—180°	3.0 „	12 „	0.7253	1.4020
3	180°—210°	3.3 „	13 „	0.7389	1.4090
4	210°—240°	5.2 „	21 „	0.7557	1.4180
5	240°—270°	7.8 „	31 „	0.7696	1.4250

mentioned above, 25 c.c. of each fraction were treated with 50 c.c. of fuming sulphuric acid with 10% SO_3, under ice-cooled water. The yield of the saturated hydrocarbons which remained unaffected by the acid treatment is shown in Table III with some physical properties.

2. Action of con. Sulphuric Acid on Neutral Substances

25 c.c. of each fraction of the neutral substance were treated with 25 c.c. of con. sulphuric acid (sp. gr. 1.84) under cooling with iced-water. The percentage of the hydrocarbons which remained in each fraction without any reaction from the acid was as follows:

Table IV

	Fraction	Yield of sat. H. C.		d_4^{25}	n_D^{25}
1	to 150°	5.3 c.c.	21. %	0.7985	1.4455
2	150°—180°	3.5 „	14. „	0.7671	1.4252
3	180°—210°	3.6 „	14 „	0.7546	1.4160
4	210°—240°	4.7 „	19 „	0.7822	1.4313
5	240°—270°	7.9 „	32 „	0.8042	1.4340

The residual hydrocarbons mentioned in the above table were again treated with fuming sulphuric acid (with 10% SO_3) and the residue from the acid treatment was determined as to quantity and also physical constants.

Table V

	Fraction	Yield		d_4^{25}	n_D^{25}
1	to 150°	2. c.c.	8. %	0.7163	1.3965
2	150°—180°	2.4 „	9. „	0.7354	1.4065
3	180°—210°	3.3 „	13 „	0.7528	1.4152
4	210°—240°	3.5 „	14 „	0.7656	1.4220
5	240°—270°	6.1 „	24 „	0.7730	1.4262

Although the sulphuric acid treatment was not an accurate method for the estimation of the aliphatic, aromatic and other unsaturated hydrocarbons in the mixture, the relative percentage of these hydrocarbons in it would be approximately determined by treating with con. sulphuric acid and fuming sulphuric acid containing 7% SO_3 successively, and the experimental results for the relative amount of these hydrocarbons in the neutral volatile oil of pityrol were as follows:

Table VI

	Fraction	Hydrocarbons.		
		paraffin	aromatic	other unsaturated
1	to 150°	8 (vol. %)	13	79
2	150°—180°	9	5	86
3	180°—210°	13	—	87
4	210°—240°	14	—	86
5	240°—270°	24	—	76

SATURATED HYDROCARBONS

For the study of the chemical nature of the saturated hydrocarbons occurring as a constituent of the neutral substances in pityrol, the isolation of individual compounds in a pure state, was undertaken; 100—250 c.c. of each fraction of the crude neutral oil were treated with sulphuric acid of sp. g. 1.84 in a cold state for 30 minutes, and the insoluble oil in the acid, separated from the acid layer, washed with water, dried and distilled, and the saturated hydrocarbons separated from the polymerized and hydrated compounds which were formed from the unsaturated hydrocarbons in the course of the acid treatment, gave the following constants:

Table VII

	Fraction (used)	Yield		d_4^{25}	n_D^{25}
1	to 150°, 145 c.c.	20 c.c.	14 %	0,7888	1.4452
2	150°—180°, 250 „	31 „	12 „	0.7561	1.4235
3	180°—210°, 250 „	40 „	16 „	0.7650	1.4267
4	210°—240°, 250 „	48 „	19 „	0.7782	1.4336
5	240°—270°, 105 „	34 „	32 „	0.7839	1.4370

Each fraction was treated again with fuming sulphuric acid containing 7% SO_3, and then washed with water, dried over calcium chloride and finally distilled on metallic sodium.

For the purification of the saturated hydrocarbons from the hydrocarbons of the polymethylen series which may be present with the former in the fractions, having escaped from the sulphuric acid treatment, each

Table VIII

	Fraction	Yield		d_4^{25}	n_D^{25}
1	to 150°	8.8 c.c.	6.7 %	0.7131	1.3950
2	150°—180°	23.6 „	9.4 „	0.7304	1.4084
3	180°—210°	32.6 „	13.5 „	0.7496	1.4180
4	220°—240°	40.5 „	16.2 „	0.7632	1.4250
5	240°—270°	27.2 „	25.9 „	0.7712	1.4300

fraction was passed, at the rate of 3 grm. an hour, on reduced nickel heated at 300°, under this treatment the polymethylene hydrocarbons should decomposed into unsaturated or aromatic hydrocarbons.

Table IX

	Fraction I	Sample passed	H_2 liberated	Fraction II	Yield	d_4^{25}	n_D^{25}
1	to 150°	4.0 c.c.	60 (c.c.)	(124°—150°)	3.7 c.c.	0.7119	1.3944
2	150°—180°	13.6 „	250 „	(150°—183°)	13.1 „	0.7299	1.4040
3	180°—210°	19.8 „	610 „	(177°—214°)	18.8 „	0.7499	1.4142
4	210°—240°	25.0 „	280 „	(208°—244°)	23.5 „	0.7627	1.4210
5	240°—270°	18.9 „	60 „	(238°—269°)	18.9 „	0.7705	1.4255

The fractions were again distilled after being treated with fuming sulphuric acid containing 10% SO_3, and determined of their physical constants, and the results are shown in Table IX.

In order to isolate the pure hydrocarbons from the fractions, the fractional distillation was repeated 13 times for each fraction the following 15 portions resulted from the physical constants and analytical results of carbon and hydrogen.

Octane (B. p. 135.8°); nonane (B. p. 149.5°); decane (B. p. 172°); undecane (B. p. 194.5°), dodecane (B. p. 95°. 15 mm.), tridecane (B. p. 114°. 15 mm.), tetradecane (B.p. 129°. 15 mm.), and pentadecane (B. p. 144°. 18 mm.), were found to be isolated in a fairly pure state from their physical constants and analytical results, from the neutral oil of pityrol among which decane $C_{10}H_{22}$, undecane $C_{11}H_{24}$, dodecane $C_{12}H_{26}$ and tridecane $C_{13}H_{28}$ occupy the principal parts of the oil.

Table X

	Fraction	Yield	n_D^{25}	d_4^{25}	Mean	
					C	H
1	to 120° ord. press.	0.5 grm.	1.3870	0.6962	84.0	15.9
2	120°—130°	1.0	1.3908	0.7047	84.0	15.7
3	130°—140°	1.1	1.3942	0.7115	84.0	15.8
4	140°—150°	3.4	1.3982	0.7205	84.1	15.7
5	150°—160°	2.2	1.4015	0.7256	84.2	15.6
6	160°—170°	3.3	1.4050	0.7327	84.3	15.5
7	170°—180°	4.0	1.4073	0.7372	84.5	15.5
8	180°—190°	3.0	1.4113	0.7447	84.4	15.3
9	190°—200°	7.4	1.4138	0.7495	84.6	15.3
10	— 95°	2.5	1.4180	0.7585	85.0	15.2
11	95°—105°	6.0	1.4185	0.7588	84.8	15.2
12	105°—115°	7.7	1.4208	0.7625	84.8	15.2
13	115°—125° 12 mm.	3.0	1.4228	0.7663	85.0	15.1
14	125°—135° „	5.7	1.4248	0.7698	84.0	15.0
15	Above 135° „	2.8	1.4260	0.7712	85.0	15.0

Unsaturated Hydrocarbons

The volatile neutral part of pityrol, which, being assumed to be a mixture of saturated and unsaturated hydrocarbons, was treated with con. sulphuric acid to remove the unsaturated compounds. The results of the treatment with conc. sulphuric acid would involve some chemical changes in the unsaturated compounds of polymerisation, the formation of sulphuric acid esters, and hydration to alcohols.

The researches into the polymers and alcohols which were formed by the treatment are therefore of considerable interest in connection with the identification of the unsaturated hydrocarbons which occurred with the saturated compounds in the volatile neutral oil.

Five fractions mentioned in the foregoing paragraph, had contained the saturated & unsaturated hydrocarbons, and the latter were supposed to yield by the action of the acid polymers which were separated by fractional distillation and their physical constants determined.

Table XI

	Original sample		B.p. polymer.	Yield of	
	B. p.	c.c.	(10—11 mm.)	Polymer.	High boiling fraction
1	to 150°	145	60°—195°	25 grm.	3 grm.
2	150°—180°	250	90°—210°	50 „	19 „
3	180°—210°	250	120°—225°	33 „	30 „
4	210°—240°	250	150°—250°	42 „	17 „
5	240°—270°	105	180°—275°	10 „	10 „

Table XII

	Fraction (10—11 mm.)	d_4^{25}	n_D^{25}
1	60°—195°	0.8672	1.4840
2	90°—210°	0.6895	1.4856
3	120°—225°	0.8733	1.4880
4	150°—260°	0.8832	1.4950
5	180°—275°	0.8857	1.4954

Each fraction was again distilled 4 times under 12 mm. to isolate, if possible, definite polymers, and divided into three parts which show physical constants, analytical results and molecular weight.

The middle part (b) of each fraction was assumed to be composed mostly of a definite compound from its physical constants, analytical results and also molecular weight measured by the cryoscopic method of the benzene solution; the hydrocarbons of the molecular formulae $C_{16}H_{26}$, $C_{18}H_{30}$, $C_{20}H_{34}$, $C_{24}H_{38}$ & $C_{28}H_{46}$ were found actually to occur in the main part of each fraction shown in Table XII.

The occurrence of these compounds in the polymers can be explained by assuming the polymerisation of the unsaturated hydrocarbons C_8H_{13}, C_9H_{15}, $C_{10}H_{17}$, $C_{12}H_{19}$ & $C_{14}H_{23}$, which takes place during the acid-treatment. It seems, however, very reasonable to assume that the mother substances which occur in the original tar and yield polymers by the acid treatment should be hydrocarbons of the C_nH_{2n} or C_nH_{2n-2} series, namely the unsaturated hydrocarbons of C_9H_{16}, $C_{10}H_{18}$, $C_{12}H_{20}$ and $C_{14}H_{24}$ are the main constituents of the volatile neutral part of pityrol.

Table XIII

	Fraction		Yield	d_4^{55}	n_D^{25}	C	H	M. W.
1	(a)	45°—135°	5.7 grm.	0.8287	1.4620	87.3	12.7	—
	(b)	135°—150°	10.4	0.8722	1.4878	88.2	11.9	218
	(c)	150°—190°	4.3	0.8915	1.4968	88.2	11.6	—
2	(a)	90°—155°	6.4	0.8153	1.4530	86.6	13.3	—
	(b)	155°—175°	30.2	0.8741	1.4882	87.9	12.2	216
	(c)	175°—210°	9.7	0.8888	1.4952	87.6	11.9	—
3	(a)	105°—185°	4.1	0.8280	1.4594	86.6	13.3	—
	(b)	185°—195°	17.4	0.8748	1.4890	87.1	12.2	287
	(c)	195°—220°	7.9	0.8870	1.4958	87.2	12.0	—
4	(a)	125°—215°	4.5	0.8161	1.4516	85.5	13.8	—
	(b)	215°—230°	19.8	0.8891	1.4982	87.1	12.0	362
	(c)	230°—260°	8.9	0.9003	1.5050	87.2	11.9	—
5	(a)	150°—240°	3.0	0.8717	1.4851	86.4	12.5	—
	(b)	240°—255°	4.3	0.8932	1.4998	87.5	12.1	383
	(c)	255°—270°	0.9	0.8988	1.5028	87.3	12.1	—

In order to isolate alcohol formed from alkyl sulphuric acid esters, as an intermediate reaction substance from the unsaturated hydrocarbon of the olefine series and sulphuric acid, by hydrolysis, the aqueous acidic solution in each fraction, which is separated from the oily layer of

Table XIV

	Fraction	Yield	d_4^{25}	n_D^{25}
1		0.9 grm.	0.8602	1.4329
2		5.0 „	0.8322	1.4257
3		6.7 „	0.8382	1.4364
4		4.7 „	0.8368	1.4435
5		1.4 „	0.8433	1.4469

hydrocarbons, was diluted with water at 0°, and the alcohols which resulted from the hydrolysis of the sulphuric acid esters were extracted by means of ether.

Distilling off the solvent, there remained an oily residue which was

composed mostly of alcohols, this was subjected to steam distillation, the oily distillate separated from water, dried and then distilled.

Each fraction was distilled again under 18 mm. 4 times and was divided into the following parts, and the physical constants and the contents of carbon & of hydrogen in the molecule determined.

Table XV

II.	Fraction	Yield	d_4^{25}	n_D^{25}	C	H	O
1	40°—50°	0.2 grm.	—	1.4115	—	—	
2	50°—60°	0.7	0.8143	1.4162	76.3	12.7	11.0
3	60°—70°	0.9	0.8257	1.4218	76.6	12.4	11.0
4	70°—80°	1.0	0.8388	1.4281	75.6	12.0	11.4
5	80°—105°	0.8	0.8702	1.4449	74.4	11.2	13.4
III.							
1	60°—70°	0.6	0.8041	1.4213	78.7	13.1	8.3
2	70°—80°	1.6	0.8176	1.4277	78.5	12.7	8.8
3	80°—90°	1.7	0.8381	1.4366	78.5	12.2	9.3
4	90°—100°	1.0	0.8571	1.4442	77.9	11.7	10.3
5	100°—117°	0.5	0.8781	1.4534	76.9	11.4	11.6
IV.							
1	80°—90°	0.6	0.8171	1.4330	80.6	12.9	6.4
2	90°—100°	1.1	0.8261	1.4388	80.4	12.9	6.7
3	100°—110°	1.0	0.8364	1.4429	79.8	12.6	7.5
4	110°—120°	0.9	0.8486	1.4489	79.2	12.3	8.4
5	120°—	0.3	—	1.4642	—	—	—

The experimental results shown in the table above, indicate alcohols of the molecular formulae from $C_8H_{18}O$ to $C_{14}H_{30}O$ occurring in the distillates, which were evidently derived from the hydrocarbons of the olefine series C_8H_{16} $C_{14}H_{28}$ by hydration in presence of con. sulphuric acid.

Neutral Substance in the Non-Volatile Oil

The non-volatile oil of pityrol was treated with a 5% sulphuric acid & a 3% caustic soda solution successively to separate neutral substance, and

1700 grm. of the remaining oil after being washed with water and dried were subjected to fractional distillation 3 times under 20 mm. and the results were:

	Fraction	Yield		d_4^{25}	n_D^{25}
		wt.	%		
1	90°—150°	167 gr.	9.8	0.8693	1.484
2	150°—200°	356	20.9	0.8564	1.477
3	200°—250°	357	21.0	0.8996	1.491
4	250°—280°	64	3.8	0.9526	1.529
	Residue	530	31.2		

These fractions were again distilled 5 times under 10 mm.

	Fraction	Yield		d_4^{25}	n_D^{25}
		wt.	%		
1	to 130°	151 gr.	10.1	0.8804	1.4837
2	130°—180	347	23.1	0.8616	1.4750
3	180°—230°	353	23.5	0.8999	1.4870
4	230°—300°	189	12.6	0.9445	1.5270

Fig. 2

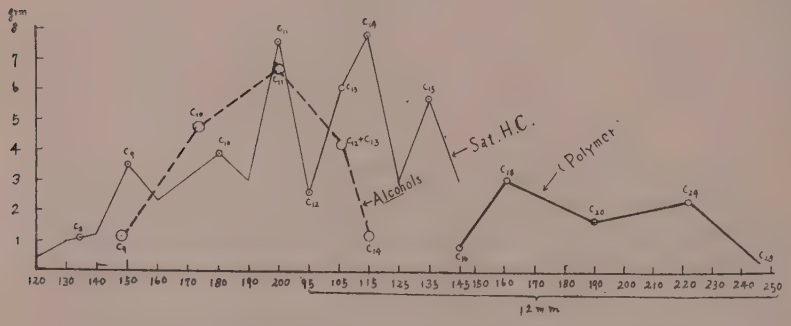

From these experimental results, the neutral non-volatile part of pityrol was assumed to be composed mostly of the hydrocarbons of the polymethylene series, which are similar in properties with those that occur

C	H	N	S
85.6	11.5	1.5	0.2
85.6	12.4	1.9	0.2
82.3	12.0	2.5	0.1
84.3	11.4	4.2	0.1

in Russian or some Japanese Petroleums and in low temperature coal tars.

The neutral constituents of pityrol, as will be indicated in the Fig 2, consist mostly of the hydrocarbons of the carbon atoms C_{10}, C_{11}, C_{14} & C_{15}.

Biochemical Studies on Pityrol, IV. Acidic Constituents of Pityrol

By

Bunkichi Masumoto

(Received September 12, 1928)

Acidic substance as one of the constituents of commercial pityrol was isolated by treating 20 lbs of the crude tar by means of a 5 % caustic soda solution in the usual way, and the yield was 90 grm. The acidic substance was a dark brown oil having a phenolic odour, partly soluble in water, and easily soluble in organic solvents. 80 grm. of this acidic oil were fractionated under 19 mm. pressure, after being dried with anhydrous sodium sulphate.

Table I

	Fraction	Yield	Colour
1	30°—120°	35.1 gr.	Very slightly coloured
2	120°—150°	32.1 „	Light yellow
3	Above 150° & loss	12.8 „	Dark brown

The second fraction, which was composed of the main portion of the acidic part, was noticed, on being kept exposed to the air, to change its colour from light yellow to brownish red, due to the oxidation of the constituents by the air. The fraction was treated with dimethyl sulphate and a caustic soda solution in order to convert the phenols and other acidic compounds into their methyl derivatives, and the methylated compounds were then fractionated under reduced pressure, and after distillation 17 times, the following 18 fractions were obtained, each fraction

being its content of carbon, of hydrogen and of the methoxyl group estimated, and also its density & index of refraction, determined with the following results:

Table II

	Fraction (7 mm.)	Yield	n_D^{25}	d_4^{25}
1	40°—50°	0.9	1.4534	0.65781
2	50°—59.6°	3.6	1.4623	0.67705
3	59.6°—65°	2.1	1.4650	0.68461
4	65°—70°	3.1	1.4668	0.68521
5	70°—74.5°	5.3	1.4698	0.69220
6	74.5°—80°	4.8	1.4723	0.69385
7	80°—84°	2.8	1.4740	—
8	84°—89°	2.7	1.4740	0.68874
9	89°—94°	2.6	1.4741	0.68673
10	94°—99°	2.9	1.4753	0.68521
11	99°—104°	2.4	1.4772	0.68825
12	104°—110°	1.9	1.4790	0.69160
13	110°—120°	2.8	1.4760	0.68386
14	120°—130°	3.0	1.4683	0.66568
15	130°—141°	2.4	1.4641	0.65690
16	141°—151°	1.9	1.4643	0.65281
17	151°—162°	1.2	1.4638	0.56175
18	162°—167°	0.6	1.4719	0.66901
19	Above 167°	1.2	—	—

Each fraction was a colourless light oil, insoluble in water and alkali, and soluble in organic solvents.

They gave no phenol test and no colour is ation with ferric chloride.

The weight-temperature-curve drawn from the results of the fractional distillation, indicates clearly that there exists at least one compound of an ethereal nature, which would occur as the main portion of the fifth fraction and having a molecular formula $C_{11}H_{18}O$ or $C_{10}H_{15}OCH_3$ since the experimental results of the analysis C=79.7; H=10.7; O=9.6;

Table III

	C	H	O	CH_3O
1	80.7	11.2	8.1	4.0
2	79.1	10.6	10.3	8.1
3	77.8	10.5	10.7	10.1
4	78.5	10.5	11.0	11.1
5	79.7	10.7	9.6	11.8
6	79.3	10.7	10.0	11.5
7	—	—	—	9.0
8	81.9	11.0	7.1	8.0
9	82.7	11.0	6.3	7.4
10	81.9	11.2	6.9	8.5
11	81.9	11.1	7.0	6.4
12	81.6	11.2	7.2	8.4
13	81.3	11.5	7.2	3.1
14	83.3	12.2	4.5	1.6
15	84.5	12.7	2.8	1.0
16	84.7	13.0	2.3	
17	85.3	13.0	1.7	

Fig. 4

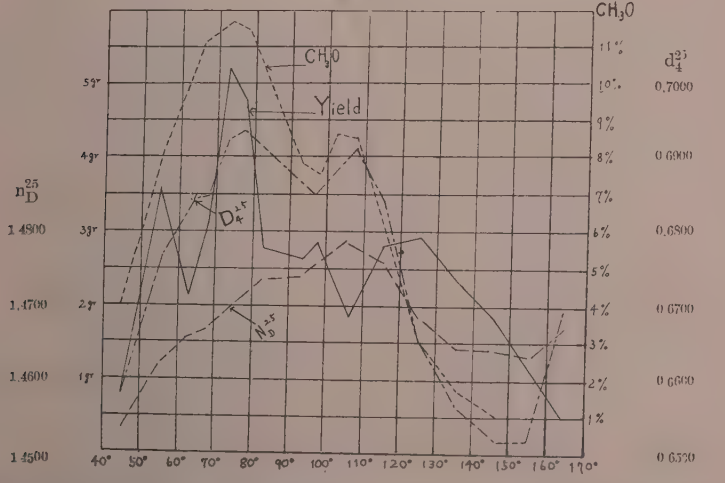

CH_3O=11.8 and the measurement of the physical constants confirm the above assumption as being correct.

Biochemical Studies on Pityrol, V.
Basic Constituents of Pityrol

By

Shigekiyo Suzuki

(Received September 12, 1928)

Although the basic fraction is composed of the smallest part of the pityrol, the odour of the drug is principally due to its presence.

It was separated from the commercial pityrol by means of dilute sulphuric acid from neutral and acidic fractions, and was a dark brown viscous liquid of a peculiar odour somewhat reminiscent of the pyridine bases.

For purification, it was subjected to steam distillation, and the basic compounds separated as an oily substance in the distillate amounted to 460 grm., and 190 grm. of the soluble bases were extracted from the distillate with ether after the insoluble oil had been separated.

Both the soluble and insoluble bases ascertained by chemical reactions

Table I

	Soluble bases.		Insoluble bases.	
B. p.	(46°–150°) 15 mm.		(41°–160°) 14 mm.	
Yield	110 grm.		390 grm.	
Density	0.9750		0.9248	
n_D^{25}	1.491		1.494	
C	66.6		77.2	
H	8.7	84.7	9.6	95.4
N	9.4		8.6	

Primary amine		
aliphatic	−	−
aromatic	+	+
Secondary amine	+	+
Tertiary amine	+	+
Pyrrol	−	−

to be composed of primary, secondary and tertiary amines, and it is of interest to note that the basic fractions especially of the latter bases, but contain not a single trace of pyrrol.

Two fractions were treated with picric acid in order to isolate only the tertiary bases as picrate, and 77 grm. and 120 grm. of the picrates were obtained from the soluble and insoluble bases respectively and the picrate which were then treated with hydrochloric acid to convert the hydrochlorides. From the hydrochlorides free bases were isolated by means of caustic soda.

The yield of free bases from both fractions is shown in Table II with their physical constants.

Table II

	Fraction	Yield	d_4^{25}	n_D^{25}
Soluble bases	100°—170°	14.5 grm.	0.9184	1.502
	above 170°	3.6 „	—	1.504
Insoluble bases	140°—200°	26.0	0.9129	1.503
	above 200°	8.4	—	1.552

The basic compouud is a colourless light oil of pyridine-like odour, and on being left exposed to the air becomes dark yellowish due to oxidation by the air.

Each low boiling fraction was carefuly distilled under ordinary pressure, and the high boiling one distilled under reduced pressure many times and the physical constants of the fractions were studied with the following results:

To isolate the basic compounds which occurring in the distillates in a pure state, the hydrochlorides of each fraction were treated with mercuric chlorides to convert them into the double salt. By repeated crystallisation

Table III
Soluble Bases

		Fraction	Yield	n_D^{25}	d_4^{25}	Double salt of $HgCl_2$	
						Yield	M. p.
Lower	1	to 130°	1.6 grm.	1.453	0.9127	0.9 grm.	(151°)
	2	130°—140°	2.0 „	1.478	0.9155	0.5 „	147°
	3	140°—150°	2.8 „	1.483	0.9222	0.2 „	147°
	4	150°—160°	3.5 „	1.486	0.9507	1.5 0.4	127° 131°
	5	Residue	0.6 „	—	—		
Higher	1	to 70° 13mm.	1.1 grm.	1.492	0.9285	No definite double salt of $HgCl_2$ and picric acid.	
	2	70°—80°	0.8	1.498	0.9393		
	3	80°—90°	1.1	1.500	0.9530		
	4	Residue	0.31	—	—		

Table IV
Insoluble Bases

		Fraction	Yield	n_D^{25}	d_4^{25}	Double salt of $HgCl_2$	
						Yield	M. p.
Lower	1	115°—130°	0.8 grm.	1.466	0.9703	0.3 grm.	151°
	2	130°—145°	2.1 „	1.483	0.9297	0.6 „ 0.5 „	154° 116°
	3	150°—157°	3.7 „	1.483	0.9689		
	4	157°—164°	3.4 „	1.485	0.9343	1.6 0.07 0.5 0.4 0.1 0.8	116° 163° 166° 127° 131° 188°
	5	164°—166°	1.0 „	1.485	0.9434	—	—
	6	166°—176°	2.6 „	1.488	0.9343	0.5 0.1	163° 127°
	7	Residue	8.4 „	—	—	—	—
Higher	1	70°—80° (13 mm.)	1.2 „	1.495	0.9962	0.1	162°*
	2	80°—90°	0.3 „	1.500	0.9974	0.05	162*
	3	90°—100°	0.7 „	1.517	0.9986	0.3	200°*
	4	100°—117°	2.1 „	1.549	1.0428	0.4	200°*
	5	Residue	—	—	—	—	picrate

from the aqueous solution, pure salts were isolated which show a definite melting point, and the results are shown in the table. The basic compounds which are difficult to isolate in a pure state by the aid of the double salt of mercuric chloride, in forming an oily salt, were accordingly converted into a picrate in an alcoholic solution after the free base was isolated from the hydrochlorides. We, however, noticed that some of the basic compounds occurring in the pityrol were difficult to isolate in a crystalline form either by means of the double salt of mercuric chloride or by means of a picrate.

The basic compounds which occur in the soluble basic fraction and form no crystalline picrates, were separated from crystals and set in a free state by means of caustic soda.

The yield of the free base was 21 grm., & it boils at 140°–230°, and shows the constants

$$n_D^{25} = 1.4989\,; \quad d_4^{25} = 0.9403$$

It was fractionated 3 times:

Table V

	Fraction	Yield	n_D^{25}	d_4^{25}
1	to 155°	1.8 grm.	1.5050	0.9031
2	155°–165°	2.6 „	1.5053	0.9158
3	165°–175°	2.9 „	1.5060	0.9256
4	175°–190°	2.0 „	1.5070	0.9419
5	190°–200°	2.4 „	1.5120	0.9550
6	Residue	1.7 „	—	—

The fraction was again treated to convert it into the double salt of mercuric chloride, and the salts isolated in a pure state by repeated crystallization were as follows:

Table VI

	Fraction	Double salt of $HgCl_2$	
		Yield	M.p.
1	to 155°	1.4	167°
2	155°–165°	8.0	157°
3	165°–175°	9.6	154°

By repeated crystallisation of these salts from their aqueous solution, they were found to be composed of the same substance which melts at 188°, and thus 2 : 6-dimethyl pyridine was confirmed to be composed mostly of these fractions.

The basic compounds which occur in the insoluble fraction to form an oily compound with picric acid, were regenerated into the free base by the usual method and distilled.

The fraction has a B.p. of 150°–270°, and its constants showed $d_4^{25}=0.9452$; $n_D^{25}=1.5170$, and it weighed 107 grm.

It contains much of the tertiary bases and some quantity of the secondary & primary bases, and accordingly it was fractionated under ordinary pressure 5 times with the following results.

Table VII

	Fraction	Yield	n_D^{25}	$d_4^{25°}$
1	145°–160°	8.1 grm.	1.4890	0.9245
2	160°–165°	4.8 „	1.4891	0.9263
3	165°–170°	5.0 „	1.4893	0.9275
4	170°–175°	5.8 „	1.4914	0.9307
5	175°–180°	7.9 „	1.4925	0.9410
6	180°–190°	5.6 „	1.4943	0.9551
7	192°–200°	7.7 „	1.5010	0.9532
8	200°–210°	6.5 „	1.5085	0.9661
9	210°–220°	5.3 „	1.5200	0.9909
10	220°–230°	1.6 „	1.5400	1.0059
11	230°–255°	5.9 „	1.5520	1.0251

To isolate the basic compounds in a pure state, the fractions were treated in their hydrochlorides with mercuric chloride, and the double salt of mercuric chloride separated in a solid form was purified by recrystallisation from the aqueous solution and the following pure salts were obtained as shown in Table VIII from the corresponding fraction.

Some of the fractions which hardly yielded to the crystalline double salt of mercuric chloride, were tried with picric acid to convert picrate as indicated in Table VIII.

From the first to the fourth fraction, their hydrochlorides form a

Table VIII

	Fraction	Double salt of $HgCl_2$	
		Yield	M.p.
1	145°–160°	8 grm. 3 „ 0.4 0.2 0.4	127° 154° 147° 110° 151°
2	160°–165°	3 grm. 0.2 „ 0.1 0.5	116° 191° 110° 112°
3	165°–170°	0.3 0.5	127° 112°
4	170°–175°	0.3 1.2	154° 106°*
5	175°–180°	0.2 0.1	157° 106°*
6	180°–190°	0.6	130 ⊕
7	192°–200°	—	—
8	200°–210°	—	—
9	210°–220°	0.2	200°*
10	220°–230°	0.3	200°*
11	230°–255°	0.5	200°*

definite double salt with mercuric chloride, and others which do not yield a definite compound in this manner, were transformed into their picrate in an alcohol solution.

The sixth fraction which seems from its physical constants to be composed of aniline, was identified to be so by transforming it into benzene azo-β-naphthol.

2-Methyl Pyridine

A basic substance which occurs in the low boiling fraction with a B.p. of 150°–160°, yields its double salt of mercuric chloride with a M.p. of 151° or 154°, shown in Tables III, IV, & VIII.

The double salt was analysed and the results for carbon, hydrogen & nitrogen all agree with the theoretical values for 2-methyl pyridine.

* Picrate.

⊕ benzene azo-β-naphthol.

Salt, m.p. 154°	CO_2	H_2O	Found		Calc for $C_6H_7NHCl_2HgCl_2$	
			C.	H.	C.	H.
12.755 mg	5.005 mg	1.419 mg	10.70	1.24	10.71	1.05
Salt, m.p. 151°						
15.048 mg	6.004 „	1.490 „	10.88	1.10	10.71	1.05
14.002 „	5.580 „	1.488 „	10.87	1.18	11	„

Salt, m.p. 154°	N (c.c.)	Found N.	Calc N.
19.605 mg.	0.37 (20°, 758 mm,)	2.09	2.08
24.747 „	0.46 (19°, 758 „)	2.08	—
Salt, m.p. 151°			
13.694 mg	0.25 (18°, 766 mm.)	2.07	—
14.243 „	0.25 (17°, 766.5 „)	2.00	

3-Methyl Pyridine

The double salt of the base with mercuric chloride, showing a m.p. of 147°–146°, in Tables III, and VIII was analysed with the following results :

Salt	N (c.c)	t.	p.	Calc for $C_6H_7NHCl_2HgCl_2$			Found		
				C	H	N	C	H	N
15.118 mg	0.30	25.5	757	10.71	1.05	2.08	10.31	1.17	2.14
16.238 „	0.32	23	758	—	—	—	—	—	2.16
13.162 „	4.976 mg CO_2 1.386 mg H_2O								

2 : 6-Dimethyl Pyridine

The double salt formed from a base with mercuric chloride, which occurs in the fractions having B.p. of 157°–164° in Table IV, and B.p. of 160°–165° in Table VIII, was found to melt at 188° & 191° respectively. The two salts were noticed to be the same substance because there was no indication of any lowering of the m.p. of the mixed salts also by analysis.

Salt, m.p. 188°	N (c.c)	Found	Theory for $C_7H_9NHClHgCl_2H_2O$.
13.801 mg	0.41 (21°, 758 mm.)	3.36	3.24
12.103 „	0.36 (22° 758, „)	3.34	„

CO_2		H_2O	C		H	
			found	theory	found	theory
11.803 mg	8.558 mg	2.704 mg	19.77	19.44	2.54	2.10
13.273 „	9.632 „	2.880 „	19.79	„	2.41	„

Salt, m.p. 191°	CO_2	H_2O	C	H
13.526 mg	9.515 mg	2.889 mg	19.18	2.37
12.303 „	8.906 „	2.448 „	19.74	2.25

	N (c.c)	Found	Theory for $C_7H_9NHClHgCl_2H_2O$
11.384	0.34, (22°, 757 mm)	3.28	3.24
11.295	0.33, (21°, 758 mm)	3.22	„

2 : 4 Dimethyl Pyridine

The base which occurs in the fractions having B.p. of 150°–160° in Table III, and B.p. of 157°–164° in Table IV; B.p. 145°–160°, and B.p. of 165°–170° in Table VIII, yields equally the double salt of mercuric chloride which shows the m.p. of 127°, was confirmed to be the salt of 2 : 4 dimethyl pyridine.

Salt		Found			Calc. for $C_7H_9NHCl2HgCl_2$		
		C	H	N	C	H	N
16.657 mg	0.31 c.c.N (20°, 758 mm.)	12.00	1.54	2.07	12.23	1.32	2.04
20.452 „	0.39 „ (22°, 758 „)	—	—	2.10			
12.272 „	5.415 mg CO_2, 1.699 mg H_2O						

2 : 4 : 6-Trimethyl Pyridine

The fractions with B.p. of 155°–175 in Table VI, B.p. of 170°–180°

in Table VIII, contain a base which yields the double salt with the mercuric chloride having a m.p. of 157° & 154°, and this was found by analysis to be the same salt derived from 2 : 4 : 6 trimethyl pyridine :

Salt, m.p. 154°	CO_2	H_2O	Found		Theory for $C_8H_{11}NHCl_2HgCl_2$	
			C	H	C	H
13.051 mg	6.700 mg	1.910 mg	14.00	1.63	13.68	1.58
12.104 „	6.205 „	1.809 „	13.98	1.66	—	—
Salt, m.p. 157°						
12.505 mg	6.197 mg	1.840 mg	13.52	1.63	13.68	1.58
13.211 „	6.584 „	1.953 „	13.59	1.64	—	—

Salt, m.p. 154°	N (c.c.)	N	
		Found	Calc. for $C_8H_{11}NHCl_2HgCl_2$
17.969 mg	0.29 (18 , 766 mm).	1.83	2.00
17.265 „	0.30 (18°, 762 „)	1.95	„

Salt, m.p. 157°		Found	Calc. for $C_8H_{11}NHCl_2HgCl_2\frac{1}{2}H_2O$
24.114 mg	0.40 (22°, 752.5)	1.81	1.97
27.864 „	0.45, (23°, 752.5)	1.79	

Aniline

This was isolated from the fraction B.p. 180°–190° shown in Table VIII in the form of phenyl azo-β-naphthol, m.p. 130°, and was confirmed to be so by analysis :

Sample		N					
		Found			Calc. for $C_6H_5N_2C_{10}H_7OH$		
		C	H	N	C	H	N
2.502 mg	0 26 c.c.N (25°, 763 mm)	76.88	4.63	11.34	77.38	4.88	11.28
4.0075 „	0.40 „ (17°, 758 „)			11.24			
4.057 „	11.437 mg CO_2, 1.691 mg H_2O						

Quinoline

The occurrence of the base in the fraction. B.p. 240°–255°, in Table VIII, and also in the high fraction with a B.p. above 117°, 13 mm. in Table IV, was confirmed by isolating it as a salt of picrate, m.p. 200°.

Salt		N					
		Found			Calc. for $C_{15}H_{10}N_4O_7$		
		C	H	N	C	H	N
2.735 mg	0.40 c.c.N (21°, 749 mm)	50.10	3.14	16.0	50.26	2.81	15.64
3.458 „	0.59 „ (20°, 752 „)			15.93			
2.298 „	4.302 mg CO_2, 0.650 mg H_2O						

Dimethyl Pyridine (2.5 ?)

The fractions with B.p. 150°–164°, B.p. 166°–176°, in Table IV, and B.p. to 155°, in Table VI, were to supposed to contain dimethyl pyridine (2.5 ?) as a constituent from the analysis and melting-point determination of its double salt of mercuric chloride.

Salt, m.p. 163°–4°	CO_2	H_2O	Found			Theory for $C_7H_9NHCl_2HgCl_2$		
			C	H	N	C	H	N
15.159 mg	6.882 mg	1.818 mg	12.38	1.33	2.04	12.33	1.32	2.04
12.643 „	5.639 „	1.525 „	12.16	1.34	—			
22.561 „	0.42 c.c.N (24°, 762 mm)				2.04			
Salt, m.p. 167°								
12.477 mg	5.665 mg	1.478 mg	12.38	1.32	2.08	„	„	„
11.032 „	4.892 „	1.026 „	12.09	1.03	—			
23.105 „	0.43 c.c.N (24°, 762 mm)							

Dimlethy Pyridine

A base which yielded the double salt of mercuric chloride with a m.p. of 110°, and gave the analytical results of a dimethyl pyridine derivative, was found to occur in the fractions. B.p. 100°–117° at 13 mm.

in Table IV, B.p. 145°–160°, 160°–165° in Table VIII.

Salt	CO_2	H_2O	Found			Calc. for $C_7H_8NHCl\ 2HgCl_2$		
			C	H	N	C	H	N
12.632 mg	5.598 mg	1.592 mg	12.09	1.40	2.06	12.23	1.32	2.04
15.050 „	6.600 „	1.946 „	11.96	1.44	—			
12.681 „	0.24 c.c.N (23°, 756 mm)							

Dimethyl Pyridine

The double salt of a base occurs in the fraction with B.p. of 165°–170° in Table VIII, melts at 112° agrees in analytical results with these of dimethyl pyridine. Although the crystalline form of the salt is similer to that of the 2 : 5 dimethyl pyridine mentioned above, a mixture of two crystals above a lowering in the melting-point.

Salt	CO_2	H_2O	Found		
			C	H	N
12.243 mg	5.652 mg	1.856 mg	12.59	1.68	2.06
13.241 „	6.020 „	1.713 „	12.40	1.50	—
13.512 „	0.25 c.c.N (23°, 756 mm)				

A Pyridine Derivative

The fractions having B.p. of 130°–145° in Table IV, and B.p. of 160°–165° in Table VIII, contain a base which forms a double salt of mercuric chloride of m.p. 116°, and gave the following analytical results of the salt, which agree fairly well with those of the pyridine salt, $C_5H_5NHCl.\ 2HgCl_2$.

Salt	CO_2	H_2O	C	H	N
12.888 mg	4.422 mg	1.173 mg	9.35	1.01	2.21
13.653 „	4.730 „	1.278 „	9.45	1.04	2.10
17.942 „	0.35 c.c.N (20°, 756.5 mm)				
22.238 „	0.41 „ (19°, 758 „)				

Tetramethyl Pyridine (?)

The fraction B.p. 170°–175°, B.p. 175°–180° in Table VIII, contains a base which gave a picrate of m.p. 106°. The analytical results of the picrate were as follows:

Salt	CO_2	H_2O	C	H
4.987 mg	7.232 mg	1.603 mg	39.55	3.57
4.402 „	6.410 „	1.320 „	39.71	3.33

A Base

The mother liquor separated from the crystals of quinoline picrate, yielded on standing for a while in a dark cold place fine crystals with a m.p. of 180° with decomposition, which on analysis gave the following results:

Sample	CO_2	H_2O	C	H
3.445 mg	5.920 mg	1.113 mg	46.87	3.59
3.212 „	5.553 „	1.120 „	47.14	3.49

The chemical nature of the base is awaiting further research which could not be attempted at this present owing to the scantiness of the sample.

Biochemical Studies on Pityrol, VI. Distillation of Palmitic Acid

By

Seiichi Shoyama

(Received September 12, 1928)

I. PREPARATION OF PALMITIC ACID

Palmitic acid, one of the chief constituents of fatty acids occurs in rice oil, which is easily obtained and in a pure state from Haze tallow. According to Dr. Tsujimoto,[1] the fatty acids of Haze tallow are composed of 84 % palmitic acid, 14 % oleic acid and 2 % Japanic acid, and the tallow was regarded by the writer as a good source in Japan, for the preparation in a pure state, of palmitic acid. The raw material which showed the constants, was saponified with a caustic soda solution, and the mixture of sodium salts of the fatty acids separated from the glycerine solution was treated with sulphuric acid. The free fatty acids-mixture was subjected to distillation under 15 mm. pressure after being dehydrated by the melting process, and the fraction B.p. 215°–220° was collected for palmitic acid which shows the following constants:

	Haze tallow	
M. p.	49°–53°	
Saponification number	227 –246	
Acid number	20 –28	
Ester numer	207 –218	
Iodine „	8.5–9	
	Palmitic Acid	
B. p.	(215°–220°)	15 mm.
M. p.	59°	
Iodine number		8.5

The yield was about 60 % of the theory. The purity of the acid was calculated from its iodine number to be about 90 %, assuming the presence of oleic acid to be an impurity.

II. DISTILLATION OF SODIUM PALMITATE

The sodium salt of the acid was prepared by neutralizing the acid with sodium carbonate, and purified by recrystallization from alcohol solution. The sodium content was determined to be Na=9.3% while the theory requires 8.7%.

25 gm. of dry sodium salt were distilled in Fischer's aluminium retort; it appears that gas is evolved up to about 380° and the distillation of tar commenced at 400°, the evolution of tar and gas rapidly increased at about 440° and is finished at about 540°. The yield of tar, coke and gas is 70%, 24% and 6% respectively.

The chemical composition of gas was determined with the following results:

CO	11.8 %
CO_2	12.2 „
C_2H_4	1.7 „
$C_nH_{2n+2}+H$	27.4 „

The coke which shows 27.6% of ignition loss, was assumed to be composed of sodium carbonate, containing Na=44.1, with some organic matter asan impurity.

2 kg. of the salt yielded by the operation 1370 grm. of tar which is a yellowish brown oil of green fluorescence and a burning odour, and was separated first by steam distillation into two fractions-volatile and non-volatile parts:

Volatile part	45 %
Non-valatile „	55 „

A. VOLATILE PART

The volatile part, having as constants, B.p. 80°–270°; d_4^{21}=0.748; iodine-no. 119, was assumed to be a mixture of saturated and unsaturated hydrocarbons of the ratio 60 and 40 by means of conc. sulphuric acid.[1]

1. Z. f. angew. Chem., **33**, 172 (1920).

1. Saturated hydrocarbons

45 grm. of the saturated hydrocarbons which remain without any reaction with conc. sulphuric acid, were fractionated carefuly on metallic sodium six times, and of each distillate the weight, specific gravity, and index of refraction were determined and the results are shown in Table I, II, III. Both the temperature-weight curve and the temperature-mol per cent curve of the fractions shown in Figs. 1 and 2, show the five maxima which indicate the presence of the hydrocarbons of the carbon atom C_8, C_9, C_{10}, C_{11}, C_{12}, and C_{13}. The assumption for the occurrence of the hydrocarbons in the distillates was confirmed by comparison of their physical constants and analytical results with those of the pure substances mentioned in the literature.

2. Unsaturated hydrocarbons

The unsaturated hydrocarbons which occur in the volatile oil were separated from the saturated ones by means of liquid sulphur dioxide according to the method suggested by Edeleanu[1], being divided by fractional

Table I

	Fraction	Yield	Δt^1	$\frac{\Delta W^2}{\Delta t}$
I	—122°	0.2	—	—
II	122°—126°	0.5	4°	0.125
III	126°—148°	3.0	24°	0.125
IV	148°—152°	1.5	4°	0.375
V	152°—171°	2.7	19°	0.142
VI	171°—175°	1.8	4°	0.450
VII	175°—193°	4.9	18°	0.272
VIII	193°—197°	1.7	4°	0.425
IX	197°—212°	3.5	15°	0.233
X	212°—216°	1.7	4°	0.425
XI	216°—232°	3.6	16°	0.225
XII	232°—236°	2.0	4°	0.500
XIII	236°—251°	1.9	15°	0.127
XIV	251°—255°	0.5	4°	0.125
XV	255°—270°	0.3	15°	0.020

1. Z. angew. Chem., **25**, 175 (1919).

Table II

Fraction		$d_4^{25°}$ (obs.)	$d_4^{t°}$	$n_D^{25°}$ (obs.)	n_D	C_n
I	—122°	0.6983		1.3890		
II	122°—126°	0.7075	$0.7185\left(\frac{0°}{4°}\right)$	1.3924	—	C_8
III	126°—148°	0.7150		1.3962		
IV	148°—152°	0.7207	$0.733\left(\frac{0°}{4°}\right)$	1.3998	—	C_9
V	152°—171°	0.7283		1.4024		
VI	171°—175°	0.7333	$0.7303\left(\frac{20°}{4°}\right)$	1.4062	*1.4136	C_{10}
VII	175°—193°	0.7398		1.4100		
VIII	193°—197°	0.7462	$0.7411\left(\frac{20°}{4°}\right)$	1.4132	1.4158	C_{11}
IX	197°—212°	0.7510		1.4152		
X	212°—216°	0.7555	$0.7511\left(\frac{20°}{4°}\right)$	1.4181	1.4209	C_{12}
XI	216°—232°	0.7589		1.4204		
XII	232°—236°	0.7660	$0.7571\left(\frac{20°}{4°}\right)$	1.4227	—	C_{13}
XIII	236°—251°	0.7707		1.4251		
XIV	251°—255°	0.7817	$0.7645\left(\frac{20°}{4°}\right)$	1.4315	*1.4358	C_{14}
XV	255°—270°	0.7965				

Table III

	Found		Calc.		C_n
	C%	H%	C%	H%	
II	84.11	15.91	84.2	15.8	C_8
IV	84.38	15.39	84.4	15.6	C_9
VI	84.42	14.87	84.5	15.5	C_{10}
VIII	84.33	15.21	84.6	15.4	C_{11}
X	84.35	15.28	84.7	15.3	C_{12}
XII	84.44	14.87	84.8	15.2	C_{13}
XIV	84.73	14.43	84.8	15.2	C_{14}

Table IV

	Fraction	Yield	I. V.		C_n
			obs.	calc.	
I	70°—100°	0.5	—		C_6
II	100°—120°	0.7	166.1	259.2	C_7
III	120°—140°	1.4	167.3	226.8	C_8
IV	140°—160°	1.7	145.6	201.6	C_9
V	160°—180°	2.5	163.1	181.4	C_{10}
VI	180°—200°	2.4	131.6	164.9	C_{11}
VII	200°—220°	2.1	126.1	151.2	C_{12}
VIII	220°—240°	2.0	109.9	139.6	C_{13}

Table V

	Fraction	$d_{4°}^{25°}$ (obs.)	$d_{4°}^{t°}$ (Beilstein)	$n_D^{25°}$	$n_D^{t°}$	C_n
I	70°—100°	—	$0.683\left(\frac{20°}{4°}\right)$	1.4022	—	C_6
II	100°—120°	0.736	$0.699\left(\frac{15°}{4°}\right)$	1.3958	—	C_7
III	120°—140°	0.737	$0.723\left(\frac{0°}{4°}\right)$	1.3966	—	C_8
IV	140°—160°	0.751	$0.743\left(\frac{20°}{4°}\right)$	1.4023	* 1.4286	C_9
V	160°—180°	0.762	$0.763\left(\frac{0°}{4°}\right)$	1.4090	* 1.4301	C_{10}
VI	180°—200°	0.773	$0.773\left(\frac{15°}{15°}\right)$	1.4147	* 1.4219 1.4376	C_{11}
VII	200°—220°	0.779	$0.773\left(\frac{0°}{4°}\right)$	1.4193	* 1.4212 1.4231	C_{12}
VIII	220°—240°	0.785	$0.844\left(\frac{0°}{4°}\right)$	1.4215	* 1.4488	C_{13}

fractions 5 times into 8 parts. The occurrence of the hydrocarbons of the carbon atoms C_7, C_8, C_9, C_{10}, O_{11}, C_{12}, C_{13}, was indicated from the analytical results and the determination of physical constants of the fractions as will be seen in Table IV, V, VI. and figure. I. (dotted line)

Table VI

	Fraction	Found		Calc.		C_n
		C%	H%	C%	H%	
I	70°—100°	—	—	85.7	14.3	C_6
II	100°—120°	85.41	13.97	85.7	14.3	C_7
III	120°—140°	85.22	13.91	85.7	14.3	C_8
IV	140°—160°	85.76	13.92	85.7	14.3	C_9
V	160°—180°	84.87	13.86	85.7	14.3	C_{10}
VI	180°—200°	85.12	13.88	85.7	14.3	C_{11}
VII	200°—220°	84.42	13.71	85.7	14.3	C_{12}
VIII	220°—240°	84.61	13.99	85.7	14.3	C_{13}

Fig. 1

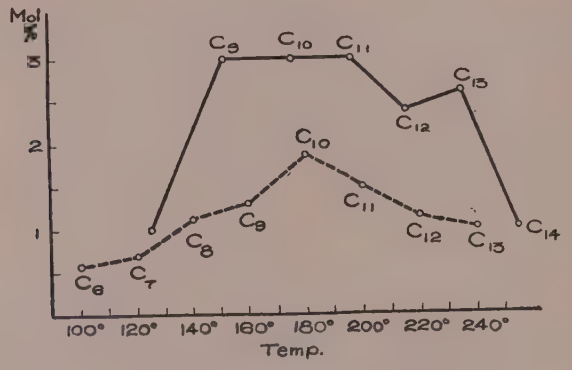

B. NON-VOLATILE PART

1. Palmitone, $(C_{15}H_{31})_2CO$

The occurrence of this ketone in the non-volatile part of the tar was previously assumed from the experiment which was carried out by Kraft,[1] and 20 grm. of the ketone were actually isolated from 270 grm. of the tar by treating with ether, and the ketone was confirmed by converting it into its oxime of m.p. 58°.[2]

1. Ber. D. Chem. Ges., **15**, 1711 (1882).
2. Kipping: J. Chem. Soc., **57**, 985 (1890).

2. Hydrocarbons

The oily part separated from the ketone, which showed by its iodine number 69 about 85% of unsaturated hydrocarbons, was fractionated under 10–12 mm. pressure.

150 grm. of the non-volatile oil free from the ketone, were divided into 18 fractions by repeating fractional distillation fives times which were confirmed as composed of hydrocarbons by determining the physical constants and chemical properties and also by analysis of the fractions. (Table VII, VIII, IX.) The proportion of saturated and unsaturated hydrocarbons in the non-volatile oil was estimated by means of iodine number of the oil, and the results are shown in Table X. Among these hydrocarbons, unsaturated compouds of the carbon atom C_{15}, C_{19}, C_{20} and C_{30} as will be seen in Table X, composed the main part of the oil and the chief saturated hydrocarbons are $C_{14}H_{30}$, $C_{18}H_{38}$ and $C_{20}H_{42}$.

Table VII

	Fraction (10—12mm.)	Yield	I. V. (obs.)	I. V. (calc.)	C_n
I	—120°	12.6	94.4	139.6	C_{13}
II	120°—130°	11.5	87.4	129.6	C_{14}
III	130°—140°	27.1	114.8	121.0	C_{15}
IV	140°—150°	7.9	111.0	113.4	C_{16}
V	150°—160°	5.5	150.8	106.7	C_{17}
VI	160°—170°	5.1	18.8	100.9	C_{18}
VII	170°—180°	6.7	59.0	96.2	C_{19}
VIII	180°—190°	10.8	42.8	90.7	C_{20}
IX	190°—200°	5.2	46.6	85.8	C_{21}
X	200°—210°	4.0	61.4	82.4	C_{22}
XI	210°—220°	4.5	58.2	78.8	C_{23}
XII	220°—230°	3.7	59.0	75.6	C_{24}
XIII	230°—240°	3.8	62.0	72.6	C_{25}
XIV	240°—250°	2.9	71.0	69.8	C_{26}
XV	250°—260°	2.9	69.2	67.2	C_{27}
XVI	260°—270°	1.2	57.5	64.8	C_{28}
XVII	270°—280°	0.7	59.0	62.6	C_{29}
XVIII	280°—290°	2.0	61.4	60.5	C_{30}
XIX	290°—300°	3.2	53.4	58.5	C_{31}

Table VIII

	Fraction (10—12mm.)	$d_4^{25°}$ (obs.)	$d_4^{t°}$ (Beilstein)	$n_D^{25°}$	C_n
I	—120°	0.7837	{0.7977(20°) 0.8445(0°)}	1.4203	C_{13}
II	120°—130°	0.7825	0.7638(30°)	1.4210	C_{14}
III	130°—140°	0.7853	—	1.4226	C_{15}
IV	140°—150°	0.7974	0.7842(0°)	1.4288	C_{16}
V	150°—160°	0.8118	0.7977(10°)	1.4345	C_{17}
VI	160°—170°	0.8033	0.7881(22°)	—	C_{18}
VII	170°—180°	0.8110	—	—	C_{19}
VIII	180°—190°	0.8166	0.7810(0°)	—	C_{20}
IX	190°—200°	0.8224	—	—	C_{21}
X	200°—210°	0.8307	—	—	C_{22}
XI	210°—220°	0.8347	—	—	C_{23}
XII	220°—230°	0.8372	—	—	C_{24}
XIII	230°—240°	0.8412	—	—	C_{25}
XIV	240°—250°	0.8433	—	—	C_{26}
XV	250°—260°	0.8458	—	—	C_{27}
XVI	260°—270°	0.8479	—	—	C_{28}
XVII	270°—280°	0.8490	—	—	C_{29}
XVIII	280°—290°	0.8500	—	—	C_{30}
XIX	290°—300°	0.8545	—	—	C_{31}

Table IX

	C%	H%	O% (by diff)
I	83.85	13.88	2.27
II	84.30	13.97	1.73
III	84.66	13.99	1.35
IV	83.20	13.33	3.47
V	82.68	13.53	3.79
VI	81.17	13.33	3.50
VII	79.09	12.80	8.11
VIII	81.89	13.54	4.57
IX	81.64	12.55	5.81
X	82.57	13.32	4.11
XI	82.52	13.22	4.26
XII	82.50	12.95	4.55
XIII	80.69	12.73	6.58
XIV	82.77	13.00	4.23
XV	83.22	13.25	3.53
XVI	83.82	12.83	3.35
XVII	82.88	12.91	4.21
XVIII	81.43	12.98	5.59
XIX	82.51	12.63	4.86

Table X

	Olefine			Paraffine	
		Yield		Yield	
	C_n	(gr.)	Mol%	(gr.)	Mol%
I	C_{13}	8.5	4.6	4.1	2.2
II	C_{14}	7.7	3.9	3.8	1.9
III	C_{15}	25.7	12.2	1.4	0.6
IV	C_{16}	7.6	3.4	0.3	0.1
V	C_{17}	5.5	2.3	0.0	0.0
VI	C_{18}	0.9	0.4	4.2	1.6
VII	C_{19}	4.0	1.5	2.7	1.0
VIII	C_{20}	4.4	1.5	6.4	2.3
IX	C_{21}	2.8	0.9	2.4	0.9
X	C_{22}	2.8	0.9	1.2	0.4
XI	C_{23}	3.2	1.0	1.3	0.4
XII	C_{24}	2.9	0.8	0.8	0.2
XIII	C_{25}	3.2	0.9	0.6	0.1
XIV	C_{26}	2.9	0.8	0.0	0.0
XV	C_{27}	2.9	0.7	0.0	0.0
XVI	C_{28}	1.0	0.2	0.2	0.0
XVII	C_{29}	0.6	0.1	0.1	0.0
XVIII	C_{30}	5.2	1.2	0.0	0.0

Fig 2

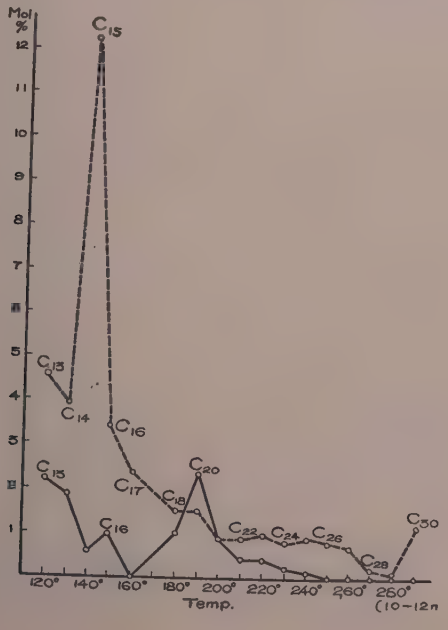

In conclusion, sodium palmitate, when distilled in Fischer's aluminum retort produces 70% of a theory-yield of tar which is composed of the following constituents.

Volatile oil	acidic oil	trace
	saturated hydrocarbons	25%
	unsaturated „	23%
Non-volatile oil	palmitone	3%
	saturated hydrocarbons	8 „
	unsaturated „	47 „

Biochemical Studies on Pityrol, VII
Distillation of Oleic Acid

By

Hiroshi Ogata

(Received September 12, 1928)

The Tsubaki oil (*Thea Japonica Nois*) was regarded by the writer as a good source in Japan for obtaining oleic acid in a pure state, since the oil, according to the investigation by I. Misumi[1], contains 90% or more of oleic acid in its fatty acids.

The oil which was used in this experiment was obtained by the courtesy of Dr. Hiraizumi from seeds grown in Hayaki, Nagasaki ken, and shows the following constants:

$d_4^{25}=0.9093$; $n_D^{25}=1.4626$; acid number 3.9; saponification number 187.7; iodine number 81.5.

A convenient and reliable procedure for the preparation of pure oleic acid[2] from Tsubaki oil was proposed after many trials by the writer as follows:

The crude sodium salt of oleic acid prepared from the oil by the usual method was converted into the lead salt which was extracted with ether and then decomposed by means of sulphuric acid into the free oleic acid.

In the purification of the crude oleic acid, it was subjected to distillation under 12–18 mm. pressure after being dried with anhydrous sodium sulphate in its ether solution, and 1.8 kg. of pure oleic acid of the following constants were obtained from 6 kg. of the Tsubaki oil; one operation is enough for obtaining the acid in such a state of purity.

---

1. J. Chem. Ind., Japan, **9**, 1 (1906).
2. Refer L. Ubbelohde: Handbuch d. Öle u. Fette 1. 55. & F. Ulzer & J. Klimont: Chemie d. Fette. 95 (1906); Monat. f. Chem., **46**, 337 (1926).

$d_4^{25}=0.8863$; $n_D^{25}=1.4535$; m.p.$=9.2°$;

solid. p.$=4.5°$; b.p.$=235°$, 18 mm., light yellow colour. iodine value 90.6.

Sodium oleate was prepared from the interaction of the acid and sodium ethylate, and purified from the alcohol solution[1].

It gave Na$=7.3$ on analysis, which agrees quite well with the theoretical value of 7.5 for $C_{15}H_{33}O_2$ Na.

When the salt was heated in Fischer's aluminium retort, gas began to evolve at 390°, tar distils at 440° and the reaction was completed at 550°. The yield of gas, tar and coke was shown in the following table with the results by the distillation of sodium oleate under reduced pressure by Pictet & Potok[2] and also of the calcium salt under ordinary pressure by Kawai.[3]

	Pictet & Potok	Kawai	The writer
Tar	70%	63%	65%
Coke	24 „	28 „	17 „
Gas & loss	6 „	9 „	18 „

The tar which was obtained by the writer shows the following constants, $d_4^{25}=0.794$; $n_D^{25}=1.445$; iodine number 142., was divided by steam distillation into volatile and non-volatile parts.

	%	B. p.	I. V.	d_4^{25}	n_D^{25}
Volatile part	47	41°—266°	158	0.766	1.427
Non-volatile „	53	—	105	0.828	1.457

The content of the unsaturated compounds in the fractions was estimated by determination of the volumetric loss to sulphuric acid of 84.5% strength[4] to be 80%, but the oil which remained unaffected by the sulphuric acid-treatment, still showed the iodine number 87 due to the presence of some unsaturated compounds in it. The liquid sulphur dioxide method proposed by Edeleanu for the determination of unsaturated compounds was tried in the hope that the determination would be an

1. L. L. Biscumshaw: J. Chem. Soc., **123**, 91 (1923).
2. A. Pictet & G. Potok: Hel. Chim. Acta, **2**, 501 (1919).
3. S. Kawai: J. Chem. Soc. Ind. Japan, **28**, 52 (1925).
4. E. Leslie: Motor Fuels, 595 (1923).

accurate measure of the unsaturation. The result indicating 92 % of unsaturation is closely in agreement with that of the sulphuric acid method.

VOLATILE PART

This was distilled under ordinary pressure and divided into the following fractions:

	Fraction	Yield	Colour
1	to 90°	8.7%	light yellow
2	90°—150°	41.0%	yellow
3	150°—200°	32.8%	deep yellow
4	200°—250°	14.8%	greenish yellow
5	250°—	2.6%	green

By repeated fractional distillation four times, the volatile part was divided into the following 18 fractions, among which the fractions boiling above 200°, were distilled under 15 mm. pressure. The yield, density, index of refraction and iodine numbers of each fraction were determined and the results are shown in Table I, with the analytical results of carbon and hydrogen.

Fig 1

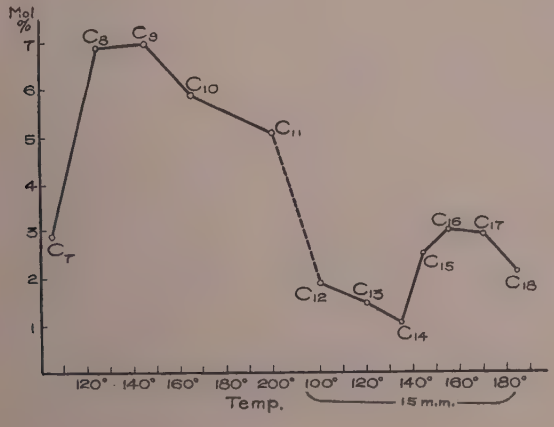

Table I

	Volatile Part								
	Fraction	Yield	d_4^{25}	n_D^{25}	I. V.		C	H	C_nH_m
					obs.	calc.			
I	75°–83°	4.4gr.	0.7915	1.4315	83.03		83.82%	10.46%	
II	83°–95°	6.3	0.7810	1.4233	101.60		84.83	10.93	
III	95°–105	1.8	0.7615	1.4124	115.70	259·1	83.78	11.86	C_7H_{14}
IV	105°–118°	0.6	0.7561	1.4075	180.27		—	—	
V	118°–125°	4.1	0.7546	1.4045	137.70	226.8	85.66	13.39	C_8H_{16}
VI	125°–135°	3.5	0.7546	1.4046			84.83	13.42	
VII	135°–144°	1.7	0.7547	1.4057	131.50	201.6	84.92	13.51	C_9H_{18}
VIII	144°–158°	7.0	0.7656	1.4104	146.36		83.67	13.43	
IX	158°–165°	2.6	0.7717	1.4135	147.20	180.15	84.59	13.80	$C_{10}H_{20}$
X	165° 175°	4.8	0.7813	1.4183	126.60	180.15	—	—	$C_{10}H_{20}$
XI	175°–185°	5.6	0.7876	1.4232	160.48		83.36	13.78	
XII	185°–198°	7.9	0.7952	1.4265	155.80	164.93	84.88	13.45	$C_{11}H_{22}$
XIII	95°–100°	2.7	0.8047	1.4334	138.10	151.19	85.51	13.30	$C_{12}H_{24}$
XIV	100°–110°	2.7	0.8140	1.4392	154.88		85·52	14.07	
XV	110°–120°	3.0	0.8271	1.4437	144.10	139.56	81.81	12.89	$C_{13}H_{26}$
XVI	125°–130°	1.8	0.8377	1.4460	126.01	129.59	83.93	12.78	$C_{14}H_{28}$
XVII	130°–150°	2.5	0.8389	1.4475	154.00	120.95	—	—	$C_{15}H_{30}$
XVIII	150°–156°	0.7	0.8430	1.4480	—	113.39	85.71	14.29	$C_{16}H_{32}$

Table II

	Non-volatile								
	Fraction (15mm.)	Yield	d_4^{25}	n_D^{25}	I. V.		C	H	C_nH_m
					obs.	calc.			
I	110°–125°	1.0gr.	0.8064	1.4315					
II	125°–133°	0.9	0.8125	1.4334	118.20	129.59	84.50	13.35	$C_{14}H_{28}$
III	133°–138°	0.2	0.8176	1.4343					
IV	138°–143°	1.9	0.8201	1.4365	131.28	120.95	81.96	11.66	$C_{15}H_{30}$
V	143°–152°	3.8	0.8208	1.4373	127.98				
VI	152°–157°	4.1	0.8225	1.4381	110.80	113 39	85.87	13.92	$C_{16}H_{32}$
VII	157°–170°	2.2	0.8267	1.4394	—	106.72			$C_{17}H_{34}$
VIII	170°–178°	4.7	0.8315	1.4425	150.55				
IX	178°–185°	3.1	0.8394	1.4450	126.56	100.79	95.76	13.95	$C_{11}H_{34}$
X	185°–200°	2.0		1.4492					
XI	200°–210°	0.8	0.8498	1.4519					
XII	210°–220°	1.4	0.8628	1.4585					

Non-Volatile Part

The tar separated from the volatile part by steam distillation was of a dark brown colour with a green fluorescence, and shows $d_4^{25} = 0.828$; $n_D^{25} = 1.457$; iodine value 105.

It contains about 10 % of sodium oleate which was carried out from the retort with the tar during the distillation.

The non-volatile tar separated from sodium oleate, was subjected to fractional distillation under 15 mm. pressure, and after three distillations, it was divided into the following 12 fractions which show the physical constants, iodine value and chemical composition of carbon and hydrogen.

The temperature-mol per cent curves of the results obtained from the volatile and non-volatile parts shown in Fig. 1 indicate the hydrocarbons of the carbon atoms C_8, C_9, C_{10}, C_{12}, C_{13}, C_{14}, C_{15}, C_{16}, C_{17} & C_{18} which occur in the tar.

The relative amount of the saturated and unsaturated hydrocarbons of the distillates was estimated by means of their iodine value.

The hydrocarbons of the olefine series of the molecular formulae C_8H_{16}, C_9H_{18}, $C_{15}H_{30}$, $C_{16}H_{32}$, $C_{17}H_{34}$ are the main constituents of the tar as the results indicate in the temperature mol per cent ratio curve shown in Fig I.

Biochemical Studies on Pityrol, VIII
Distillation of Sucrose

By

Yoshinori Hidaka

(Received September 12, 1928)

Sucrose purified by recrystallisation of commercial cane sugar, was found to melt at 170°–171° and showed $[\alpha]_D = 64°$.

30 grm. of the sugar were distilled at ordinary pressure in an iron retort of 500 c.c. capacity, the reaction began to take place vigorously at about 240°, and then ceased after 2 hours. The highest temperature of the retort during the reaction was about 610°. 100 grm. of the sample, thus, yield 25 grm. of tar and water liquor, 45 grm. of charcoal and 20 litres of gas.

The distillate, which contains tarry matter, was a dark reddish-brown acidic liquor of a density of 1.06, the colour on standing, changing gradually to a dark brown, forming a dark brown solid deposit at the bottom of the vessel.

The distillate separated from the brown deposit, was treated with ether for 5 hours to extract furfurals and some organic acids formed from the sugars by distillation, and distilling off the solvent, there was found an oily residue which consisted of acidic and neutral substances. The solid substance in the aqueous distillate, which was insoluble in ether was ascertained from its chemical nature to be humus. The percentage of these substances in the distillate was as follows:

Water	75
Neutral substance	4.5
Acidic substance	1.5
Humus	8.5

1. Neutral Substance

11.5 grm. of the neutral substance were subjected to fractional distillation under 7 mm. pressure, and the following fractions of the constants resulted:

	Fraction	Yield	d_4^{25}	n_D^{25}
1	34°–42°	0.6 grm.	1.1449	1.5188
2	42°–47°	0.1 „	—	1.5179
3	47°–65°	1.8 „	1.1219	1.5147
4	65°–140°	0.3 „	—	1.5118
5	140°–142°	0.6 „	1.2065	1.5366
6	Residue	4. „	—	—

A. Furfural.

The first fraction was confirmed to be composed of furfural by its analysis and also by its physical constants.

C=62.5; H=4.5, theory requires C=62.5; H=4.2 for $C_5H_4O_2$

B. Methyl Furfural.

The third fraction was analysed, and the results agree with the theoretical value for methylfurfural.

C=63.2; 65.8: H=5.2; 5.1: theory requires C=65.5; H=5.4 for $C_6H_6O_2$.

C. Oxymethyl Furfural.

The fifth fraction was assumed to consist mostly of oxymethyl furfural by analysis of the results.

C=59.7; 59.3; H=5.6; 5.7; theory C=57.1; H=4.8 for $C_6H_6O_3$.

2. Acidic Substance

The acidic substance consists of volatile and non-volatile acids and the former was found by its chemical properties to be formic acid and the latter laevulinic acid.

3. Humus Substance

The brown solid substance which occurs in the distillate and is insoluble in ether, was analysed with the following results

C=62.65; H=4.55.

4. Charcoal

The non volatile substance which remained in the retort was analysed with the following results :

C=70.45 ; 67.56 ; H=4.59 ; 4.92.

5. Quantitative Estimation of the Substances in the Distillate

The quantity of furfural and methyl furfural substance in the distillate was determined by means of phloroglucin, and the content of the oxy-methyl furfural was also determined in the non-volatile neutral substance.

The quantitative estimation of the formic acid and the laevulinic acid in the distillate was performed by determining the total volatile acids by titration with a dilute caustic soda solution and the results are as follows :

Oxymethyl furfural	1 %
Furfural	2.6 „
Methyl furfural	2.5 „
Formic acid \	3.1 „
Laevulinic acid \	0.4 „

The further researches on Pityrol are now being studies in Professor Matsumoto and my laboratories and the result will be communicated in a near future.

The writer (S.K.) wishes to express his thanks to Mr. Ichinose for the valuable material which has donated.

Aug. 3, 1928.

Laboratory of Bio- & Organic-Chemistry.

INDEX OF AUTHORS TO VOLUME XI

PAGE

Ando, G.—On the Reflective Power of Some Eutectic Alloys in Relation to their Micro-Structures 43

Ando, G.—The Quantitative Determination of the Degree of Tarnishing of a Metallic Surface by its Reflective Power 65

Fujita, S.—Biochemical Studies on Pityrol, II. Distillation of Rice Bran 497

Fujiwara, T.—Laue-Photograph taken with Convergent X-Rays 283

Fukushima, H.—The Arrangement of Micro-Crystals in the Banded "Supposed Aragonite (Arareishi)"... 223

Fukushima, H. (See **Yoshida, U., Fukushima, H. and Iso, M.**) 451

Furutani, N.—On the Measurements of the Vapour Pressures of Concentrated Aqueous Solutions of Potassium Iodide 149

Hidaka, Y.—Biochemical Studies on Pityrol, VIII. Distillation of Sucrose 549

Hirata, H.—On the Arrangements of the Micro-Crystals in Bismuth and Antimony deposited by Electrolysis 429

Horiuchi, R.—On the Transformation of Aliphatic Terpenes into Monocyclic Terpenes—A Synthesis of Menthol 171

Iso, M. (See **Yoshida, U., Fukushima, H. and Iso, M.**) 451

Kawai, H.—On the Brinell Hardness of the Ternary Alloys consisting of Copper, Zinc and Aluminium as an α-Solid Solution 137

Koidzumi, S.—The Electrolytic Oxidation of Alcohols, III. Electrolytic Oxidation of Benzylalcohol 383

Koidzumi, S.—The Electrolytic Oxidation of Alcohols, IV. Electrolytic Oxidation of Propylacohol in Alkaline Solutions... 391

Komatsu, S. and Kurata, M.—Studies on Catalytic Action, XXII. Catalytic Action of Reduced Copper on Unsaturated Hydrocarbons 163

Komatsu, S. and Matsunami, N.—On Kakishibu, IV. Constitution of Shibuol, III 205

Komatsu, S., Matsunami, N. and Kurata, M.—On Kakishibu, V. Methylation of Shibuol 211

Komatsu, S.—Biochemical Studies on Pityrol, I. Introduction to the Biochemistry of Pityrol... 481

Kurata, M. (See **Komatsu, S. and Kurata, M.**) 163

Kurata, M. (See **Komatsu, S., Matsunami, N. and Kurata, M.**) 211

Masumoto, B.—Biochemical Studies on Pityrol, IV. Acidic Constituents of Pityrol ... 517

Matsumoto, T.—Group-Theory of Sequences of Numbers 11

Matsumoto, T.—On Paradoxes and Definitions 367

Matsunami, N. (See **Kamatsu, S. and Matsunami, N.**) 205

Matsunami, N. (See **Komatsu, S., Matsunami, N. and Kurata, M.**) 211

Nakaseko, R.—Studies in Micro-Estimation of Metallic Elements, Part I. The Micro-Chemistry of Potassium Ferrocyanide 95

PAGE

Nakaseko, R.—Studies in Micro-Estimation of Metallic Elements, Part. II. The Micro-Detection of Iron with Dimethylglyoxime 113
Ogata, H.—Biochemical Studies on Pityrol, VII. Distillation of Oleic Acid 543
Sakami, S.—Biochemical Studies on Pityrol, III. Neutral Constituents of Pityrol ... 505
Sakao, T.—On the Destruction of the Single Crystal of Aluminium by the Process of Rolling... 279
Shima, G.—On the Electrolytic Reduction of Aldehydes, Part II. Metanitrobenzaldehyde 1
Shima, G.—On the Electrolytic Reduction of Aldehydes, Part III. Ortho and Para-Oxybenzaldehydes 407
Shima, G.—On the Electrolytic Reduction of Aldehydes, Part IV. Vanillin and Piperonal 419
Shoyama, S.—Biochemical Studies on Pityrol, VI. Distillation of Palmitic Acid ... 533
Suzuki, S.—Biochemical Studies on Pityrol, V. Basic Constituents of Pityrol 521
Takeyama, S.—A Method of Determining the Orientation of Crystal-Axes by X-Rays 469
Tanaka, K.—Bending of Aluminium-Crystals 199
Tanaka, K.—The Recrystallization of Aluminium 229
Tanaka, K.—The Orientation of Single-Crystals of Zinc 361
Terada, T.—"The Reversal-like Phenomena" of the Secondary and the Tertiary Discharge-Figures impressed on Photographic Plates 355
Tsuboi, S.—On the Fibrous Structure in Metals Deposited by the Difference of Electrolytic Solutional Pressures 271
Tsuboi, S.—The Arrangement of the Micro-Crystals in Compressed Magnesium and Aluminium Plates 375
Tsutsumi, J.—An Examination of the Micro-Crystals of Calcium Carbonate in Molluscan Shells by means of X-Rays, Part I 217
Tsutsumi, J. (See **Yoshida, U. and Tsutsumi, J.**) 267
Tsutsumi, J.—An Examination of the Micro-Crystals of Calcium Carbonate in Molluscan Shells by means of X-Rays, Part II 401
Watanabe, Y.—On some Functions defined by certain Infinite Products 311
Yamamoto, I.—The Influence of the Heliographic Activity upon the Solar Constant, with two Appendices 233
Yamamoto, I.—Some Notes on Solar Research 303
Yamamoto, T.—On the Arrangements of the Micro-Crystals in Zinc and Cadmium obtained by Sublimation 39
Yamashita, K.—On the Theory of Reverberation 119
Yoshida, U. and Tsutsumi, J.—A Peculiar Reversal of the Discharge-Figures on Photographic Plates 267
Yoshida, U., Fukushima, H. and Iso, M.—The Probability of Lightning Strokes ... 451

INDEX OF SUBJECTS TO VOLUME XI

PAGE

Acidic Constituents of Pityrol, Biochemical Studies on Pityrol, IV., (*Masumoto*) 517

Alcohols, The Electrolytic Oxidation of, III. Electrolytic Oxidation of Benzylalcohol (*Koidzumi*)... 383

Alcohols, The Electrolytic Oxidation of, IV. Electrolytic Oxidation of Propylalcohol in Alkaline Solutions (*Koidzumi*) 391

Aldehydes, On the Electrolytic Reduction of, Part II. Metanitrobenzaldelydes (*Shima*)... 1

Aldehydes, On the Electrolytic Reduction of, Part III. Ortho- and Para-Oxybenzaldehydes (*Shima*) 407

Aldehydes, On the Electrolytic Reduction of, Part IV. Vanillin and Piperonal (*Shima*) ... 419

Aliphatic Terpenes, On the Transformation of, into Monocyclic Terpenes—A Synthesis of Menthol (*Horiuchi*) 171

Alkaline Solutions, Electrolytic Oxidation of Alcohols, IV. Electrolytic Oxidation of Propylalcohol in, (*Koidzumi*) 391

α Solid Solution, On the Brinell Hardness of the Ternary Alloys consisting of Copper, Zinc and Aluminium as an, (*Kawai*) 137

Aluminium-Crystals, Bending of, (*Tanaka*) 109

Aluminium, The Recrystallization of, (*Tanaka*) 220

Aluminium, On the Destruction of the Single Crystal of, by the Process of Rolling (*Sakao*)... 279

Aluminium Plates, The Arrangement of the Micro-Crystals in Compressed Magnesium and, (*Tsuboi*) 375

Antimony, On the Arrangements of the Micro-Crystals in Bismuth and, deposited by Electrolysis (*Hirata*)... 429

Aqueous Solutions, On the Measurements of the Vapour Pressures of Concentrated, of Potassium Iodide (*Furutani*) 140

Aragonite (Araregishi), The Arrangement of Micro-Crystals in Banded Supposed, (*Fukushima*) 223

Basic Constituents of Pityrol, Biochemical Studies on Pityrol, V., (*Suzuki*) 521

Bending of Aluminium-Crystals (*Tanaka*)... 109

Benzylalcohol, The Electrolytic Oxidation of Alcohols, III. Electrolytic Oxidation of, (*Koidzumi*)... 383

Biochemical Studies on Pityrol, I. Introduction to the Biochemistry of Pityrol (*Komatsu*) ... 481

Biochemical Studies on Pityrol, II. Distillation of Rice Bran (*Fujita*) 497

Biochemical Studies on Pityrol, III. Neutral Constituents of Pityrol (*Sakami*) 505

Biochemical Studies on Pityrol, IV. Acidic Constituents of Pityrol (*Masumoto*) 517

Biochemical Studies on Pityrol, V. Basic Constituents of Pityrol, (*Suzuki*) 521

Biochemical Studies on Pityrol, VI. Distillation of Palmitic Acid (*Shoyama*) 533

Biochemical Studies on Pityrol, VII. Distillation of Oleic Acid, (*Ogata*) 543

Biochemical Studies on Pityrol, VIII. Distillation of Sucrose (*Hidaka*) 549

Bismuth and Antimony, On the Arrangements of the Micro-Crystals in, deposited by Electrolysis, (*Hirata*) 429

Brinell Hardness, On the, of the Ternary Alloys consisting of Copper, Zinc and Aluminium as an α-Solid Salution (*Kawai*) 137

PAGE

Cadmium, On the Arrangements of the Micro-Crystals in Zinc and, obtained by Sublimation (*Yamamoto*) ... 39

Calcium Carbonate, An Examination of the Micro-Crystals of, in Molluscan Shells, by means of X-Rays, Part I (*Tsutsumi*) ... 217

Calcium Carbonate, An Examination of the Micro-Crystals of, in Molluscan Shells by means of X-Rays, Part II (*Tsutsumi*) ... 401

Catalytic Action, Studies on, XXII. Catalytic Action of Reduced Copper on Unsaturated Hydrocarbons (*Komatsu and Kurata*) ... 163

Compressed Magnesium and Aluminium Plates, The Arrangement of the Micro-Crystals in, (*Tsuboi*) ... 375

Convergent X-Rays, Laue-Photograph taken with, (*Fujiwara*) ... 283

Crystal-Axes, A Method of Determining the Orientation of, by X-Rays (*Takeyama*) ... 469

Crystals of Zinc, The Orientation of Single, (*Tanaka*) ... 361

Definitions, On Paradoxes and, (*Matsumoto*) ... 367

Destruction of the Single Crystal of Aluminium by the Process of Rolling (*Sakao*)... ... 279

Dimethylglyoxime, Studies in Micro-Estimation of Metallic Elements, Part II. The Micro-Detection of Iron with, (*Nakaseko*)... ... 113

Discharge-Figures, A Peculiar Reversal of the, on Photographic Plates (*Yoshida and Tsutsumi*) ... 267

Discharge-Figures, The Reversal-like Phenomena of the Secondary and the Tertiary, impressed on Photographic Plates (*Terada*) ... 355

Electrolysis, On the Arrangements of the Micro-Crystals in Bismuth and Antimony deposited by, (*Hirata*) ... 429

Electrolylic Oxidation of Alcohols, III Electrolytic Oxidation of Benzylalcohol (*Koidzumi*) 383

Electrolytic Oxidation of Alcohols, IV. Electrolytic Oxidation of Propylalcohol in Alkaline Solutions (*Koidzumi*)... ... 391

Electrolytic Reduction, On the, of Aldehydes, Part II. Metanitrobenzaldehydes (*Shima*) ... 1

Electrolytic Reduction, On the, of Aldehydes, Part III. Ortho-and Para-Oxybenzaldehydes (*Shima*) ... 407

Electrolytic Reduction, On the, of Aldehydes, Part IV. Vanillin and Piperonal (*Shima*) 419

Electrolytic Solutional Pressures, On the Fibrous Structure in Metals Deposited by the Difference of, (*Tsuboi*) ... 271

Eutectic Alloys, On the Reflective Power of some, in Relation to their Micro-Structures (*Ando*) ... 43

Fibrous Structure, On the, in Metals Deposited by the Difference of Electrolytic Solutional Pressures (*Tsuboi*) ... 271

Functions, On some, defined by certain Infinite Products (*Watanabe*)... ... 311

Group-Theory of Sequences of Numbers (*Matsumoto*) ... 11

Heliographic Activity, the Influence of the, upon the Solar Constant, with two Appendices (*Yamamoto*) ... 233

Infinite Products, On some Functions defined by certain, (*Watanabe*) ... 311

Iron with Dimethylglyoxime, Studies in Micro-Estimation of Metallic Elements, Part II. The Micro-Detection of, (*Nakaseko*) ... 113

Kakishibu, IV. Constitution of Shibuol, III (*Komatsu and Matsunami*) ... 205

Kakishibu, V. Methylation of Shibuol (*Komatsu, Matsunami and Kurata*) ... 211

Laue-Photograph taken with Convergent X-Rays (*Fujiwara*) ... 283

Lightning Strokes, The Probability of, (*Yoshida, Fukushima and Iso*) ... 451

Magnesium and Aluminium Plates, The Arrangement of the Micro-Crystals in Compressed, (*Tsuboi*) ... 375

PAGE
Menthol, On the Transformation of Aliphatic Terpenes into Mono-Cyclic Terpenes—A Synthesis of, (*Horiuchi*) 171
Metallic Elements, Studies in Micro-Estimation of, Part I. The Micro-Chemistry of Potassium Ferrocyanide (*Nakaseko*) 95
Metallic Elements, Studies in Micro-Estimation of, Part II. The Micro-Detection of Iron with Dimethylglyoxime, (*Nakaseko*)... 113
Metal Surface, The Quantitative Determination of the Degree of Tarnishing of a, by its Reflective Power (*Ando*) 65
Metals, On the Fibrous Structure in, Deposited by the Difference of Electrolytic Solutional Pressures (*Tsuboi*) 271
Metanitrobenzaldehyde, On the Electrolytic Reduction of Aldehydes, Part II., (*Shima*) ... 1
Methylation of Shibuol, On Kakishibu V., (*Komatsu, Matsunami and Kurata*) 211
Micro-Crystals, On the Arrangements of the, in Zinc and Cadmium obtained by Sublimation (*Yamamoto*) 39
Micro-Crystals, The Arrangement of, in the Banded "Supposed Aragonite (Araragishi)" (*Fukushima*) 223
Micro-Crystals, The Arrangement of the, in Compressed Magnesium and Aluminium Plates (*Tsuboi*) 375
Micro-Crystals, An Examination of the, of Calcium Carbonate in Molluscan Shells by means of X-Rays, Part I (*Tsutsumi*) 217
Micro-Crystals, An Examination of the, of Calcium Carbonate in Molluscan Shells by means of X-Rays, Part II (*Tsutsumi*)... 401
Micro-Crystals, On the Arrangements of the, in Bismuth and Antimony deposited by Electrolysis, (*Hirata*) 429
Micro-Estimation, Studies in, of Metallic Elements, Part I. The Micro-Chemistry of Potassium Ferrocyanide (*Nakaseko*)... 95
Micro-Estimation, Studies in, of Metallic Elements, Part II. The Micro-Detection of Iron with Dimethylglyoxime (*Nakaseko*)... 113
Micro-Structures, On the Reflective Power of some Eutectic Alloys in Relation to their, (*Ando*) 43
Molluscan Shells, An Examination of the Micro-Crystals of Calcium Carbonate in, by means of X-Rays, Part I (*Tsutsumi*) 217
Molluscan Shells, An Examination of the Micro-Crystals of Calcium Carbonate in, by means of X-Rays, Part II (*Tsutsumi*)... 401
Monocyclic Terpenes, On the Transformation of Aliphatic Terpenes into,—A Synthesis of Menthol (*Horiuchi*) 171
Neutral Constituents of Pityrol, Biochemical Studies on Pityrol, III., (*Sakami*)... 505
Numbers, Group-Theory of Sequences of, (*Matsumoto*) 11
Oleic Acid, Biochemical Studies on Pityrol, VII. Distillation of, (*Ogata*) 543
Ortho-and Para-Oxybenzaldehydes, On the Electrolytic Reduction of Aldehydes, Part II., (*Shima*) 407
Palmitic Acid, Biochemical Studies on Pityrol, VI. Distillation of, (*Shoyama*) 533
Paradoxes and Definitions (*Matsumoto*) 367
Para-Oxybenzaldehydes, On the Electrolytic Reduction of Aldehydes, Part III. Ortho-and, (*Shima*) 407
Peculiar Reversal of the Discharge-Figures on Photographic Plates (*Yoshida and Tsutsumi*) 267
Piperonal, On the Electrolytic Reduction of Aldehydes, Part IV. Vanillin and, (*Shima*) 419
Pityrol, Biochemical Studies on, I. Introduction to the Biochemistry of Pityrol (*Komatsu*) 481
Pityrol, Biochemical Studies on, II. Distillation of Rice Bran (*Fujita*) 497

PAGE
Pityrol, Biochemical Studies on, III. Neutral Constituents of Pityrol (*Sakami*) 505
Pityrol, Biochemical Studies on, IV. Acidic Constituents of Pityrol (*Masumoto*) 517
Pityrol, Biochemical Studies on, V. Basic Constituents of Pityrol (*Suzuki*) 521
Pityrol, Biochemical Studies on, VI. Distillation of Palmitic Acid (*Shoyama*) 533
Pityrol, Biochemical Studies on, VII. Distillation of Oleic Acid (*Ogata*) 543
Pityrol, Biochemical Studies on, VIII. Distillation of Sucrose (*Hidaka*) 549
Potassium Ferrocyanide, Studies in Micro-Estimation of Metallic Elements, Part I. The Micro-Chemistry of, (*Nakaseko*) 95
Potassium Iodide, On the Measurements of the Vapour Pressures of Concentrated Aqueous Solutions of, (*Furutani*) 149
Probability of Lightning Strokes (*Yoshida, Fukushima and Iso*)... 451
Propylalcohol, The Electrolytic Oxidation of Alcohols, IV. Electrolytic Oxidation of, in Alkaline Solutions (*Koidzumi*) 391
Recrystallization of Aluminium (*Tanaka*)... 229
Reduced Copper, Studies on Catalytic Action, XXII. Catalytic Action of, on Unsaturated Hydrocarbons (*Komatsu and Kurata*) 163
Reflective Power, On the, of some Eutectic Alloys in Relation to their Micro-Structures (*Ando*) 43
Reflective Power, The Quantitative Determination of the Degree of Tarnishing of a Metal Surface by its, (*Ando*) 65
Reverberation, On the Theory of, (*Yamashita*) 119
Reversal-like Phenomena of the Secondary and the Tertiary Discharge-Figures impressed on Photographic Plates (*Terada*) 355
Rice Bran, Biochemical Studies on Pityrol, II. Distillation of, (*Fujita*) 497
Rolling, On the Destruction of the Single Crystal of Aluminium by the Process of, (*Sakao*) 279
Sequences of Numbers, Group-Theory of, (*Matsumoto*) 11
Shibuol, On Kakishibu, IV. Constitution of, III. (*Komatsu and Matsunami*) 205
Shibuol, On Kakishibu, V. Methylation of, (*Komatsu, Matsunami and Kurata*)... ... 211
Single Crystal of Aluminium, On the Destruction of the, by the Process of Rolling (*Sakao*) 279
Single Crystals of Zinc. The Orientation of, (*Tanaka*)... 361
Solar Constant, The Influence of the Heliographic Activity upon the, with two Appendices (*Yamamoto*)... 233
Solar Research, Some Notes on, (*Yamamoto*)... 303
Sublimation, On the Arrangements of the Micro-Crystals in Zinc and Cadmium obtained by, (*Yamamoto*)... 39
Sucrose, Biochemical Studies on Pityrol, VIII. Distillation of, (*Hidaka*) 549
Synthesis of Menthol, On the Transformation of Aliphatic Terpenes into Monocyclic Terpenes-, (*Horiuchi*) 171
Tarnishing of a Metal Surface by its Reflective Power, The Quantitative Determination of the Degree of, (*Ando*) 65
Ternary Alloys, On the Brinell Hardness of the, consisting of Copper, Zinc and Aluminium as an α-Solid Solution (*Kawai*) 137
Unsaturated Hydrocarbons, Studies on Catalytic Action, XXII. Catalytic Action of Reduced Copper on, (*Komatsu and Kurata*) 163
Vanillin and Piperonal, On the Electrolytic Reduction of Aldehydes, Part IV., (*Shima*) 419
Vapour Pressures, On the Measurements of the, of Concentrated Aqueous Solutions of Potassium Iodide (*Furutani*) 149
X-Rays, An Examination of the Micro-Crystals of Calcium Carbonate in Molluscan Shells by means of, Part I (*Tsutsumi*) 217

PAGE

X-Rays, An Examination of the Micro-Crystals of Calcium Carbonate in Molluscan Shells by means of, Part II (*Tsutsumi*) 401

X-Rays, Laue-Photograph taken with Convergent, (*Fujiwara*) 283

X-Rays, A Method of Determining the Orientation of Crystal-Axes by (*Takeyama*) ... 469

Zinc and Cadmium, On the Arrangements of the Micro-Crystals in, obtained by Sublimation (*Yamamoto*) 39

Zinc, The Orientation of Single Crystals of, (*Tanaka*) 361

Vol. XI, No. 6, Published November 25, 1928

Price - - - Yen 1·500

These Memoirs are on Sale at

MARUZEN COMPANY, LTD.

TOKYO, OSAKA, KYOTO, NAGOYA, YOKOHAMA, FUKUOKA
& SENDAI

昭和三年十一月二十日印刷
昭和三年十一月廿五日發行

編纂兼發行者　京都帝國大學理學部

印刷者　須磨勘兵衛
京都市下京區北小路通新町西入

印刷所　內外出版印刷株式會社
京都市下京區西洞院七條南

賣捌所　丸善株式會社
東京、大阪、京都、名古屋、横濱、福岡、仙臺

CONTENTS

The Probability of Lightning Strokes
By Usaburo Yoshida, Hidehiko Fukushima and Megumu Iso . . . 451
A Method of Determining the Orientation of Crystal-Axes by X-Rays
By Setsuzo Takeyama 469
Biochemical Studies on Pityrol, I. Introduction to the Biochemistry of Pityrol
By Shigeru Komatsu 481
Biochemical Studies on Pityrol, II. Distillation of Rice Bran
By Shinzaburo Fujita 497
Biochemical Studies on Pityrol, III. Neutral Constituents of Pityrol
By Saburo Sakami 505
Biochemical Studies on Pityrol, IV. Acidic Constituents of Pityrol
By Bunkichi Masumoto 517
Biochemical Studies on Pityrol, V. Basic Constituents of Pityrol
By Shigekiyo Suzuki 521
Biochemical Studies on Pityrol, VI. Distillation of Palmitic Acid
By Seiichi Shoyama 533
Biochemical Studies on Pityrol, VII. Distillation of Oleic Acid
By Hiroshi Ogata 543
Biochemical Studies on Pityrol, VIII. Distillation of Sucrose
By Yoshinori Hidaka 549